Distribution, Dimerization and Function of Human Cannabinoid Receptor Type 1 Coding Region Splice Variants

by

Amina Mustafa Bagher

Submitted in partial fulfilment of the requirements
for the degree of Master of Science

at

Dalhousie University
Halifax, Nova Scotia
July 2012

DALHOUSIE UNIVERSITY
DEPARTMENT OF PHARMACOLOGY

The undersigned hereby certify that they have read and recommend to the Faculty of Graduate Studies for acceptance a thesis entitled "Distribution, Dimerization and Function of Human Cannabinoid Receptor Type 1 Coding Region Splice Variants" by Amina Mustafa Bagher in partial fulfilment of the requirements for the degree of Master of Science.

Dated: 19-July-2012

Co-Supervisors: _____

_____

Readers: _____

_____

Departmental Representative: _____

DALHOUSIE UNIVERSITY

DATE: 19-July-2012

AUTHOR: Amina Mustafa Bagher

TITLE: Distribution, Dimerization and Function of Human Cannabinoid Receptor Type 1 Coding Region Splice Variants.

DEPARTMENT OR SCHOOL: Department of Pharmacology.

DEGREE: M.Sc. CONVOCATION: October YEAR: 2012

_____

Signature of Author

Table of Contents

List of Tables

List of Figures

Abstract

The pharmacological functions of the type 1 human cannabinoid receptor (hCB_1) are thought to be modulated through the isoform encoded by the fourth exon of the *CNR1* gene. Two other mRNA variants of the coding region of this receptor have been described, hCB_{1a} and hCB_{1b}. The contribution of these variants to endocannabinoid physiology and pharmacology remains unclear. In the present study, the three hCB_1 coding region variants mRNAs were detected in all human brain regions examined. Western blot analysis of homogenates from different regions of the monkey brain demonstrated that proteins with the expected molecular weights of CB_1, CB_{1a} and CB_{1b} receptors are present throughout the brain. In HEK cells, each of the receptor variants could form homodimers and variants formed heterodimers. Heterodimerization affected both the trafficking of hCB_1 receptor complexes and signalling in response to cannabinoid agonists.

List of Abbreviations and Symbols Used

2-AG	2-arachidonyl glycerol
A	adenosine
AEA	N-arachidonoylethanolamine, or anandamide
AM251	(N-(piperidin-1-yl)-5-(4-iodophenyl)-1-(2,4-dichlorophenyl)-4-methyl-1H- pyrazole-3-carboxamide)
ANOVA	analyses of variance
ATG	translation initiation codon
β_2AR	β_2 adrenergic receptor
BiFC	bimolecular fluorescence complementation
bp	base pair
BRET	bioluminescence resonance energy transfer
BSA	bovine serum albumin
cAMP	cyclic adenosine monophosphate
CCK	cholecystokinin
CCKR5	cholecystokinin receptor 5
CHO	Chinese hamster ovary cells
CNS	central nervous system
Co-IP	co-immunoprecipitation
$CRIP_{1a}$	cannabinoid receptor-interacting protein 1a
$CRIP_{1b}$	cannabinoid receptor-interacting protein 1b
D_{2S}	dopamine receptor 2 short isoform
D_{2L}	dopamine receptor 2 long isoform
D_3	dopamine receptor 3
DGL	diacylglycerol lipase
DTT	dithiothreitol
DMEM	Dulbecco's modified eagle's medium
DMSO	dimethyl sulfoxide
dNTP	deoxyribonucleotide

DNA	deoxyribonucleic acid
DRC	dose-response curve
ECS	endocannabinoid system
EDTA	ethylenediaminetetraacetic acid
ER	endoplasmic reticulum
ERK	extracellular-signal regulated kinase
G	guanine
FBS	fetal bovine serum
GABA	γ-aminobutyric acid
GFP^2	green fluorescent protein2
GDP	guanosine diphosphate
GPCR	G-protein coupled receptor
G protein	guanine nucleotide binding protein
GRK	g protein kinase
GTP	guanosine triphosphate
FITC	fluorescein isothiocyanate
FRET	fluorescence resonance energy transfer
H_2O	water
hMOR	human mu opioid receptor
HEPES	(4-(2-hydroxyethyl)-1-piperazineethanesulfonic acid)
HERG	human *ether--a--go--go* related gene
HEK	human embryonic kidney
HIV	human immunodeficiency virus
h	hours
IgG	immunoglobulin G
kDa	kilodaltons
m	minute
MAP kinase	mitogen activated protein kinase
mGluR6	metabotropic glutamate receptor 6
mGluR1	metabotropic glutamate receptor 1
mRNA	messenger RNA

NAT	N-acyltransferase
NCBI	National center for biotechnology information
O-2050	((6aR,10aR)-3-(1-Methanesulfonylamino-4-hexyn-6-yl)-6a,7,10,10a-tetrahydro-6,6,9-trimethyl-6H-dibenzo[b,d]pyran)
ORF	open reading frame
PBS	phosphate-buffered saline
PBST	phosphate-buffered saline with 0.1%tween-20
PCR	polymerase chain reaction
PFA	paraformaldehyde
PKA	protein kinase A
PTx	pertussis toxin
qPCR	quantitative polymerase chain reaction
RGS	regulator of G protein signaling proteins
Rluc	*Renilla* luciferase
RNA	ribonucleic acid
RT-PCR	reverse transcription polymerase chain reaction
s	seconds
SDS-PAGE	sodium dodecyl sulfate polyacrylamide gel electrophoresis
THC	Δ9-tetrahydrocannabinol
T	thymidine
TM	transmembrane
UTR	untranslated regions
VGCC	voltage gated calcium channel
WIN 55,212-2	WIN (R)-(+)-WIN55,212-2 mesylate (WIN) ((R)-(+)-[2,3-Dihydro-5-methyl-3-(4-morpholinylmethyl)pyrrolo[1,2,3-de]-1,4-benzoxazin-6 yl]-1-naphthalenylmethanone mesylate

Acknowledgements

In the name of ALLAH (GOD), the most merciful, the most compassionate

"The more you thank Me, the more I give you." Quran, 14:7

"Say: My Lord increase me in knowledge." Quran, 20:114

First of all, I would like to thank my supervisor Dr. Melanie Kelly for giving me this great opportunity to be a grad student at Dalhousie University and for her guidance. I also would like to thank my co-supervisor Dr. Eileen Denovan-Wright for her outstanding supervision, support and patience, without her guidance, I would not have been able to finish this thesis. I would like to thank my parents Norma and Mustafa for their support and encouragement who without them I would not be here. Thanks to my siblings Sarah, Kassem and Mariam for their support through the years. Thanks to my husband Abdullah and my big boy Louie for their love and patience. Thanks to our lovely lab technician Kay Murphy for all her technical help, and thanks to all the current and the past members of the Denovan-Wright lab, Robert Laprairie, Gregory Hosier, Mathew Hogel, Sophie Rowlands and Sarah Hutchings for their continuous help and sharing a good time. Finally I need to thank all the faculty and staff of the Department of Pharmacology for their help and support, in particular the members of my thesis advisory committee and examining committee, Dr. Christopher Sinal, Dr. Elizabeth Cowley and Dr. Denis Dupré.

Chapter 1: Introduction

G protein-coupled receptors (GPCRs) are the largest family of transmembrane receptors. GPCRs can physically interact with each other to form homo- and heterodimers. These interactions have profound impact on receptor trafficking, ligand binding and G protein coupling (Milligan, 2004). GPCR transcripts can undergo alternative splicing within their coding regions to generate receptor variants that may differ in their pharmacological, signaling and regulatory properties (Kilpatrick *et al*., 1999). The human cannabinoid receptor 1 (hCB_1), a GPCR that is highly expressed in the central nervous system, plays an important role in regulating neurotransmitter release (Howlett *et al*., 2004). Two mRNA variants of the hCB_1 coding region have been identified: hCB_{1a} and hCB_{1b} (Shire *et al*., 1995; Ryberg *et al*., 2005). The main aim of my thesis was to examine the distribution of CB_1 variant transcripts in human and monkey brain, to examine if hCB_{1a} and hCB_{1b} protein are expressed in the monkey brain, and to study physical interactions between hCB_1 receptor variants.

1.1 G Protein-Coupled Receptors

G protein-coupled receptors (GPCRs) are integral membrane proteins involved in signal transduction (Millar and Newton, 2010). GPCRs share a common architecture, which consists of an extracellular amino (N)-terminus, seven transmembrane spanning segments (TM) and an intracellular carboxyl (C)-terminus. They are activated by a diverse range of ligands including: light, odorants, hormones, neurotransmitters, chemokines, amino acids and Ca^{+2} ions. GPCRs can be broadly subdivided into five families according to their protein sequence and receptor function, including the

rhodopsin family, the secretin family, the glutamate family, the adhesion family, and the frizzled/taste2 family (Gurevich, 2008; Millar & Newton, 2010).

Signal transduction at GPCRs begins with an agonist binding to the receptor, which in turn switches the receptor from an inactive state to an active state conformation (Fig. 1.1). The activated receptor catalyzes the exchange of GDP for GTP on the α-subunit of heterotrimeric G proteins (Gαβγ), which in turn engages conformational and/or dissociational events between the Gα and dimeric Gβγ subunits. Both the GTP-bound Gα subunit and the Gβγ dimer can then initiate or suppress the activity of effector enzymes (*e.g*. adenylyl cyclases, phosphodiesterases, phospholipases), and ion channels (*e.g*. G protein-activated inwardly rectifying K+ channels) that modulate diverse signaling pathways (Vilardaga *et al*., 2009). Signaling ceases when GTP is hydrolyzed to GDP by intrinsic GTPase activity of the Gα subunit. The primary pathway leading to desensitization of a GPCR is initiated by phosphorylation of the intracellular C-terminus of the receptor by G-protein receptor kinase (GRK). Following phosphorylation, an arrestin scaffolding protein facilitates the internalization of the receptor, where it may either be degraded or recycled back to the cell surface (Millar & Newton, 2010; Duvernay *et al*., 2005).

In recent years, it has become clear that GPCR signaling is more complex and diverse than has been previously known. This complexity in signaling arises from numerous factors, among which are the ability of GPCRs to form both homo- and heterodimers, which modulates nearly every aspect of receptor pharmacology and function; the ability of receptors to adopt multiple "active" states with different effector coupling profiles; and the ability of non-G protein effectors to mediate some aspects of

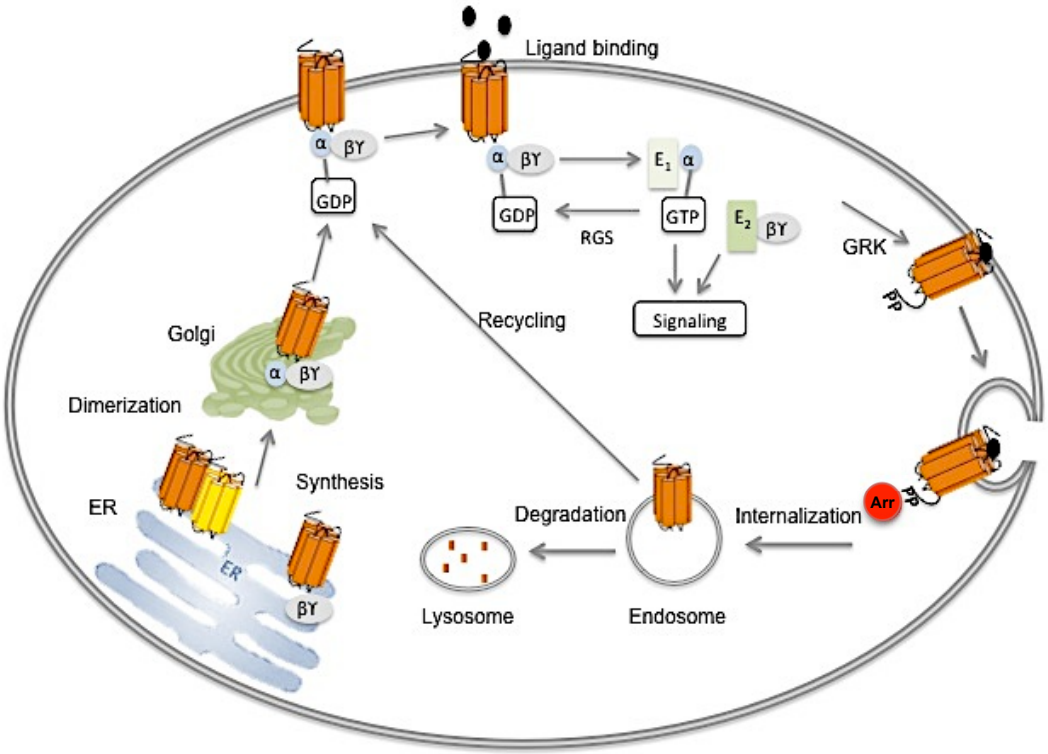

Figure 1.1: The life-cycle of a GPCR. GPCRs are synthesized and folded in the endoplasmic reticulum. Following this, the receptor is transported via secretory vesicle to the Golgi apparatus and eventually to the plasma membrane. Signal transduction at GPCRs begins with the agonist binding to the receptor, which catalyzes the exchange of GDP for GTP on the α-subunit of heterotrimeric G proteins (Gαβγ). This allows the activated G protein to act on downstream effectors and produce a biological response through their own effector 1 (E_1) and effector 2 (E_2). Signaling is then turned off by the hydrolysis of GTP back to GDP by the regulator of G protein signaling (RGS) proteins. The receptor will be internalized by phosphorylation of the intracellular region of the receptor by G protein kinase (GRK) and the recruitment of arrestin protein (Arr). The internalized receptor will either be degraded by the lysosome, or recycled back to the cell surface. GPCR dimerization persists throughout the cycle (Figure was modified from Wilkie *et al.,* 2001).

GPCR signaling (Maudsley *et al*., 2005). In addition, the discovery that GPCRs can undergo alternative splicing to generate multiple isoforms with distinct biochemical properties further increases the complexity of GPCR (Kilpatrick *et al*., 1999).

1.2 Alternative Splicing of GPCRs

Alternative splicing is a mechanism that increases the diversity of proteins that are encoded by the genome. Alternative splicing is the process by which introns are removed from precursor-mRNA (pre-mRNA) and exons are reconnected in multiple ways, resulting in alternative and sometimes multiple mature mRNA variants. The resulting different mRNA may be translated into different protein isoforms. Thus, a single gene may code for multiple proteins. In humans, over 90% of genes undergo alternative splicing giving rise to the exceptional complexity of human proteins (Kilpatrick *et al*., 1999; Markovic and Challiss, 2009). To date, alternative splicing has been reported for more than 50 GPCRs and some GPCRs have multiple variants (Markovic and Grammatopoulos, 2009). Alternative splicing of GPCRs can result from exon skipping, alternative exon insertion, and intron retention and consequently several receptor isoforms may be encoded by the same gene (Kilpatrick *et al*., 1999; Minneman, 2001). Many members of the rhodopsin family are expressed as multiple isoforms and all members of the secretin and glutamate families identified to date undergo extensive alternative splicing (Markovic and Challiss, 2009). Interestingly, alterative splicing of GPCRs is not limited to the open reading frame (ORF), but it can also occur in the 5'-untranslated region (5'-UTR) of the pre-mRNAs. The retention of alternate 5'-UTR may play an important role in controlling the translational efficiency, message stability and

subcellular localization of mRNAs (Hughes, 2006). GPCR splice variants have been identified by reverse transcriptase- polymerase chain reaction (RT-PCR) and by *in situ* hybridization. Whether alternatively spliced coding regions GPCRs are translated and expressed *in vivo* as receptors, or they undergo degradation, has not been determined for all alternatively spliced GPCRs mRNAs (Minneman, 2001).

1.2.1 Influence of Alternative Splicing on GPCRs Structure and Function

GPCR open reading frame splice variants can differ in the amino acid sequence of their C-terminal tails, N-terminal tails or transmembrane regions (Kilpatrick *et al*., 1999). There is a growing body of evidence showing that alternatively spliced GPCR isoforms might exhibit altered pharmacological properties, ranging from changes in ligand binding, signaling, G-protein coupling, constitutive activity and distribution (Minneman, 2001).

Knowing the sites of variation in GPCR structures that arise through splicing may give an insight regarding their pharmacological differences (Minneman, 2001). For example, the N-termini of GPCRs are usually involved in ligand recognition and binding. It has been reported that some N-terminal GPCR splice variants display altered ligand-binding properties. Cholecystokinin ΔCCK-B, an isoform of the CCK-B receptor, has lower affinity for CCK and gastrin compared to the full-length isoform (Miyake *et al*., 1995). In contrast, human μ opioid receptor (hMOR-1i), a splice variant for hMOR-1, having an additional 93 amino acids at the N-terminus, shows no significant difference in binding affinity compared to the hMOR-1 (Xu *et al*., 2009). Alternative splicing at the C-

terminal and the transmembrane domains of GPCRs has effects on the signaling pathways used by the receptors. For instance, the $mGluR_{1a}$ receptor, a C-terminal splice variant of the metabotropic glutamine receptor ($mGluR_1$), stimulates adenylate cyclase, as well as the production of inositol phosphate, unlike the other C-terminal splice variants that don't activate inositol phosphate (Coon and Pin, 1997). In addition to ligand binding and signaling, alternative GPCR splicing at the C-terminus has also been reported to alter the constitutive activity of the receptor. For example, $5\text{-}HT_{4a}$, a splice variant of the $5\text{-}HT_4$ receptor, has a much higher constitutive activity compared to the full-length receptor (Claeysan *et al*., 1999). However, constitutive activity is difficult to quantify, and is generally inferred from differences in second messenger levels caused by changes in receptor density following heterologous overexpression (Minneman, 2001). Lastly, GPCR splice variants might also exhibit different distribution patterns. A well-known example is the D_2 dopamine receptor, which exists in two isoforms including the short isoform (D_{2S}) and long isoform (D_{2L}). D_{2S} and D_{2L} receptors are formed by alternate splicing of the third intracellular loop. D_2 variants are differentially localized in central nervous system (CNS) neurons; the short isoform is localized pre-synaptically, especially in the hypothalamus and mesencephalon regions known to synthesize and release dopamine, while the long isoform is localized post-synaptically in the striatum and nucleus accumbens regions that receive dopaminergic output (Khan *et al*., 1998).

1.3 GPCRs Dimerization and its Functional Consequences

For many years, GPCRs were thought to exist and function as monomers. However, recent evidence has shown that many GPCRs can physically interact to form functional

homodimers, and can physically interact with other member of GPCRs to form heterodimers (Milligan, 2004; Prinster *et al*., 2005). Dimerization of GPCRs has been reported to have profound effects on receptor biosynthesis, trafficking, ligand binding and signal transduction (Rios *et al*., 2001; Terrillon and Bouvier, 2004).

Dimerization occurs early during the biosynthesis of the receptor in the endoplasmic reticulum (ER), and appears to persist through all phases of receptor trafficking to the cell membrane (Dupré *et al.*, 2006). Several studies have demonstrated that GPCR heterodimerization can affect receptor synthesis and trafficking to the plasma membrane. A good example is the gamma-aminobutyric acid B receptor ($GABA_B$), which exists as a heterodimer composed of $GABA_{B1}$ and $GABA_{B2}$. When each receptor is expressed alone, $GABA_{B1}$ is retained in the ER, whereas $GABA_{B2}$ reaches the cell surface as a nonfunctional receptor. Co-expression of $GABA_{B1}$ and $GABA_{B2}$ results in efficient surface expression of the receptor and the agonist affinity of these heterodimeric receptors were similar to the native $GABA_B$ receptor (Galvez *et al*., 2001). This observation confirms that dimerization of GPCRs is required for the appropriate maturation and trafficking of these receptors from the ER to the cell membrane (Milligan, 2004). Another aspect of GPCR function that is affected by dimerization is the ligand pharmacology of the interacting receptors. It has been reported that GPCR heterodimerization leads to both positive and negative ligand binding cooperativity between the receptors (Terrillon and Bouvier, 2004). An interesting consequence of dimerization with respect to ligand pharmacology is the concept that heterodimer-selective ligands could be created, which may be useful in reducing the side-effect of drug, as they act only on cells expressing the heterodimer (Milligan *et al*., 2004; Terrillon

and Bouvier, 2004). Another aspect of GPCR function that is altered by dimerization is signal transduction. Many studies have shown that the G-protein coupling preference for receptors may be altered by heterodimerization, while others have simply suggested that heterodimerization may either potentiate or inhibit receptor signaling through specific pathways (Bai, 2003; Milligan *et al*., 2004; Terrillon and Bouvier, 2004). A final aspect of GPCR function that is affected by dimerization is desensitization and internalization of the GPCRs following agonist activation. In a heterodimer, it has been found that activation of one receptor will lead to a cross-internalization and a cross-desensitization of the second receptor. These findings are supported by the observation that dimers appear to internalize as intact entities, instead of disassociating prior to internalization (Terrillon and Bouvier, 2004).

1.4 Physiological and Pathophysiological Roles of GPCR Splice Variants

There is a growing body of evidence that suggests that GPCR splice variants play important roles under normal as well as diseased conditions (Markovic and Grammatopoulos, 2009). Changes in expression of the full-length and spliced mRNAs during development have been reported for some GPCRs. A good example is the mGlu1b receptor variant. The $mGluR_{1b}$ mRNA was found to be the predominant isoform in embryonic mouse olfactory mitral cells, compared to postnatal day 7 when this variant is a minor component and the $mGluR_{1a}$ receptor predominates. This finding suggests a physiological function for $mGluR_{1b}$ in mitral embryonic cell maturation (Bovolin *et al.*, 2009). Moreover, it has been reported that some GPCRs are capable of physically

interacting with their splice variants to form heterodimers. Such interaction was found to affect every aspect of the full-length receptor function. Many members of the rhodopsin family GPCRs have been reported to dimerize with their splice variants, including GnRH gonadotropin-releasing hormone (Grosse *et al*., 1997; McElvaine and Mayo, 2005), vasopressin V2R (Zhu and Wess, 1998), D3 dopamine (Karpa *et al.*, 2000), and CCR5 chemokine receptors (Benkirane *et al.*, 1997; Shioda *et al*., 2001) and hLHR human luteinizing hormone (Nakamura *et al*., 2004; Apaja *et al.*, 2006). In all cases, it was found that the co-expression of the full-length receptor and its splice variants in a heterologous expression system resulted in a reduction in the cell surface expression of the full-length receptor. Studies suggest that this reduction in cell-surface expression is due to the retention of the wild-type receptor in the ER (Bai, 2003).

Dimerization of GPCRs with their splice variants has been linked to the pathophysiology of some diseases. For example, increase in the expression level of the truncated dopamine D_{3nf} mRNA was observed in the cortex of postmortem tissue from schizophrenia patients. D_{3nf} expression inhibits dopamine binding to full-length D_3 receptor, and also redirects full-length D_3 receptor localization away from the plasma membrane, and instead into an intracellular compartment. Alternation in the expression level of the truncated D_3 receptor was hypothesized to contribute to the abnormal dopamine activity observed in schizophrenia (Richtand, 2006; Karpa *et al*, 2000). Another example is the CCR5 receptor. It has been shown that a truncated variant of the human CCR5 receptor can reduce cell surface expression of the full-length CCR5 receptor, which inhibits CCR5 receptor-mediated human immunodeficiency virus (HIV) infection in individuals who are heterozygous for the mutant GPCR by forming

heterodimers with the wild-type receptor and thereby preventing its transport and delaying the development of HIV syndromes by 2-4 years (Benkirane *et al.*, 1997; George *et al*., 2002). Clearly, dimerization of GPCRs with their variants has profound influences on the full-length receptor functions.

1.5 The Cannabinoid System: the Cannabinoid Receptor 1 (CB_1)

The plant *Cannabis sativa* has been used for centuries for medical, religious, and recreational purposes due to its antiemetic, sedative, anti-inflammatory and psychotropic effects (Mechoulam & Gaoni, 1967). These effects have been attributed to the effect of delta-9-tetrahydrocannabinol (Δ9-THC), one of the active constituent of the plant, on two GPCRs: the cannabinoid receptor 1 (CB_1), predominantly found in the CNS and other peripheral tissues, and the cannabinoid receptor 2 (CB_2), mainly associated with immune cells (Mechoulam, 1970; Matsuda *et al*., 1990; Munro *et al.*, 1993). The CB_1 receptor regulates a variety of central and peripheral physiological functions, including neuronal development, neuromodulatory processes, energy metabolism as well as cardiovascular, respiratory and reproductive functions. The CB_2 receptor plays a role in modulating the immune system (Howlett *et al*., 2004; Bosier *et al.,* 2010).

The cannabinoid receptors, their endogenous ligands (endocannabinoids) and enzymes for their synthesis and degradation are referred to as the endocannabinoid system (ECS). The ECS activity is regulated by the enzymes responsible for the synthesis and the degradation of the endocannabinoids. Endocannabinoids are lipid neurotransmitters derived from arachidonic acid. The primary endocannabinoids are arachidonylethanolamide (anandamide or AEA), 2-arachidonoylglycerol (2-AG),

virodhamine and noladin ether (Devane *et al*., 1992; Mechoulam *et al*., 1995). These endocannabinoids are synthesized on demand at the site of action in response to specific signals, such as increases in intracellular calcium or activation of phospholipase Cβ by $G_{q/11}$ metabotropic receptors. Degradation of the endocannabinoids occurs locally by fatty-acid amide hydrolase (FAAH) and monoacylglycerol lipase (MGL; Howlett *et al*., 2004; Bosier *et al.,* 2010).

In the CNS, the CB_1 receptor is located presynaptically where it plays a modulatory role in the regulation of neurotransmitters release including: noradrenaline, acetylcholine, dopamine, GABA, glutamine, serotonin and glycine (Fig. 1.2; Abood & Martin, 1992; Wilson & Nicoll, 2001; Howlett *et al*., 2004). The CB_1 receptor preferentially couples to $G\alpha_i$, and CB_1 activation is associated with inhibition of adenylyl cyclase, decreases in the concentrations of cAMP, and activation of mitogen activated protein kinases (MAP kinase). In addition, CB_1 receptors are associated with inhibition of voltage-gated Ca^{2+} channels and activation of inward rectifying K^+ channels. In some cells CB_1 has been shown to signal through both $G\alpha_s$ and $G\alpha_{q/11}$ pathways to increase cAMP, and intracellular Ca^{2+}, respectively (Demuth and Molleman, 2006; Bosier *et al.,* 2010).

Cannabinoid agonists are divided into four structurally distinct groups. The first group contains the 'classical cannabinoids' derived from the plant *C. sativa* such as Δ9-THC and related synthetic derivatives such as, HU-210. The second group contains the non-classical cannabinoids, which are synthetic derivatives of the classical cannabinoids that lack the dihydropyran ring, for example, CP 55,940. The third group contains aminoalkylindoles, such as WIN 55212-2 and its related compounds. The fourth group

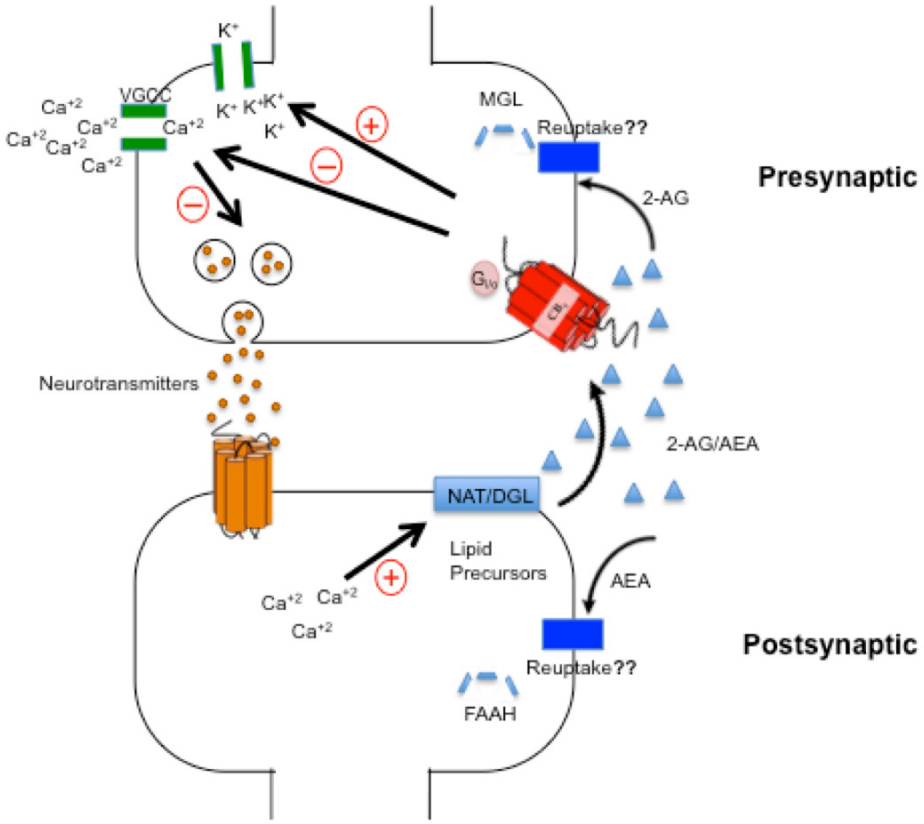

Figure 1.2: Diagram of CB_1 retrograde inhibition of neurotransmitter release. The increase in intracellular calcium levels in the postsynaptic terminal activates N-acyltransferase (NAT) or diacylglycerol lipase (DGL), which synthesize anadamide (AEA) or 2-arachidonyl glycerol (2-AG), respectively, from cellular phospholipids. AEA and 2-AG then travel back to the presynaptic terminal to activate CB_1 receptors (retrograde signaling). Activation of CB_1 receptors inhibit voltage gated calcium channel (VGCC), in addition to other presynaptic changes, which lowers the probability of Ca^{+2} dependent neurotransmitter release. Then, AEA is taken back up by the postsynaptic terminal, possibly by a plasma membrane protein transporter and/or by passive diffusion, and its signaling function terminated by conversion to arachidonic acid by fatty acid amide hydrolase (FAAH), while the 2-AG is taken up by the presynaptic terminal and is degraded by monoacylglycerol lipase (MGL; Figure was modified from Hosking, R.D. & Zajicek, J.P., 2008).

contains the endocannabinoids, which are eicosanoid compounds rather than cannabinoid compounds and includes the endocannabinoids AEA and 2-AG (Bosier *et al.,* 2010).

1.5.1 Human CB_1 Gene Structure and Splicing Pattern

The human CB_1 gene (*CNR1*) is located on chromosome 6 locus q14-q15. The *CNR1* gene was originally described as consisting of four exons and three introns. Exon 4 contains the entire protein coding regions of hCB_1, while the three non-coding exons, named exon 1, 2, and 3 are located 5' to the protein-coding region and are separated by three introns (introns 1, 2, and 3; Zhang *et al*., 2004). Alternative splicing of the 5'-UTR of the hCB_1 gene results in the formation of six hCB_1 transcripts with variable 5' UTR, termed variants 1, 2, 3, 4, 5 and 6 (Fig. 1.3). Each of these variants has a unique 5'- UTR, transcription initiation site and distribution pattern in the human brain and peripheral tissues. Alternations in the relative abundance of these variants have been reported in the visceral adipose tissue of obese patients (Sarzania *et al*., 2009). The translation of the hCB_1 receptor starts at the first ATG located at the 5' end of unspliced exon 4 and produces a polypeptide chain of 472 amino acids. This chain forms an exceptionally long extracellular N-terminal tail of 116 amino acids connected to seven transmembrane domains and ended by an intracellular carboxyl terminus (The National Center for Biotechnology Information, NCBI; Zhang *et al*., 2004). Alternative splicing of hCB_1 within the coding region has been totally ignored, as the fourth exon of the *CNR1* gene, that encodes the whole coding region of hCB_1 receptor was thought to be intronless,

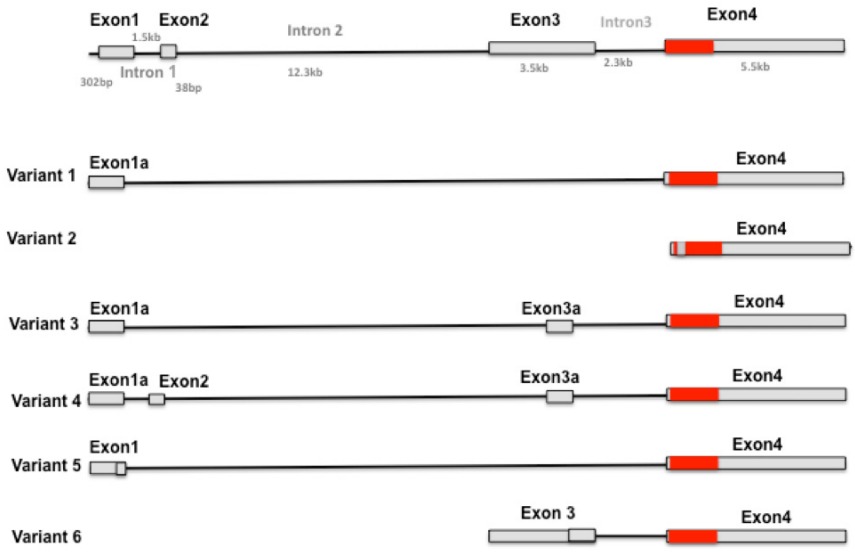

Figure 1.3: Schematic diagram of the human *CNR1* gene and mRNA variants. Six splice variants of the 5'UTR of hCB_1 gene have been identified. Exons are indicated by boxes, while introns are indicated by interconnecting lines. The coding region is indicated in red, while the non-coding region is indicated in grey (Figure was modified from Zhang *et al*., 2004).

which led to the belief that hCB_1 mRNA is not subjected to alternative splicing. As a result, all the pharmacological functions of the hCB_1 were thought to be modulated through the isoform encoded by the fourth exon of the *CNR1* gene. However, this view has now changed with the identification of the first hCB_1 receptor mRNA coding region splice variant, hCB_{1a} (411 amino acids; Shire *et al.*, 1995). Subsequently, the second hCB_1 splice variant mRNA, hCB_{1b} (439 amino acids) has been identified (Ryberg *et al*, 2005). Splicing within the coding region of transcript variant 2 results in the formation of hCB_{1a} and hCB_{1b} transcripts. The hCB_{1a} transcript lacks an internal segment of 167 base pairs within the sequence encoding the N-terminal tail of the receptor. Translation of the hCB_{1a} receptor starts at the second ATG located at the 5' end of exon 4 (Fig.1.4). The resulting receptor is shorter than hCB_1 by 61 amino acids at its N-terminus. In addition, the first 28 amino acids of the N-terminus are totally different to hCB_1, while the remaining 27 amino acids are similar to the hCB_1 receptor (Fig. 1.5 &1.6). hCB_{1a} also lacks two out of three glycosylation sites and resulted in a more hydrophobic receptor. hCB_{1b} transcript is missing an internal segment of 99 base pairs resulting in a protein lacking 33 amino acids at the N-terminus tail. However, unlike hCB_{1a}, translation of hCB_{1b} starts at the first ATG located in exon 4 as hCB_1 (Fig. 1.4, 1.5. & 1.6; Shire *et al*., 1995; Ryberg *et al*., 2005; Zhang *et al*., 2004). It has not been demonstrated yet if the hCB_{1a} and hCB_{1b} mRNAs are translated and expressed as functional receptors *in vivo*. Transcripts formed through alternative splicing within the coding region of the gene are of particular interest, as they have the potential to alter the biological function of the expressed protein (Tress *et al*., 2007).

Figure 1.4: Aligned sequences of the 5' end of hCB_1, hCB_{1b} and hCB_{1a} cDNA. hCB_1 translation start at the first ATG from mRNA that is unspliced in the coding region. hCB_{1b} translation starts at the same ATG from mRNA that is spliced at the 5' end of the coding region. Specifically, hCB_{1b} results from a 99-nucleotide excision between donor (5'hCB_{1b}) and acceptor (3' hCB_{1b}). hCB_{1a} results from a 167-nucleotide excision between donor (5'hCB_{1a}) and acceptor (3' hCB_{1a}),while translation starts at the second ATG. TM1 codes for the first transmembrane region. Splicing sites are indicated in red boxes. Dashes represent gaps. (Figure was modified from Shire *et al*., 1995; Xiao *et al*., 2008; NCBI).

```
hCB1    MKSILDGLAD TTFRTITTDL LYVGSNDIQY EDIKGDMASK LGYFPQKFPL          1
hCB1b   MKSILDGLAD TTFRTITTDL L--------- ---------- ----------
hCB1a         MALQ IPPSAPSPLT SCTWAQMTFS TKTSK----- ----------

                                       *      *
hCB1    TSFRGSPFQE KMTAGDNPQL VPADQVNITE FYNKSLSSFK ENEENIQCGE         51
hCB1b   ----GSPFQE KMTAGDNPQL VPADQVNITE FYNKSLSSFK ENEENIQCGE
hCB1a   ---------- ---------- ---------- ---------- ENEENIQCGE

                    *
hCB1    NFMDIECFMV LNPSQQLAIA VLSLTLGTFT VLENLLVLCV ILHSRSLRCR        101
hCB1b   NFMDIECFMV LNPSQQLAIA VLSLTLGTFT VLENLLVLCV ILHSRSLRCR
hCB1a   NFMDIECFMV LNPSQQLAIA VLSLTLGTFT VLENLLVLCV ILHSRSLRCR

hCB1    PSYHFIGSLA VADLLGSVIF VYSFIDFHVF HRKDSRNVFL FKLGGVTASF        151
hCB1b   PSYHFIGSLA VADLLGSVIF VYSFIDFHVF HRKDSRNVFL FKLGGVTASF
hCB1a   PSYHFIGSLA VADLLGSVIF VYSFIDFHVF HRKDSRNVFL FKLGGVTASF

hCB1    TASVGSLFLT AIDRYISIHR PLAYKRIVTR PKAVVAFCLM WTIAIVIAVL        201
hCB1b   TASVGSLFLT AIDRYISIHR PLAYKRIVTR PKAVVAFCLM WTIAIVIAVL
hCB1a   TASVGSLFLT AIDRYISIHR PLAYKRIVTR PKAVVAFCLM WTIAIVIAVL

hCB1    PLLGWNCEKL QSVCSDIFPH IDETYLMFWI GVTSVLLLFI VYAYMYILWK        251
hCB1b   PLLGWNCEKL QSVCSDIFPH IDETYLMFWI GVTSVLLLFI VYAYMYILWK
hCB1a   PLLGWNCEKL QSVCSDIFPH IDETYLMFWI GVTSVLLLFI VYAYMYILWK

hCB1-   AHSHAVRMIQ RGTQKSIIIH TSEDGKVQVT RPDQARMDIR LAKTLVLILV        301
hCB1b   AHSHAVRMIQ RGTQKSIIIH TSEDGKVQVT RPDQARMDIR LAKTLVLILV
hCB1a   AHSHAVRMIQ RGTQKSIIIH TSEDGKVQVT RPDQARMDIR LAKTLVLILV

hCB1    VLIICWGPLL AIMVYDVFGK MNKLIKTVFA FCSMLCLLNS TVNPIIYALR        351
hCB1b   VLIICWGPLL AIMVYDVFGK MNKLIKTVFA FCSMLCLLNS TVNPIIYALR
hCB1a   VLIICWGPLL AIMVYDVFGK MNKLIKTVFA FCSMLCLLNS TVNPIIYALR

hCB1    SKDLRHAFRS MFPSCEGTAQ PLDNSMGDSD CLHKHANNAA SVHRAAESCI        401
hCB1b   SKDLRHAFRS MFPSCEGTAQ PLDNSMGDSD CLHKHANNAA SVHRAAESCI
hCB1a   SKDLRHAFRS MFPSCEGTAQ PLDNSMGDSD CLHKHANNAA SVHRAAESCI

hCB1    KSTVKIAKVT MSVSTDTSAE AL                                      451
hCB1b   KSTVKIAKVT MSVSTDTSAE AL
hCB1a   KSTVKIAKVT MSVSTDTSAE AL
```

Figure 1.5: Amino acid sequence alignment of hCB_1, hCB_{1b} and hCB_{1a}. The N-terminus of the hCB_1 receptor consists of 116 amino acids, indicated in bold. The hCB_{1b} receptor lacks an internal segment of 33 amino acids within the sequence encoding the amino-terminal tail of the receptor, resulting in a receptor with 84-amino acid N-terminal tail. The hCB_{1a} receptor uses a different initiation coding leading to a frameshift from the reading frame of hCB_1; in addition it misses an internal segment of 56 amino acids. This results in a receptor with only 55 amino acids N-terminal tail that differs from hCB_1 in the first 28 amino acids (highlighted in grey). However, after the splice junction, the reading frame of hCB_1 is restored, and the remaining 27 amino acids of the NH_2 terminal of hCB_{1a} are identical to hCB_1. Glycosylation sites are indicated in red *. Dashes represent gaps

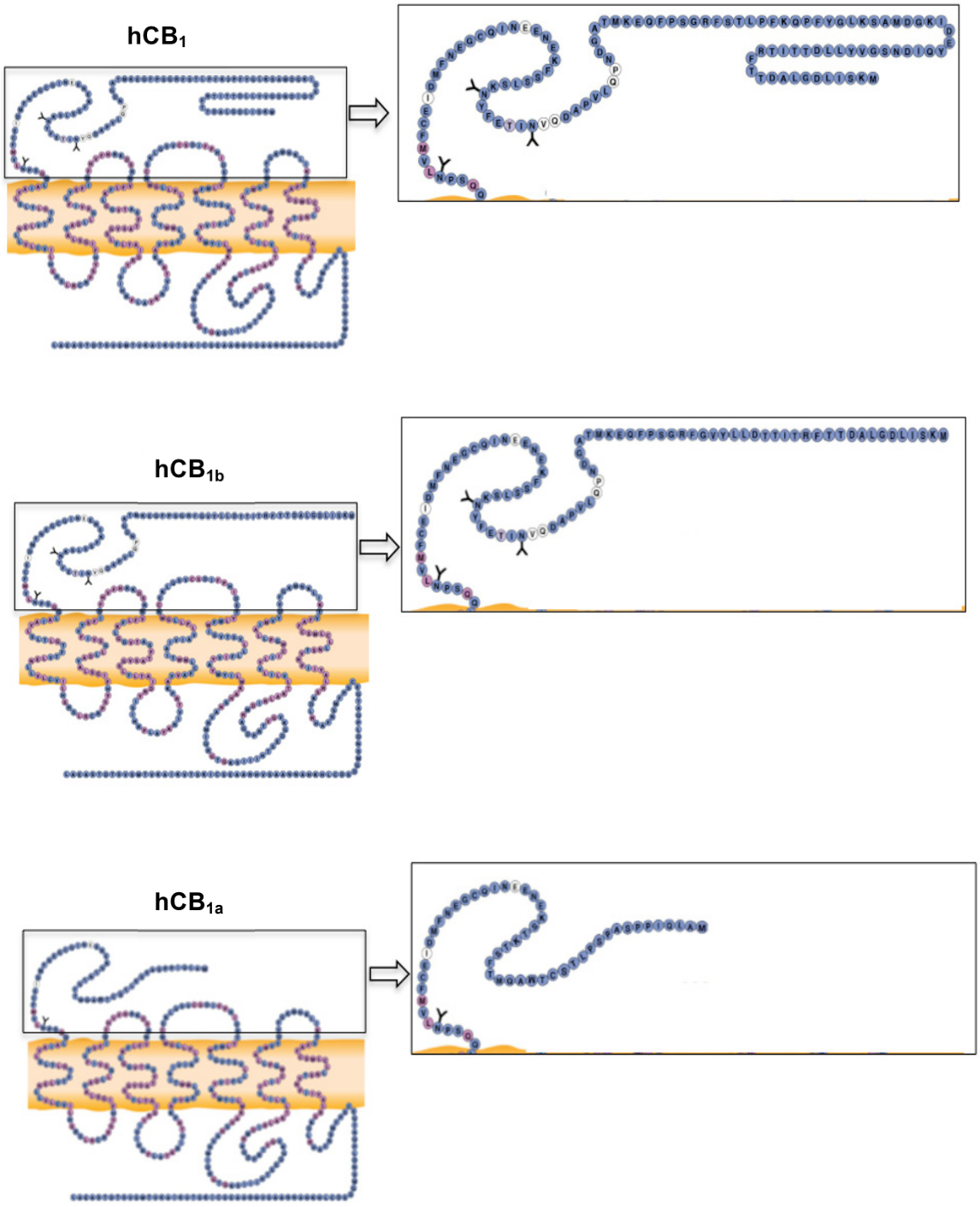

Figure 1.6: Schematic illustration of the amino acid sequences of hCB_1, hCB_{1b} and hCB_{1a} (Modified with permission of Cayman chemical company).

1.5.2 Distribution of hCB_1, hCB_{1a} and hCB_{1b} Receptors

The distribution of hCB_1 receptors has been extensively mapped by quantitative autoradiography, *in situ* hybridization and immunocytochemistry. High levels of the hCB_1 are expressed in neocortical association areas such as the prefrontal cortex and the cingulate cortex, which are known to mediate executive functions. Other brain regions involved in cognitive functioning, such as the hippocampus, basal ganglia, and cerebellum, also express high levels of the hCB_1. hCB_1 transcript is expressed in many regions of the human brain as early as the prenatal age (Wang *et al.,* 2003). The hCB_1 mRNA expression levels change during development. In the visual cortex of infants (<1 year) and pre-teens (5–11 years), the hCB_1 mRNA levels are about 40% higher compared to young children (1–2 years), adults (21–55 years), and the elderly (>55 years) (Pinto *et al*., 2010). In addition to the CNS, hCB_1 is expressed in several peripheral organs including the eye, gut, uterus, testis, vascular endothelium, spleen, and tonsils (Howlett *et al.,* 2004; Mackie, 2005).

The mRNAs of the hCB_{1a} and hCB_{1b} are expressed in the human brain and some peripheral tissues. Alteration in the distribution profiles of these transcripts has been reported during development and disease states (Shire *et al.,* 1995; Ryberg *et al.,* 2005; Xiao *et al*., 2008; Gustafsson *et al*., 2008). In the human brain, the hCB_1 and hCB_{1a} transcripts have been detected, using RT-PCR, in human adult total brain, brain stem, cortex, cerebellum, inferior hemisphere and temporal lobe (Shire *et al.,* 1995). Unlike hCB_1, hCB_{1a} mRNA was not detected in all the tested human infant brain regions including the brain stem and temporal lobe. The expression of the hCB_{1b} transcript has only been investigated in human fetal and adult total brain. It has not yet been determined if there is an overlap in the distribution patterns of the mRNAs of the three hCB_1 protein

variants in different regions of human adult brain. In the periphery, the transcripts of three hCB_1 coding region variants were detected in many peripheral tissues (adipose, testis, lung, kidney, jejunum, uterus, muscle, duodenum, and colon; Ryberg *et al.,* 2005). hCB_{1a} and hCB_{1b} transcripts were reported to be the minor transcripts compared to the hCB_1 transcript, as they represent fewer than 5% of the total hCB_1 transcripts depending on the examined tissues (Shire *et al,* 1995; Ryberg *et al.,* 2005; Xiao, 2008).

1.5.3 Functional Differences Between of hCB_1 and its Splice Variants

The existence of three isoforms of the human cannabinoid receptor 1 (hCB_1, hCB_{1a} and hCB_{1b}) has raised questions concerning their functional variations. A limited number of studies have attempted to address the functional differences between the hCB_1 receptor and its splice variants, as well as their physiological significance of these variants on the endocannabinoid system. One of the initial reports that characterized the hCB_{1a} splice variant, found that the binding of THC, CP55940 and WIN 5521-2 was slightly higher for hCB_1 than hCB_{1a} receptor, when either isoform was stably expressed in Chinese hamster ovary (CHO) cells. However, the endocannabinoid anandamide showed a similar affinity for both isoforms. Activation of hCB_{1a} by the cannabinoid agonists is able to inhibit cAMP and increase MAP kinase phosphorylation in a slightly lower extent compared to the full-length hCB_1 receptor (Rinaldi-Carmona *et al*., 1996). These results are consistent with the findings of Xiao *et al*. (2008). In this study, no significant difference in ligand binding and cAMP levels was observed among hCB_1, hCB_{1a} and hCB_{1b} receptors, in CHO cells, in responses to either endogenous cannabinoids (anandamide, 2-AG,

virodhamine and noladin ether) or synthetic cannabinoid ligands (CP55940 and AM251). In contrast, a study carried out by Ryberg *et al.*, (2005), reported that expression of hCB_{1a} and hCB_{1b} variants in human embryonic kidney (HEK) 293 cells displayed significantly less affinity and efficacy when treated with the endogenous cannabinoid ligands (anandamide, virodhamine and noladin ether) compared to hCB_1 receptor. In this study, 2-AG was found to act as an inverse agonist on both hCB_{1a} and hCB_{1b} receptors, while it acted as a full agonist on the hCB_1 receptors. The three receptors showed similar binding affinity and efficacy to synthetic ligands (Δ9-THC, CP55940, WIN 5521-2, HU210 and SR141716; Ryberg *et al*., 2005). A more recent study published in 2011 by Straiker *et al*., reported that hCB_1 variants signal more robustly compared to the hCB_1 in cultured hippocampal neurons. Given differences in general studies, the signaling properties for the hCB_1 variants are still poorly understood and further investigation is required.

1.5.4 Dimerization of the Cannabinoid Receptor 1 (CB_1)

Similar to other member of the Rhodopsin family of GPCR, the hCB_1 receptor forms both homodimers (Wager-Miller *et al*., 2002) and heterodimers with other GPCRs such as the D_2 dopamine receptor (Glass and Felder, 1997; Kearn *et al*., 2005), μ-, κ- and δ-opioid receptors (Rios *et al.,* 2006), orexin-1 (Ellis *et al*., 2006), A_{2a} adrenergic receptor (Carriba *et al.,* 2007) β_2-adrenergic receptor (β_2-AR; Hudson *et al*., 2010) and angiotensin II receptor (Rozenfeld *et al.,* 2011). These interactions have a profound functional implications on the function and pharmacology of the CB_1 receptor, including receptor trafficking, G protein coupling and signaling.

Homodimerization of the CB_1 receptor has been demonstrated by the observation of

a high molecular weight band on SDS-PAGE using an antibody directed against the C-terminal tail of CB_1 receptor; the high molecular weight bands have been anticipated as a dimer of higher molecular (Wager-Miller *et al.*, 2002). Homodimerization of the CB_1 receptor was further confirmed using the bioluminescence resonance energy transfer (BRET; Hudson *et al*., 2010). There is substantial evidence, using a variety of techniques, demonstrating that CB_1 can form dimers and higher order oligomers with a number of members the rhodopsin family of GPCRs. The first receptor demonstrated to form a heterodimer with CB_1 was the D_2 dopamine receptor. The functional interaction between the two receptors was first observed by Glass and Felder in 1997. They demonstrated that the co-activation of D_2 and CB_1, in both transfected cell lines and cultured striatal neurons, caused an increase in cAMP production, however stimulation of only one of the receptor results in an inhibition of cAMP. This response was found to be the result of stabilizing the CB_1 active state with increased coupling to G_s instead of G_i when the two receptors were co-activated (Kearn *et al.*, 2005). Physical interaction between the CB_1 and the D_2 receptors was confirmed using co-immunoprecipitation (Co-IP), fluorescence resonance energy transfer (FRET) and bimolecular fluorescence complementation (BiFC; Marcellino *et al.*, 2008, Przybyla and Watts, 2010). The CB_1 receptor has also been reported to form heterodimers with the μ, κ and δ opioid receptors using the BRET and FRET. The functional result of the CB_1/μ opioid receptor interaction is that signaling from both receptors is attenuated in the heterodimer, only when agonists for both receptors are present (Rios *et al.*, 2006). Using the fluorescence resonance energy transfer (FRET) technique, Ellis *et al.* (2006), reported that the CB_1 receptor dimerize with the orexin-1 receptor. In this study, it was shown that co-expression of the CB_1 and orexin-1

receptors altered the distribution of orexin-1 to a more intracellular distribution, similar to that of CB_1. Inverse agonists for either receptor were then able to return both receptors to the cell surface (Ellis *et al.*, 2006). In addition to D_2, opioid and orexin-1 receptors, the CB_1 receptor has also been reported to heterodimerize with the A_{2A} adenosine receptor. This was demonstrated both by Co-IP from rat striatal membranes, and by BRET in HEK 293 cells (Carriba *et al.*, 2007). Such an interaction was found to influence CB_1 signaling, such that CB_1 receptor did not signal through $G\alpha_i$ in HEK 293 cells co-expressing A_{2A} (Carriba *et al.*, 2007). Recently, Hudson *et al.*, (2010) was able to demonstrate functional and physical interactions between the hCB_1 receptor and the β_2-adrenergic receptor (β_2-AR) in both HEK 293 cells and primary human ocular cells using BRET. In HEK 293H cells, co-expression of β_2-AR increased cell surface expression of hCB_1 receptors and altered the signaling properties of CB_1 receptors, resulting in increased $G\alpha_i$ -dependent ERK phosphorylation, but decreased non-$G\alpha_i$-mediated CREB phosphorylation. Lastly, the CB_1 receptor has been reported to form heterodimers with the angiotensin II receptor (AT1R) using Co-IP, BRET and heteromer-selective antibodies (Rozenfeld *et al.,* 2011). Such an interaction was found to potentiate AT1R signaling and resulted in coupling of AT1R to multiple G proteins. In the same study, the physiological relevance of this interaction was examined in hepatic stellate cells from ethanol-administered rats in which CB_1 receptor is down regulated. They found a significant upregulation of AT1–CB_1 heteromers and enhancement of angiotensin II-mediated signaling, as compared with cells from control animals (Rozenfeld *et al.,* 2011).

1.6 Research Objectives

Similar to other members of the family of type A GPCRs, the hCB1 receptor is able to physically interact and form heterodimers with other type A GPCRs. Homo- and heterodimerization between and among hCB_1 variants has not been examined. The overlapping patterns of distribution of the mRNAs of the three coding region variants in addition to alterations in the relative abundance of the mRNAs of the three variants raises the possibility that dimerization may occur and influence the function of hCB_1 receptor complexes. Therefore, the present study aimed to address these issues with four primary research objectives:

1- Determine the relative distribution of the human cannabinoid hCB_1 receptor and its splice variant mRNAs in selected regions of the human brain.

2-Determine if the CB_1 variant proteins are expressed in the monkey (*Macaca fascicularis*) brain.

3- Determine the functional differences among the human cannabinoid hCB_1 receptor and its variants.

4- Determine if physical interactions occur between and among human cannabinoid hCB_1 receptor and its variants when expressed in heterologous expression systems and examine the functional consequences of these interactions.

Chapter 2: Methods

2.1 Isolation of Total RNA from *Macaca Fascicularis*, Mouse and Rat Brains

All animal work was done in accordance with the Canadian Council on Animal Care guidelines and is approved by the University Committee on Laboratory Animals at Dalhousie University. The *Macaca fascicularis* brain tissue was a kind gift from Dr. Jim C. Gourdon, McGill University, Montreal. The brain tissue was obtained from animals that were part of a research study of McGill University. All animal care, use and handling were approved by the McGill Animal Care Committee. The use of the post-mortem tissue was approved by Dalhousie University Committee on Laboratory Animals. The *Macaca fascicularis* brain was stored and handled following the standard operating procedure (McGill University) for hazardous material. The brain was shipped on dry ice and it was stored at -80ºC until use. Human brain RNA from different brain regions (total brain, frontal cortex, parietal cortex, caudate/putamen and cerebellum) from a 71-year-old female donor was obtained from Agilent Technologies (Cedar Creek, TX).

Total brain RNA from different brain regions (total brain, frontal cortex, parietal cortex, striatum, cerebellum, hippocampus, substantia nigra and brain stem) was isolated from mouse, rat and *Macaca fascicularis* brains. The isolated RNA was used in RT-PCR analysis to determine whether the CB_1 splice variant transcripts were expressed. RNA was isolated following the protocol described previously (Denovan-Wright *et al*., 2001). Briefly, the brain tissue was added to a tube containing 1 ml of TRIzol® reagent (Invitrogen Canada Inc., Burlington, ON, CA) per 50 mg of brain tissue. The tissue was homogenized using a Dounce homogenizer before 0.2 ml of chloroform was added.

Then, the homogenate was mixed vigorously for 15 s, incubated for 3 m on ice and centrifuged at 12,000 x *g* for 15 m at 4°C. The aqueous phase was removed to a new microcentrifuge tube and 0.5 ml of isopropanol was added. The solution was mixed well and placed on ice for 15 m before being centrifuged at 12,000 x *g* for 15 m at 4°C. The supernatant was then removed and the RNA pellet was washed twice using 1.0 ml of 75% ethanol, vortexed and centrifuged at 7,500 x *g* for 3 m at 4°C. The RNA pellet was allowed to air dry for approximately 10 m before being suspended in ddH_2O. The purity and concentration of the collected RNA were determined by measuring the A260/280 ratio of the samples. RNA samples were stored at -70°C.

2.2 Reverse Transcription Polymerase Chain Reaction (RT-PCR)

RT-PCR analysis was conducted to determine the relative abundance of the CB_1 variants and CNS distribution in human, monkey and rodents brains. Using human RNA, first strand cDNA was generated using 2 µg RNA from each brain region using reverse transcriptase SuperScript® II (GibcoBRL, ON, CA) following the protocol supplied by the manufacturer in a 20 µl reaction volume. The forward Human-CB_1-F and the reverse Human-CB_1-R primers (Table 2.1) common to the three-hCB_1 mRNAs were used to amplify cDNA (Fig. 2.1). PCR reactions contained 5 µl of 1/100 dilution of RT reaction, 2 µl 10X *Pfu* buffer with $MgSO_4$ (final concentration of 2 mM), 2 mM each deoxyribonucleoside triphosphate and 1 unit of *Pfu* DNA polymerase (Fermentas, ON, CA). These reactions were subjected to an initial denaturation step at 95°C for 3 m, and then 30 cycles of amplification at 95°C for 30 s, primer annealing at 54°C for 30 s and

A

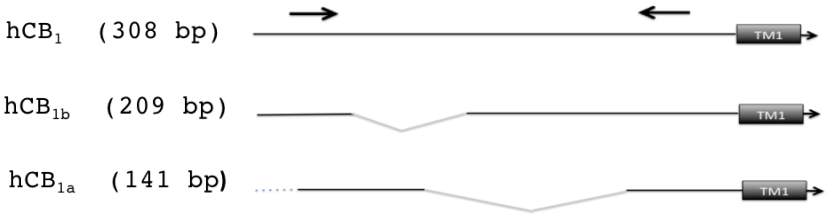

B

```
                                    Human-CB1-F
hCB1    ATGAAGTCGA TCCTAGATGG CCTTGCAGAT ACCACCTTCC GCACCATCAC       1
hCB1b   ATGAAGTCGA TCCTAGATGG CCTTGCAGAT ACCACCTTCC GCACCATCAC
hCB1a   ---------- ------ATGG CCTTGCAGAT ACCACCTTCC GCACCATCAC

hCB1    CACTGACCTC CTGTACGTGG GCTCAAATGA CATTCAGTAC GAAGACATCA      51
hCB1b   CACTGACCTC CT-------- ---------- ---------- ----------
hCB1a   CACTGACCTC CTGTACGTGG GCTCAAATGA CATTCAGTAC GAAGACATCA

hCB1    AAGGTGACAT GGCATCCAAA TTAGGGTACT TCCCACAGAA ATTCCCTTTA     101
hCB1b   ---------- ---------- ---------- ---------- ----------
hCB1a   AAG------- ---------- ---------- ---------- ----------

hCB1    ACTTCCTTTA GGGGAAGTCC CTTCCAAGAG AAGATGACTG CGGGAGACAA     151
hCB1b   ---------- -GGGAAGTCC CTTCCAAGAG AAGATGACTG CGGGAGACAA
hCB1a   ---------- ---------- ---------- ---------- ----------

hCB1    CCCCCAGCTA GTCCCAGCAG ACCAGGTGAA CATTACAGAA TTTTACAACA     201
hCB1b   CCCCCAGCTA GTCCCAGCAG ACCAGGTGAA CATTACAGAA TTTTACAACA
hCB1a   ---------- ---------- ---------- ---------- ----------

hCB1    AGTCTCTCTC GTCCTTCAAG GAGAATGAGG AGAACATCCA GAGAATGAGG     251
hCB1b   AGTCTCTCTC GTCCTTCAAG GAGAATGAGG AGAACATCCA GAGAATGAGG
hCB1a   ---------- ---------- GAGAATGAGG AGAACATCCA GAGAATGAGG

                   Human-CB1-R
hCB1    AGAACATCCA GTGTGGGGAG AACTTCATGG ACATAGAGTG TTTCATGGTC     301
hCB1b   AGAACATCCA GTGTGGGGAG AACTTCATGG ACATAGAGTG TTTCATGGTC
hCB1a   AGAACATCCA GTGTGGGGAG AACTTCATGG ACATAGAGTG TTTCATGGTC

hCB1    CTGAACCCCA GCCAGCAGCT GGCCATTGCA GTCCTGTCCC TCACGCTGGG     351
hCB1b   CTGAACCCCA GCCAGCAGCT GGCCATTGCA GTCCTGTCCC TCACGCTGGG
hCB1a   CTGAACCCCA GCCAGCAGCT GGCCATTGCA GTCCTGTCCC TCACGCTGGG
                                  TM1
```

Figure 2.1: **Detecting the human CB_1 receptor variants in the human brain using RT-PCR (A)** A schematic diagram of primers used for RT-PCR (indicated by arrows) and the expected length of the PCR products corresponding to hCB_1 (308 bp), hCB_{1b} (209 bp) and hCB_{1a} (141 bp). **(B)** Aligned sequences of the 5' end of hCB_1, hCB_{1b} and hCB_{1a} cDNA. The forward Human-CB_1-F and the reverse Human-CB_1-R primers used to detect hCB_1, hCB_{1a} and hCB_{1b} are underlined. TM1 codes for the first transmembrane region. Dashes represent gaps (Figure was modified from Ryberg *et al.,* 2005

Table 2.1: Primer sequences used in RT-PCR and cloning. Restriction sites are shown in bold.

Primer Name	Orientation	Primer sequence (5' to 3')	References
Human-CB_1-F	Sense	ATGGCCTTGCAGATACCACC	
Human-CB_1-R	Anti-sense	AGTTCTCCCCACACTGGATG	Ryberg *et al*., 2005
Mouse-CB_1-F	Sense	ACGGACTTGGAGACACCACC	
Rat-CB_1-F	Sense	ATGGCCTTGCAGACACCACC	
hCB_{1a}-87-F	Sense	CGAC**GAATTC**ATGGCCTTGCAGATACCACC	
hCB_{1a}-87-R	Anti-sense	PCTTTGATGTCTTCGTACTGAATGTCATTT GAGCC	
hCB_{1a}-1146-F	Sense	PGAGAATGAGGAGAACATCCAGTGTGGGGA GAAC	
hCB_{1a}-1146-R	Anti-sense	TGACAT**GGATCC**CACAGAGCCTCGGCAGAC	Hudson *et al*., 2010
hCB_{1b}-63-F	Sense	CGAC**GAATTC**ATGAAGTCGATCCTAGATGG CC	
hCB_{1b}-63-R	Anti-sense	PCAGGAGGTCAGTGGTGATGGTG	
hCB_{1b}-1254-F	Sense	PGGGAAGTCCCTTCCAAGAGAAG	
hCB_{1b}-1254-R	Anti-sense	TGACAT**GGATCC**CACAGAGCCTCGGCAGAC	Hudson *et al.*, 2010
Myc-hCB_1-F	Sense	CGAC**GAATTC**GCGCCATGGAACAAAAACTT ATTTCTGAAGAAGATCTGAAGTCGATCCTA GATGGCC	
Myc-hCB_1-R	Anti-sense	TGACAT**AAGCTT**ACAGAGCCTCGGCAGACG TGCTG	
HA-hCB_{1a}-F	Sense	CGAC**GAATTC**GCGCCATGTACCCATACGAT GTTCCAGATTACGCTGCCTTGCAGATACCA CCTTCC	
HA-hCB_{1b}-F	Sense	CGAC**GAATTC**GCGCCATGTACCCATACGAT GTTCCAGATTACGCTAAGTCGATCCTAGAT GGCC	

extension at 72°C for 40 s with a final extension at 72°C for 10 m. Products were fractionated on a 2% agarose gel containing 0.5 μg/ml ethidium bromide and visualized with a UV transilluminator and Kodak EDAS 290 docking station. Similar RT-PCR conditions were used to examine the expression and relative abundance of the CB_1 variants and CNS distribution in the *Macaca fascicularis* brain. The RT-PCR analysis was also used to examine whether the two splice variants, CB_{1a} and $CB_{1b,}$ are expressed in the rodent brains. The RT-PCR was conducted using the same conditions described to amplify human CB_1 variants with the exception that the forward primer used was Mouse-CB_1-F or Rat-CB_1-F for mouse and rat samples, respectively (Table 2-1). The reverse primer was Human-CB_1-R primer.

2.3 *Macaca Fascicularis* Tissue Preparation

In order to extract total protein from the brain, the protocol previously described by Miller *et al.,* (2002) was followed. In brief, frozen brain tissue was allowed to thaw slightly on dry ice and sterile razor blades were used to dissect tissues from the brain regions. The tissue pieces were immediately homogenized in 10:1 volume:weight of 4ºC homogenization buffer (25 mM HEPES pH 7.4, 1 mM EDTA, 6 mM $MgCl_2$, 1mM DTT, 1 tablet Complete mini protease inhibitor/10 ml buffer; Roche Canada, Mississauga, ON). Samples were centrifuged at 700 x *g* at 4ºC. Supernatants were collected and the pellets were re-extracted in homogenization buffer. The pellets were then discarded and supernatants were centrifuged at 14,000 x *g* for 30 m at 4ºC. The protein pellets were resuspended in homogenization buffer, quantified using Bio-Rad reagent (Bio-Rad Laboratories, Mississauga, ON), and adjusted to a final concentration of 5 mg/ml in

homogenization buffer. Samples were divided into aliquots and were stored at -80ºC

2.4 Western Blot Analysis

Macaca fascicularis total protein samples (20 µg) were mixed with double the volume Laemmli sample buffer containing 10% ß-mercaptoethanol. The proteins were separated on a 4–20% tris-glycine gel (Bio-Rad) at 90 volts for 20 m, followed by 120 volts for 180 m. The fractionated proteins were transferred to 0.2 mm nitrocellulose at 100 volts for 120 m (Bio-Rad). Membranes were allowed to air-dry overnight before being blocked with 100% Odyssey blocking buffer (Li-Cor Biotechonology, Lincoln, NE) for 3 h at room temperature with shaking. The primary antibody, rabbit anti-CB_1 C-terminus antibody (Caymen Chemical, Ann Arbor, MI) was diluted 1:10000 in the diluted Odyssey blocking buffer (1:10 Odyssey blocking buffer in 1X PBS with 0.1% Tween-20; PBST). Blots were incubated overnight at 4ºC in antibody. Following overnight incubation blots were then washed three times with PBST for 5 m each, and then incubated for 1 h with anti-rabbit IR800CW secondary antibody (Rockland Immunochemical, Gilbertsville, PA) diluted 1:1000. The blots were washed three times with PBST, once with 1X PBS and ddH_2O. The membrane was scanned using an Odyssey infrared imaging system (Li-Cor Biotechnologis) with intensity settings of 5 for 800 nm channel and a focus offset of 0 mm.

2.5 Generating hCB_{1a} and hCB_{1b} Receptors

The hCB_1 receptor splice variants in the coding region, hCB_{1a} and hCB_{1b}, were genetically engineered using a full-length human CB_1 receptor cDNA clone as a template

(kind gift from Tom Bonner, NIH, Bethesda, MD). To generate hCB_{1a} (Fig. 2.2, 2.3), the 5'-end of the coding region of the hCB_{1a} receptor (87 nucleotides) was amplified from hCB_1 by PCR utilizing a high fidelity *Pfu* DNA polymerase (Fermentas) with the forward primer hCB_{1a}-87-F possessing an *EcoR1* restriction site and the reverse primer hCB_{1a}-87-R that was manufactured with a 5'phosphate. The 3'-end of the hCB_{1a} receptor-coding region (1146 bp) was amplified using hCB_{1a}-1146-F and hCB_{1a}-1146-R containing a *BamH1* site. The PCR products were then fractionated on a 2% gel containing ethidium bromide and the bands were extracted using GenElute™ Gel Extraction Kit (Sigma, ON). To generate the complete coding sequence of hCB_{1a} receptor, the two PCR products 87 bp and 1146 bp were blunt-end ligated overnight using T4 DNA ligase. The ligation mixture contained 100 ng of each PCR product, 1 µl ligase 10X buffer and 1 unit T4 DNA ligase in 10 µl reaction (Promega Fisher Scientific Ltd., Ottawa, CA). The ligation products (1233 bp) were amplified using *Taq* polymerase to make the products combatable for TA cloning (Fermentas), forward primer hCB_{1a}-87-F and the reverse primer hCB_{1a}-1148-R were used. The PCR products (1233 bp) were cloned into pGEM®-T vector (Promega), and transformed using One Shot® TOP10 Chemically Competent *E. coli* (Invitrogen). Transformed cells were plated on LB/carbenicillin plates with 30 µl of 20 µg/ml X-gal for a blue/white screen. White colonies were cultured in 2 ml LB broth with 50 µg/ml of carbenicillin. Plasmids were extracted using a GenElute™ Plasma Miniprep Kit (Sigma), and clones containing appropriate inserts were identified by restriction digestion of each individual DNA sample with *EcoR1* and *BamH1* followed by gel electrophoresis. A clone containing appropriate sized insert was subjected to

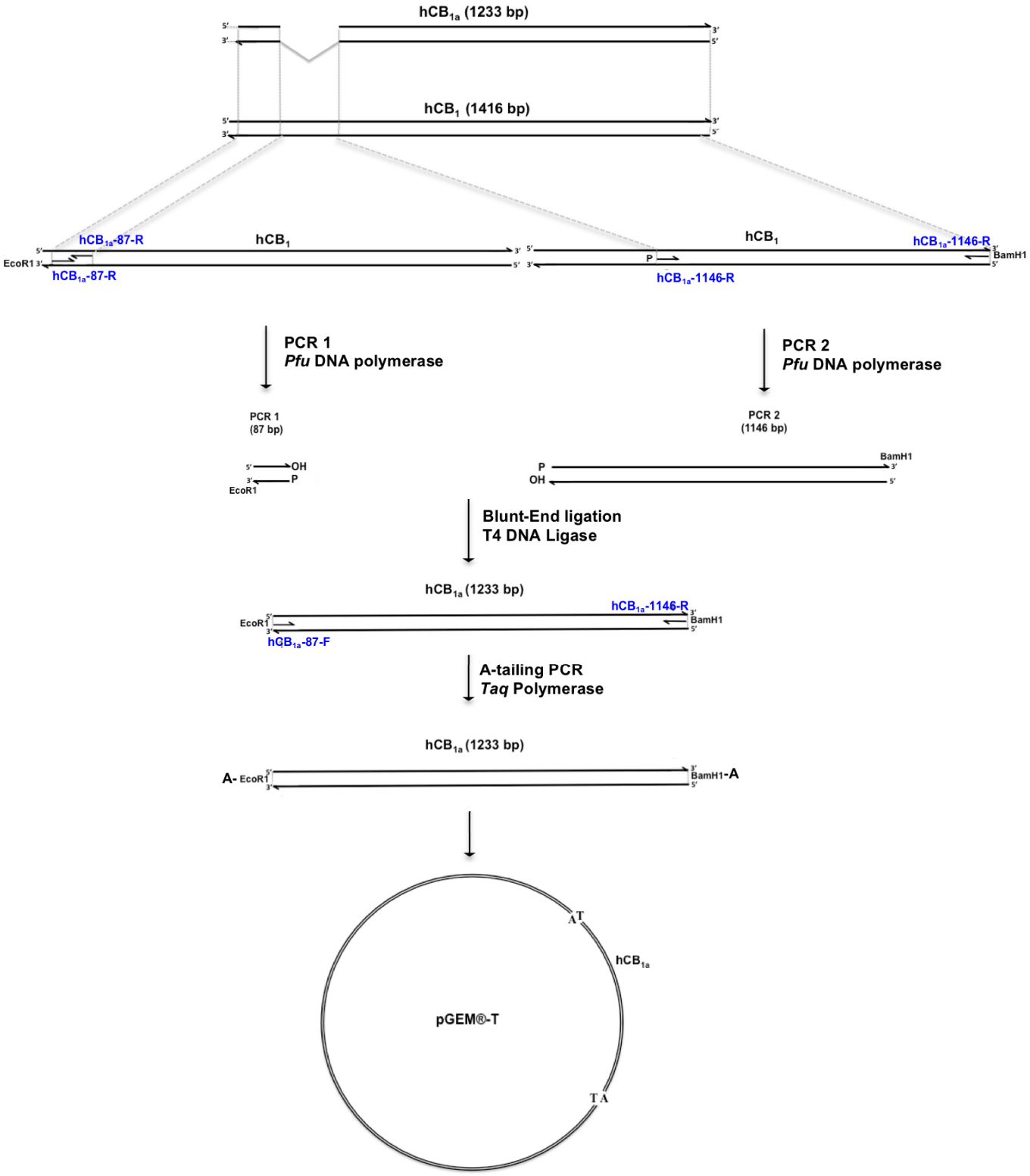

Figure 2.2: A schematic diagram of the cloning strategy of the hCB_{1a} receptor using the hCB_1 as a template. All PCR products have 5' and 3' hydroxyl groups.

hCB$_{1a}$-87-F

```
ATGAAGTCGA TCCTAGATGG CCTTGCAGAT ACCACCTTCC GCACCATCAC       1
```

hCB$_{1a}$-87-R

```
CACTGACCTC CTGTACGTGG GCTCAAATGA CATTCAGTAC GAAGACATCA      51

AAGGTGACAT GGCATCCAAA TTAGGGTACT TCCCACAGAA ATTCCCTTTA     101

ACTTCCTTTA GGGGAAGTCC CTTCCAAGAG AAGATGACTG CGGGAGACAA     151

CCCCCAGCTA GTCCCAGCAG ACCAGGTGAA CATTACAGAA TTTTACAACA     201
```

hCB$_{1a}$-1146-F

```
AGTCTCTCTC GTCCTTCAAG GAGAATGAGG AGAACATCCA GTGTGGGGAG     251

AACTTCATGG ACATAGAGTG TTTCATGGTC CTGAACCCCA GCCAGCAGCT     301

GGCCATTGCA GTCCTGTCCC TCACGCTGGG ACCTTCACGG TCCTGGAGAA     351
CCTCCTGGTG CTGTGCGTCA TCCTCCACTC CCGCAGCCTC CGCTGCAGGC     401
CTTCCTACCA CTTCATCGGC AGCCTGGCGG TGGCAGACCT CCTGGGGAGT     451
GTCATTTTTG TCTACAGCTT CATTGACTTC CACGTGTTCC ACCGCAAAGA     501
TAGCCGCAAC GTGTTTCTGT TCAAACTGGG TGGGGTCACG GCCTCCTTCA     551
CTGCCTCCGT GGGCAGCCTG TTCCTCACAG CCATCGACAG GTACATATCC     601
ATTCACAGGC CCCTGGCCTA TAAGAGGATT GTCACCAGGC CCAAGGCCGT     651
GGTGGCGTTT TGCCTGATGT GGACCATAGC CATTGTGATC GCCGTGCTGC     701
CTCTCCTGGG CTGGAACTGC GAGAAACTGC AATCTGTTTG CTCAGACATT     751
TTCCCACACA TTGATGAAAC CTACCTGATG TTCTGGATCG GGGTCACCAG     801
CGTACTGCTT CTGTTCATCG TGTATGCGTA CATGTATATT CTCTGGAAGG     851
CTCACAGCCA CGCCGTCCGC ATGATTCAGC GTGGCACCCA GAAGAGCATC     901
ATCATCCACA CGTCTGAGGA TGGGAAGGTA CAGGTGACCC GGCCAGACCA     951
AGCCCGCATG GACATTAGGT TAGCCAAGAC CCTGGTCCTG ATCCTGGTGG    1001
TGTTGATCAT CTGCTGGGGC CCTCTGCTTG CAATCATGGT GTATGATGTC    1051
TTTGGGAAGA TGAACAAGCT CATTAAGACG GTGTTTGCAT TCTGCAGTAT    1101
GCTCTGCCTG CTGAACTCCA CCGTGAACCC CATCATCTAT GCTCTGAGGA    1151
GTAAGGACCT GCGACACGCT TTCCGGAGCA TGTTTCCCTC TTGTGAAGGC    1201
ACTGCGCAGC CTCTGGATAA CAGCATGGGG GACTCGGACT GCCTGCACAA    1251
ACACGCAAAC AATGCAGCCA GTGTTCACAG GGCCGCAGAA AGCTGCATCA    1301

AGAGCACGGT CAAGATTGCC AAGGTAACCA TGTCTGTGTC CACAGACACG    1351
```

hCB$_{1a}$-1146-R

```
TCTGCCGAGG CTCTGT                                        1401
```

Figure 2.3: The sequence of hCB$_1$ cDNA and primers sequences used to generate hCB$_{1a}$. Primers are indicated in (Table 2.1).

bidirectional sequencing using M13 forward and reverse universal primers (Genewiz, NJ).

The coding sequence of the hCB_{1b} receptor was generated using a similar cloning strategy and initial template as was described for hCB_{1a} (Fig. 2.4, 2.5). The 5'-end of the coding region of the hCB_{1b} receptor (63 bp) was amplified from the hCB_1 using *Pfu* polymerase and hCB_{1b}-63-F containing an *EcoR1* restriction site, and hCB_{1b}-63-R that was manufactured with a 5'phosphate. The 3'-end of the coding region of the hCB_{1b} (1254 bp) was amplified using the forward primer hCB_{1b}-1254-F and the reverse primer hCB_{1b}-1256-R possessing a *BamH1* site. The two PCR products (63 bp and 1254 bp) were blunt-end ligated, amplified using *Taq* polymerase and cloned into a pGEM®-T vector. The hCB_{1b}-pGEM-T was subjected to bidirectional sequencing using M13 forward and reverse primers (GeneWiz).

2.6 hCB_1, hCB_{1a} and hCB_{1b} Constructs

Both hCB_{1a} and hCB_{1b} receptors were cloned such that either Green Fluorescent protein^2 (GFP^2) or *Renilla* luciferase (Rluc) was expressed as fusion protein at the intracellular carboxy terminus of each receptor. To generate hCB_{1a}-GFP^2 and hCB_{1a}-Rluc, the hCB_{1a} was digested from hCB_{1a}-pGEM-T using *EcoR1* and *BamH1* restriction enzymes. The same restriction enzyme digestions were performed on the pGFP^2-N3 and pRluc-N1 plasmids (PerkinElmer, Waltham, MA). The digested hCB_{1a} and plasmids were run on 1% agarose gel and the bands were extracted using GenElute™ Gel Extraction Kit (Sigma). The hCB_{1a} was inserted into both plasmids using a T4 DNA ligase and the ligated plasmids were then transformed using One Shot® TOP10

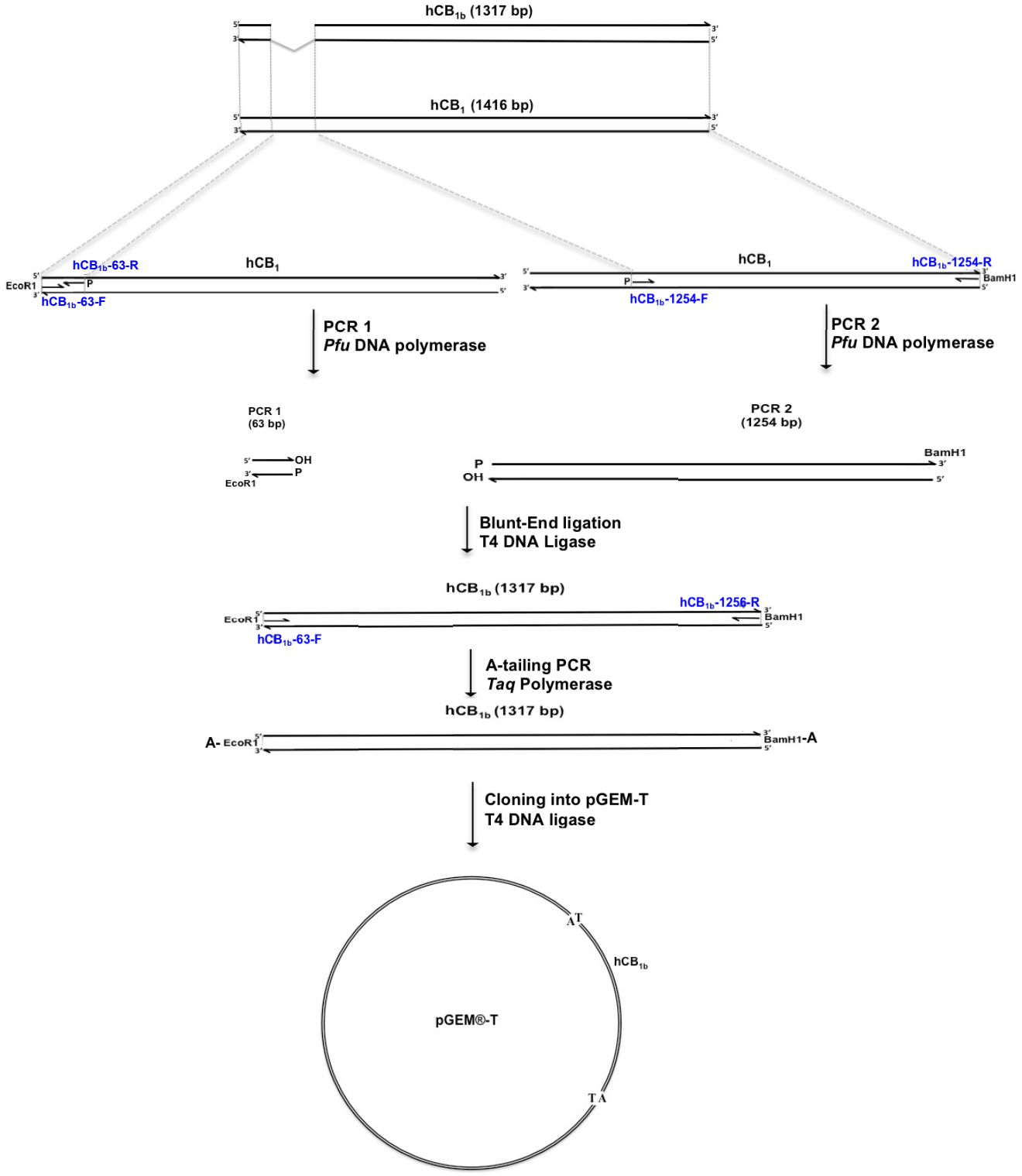

Figure 2.4: A schematic diagram of the cloning strategy of the hCB_{1b} receptor using the hCB_1 as a template. All PCR products have 5' and 3' hydroxyl groups.

hCB$_{1b}$-63-F

```
ATGAAGTCGA TCCTAGATGG CCTTGCAGAT ACCACCTTCC GCACCATCAC       1
```

hCB$_{1b}$-63-R

```
CACTGACCTC CTGTACGTGG GCTCAAATGA CATTCAGTAC GAAGACATCA      51

AAGGTGACAT GGCATCCAAA TTAGGGTACT TCCCACAGAA ATTCCCTTTA     101
```

hCB$_{1b}$-1254-R

```
ACTTCCTTTA GGGGAAGTCC CTTCCAAGAG AAGATGACTG CGGGAGACAA     151

CCCCCAGCTA GTCCCAGCAG ACCAGGTGAA CATTACAGAA TTTTACAACA     201
AGTCTCTCTC GTCCTTCAAG GAGAATGAGG AGAACATCCA GTGTGGGGAG     251
AACTTCATGG ACATAGAGTG TTTCATGGTC CTGAACCCCA GCCAGCAGCT     301
GGCCATTGCA GTCCTGTCCC TCACGCTGGG ACCTTCACGG TCCTGGAGAA     351
CCTCCTGGTG CTGTGCGTCA TCCTCCACTC CCGCAGCCTC CGCTGCAGGC     401
CTTCCTACCA CTTCATCGGC AGCCTGGCGG TGGCAGACCT CCTGGGGAGT     451
GTCATTTTTG TCTACAGCTT CATTGACTTC CACGTGTTCC ACCGCAAAGA     501
TAGCCGCAAC GTGTTTCTGT TCAAACTGGG TGGGGTCACG GCCTCCTTCA     551
CTGCCTCCGT GGGCAGCCTG TTCCTCACAG CCATCGACAG GTACATATCC     601
ATTCACAGGC CCCTGGCCTA TAAGAGGATT GTCACCAGGC CCAAGGCCGT     651
GGTGGCGTTT TGCCTGATGT GGACCATAGC CATTGTGATC GCCGTGCTGC     701
CTCTCCTGGG CTGGAACTGC GAGAAACTGC AATCTGTTTG CTCAGACATT     751
TTCCCACACA TTGATGAAAC CTACCTGATG TTCTGGATCG GGGTCACCAG     801
CGTACTGCTT CTGTTCATCG TGTATGCGTA CATGTATATT CTCTGGAAGG     851
CTCACAGCCA CGCCGTCCGC ATGATTCAGC GTGGCACCCA GAAGAGCATC     901
ATCATCCACA CGTCTGAGGA TGGGAAGGTA CAGGTGACCC GGCCAGACCA     951
AGCCCGCATG GACATTAGGT TAGCCAAGAC CCTGGTCCTG ATCCTGGTGG    1001
TGTTGATCAT CTGCTGGGGC CCTCTGCTTG CAATCATGGT GTATGATGTC    1051
TTTGGGAAGA TGAACAAGCT CATTAAGACG GTGTTTGCAT TCTGCAGTAT    1101
GCTCTGCCTG CTGAACTCCA CCGTGAACCC CATCATCTAT GCTCTGAGGA    1151
GTAAGGACCT GCGACACGCT TTCCGGAGCA TGTTTCCCTC TTGTGAAGGC    1201
ACTGCGCAGC CTCTGGATAA CAGCATGGGG GACTCGGACT GCCTGCACAA    1251
ACACGCAAAC AATGCAGCCA GTGTTCACAG GGCCGCAGAA AGCTGCATCA    1301

AGAGCACGGT CAAGATTGCC AAGGTAACCA TGTCTGTGTC CACAGACACG    1351
```

hCB$_{1b}$-1254-R

```
TCTGCCGAGG CTCTGTGA                                      1401
```

Figure 2.5: The sequence of hCB$_1$ cDNA and primers sequences used to generate hCB$_{1b}$. Primers are indicated in (Table 2.1).

chemically Competent *E. coli* (Invitrogen). Positive colonies were selected on an agar plate containing either Zeocin (25 μg/ml) or kanamycin (25 μg/ml) for GFP^2 –N3 and Rluc-N1 constructs, respectively. Similarly, hCB_{1b} receptor was cloned into $pGFP^2$-N3 and pRluc-N1 plasmids, using *EcoR1* and *BamH1* sites, to generate hCB_{1b}-GFP^2 and hCB_{1b}-Rluc constructs. The hCB_1 receptor had been previously cloned with GFP^2 and Rluc tags in the laboratory by Brian Hudson (Hudson *et al*., 2010). The carboxy-terminus fusion GFP^2 of the human ether-a-go-go-related gene construct (HERG-GFP^2) was provided by Dr. Terry Herbert and was previously described (Dupré *et al*., 2007). The carboxy-terminus construct of the human metabotropic glutamate receptor type 6 (mGluR6-GFP^2) was provided by Dr.Robert Duvoisin of the Oregan Health and Science University, Portland, OR.

The hCB_1 receptor was tagged with the Myc-tag at the N-terminus of the receptor (Myc-hCB_1) using PCR. Myc-hCB_1-F and Myc-hCB_1-R were used in PCR reaction containing hCB_1 cDNA as a template. The PCR products were digested with *EcoR1* and *HindIII* before being ligated into pcDNA3.1/Zeo(-) (Invitrogen). Following transformation, positive colonies were selected on agar plates containing 50 μg/ml carbenicillin. The hCB_1 splice variants, hCB_{1a} and hCB_{1b}, were tagged with the influenza hemagglutinin tag (HA tag) at their N-terminal extremities. HA-hCB_{1a} and HA-hCB_{1b} constructs were generated in the same manner as the Myc-hCB_1 construct, with the exception of using the forward primer HA-hCB_{1a}-F or HA-hCB_{1b}-F for HA-hCB_{1a} and HA-hCB_{1b}, respectively. All of the generated constructs were sequenced to confirm the correct reading frame and insert sequence (Genewize, NJ).

2.7 Cell Culture

All the experiments were performed using human embryonic kidney HEK 293A cells (HEK 293A) a kind gift from Dr. Denis J. Dupré, Dalhousie University, Canada. Cells were maintained in high glucose Dulbecco's Modified Eagle Medium (DMEM; Invitrogen) supplied with 10% Fetal Bovine Serum (FBS), 100 U/ml penicillin and 100 µg/ml streptomycin. Cells were cultured in cell culture treated flasks (BD) at 37ºC and 5% CO_2. At confluency, cells were subcultured at a 1:10 ratio. All experiments were carried out using cells between passages 3-15.

2.8 Transfection

HEK 293A cells were transfected using Lipofectamine 2000 reagent (Invitrogen) following the manufacturer's protocol. For BRET experiments, HEK 293A cells were plated on a 6-well plate (10 cm^2/ml) with DMEM and 10% FBS for 24-48 h, until cells reached 90% confluence. Each well of the 6-well plate received 4 µg of the required plasmids diluted in 250 µl Opti-MEM® Reduced-Serum Medium (Invitrogen; the total amount of DNA/well was kept constant by using pcDNA3.1+ empty vector as required), and mixed with 250 ul Opti-MEM® Reduced-Serum Medium containing 10 µl of Lipofectamine® 2000 reagent. The solution was then incubated at room temperature for 20 m before being added to one well of the 6-well plate containing fresh DMEM media without serum. Cells were cultured at 37°C and 5% CO_2 for 48 h. The same method was used to transfect HEK 293A cells used for confocal microscopy using 24 well plates, and for In- and On-cell western® analysis using poly-D-lysine-coated 96 well plates (Nunc, Rochester, NY).

2.9 Bioluminescence Resonance Energy Transfer 2 ($BRET^2$)

$BRET^2$ was used to study the physical interaction between the hCB_1 receptor and hCB_{1a} and hCB_{1b} splice variants. In $BRET^2$, Renilla luciferase (Rluc) is used as the donor protein, while green-fluorescent protein 2 (GFP^2) is used as the acceptor protein (Fig. 2.6). $BRET^2$ utilizes a unique Rluc substrate, coelenterazine 400 a, that emits light between 290-400 nm. If the Rluc molecule is in sufficiently close proximity (approximately 50-100 Å) to the GFP^2 molecule, then there will be a non-radiative resonance energy transfer to the GFP^2, which in turn will lead to its subsequent fluorescent emission at 505-508 nm. The efficiency of this energy transfer is dependent upon a number of factors including the relative distance between the donor and acceptor molecules, estimated to be less than 100 Å, and their relative orientation (Pfleger and Eidne, 2005).

To carry out $BRET^2$ experiments, HEK 293A cells were plated in a 6-well plate and transfected with the required constructs. Forty-eight h post-transfection, the $BRET^2$ experiment was conducted. Cells were washed twice with cold 1X PBS before being suspended in 90 µl of PBS supplemented with glucose (1 mg/ml), benzamidine (10 mg/ml), leupeptin (5 mg/ml) and a trypsin inhibitor (5 mg/ml). Cells were dispensed into a white 96 well plate (PerkinElmer). Following the addition of 10 µl of 50 µM coelenterazine 400a substrate (Biotium, Hayward, CA, USA) emissions of Rluc and GFP^2 were measured at 405 nm and 510 nm using Luminoskan Ascent plate reader (Thermo Scientific, Waltham, MA), with the integration time set to 10 s and the photomultiplier tube voltage set to 1200 volts. The ratio of 510/405 nm was converted to

A

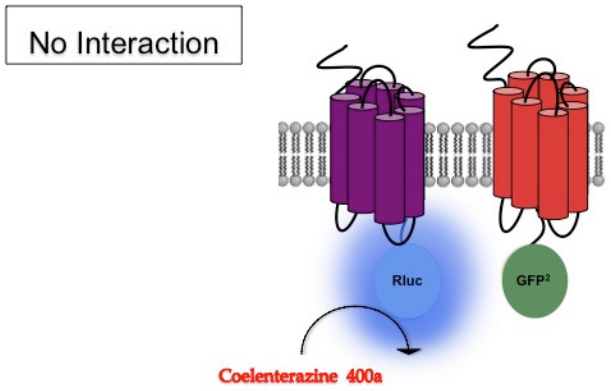

B

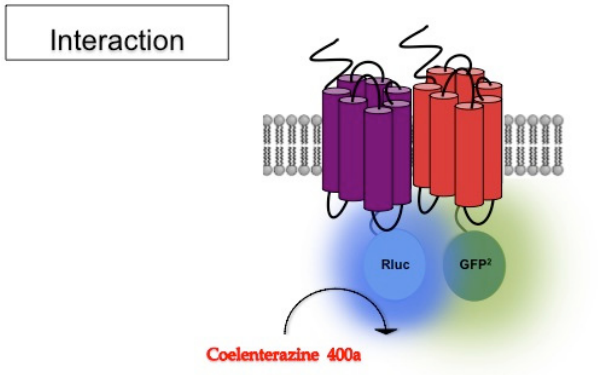

Figure 2.6: Bioluminescence Resonance Energy Transfer 2 (BRET^2). GPCRs are tagged at their carboxy-termini with either Rluc or GFP2. **(A)** GPCRs are not interacting. Thus, on the addition of the Rluc substrate, coelenterazine 400a, blue light is emitted by Rluc, but no energy is transferred to GFP^2, and therefore no green light is emitted. **(B)** GPCRs are interacting. As a result of this, on the addition of coelenterazine 400a blue light is still emitted by Rluc, but since GFP^2 is now in close enough proximity to Rluc, resonance energy transfer to GFP^2 occurs, resulting in the emission of green light (Figure was modified from Pfleger and Eidne, 2005).

BRET efficiency ($BRET_{Eff}$) by first determining the 510/405 ratio of each sample, subtracting the minimum 510/405 nm emission obtained from cells expressing only a Rluc-N1 construct, then divided by the maximum measurable 510/405 nm ratio obtained from cells expressing a GFP^2-Rluc fusion construct (PerkinElmer).

The most common problem with using BRET experiments is that because the receptor constructs are heterologously expressed, there is the possibility that an observed BRET signal may be the result of random collisions of the over-expressed receptors within the cell membrane (Pfleger and Eidne, 2005). This problem has been resolved by several modifications to the BRET assay, specifically the use of BRET saturation and competition assays, both of them help demonstrate the specificity of the interaction being measured by BRET (Pfleger and Eidne, 2005).

In BRET saturation experiments cells were transfected with fixed amounts of the BRET donor (Rluc-tagged receptor), together with increasing amounts of BRET acceptor (GFP^2- tagged receptor). $BRET_{Eff}$ values were then plotted against the ratio of GFP^2 to Rluc concentration. The resulting data was then fit to a rectangular hyperbola curve. If the interaction is specific this should result in a hyperbolic increase in BRET signal to a maximum value, or $BRET_{Max}$, while non-specific interactions will only result in a gradual linear increase. An added benefit to the BRET saturation approach is that by comparing the amount of receptor required to achieve 50% of the maximum BRET signal, the $BRET_{50}$, a rough estimate for the affinity of the interaction can be inferred. B_{Max} and K_d determinations were taken as the $BRET_{Max}$ and $BRET_{50}$, respectively (Pfleger and Eidne, 2005).

BRET competition experiments have also been used to demonstrate the specificity of an interaction between the donor and the acceptor. In these experiments, cells were transfected with constant amount of both donor (Rluc-tagged receptor), and BRET acceptor (GFP^2- tagged receptor) and increasing amounts of one of the interacting receptors untagged with either donor or acceptor is expressed. The untagged receptor should compete with the acceptor-tagged construct for the available donor-tagged constructs, thus reducing the BRET signal.

In BRET experiments examining the effect of CB_1 ligands on $BRET_{Eff}$ signal, HEK 293A cells were plated in 6 well-plate 24 h before being transfected with the required constructs. Forty-eight h later, the cells were collected from each well, washed and resuspended in 300 µl BRET buffer. The 300 µl of the resuspended cells were dispensed into four wells of a 96 well plate. Cells were treated with 10 µl of either vehicle, WIN 55,212-2 (agonist), AM-251 (inverse agonist) or O-2050 (neutral antagonist) to reach final concentrations of 10 µM for 30 m (Tocris Bioscience, Ellisville, MO). BRET signals were measured at 510 and 405 nm immediately after the addition of 10 µl of a 50 µM Coelenterazine 400a substrate.

2.10 Confocal Microscopy and Immunofluorescence

HEK 293A cells were plated onto glass cover slips in a 24-well plate. At 50% confluence, cells were transfected with HA and/or GFP^2 tagged receptors using Lipofectamine 2000 reagent. Forty-eight h post-transfection, culture media was removed and cells were fixed with ice-cold 100% ethanol for 5 m. After washing the cells three times with 1X PBS, cells were blocked with 1% bovine serum albumin (BSA) for 60 m at

room temperature. Cells expressing HA-tagged receptors were incubated with 1:1000 primary monoclonal mouse anti-HA antibody overnight at 4°C (Covance, Emeryville, CA). The next day, the cells were washed three times with 1X PBS and incubated with a Cy^3-conjugated anti-mouse immunoglobulin G (IgG) secondary antibody, 1:500 (Jackson Immuno Research Laboratories Inc., West Grove, PA) for 1 h at room temperature, then washed 3 times with 1X PBS and once with ddH_2O. Finally, cover slips were mounted on microscopic slides (Fisher Scientific) using Fluorsave reagent® (Calbiochem, San Diego, CA). Images of cells were acquired with a Nikon Eclipse E800 microscope attached to the D-Eclapse C1 confocal system (Nikon Canada Inc., Mississauga, ON). Cy^3 was imaged by a 543 nm Helium-Neon laser (JDS Uniphase, Milpitas, CA), while GFP^2 was imaged using a 488 nm air-cooled argon laser (Spectra-Physics Lasers Inc., Mountain View, CA). Images were taken using a 100X oil immersion objective.

2.11 In-Cell Western™ Analysis

In-cell western analysis was used to measure phosphorylation of the extracellular kinase 1 and 2 (ERK). HEK 293A cells were plated in poly-D-lysine coated 96 well plates and cultured for 24-48 h or until confluency. Culture media was then removed and replaced with serum free DMEM and transfected with 200 ng of the required constructs. Twenty-four h later, cells were treated with vehicle (0.05% DMSO) or 1 μM WIN 55,212-2 in 0.05% DMSO for 5 m. HEK 293A cells were fixed for 20 m at room temperature with 4% paraformaldehyde (PFA) in 0.1 M $NaPO_4$ buffer pH 7.4. Cells were washed three times with PBS, permeabilized with 0.1% Triton X-100 in PBS for 1 h at room temperature and then washed again three times with PBS. Cells were blocked using

1% BSA in PBST for 90 m at room temperature. Cells were then incubated overnight at 4°C with rabbit anti phospho-ERK antibody (Tyr 204; Santa Cruz Biotechnology Inc., Santa Cruz, CA), diluted 1:200 in the blocking buffer. After washing the cells three times with PBST, the cells were incubated for 1 h with the IR800CW conjugated anti-rabbit IgG secondary antibody, diluted 1:500 in the blocking buffer (Rockland Immunochemical). Plates were washed three times with PBST, and incubated with goat anti-total ERK2 primary antibody (c-14,; Santa Cruz Biotechnology) for 1 h, diluted 1:200 in PBST containing 1% BSA. After washing three times with PBST, cells were incubated for 1 h with Alexa Fluor 680 anti-goat secondary antibody diluted 1:800 (Invitrogen), washed three times with PBST, three times with PBS and once with ddH_2O before being allowed to air-dry. Plates were scanned using the Odyssey infrared imaging system (Li-Cor Biotechnology), with intensity settings of 5 for both 700 nm and 800 nm channel and a focus offset of 5 mm.

To obtain relative pERK, the background fluorescence was determined from wells receiving only the secondary antibodies and the background was then subtracted from the pERK and total ERK2 signals. The ratio of the background-subtracted pERK/total ERK2 signals was then determined for each well and normalized to the ratios obtained from the wells treated with vehicle (0.05% DMSO).

2.12 On- Cell Western™ Analysis

To measure cell surface expression of Myc-hCB_1, HA-hCB_{1a} and HA-$hCB_{1b,}$ on-cell western analysis was used. The protocol described previously by Miller *et al*. (2004) was followed. HEK 293A cells were plated on poly-D-lysine-coated 96 well plates and

cultured for 24 h to confluence. Twenty-four h post-transfection, the cells were fixed with 4% paraformaldehyde for 1 h at room temperature and washed three times with PBS. Cells were blocked using 1% BSA in PBS for 90 m at room temperature. Wells expressing HA-tagged receptors were incubated with 1:1000 primary monoclonal mouse anti-HA antibody (Covance), while wells expressing Myc-tagged receptors received 1:1000 primary rabbit anti-Myc antibody (Abcam, Cambridge, MA) overnight at 4°C. The following day, cells were washed three times with PBS, before being incubated with an anti-rabbit IR800CW conjugated secondary antibody (Rockland Immunochemicals) diluted 1:800 in 1% BSA in PBS. Cells were washed three times with PBS, then incubated with an Alexa Flour 680 conjugated anti-mouse IgG secondary antibody (Invitrogen) diluted 1:500 with 1% BSA in PBS. Finally, cells were washed 5 times in PBS and once with ddH_2O. The plates were allowed to air-dry and scanned using an Odyssey infrared imaging system (Li-Cor Biotechnology) with intensity settings of 5 for both the 700 and 800 nm channels and a focus offset of 3 mm.

After imaging the cell surface expression of the receptors using the Odyssey, the same wells were used to determine the total receptor expression. The cells were permeabilized using 0.1% Triton X-100 in PBS for 1 h at room temperature and washed three times with PBS. Cells were then exposed to primary anti-HA and/or anti-Myc antibodies, secondary antibodies and scanned following the same protocol described for on cell-western. To obtain the percent of basal surface expression, the background fluorescence was determined from wells receiving only the secondary antibodies and the background was then subtracted from the surface and total receptor expression signals.

The ratio of the background-subtracted surface/total signals was then determined for each well.

2.13 Statistics

Statistical analysis was performed using Graphpad Prism v.4 (GraphPad Software Inc. San Diego, CA). All data are reported as mean ± standard error of the mean (SEM). One-way and two-way ANOVA with the statistical significance set at $P < 0.05$ were performed. Tukey's post-hoc test was applied.

Chapter 3: Results

3.1 CB_1, CB_{1a} and CB_{1b} mRNAs were Distributed Throughout Human and Monkey Brains

The first aim of this study was to determine the relative abundance and CNS distribution of the hCB_1 variants in the human brain. RT-PCR was carried out using a primer set capable of amplifying the three hCB_1 variants with products of 308, 141 and 209 bp corresponding to hCB_1, hCB_{1a} and hCB_{1b}, respectively. Five regions of the human brain were examined, including total brain, frontal cortex, parietal cortex, cerebellum and caudate/putamen. After 30 cycles, PCR products were subjected to electrophoresis on a 2% agarose gel (Fig. 3.1). Three amplicons were detected of the expected sizes for hCB_1, hCB_{1a} and hCB_{1b} in each cDNA sample derived from different regions of the human brain. All of the PCR products were extracted from the agarose gel and sequenced to confirm their identities (GeneWiz).

Several hCB_1 variant-specific primer pairs were designed and tested by PCR reaction using plasmid DNA templates containing the full sequence of each variant. None of the tested primer sets specifically amplified the individual variants despite several attempts to optimize annealing temperature, buffer conditions and cycling parameters. For this reason we were unable to perform quantitative PCR (qPCR) analysis. We did attempt to examine the relative abundance of variants after different numbers of PCR amplification cycles. However, the relative abundance of the three receptors did not differ irrespective of different numbers of PCR amplification (results not shown). Our results showed that hCB_1, hCB_{1a} and hCB_{1b} mRNAs are distributed throughout the regions of the human

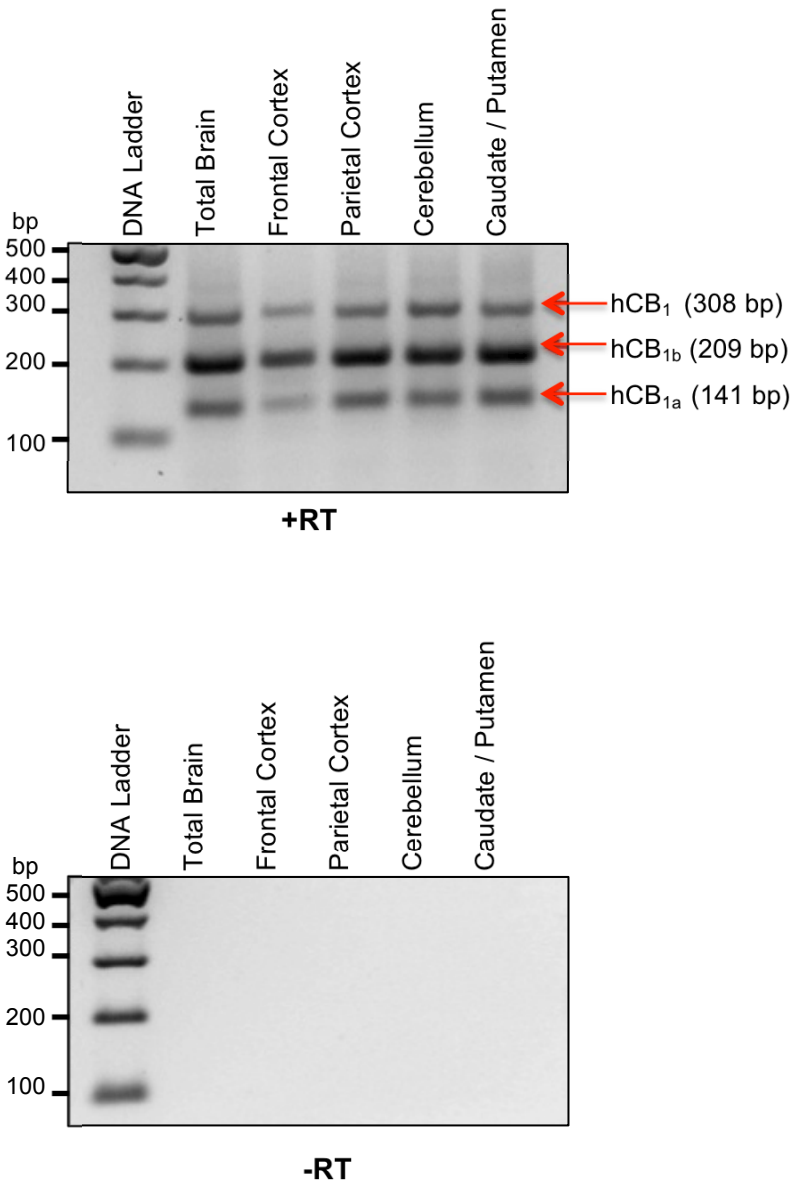

Figure 3.1: The hCB_1, hCB_{1a} and hCB_{1b} mRNAs are distributed throughout the human brain. PCR products obtained using a primer set that amplifies the three-hCB_1 variants. PCR products were fractionated on 2% agarose gel containing ethidium bromide and visualized under UV light.

brain tested and can easily be detected via RT-PCR.

Next, we wanted to determine if CB_{1a} and CB_{1b} mRNAs are expressed in the brain of different species. To examine whether the CB_1 splice variants are expressed in rodent brains, RT-PCR was performed on RNA extracted from various tissues of adult mouse and rat brains using species-specific primers. We employed multiple primer sets, PCR conditions and buffer compositions to attempt to amplify the CB_1 splice variants in the rat and mouse brains. Other than CB_1, we could not detect the variants CB_{1a} and CB_{1b} in rodent cDNA (data not shown).

We tested if the two splice variants, CB_{1a} and $CB_{1b,}$ were expressed in the brain of a non-human primate (*Macaca fascicularis)*. First, RT-PCR was conducted on RNA extracted from different brain regions of the *Macaca fascicularis* using similar primers and reaction conditions to those used to amplify human CB_1 variants using human brain RNA. Three bands were detected at the expected sizes for CB_1, CB_{1a} and CB_{1b} (Fig. 3.2). PCR products were extracted from the agarose gel and sequenced to confirm their identities (GeneWiz). Our results showed that the monkey brain expresses CB_1, CB_{1a} and CB_{1b}.

3.2 CB_1, CB_{1a} and CB_{1b} Proteins were Expressed in the Monkey Brain

It still remains unclear whether the hCB_1 splice variants mRNAs are translated into proteins *in vivo*. In addition, GPCR mRNA and protein levels do not necessarily correlate (Markovic and Challiss, 2009). Therefore, it was important not only to demonstrate the presence of the transcript of each isoform, but also to determine the relative protein level

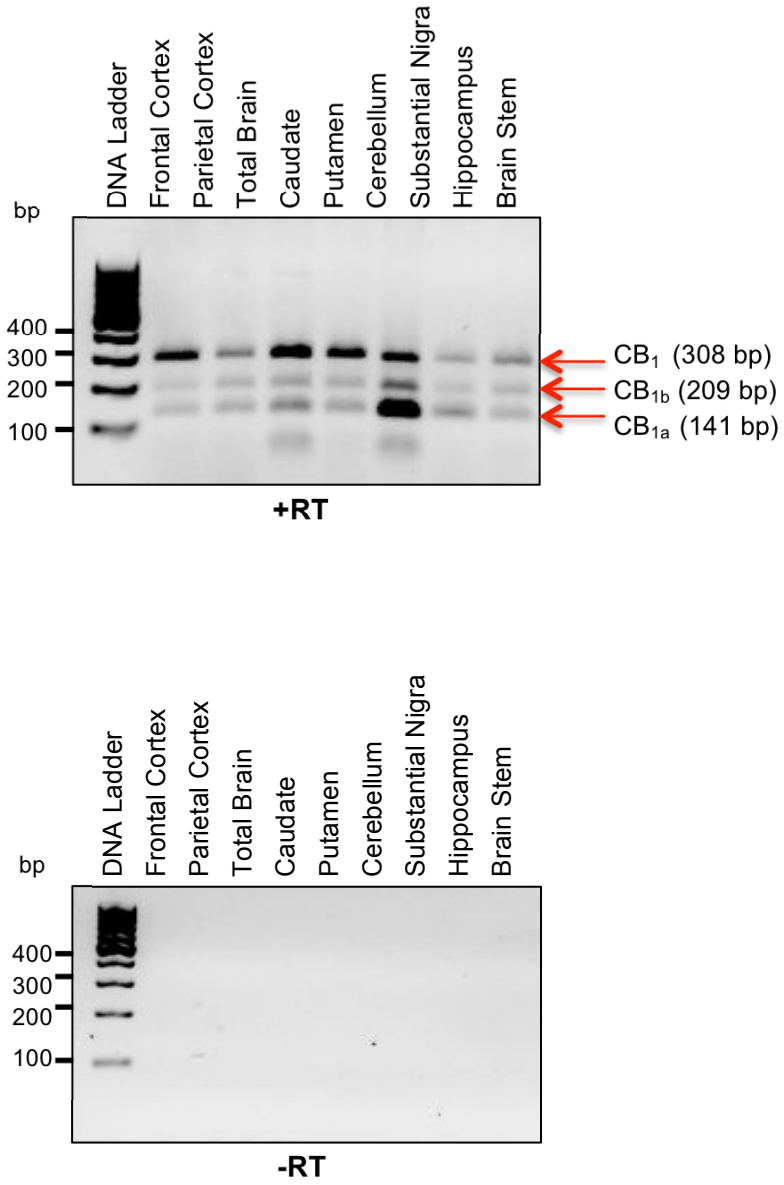

Figure 3.2: The CB_1, CB_{1a} and CB_{1b} mRNAs are distributed throughout the *Macaca Fascicularis* brain. PCR products using a primer set that amplify the three-hCB_1 variants. PCR products were fractionated on 2% agarose gel containing ethidium bromide and visualized under UV light. Upper panel represents positive reverse transcriptase (+RT) reaction, while lower panel represent negative reverse transcriptase (-RT) reaction.

in different brain regions. Since we showed that rodents don't express the CB_1 variants, and we were unable to obtain fresh or frozen human brain tissue for appropriate analysis, we chose to determine the expression levels of CB_1 variants in different brain regions of the monkey (*Macaca fascicularis)* brain. Human and monkey CB_1 receptors exhibit 100% sequence identity at the amino acid level over the complete protein (NCBI). A variety of cortical and subcortical structures from the monkey (*Macaca fascicularis*) brain were dissected and analyzed for CB_1 by western blotting. The antibody used was raised against the C-terminal (amino acids 461-472) intracellular sequences common to all three hCB_1 receptor variants (Cayman Chemical, Ann Arbor, MI). Western blot analysis of homogenates from different regions of the monkey brain revealed a prominent immunoreactive band with a molecular mass of ≈53 kDa, which is consistent with the predicted band size for human CB_1. In addition, two less abundant bands at approximately ≈49 kDa and ≈46 kDa were detected, which is the predicted size for CB_{1b} and CB_{1a}, respectively (Fig. 3.3A). The antibody detected the three different molecular weight bands in all tested brain regions. There were only slight differences in the band intensity across different brain regions. These bands were not detected when the C-terminal antibody was pre-incubated with the blocking peptide (Fig. 3.3C), or when the secondary antibody was applied alone without the primary antibody (Fig. 3.3D). We did not have enough numbers of animals to quantify the relative amounts of each variant in different brain regions. However, we can conclude that the monkey brain expressed proteins with the expected molecular weights of CB_1, CB_{1a} and CB_{1b} receptors. Although, CB_1 receptor appeared to be most abundant; the other variants were present in approachable quantities.

Figure 3.3: The CB_1, CB_{1a} and CB_{1b} proteins are distributed throughout the *Macaca fascicularis* brain. Western blot of proteins extracted from different regions of monkey brain using CB_1 antibody directed against the C-terminal tail (A) and housekeeping gene β-III tubulin **(B)**. Bands were detected at the expected molecular weight for CB_1 (53kDa) CB_{1a} (46 kDa), CB_{1b} (49 kDa) and β-III tubulin (55 kDa). No bands were detected when the antibody was pre-incubated with a blocking peptide (1:10 dilution) **(C)** or when the membrane was incubated with the secondary antibody alone **(D)**.

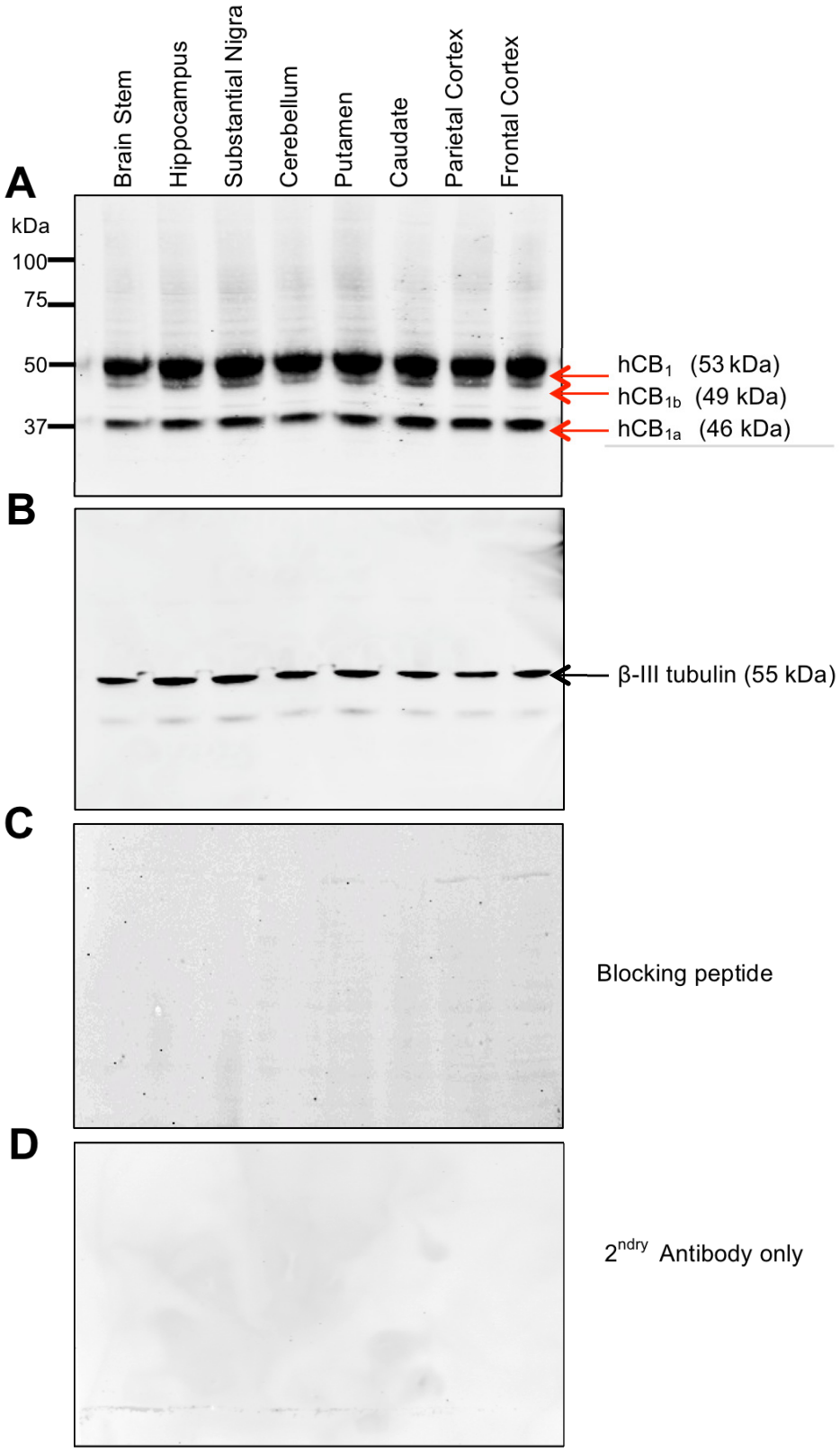
A
Brain Stem
Hippocampus
Substantial Nigra
Cerebellum
Putamen
Caudate
Parietal Cortex
Frontal Cortex
kDa
100
75
50
37
hCB1 (53 kDa)
hCB1b (49 kDa)
hCB1a (46 kDa)
B
β-III tubulin (55 kDa)
C
Blocking peptide
D
2ndry Antibody only

3.3 Dimerization of hCB_1 Receptor and its Splice Variants

3.3.1 Homodimerization of hCB_1 Receptor Splice Variants

$BRET^2$ was used to determine whether hCB_1 splice variants could form homodimers in HEK 293A cells. Cells were co-transfected with hCB_{1a}-Rluc and hCB_{1a}-GFP^2, or with two two-membrane proteins that do not interact with hCB_1, HERG-GFP^2, a membrane localized K^+ channel, or mGluR6-GFP^2 (Hudson *et al*., 2010). Forty-eight hours later, BRET efficiency ($BRET_{Eff}$) was measured. The combination of hCB_{1a}-Rluc and hCB_{1a}-GFP^2 resulted in an increased $BRET_{Eff}$ compared with the $BRET_{Eff}$ observed when hCB_{1a}-Rluc was co-transfected with mGluR6-GFP^2 or HERG-GFP^2 ($P < 0.001$; Fig. 3.4A). A BRET saturation curve was generated to demonstrate the ability of hCB_{1a} to form homodimers at constant donor expression levels and increasing acceptor expression levels. For the BRET saturation curve, cells were co-transfected with a constant amount of hCB_1-Rluc with increasing amounts of hCB_{1a}-GFP^2 or HERG-GFP^2. The combination of hCB_{1a}-Rluc with hCB_{1a}-GFP^2 resulted in a significantly different saturation curve ($P < 0.001$) than the control curve, which was generated with a combination of hCB_{1a}-Rluc with HERG-GFP^2 (Fig. 3.4B). The hCB_{1a} homodimer saturation curve resulted in a $BRET_{Max}$ of 0.32 ± 0.02 and a $BRET_{50}$ of 0.39 ± 0.043.

Similar experiments were also carried out to demonstrate the ability of hCB_{1b} to form homodimers in HEK 293A cells. A significantly higher $BRET_{Eff}$ resulted ($P < 0.001$) when hCB_{1b}-Rluc and hCB_{1b}-GFP^2 constructs were co-expressed, compared to the two controls (Fig. 3.5A). The hCB_{1b} homodimer saturation curve resulted in a $BRET_{Max}$ of 0.31 ± 0.016 ($P < 0.001$), and $BRET_{50}$ of 0.40 ± 0.048 ($P < 0.001$) (Fig. 3.5B).

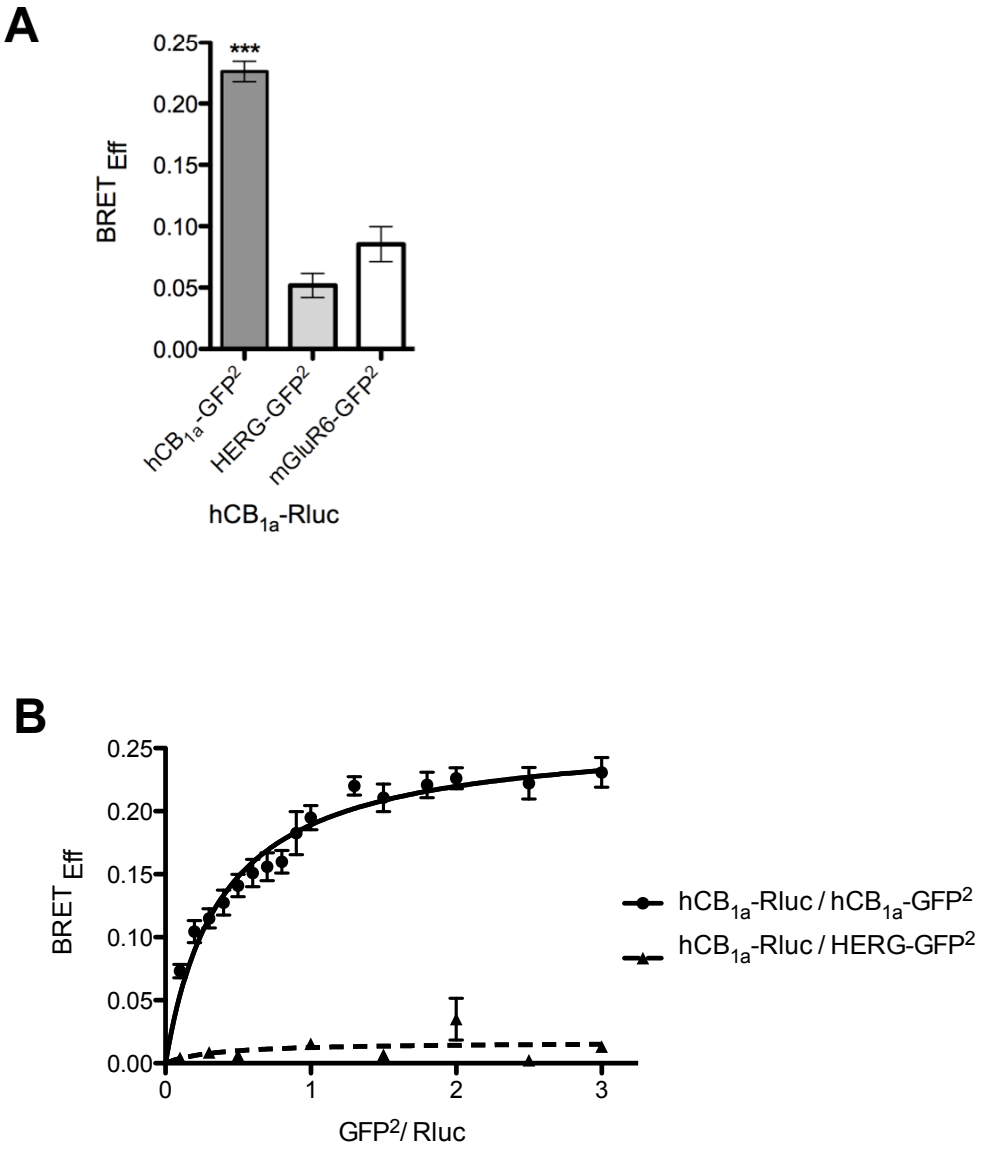

Fig. 3.4: The hCB_{1a} receptor forms homodimers in HEK 293A cells. **(A)** The co-expression of hCB_{1a}-Rluc and hCB_{1a}-GFP^2 in HEK 293A cells resulted in a higher $BRET_{Eff}$ value, compared to when hCB_{1a}-Rluc was co-expressed with either HERG-GFP^2 or mGluR6-GFP^2 controls. **(B)** BRET saturation curve obtained from cells transiently transfected with hCB_{1a}-Rluc/hCB_{1a}-GFP^2 was higher than the curve of hCB_{1a}-Rluc/HERG-GFP^2. Data are presented as mean ± SEM of three independent experiments, n=6-8. Statistical significance was determined by using one-way ANOVA, followed by Tukey's post hoc test. *** $P < 0.001$ compared to controls.

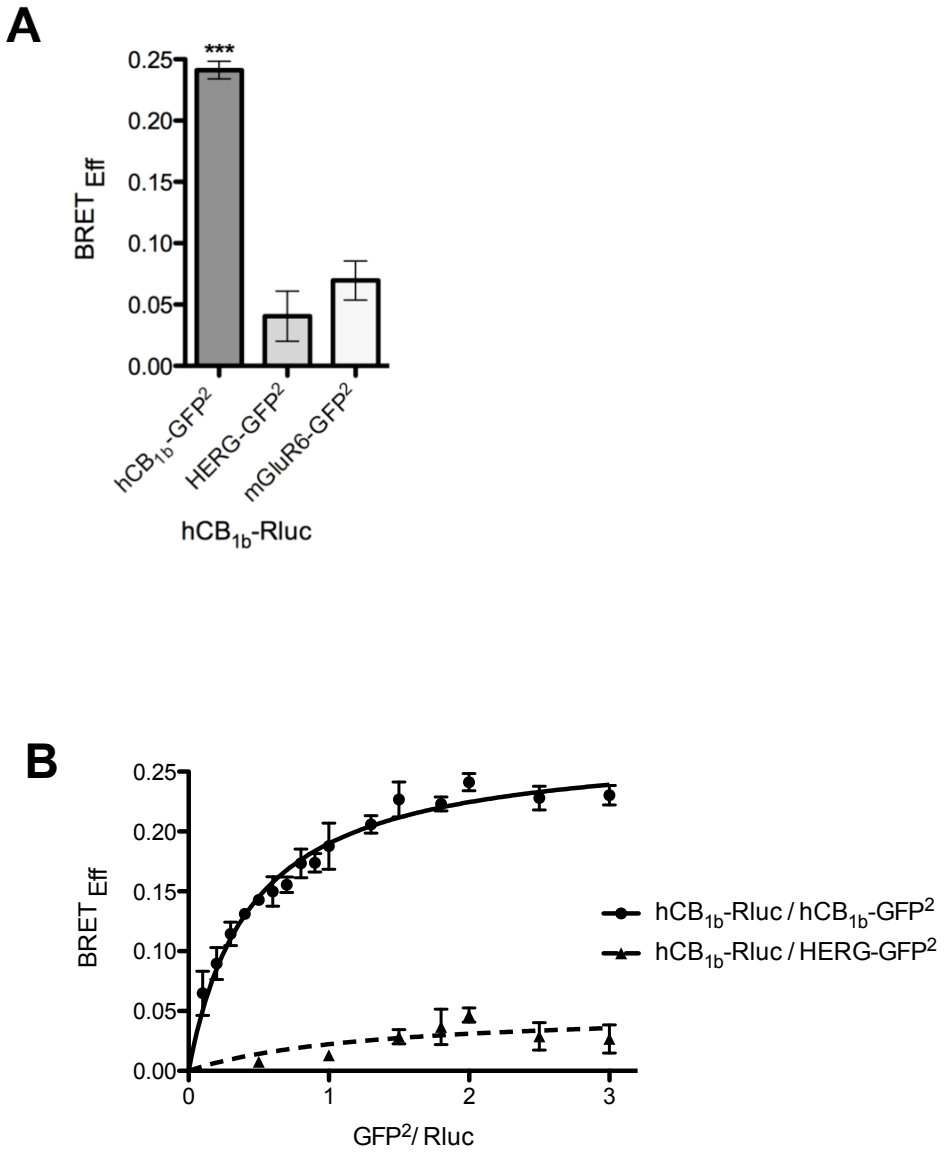

Figure 3.5: The hCB_{1b} receptor forms homodimers in HEK 293A cells. (A) The co-expression of hCB_{1b}-Rluc and hCB_{1b}-GFP^2 in HEK cells resulted in a higher $BRET_{Eff}$ value, compared when hCB_{1b} was co-expressed with either HERG-GFP^2 or mGluR6-GFP^2 controls. **(B)** The BRET saturation curve obtained from cells transiently transfected with hCB_{1b}-Rluc/hCB_{1b}-GFP^2 increases exponentially and had $BRET^{Eff}$ higher than the hCB_{1b}-Rluc/HERG-GFP^2, which showed a linear change curve over full range. Data are presented as mean ± SEM of three independent experiments, n=6-8. Statistical significance was determined by using one-way ANOVA, followed by Tukey's post hoc test. *** $P < 0.001$ compared to controls.

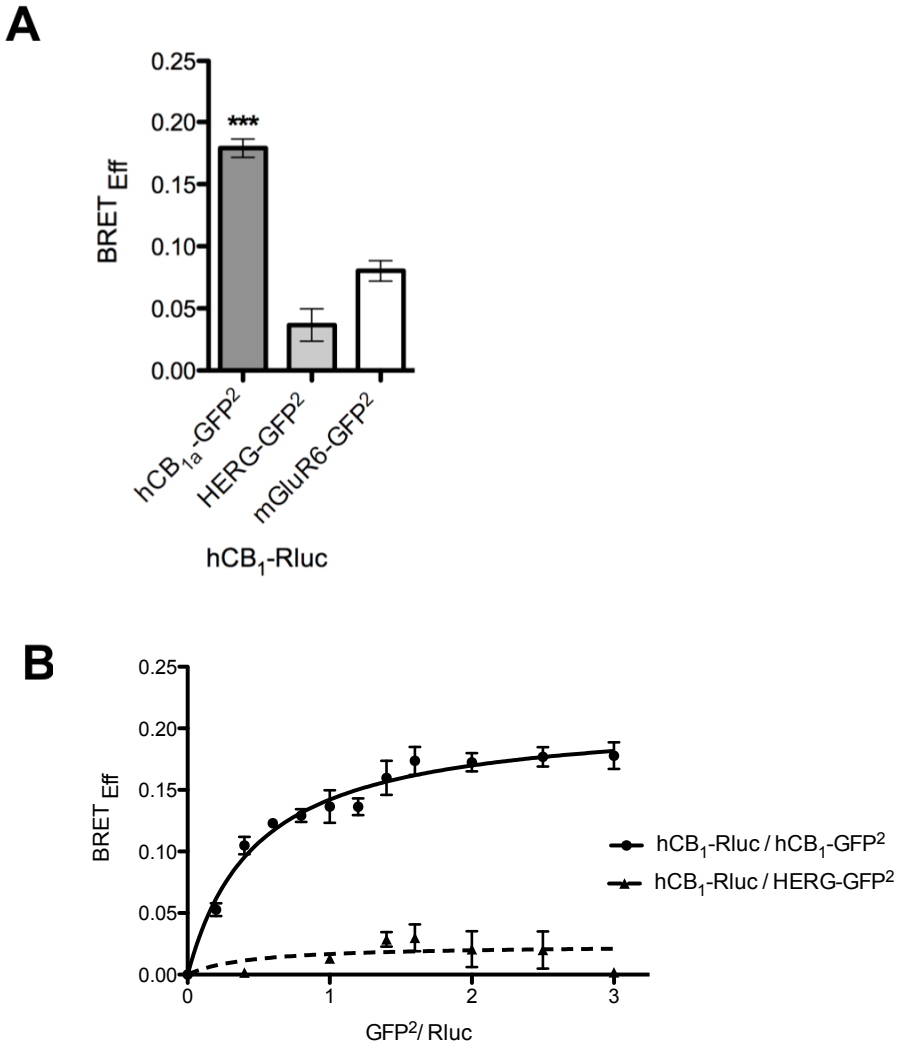

Figure. 3.6: The hCB_1 receptor forms homodimers in HEK 293A cells. **(A)** The co-expression of hCB_1-Rluc and hCB_1-GFP^2 in HEK 293A cells resulted in a higher $BRET_{Eff}$ value, compared when hCB_{1a}-Rluc was co-expressed with either HERG-GFP^2 or mGluR6-GFP^2 controls; ***p<0.001, n=6-8 of three independent experiments. **(B)** BRET saturation curve obtained from cells transiently transfected with hCB_1-Rluc/hCB_1-GFP^2 was higher than the curve of hCB_{1a}-Rluc/HERG-GFP^2. Data are presented as mean ± SEM of three independent experiments, n=6-8. Statistical significance was determined by using one-way ANOVA, followed by Tukey's post hoc test. *** $P < 0.001$ compared to controls.

Homodimerization of hCB_1 receptor was also carried out. A significantly higher $BRET_{Eff}$ resulted ($P < 0.001$) when hCB_1-Rluc and hCB_1-GFP^2 constructs were co-expressed, compared to the two controls (Fig. 3.6A). BRET saturation curve for the hCB_1 receptor resulted in a $BRET_{Max}$ of 0.23 ± 0.02 ($P < 0.001$), and $BRET_{50}$ of 0.48 ± 0.05 ($P < 0.001$; Fig. 3.6B), which further confirm previously published data of hCB_1 homodimerization (Wager-Miller *et al*., 2002; Hudson *et al*., 2010). Taken together, the $BRET^2$ data suggest that hCB_1, hCB_{1a} and hCB_{1b} are capable of forming homodimers, when expressed in HEK 293A cells.

3.3.2 Heterodimerization Between hCB_1 Receptor and its Splice Variants

GPCRs have been reported to physically interact with their splice variants under normal physiological conditions to form heterodimers (Rios *et al*., 2001; Milligan, 2004; Pfleger and Edine, 2005). These interactions were found to have substantial effects on the trafficking and signaling of the full-length receptors (Milligan, 2004). RT-PCR and western blot assays indicated that there was an overlapping pattern of distribution of the mRNAs and proteins of the three CB_1 coding region variants in different regions of the human and monkey brain, raising the possibility that heterodimerization may occur and influence the function of CB_1 receptor complexes in these tissues. For this reason, the next aim of this study was to determine whether dimerization would occur between the hCB_1 receptor and hCB_{1a} and hCB_{1b} splice variants. For these experiments, $BRET^2$ was also used to demonstrate dimerization between hCB_1 and hCB_{1a} and hCB_{1b} splice variants in HEK 293A cells. $BRET_{Eff}$ was measured from cells co-transfected with either hCB_1-

Rluc or hCB_{1a}-Rluc, and one of the following: hCB_1-GFP^2, hCB_{1a}-GFP^2, HERG-GFP^2 or mGluR6-GFP^2 (Fig. 3.7A). The co-expression of hCB_{1a}-Rluc and hCB_1-GFP^2 produced an increased $BRET_{Eff}$ ($P < 0.01$) compared to the two controls. Similarly, when hCB_1-Rluc was co-expressed with hCB_{1a}-GFP^2 it produced an increased $BRET_{Eff}$ ($P < 0.001$) compared with either HERG-GFP^2 or mGluR6-GFP^2. A BRET saturation curve was also generated (Fig. 3.7B). The hCB_1-Rluc/hCB_{1a}-GFP^2 saturation curve was higher than the curve for the hCB_{1a}-Rluc/ HERG-GFP^2 ($p<0.001$). The saturation curve yielded a $BRET_{Max}$ of 0.28 ± 0.018 and $BRET_{50}$ of 0.7 ± 0.064. To confirm the specificity of the interaction between hCB_1 and hCB_{1a}, a BRET competition assay was carried out. In a BRET competition assay, cells were transfected with constant amounts of hCB1-Rluc/hCB_{1a}-GFP^2 and an increasing amount of non-fluorescent HA-hCB_{1a} as competitor (Fig. 3.7C). The $BRET_{Eff}$ of hCB_1-Rluc/hCB_{1a}-GFP^2 was decreased by the co-expression of 1 μg of HA-hCB_{1a} ($P < 0.05$). Increasing the HA-hCB_{1a} concentration to 2 and 3 μg resulted in a further reduction in $BRET_{Eff}$ values ($P < 0.001$) and ($P < 0.01$), respectively. The physical interaction between hCB_1 and hCB_{1b} was also studied using $BRET^2$ experiments (Fig. 3.8). The BRET saturation curve of hCB_1-Rluc/hCB_{1b}-GFP^2 resulted in a $BRET_{Max}$ of 0.27 ± 0.017 and $BRET_{50}$ of 0.71 ± 0.05 (Fig.3.8B). Our results demonstrate that there is a specific interaction between hCB_1 and its splice variants, when hCB_1 is co-expressed with hCB_{1a} or hCB_{1b}.

The effect of several CB_1 ligands on the dimerization of hCB_1 with its splice variants was studied (Fig. 3.9). Treating cells expressing hCB_1-Rluc/hCB_{1a}-GFP^2 or hCB_1-Rluc/hCB_{1b}-GFP^2 for 30 m with either an inverse agonist AM-251, full agonist WIN 55212-2, or neutral antagonist, O-2050, did not significantly alter the observed $BRET_{Eff}$

Figure 3.7: The hCB_1 receptor can forms heterodimers with its splice variant hCB_{1a} in HEK 293A cells. **(A)** The co-expression of hCB_{1a}-Rluc and hCB_1-GFP^2 in HEK cells resulted in a higher $BRET_{Eff}$ value, compared when hCB_{1a}-Rluc was co-expressed with either HERG-GFP^2 or mGluR6-GFP^2 controls; ** $P < 0.01$. Similarly, the co-expression of hCB_1-Rluc and hCB_{1a}-GFP^2 in HEK cells resulted in a higher $BRET_{Eff}$ value, compared to the controls; *** $P < 0.001$. **(B)** BRET saturation curve obtained from cells transiently transfected with hCB_1-Rluc/hCB_{1a}-GFP^2 was higher than the curve of hCB_{1b}-Rluc/HERG-GFP^2. **(C)** BRET competition experiment was performed with HEK cells transfected with a constant amount of hCB_1-Rluc and hCB_{1a}-GFP^2 and increasing amounts of HA-hCB_{1a} or HERG-GFP^2. * $P < 0.05$, ** $P < 0.01$ and *** $P < 0.001$ compared to cells expressing only hCB_1-Rluc/hCB_{1a}-GFP^2. Data are presented as mean ± SEM of three independent experiments, n=6. Statistical significance was confirmed by using one-way ANOVA, followed by Tukey's post hoc test.

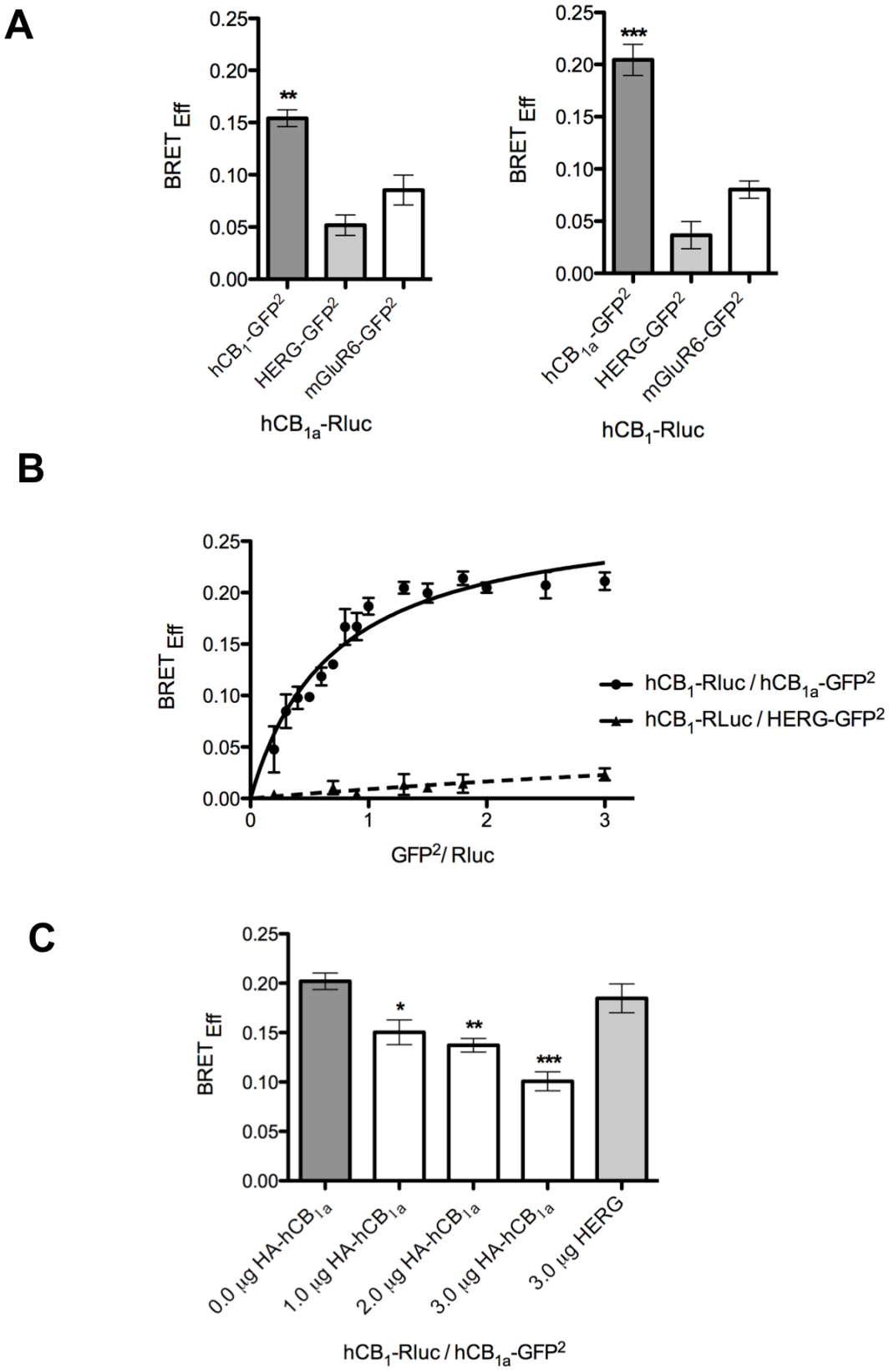
A
BRET Eff
0.25
0.20
0.15
0.10
0.05
0.00
**
hCB1-GFP2
HERG-GFP2
mGluR6-GFP2
hCB1a-Rluc
***
hCB1a-GFP2
hCB1-Rluc
B
GFP2/ Rluc
hCB1-Rluc / hCB1a-GFP2
hCB1-RLuc / HERG-GFP2
C
*
**
***
0.0 µg HA-hCB1a
1.0 µg HA-hCB1a
2.0 µg HA-hCB1a
3.0 µg HA-hCB1a
3.0 µg HERG
hCB1-Rluc / hCB1a-GFP2

Figure 3.8: The hCB_1 receptor can form heterodimers with its splice variant hCB_{1b} in HEK 293A cells. (A) The co-expression of hCB_{1b}-Rluc and hCB_1-GFP^2 in HEK cells resulted in a higher $BRET_{Eff}$ value, compared when hCB_{1a}-Rluc was co-expressed with either HERG-GFP^2 or mGluR6-GFP^2 controls; ** $P < 0.01$. Similarly, the co-expression of hCB_1-Rluc and hCB_{1a}-GFP^2 in HEK cells resulted in a higher $BRET_{Eff}$ value, compared to the controls; *** $P < 0.001$. **(B)** BRET saturation curve obtained from HEK cells transiently transfected with a constant amount of hCB_{1b}-Rluc and increasing amount of hCB_{1b}-GFP^2 was higher than the curve of hCB_{1b}-Rluc/HERG-GFP^2. **(C)** BRET competition experiment was performed with HEK 293A cells transfected with a constant amount of hCB_1-Rluc and hCB_{1b}-GFP^2 and increasing amounts of HA-hCB_{1b} or HERG-GFP^2 . * $P < 0.05$, ** $P < 0.01$ and *** $P < 0.001$ compared to the cells expressing only hCB_1-Rluc/hCB_{1b}-GFP^2. Data are presented as mean ± SEM of three independent experiments, n=6. Statistical significance was determined by using one-way ANOVA, followed by Turkey's post hoc test.

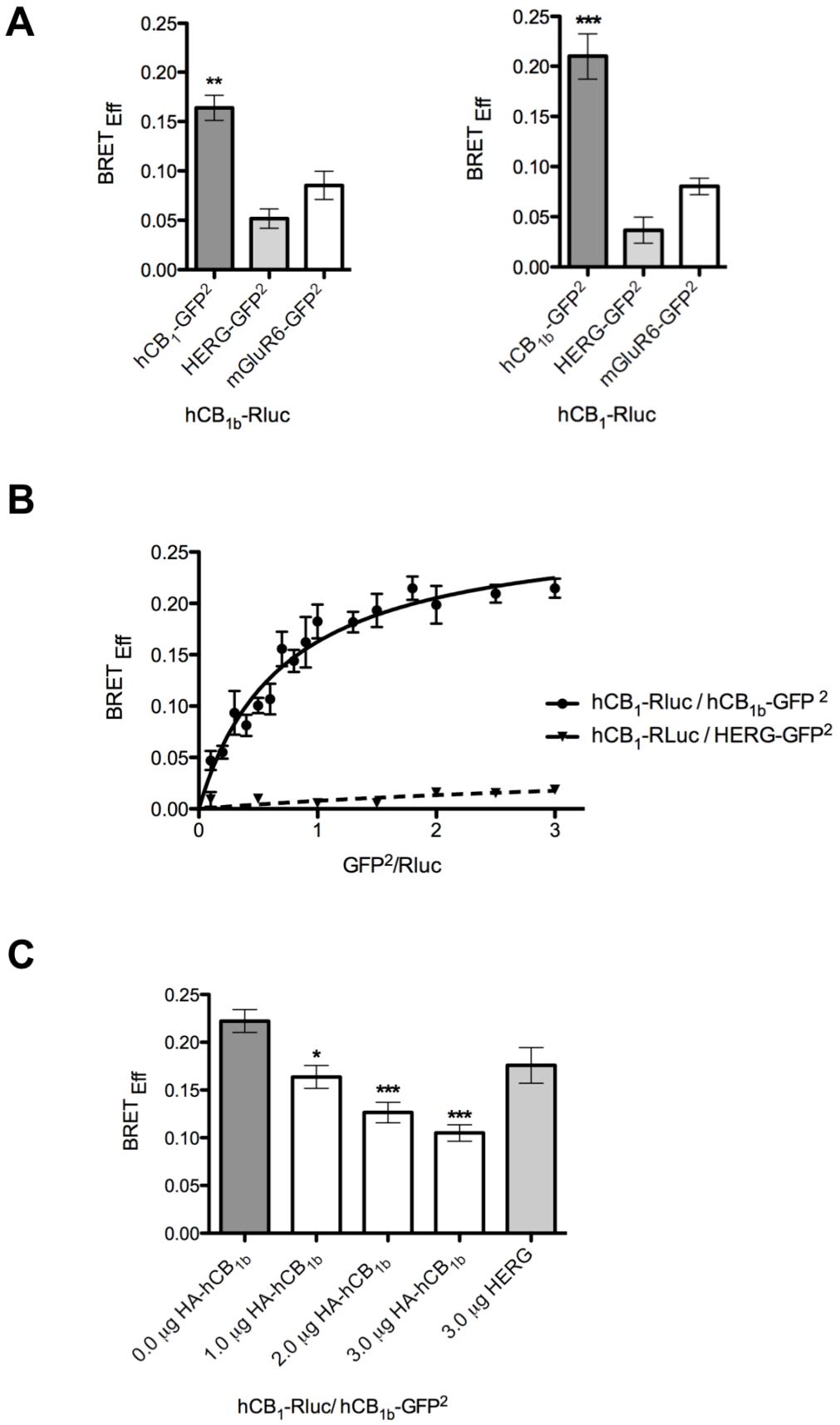
A
BRET Eff
0.25
0.20
0.15
0.10
0.05
0.00
**
***
hCB1-GFP2
HERG-GFP2
mGluR6-GFP2
hCB1b-Rluc
hCB1-Rluc
B
BRET Eff
GFP2/Rluc
hCB1-Rluc / hCB1b-GFP 2
hCB1-RLuc / HERG-GFP2
C
BRET Eff
*
***
0.0 µg HA-hCB1b
1.0 µg HA-hCB1b
2.0 µg HA-hCB1b
3.0 µg HA-hCB1b
3.0 µg HERG
hCB1-Rluc/ hCB1b-GFP2

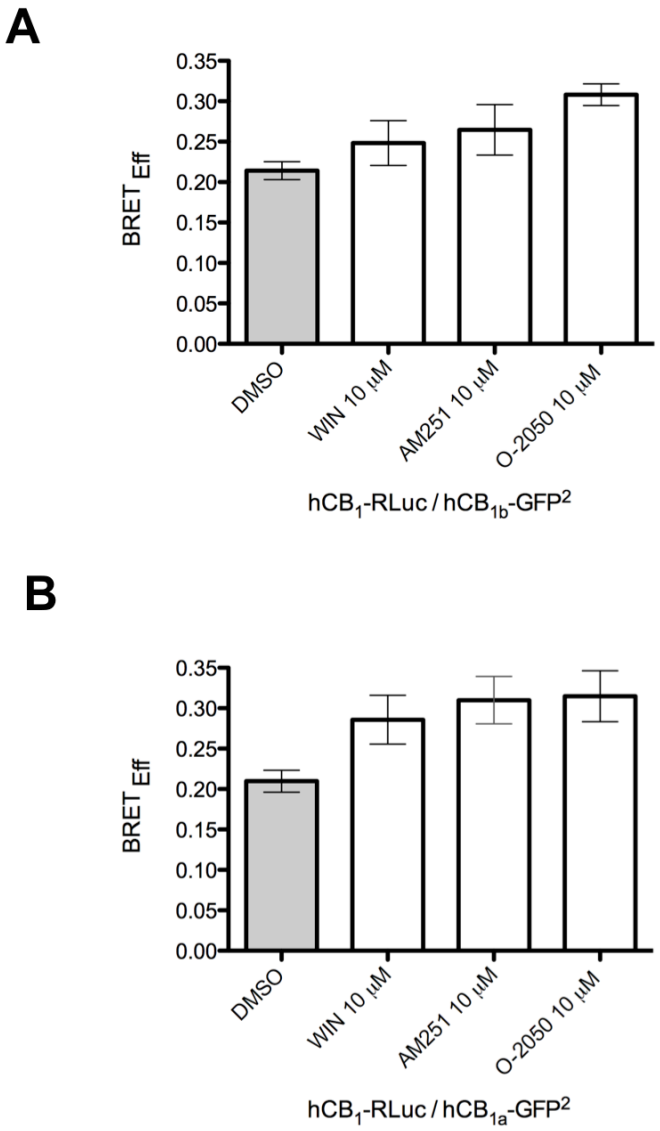

Figure 3.9: Dimerization of the hCB_1 receptor with its splice variants is not affected by CB_1 ligand treatment. $BRET_{Eff}$ obtained from cells transfected with hCB_1-Rluc/hCB1a-GFP^2 **(A)**, and hCB_1 –Rluc/hCB_{1b}-GFP^2 **(B)**, forty-eight hours later cells were treated with either DMSO (0.05%), WIN (10 µM), AM251 (10 µM) or O-2050 (10 µM) for 30 min before $BRET_{Eff}$ was measured. Data are presented as mean ± SEM of three independent experiments; n=4-6. n.s., $P > 0.05$ compared to cells treated with DMSO. Statistical significance was determined by using one-way ANOVA, followed by Tukey's post hoc test.

signals. This finding suggested that heterodimerization of hCB_1 with its splice variants is independent of ligand binding.

3.3.3 Heterodimerization Between hCB_{1a} and hCB_{1b} Receptors

We examined whether dimerization could occur between the splice variants hCB_{1a} and hCB_{1b}. HEK 293A cells were transfected with hCB_{1a}-Rluc or hCB_{1b}-Rluc, in addition to one of the following constructs: hCB_{1b}-GFP^2, hCB_{1a}-GFP^2, HERG-GFP^2 or mGluR6-GFP^2. Cells co-expressing either hCB_{1a}-Rluc/hCB_{1b}-GFP2 or hCB_{1b}-Rluc/hCB_{1a}-GFP^2 revealed a higher $BRET_{Eff}$ values compared to the controls ($P < 0.001$; Fig. 3.10A). The BRET saturation curve was also used to confirm the specificity of the interaction between the two hCB_1 splice variants and resulted in a $BRET_{Max}$ of 0.29 ± 0.015 and $BRET_{50}$ of 0.27 ± 0.014 (Fig. 3.10B). These results revealed that hCB_{1a} and hCB_{1b} were able to form heterodimers when expressed together in HEK 293A cells.

3.4 Pharmacological Characterizations of hCB_1 Splice Variants

The hCB_1 receptor preferentially couples to $G_{i/o}$, and its activation is typically associated with inhibition of adenylyl cyclase, a decrease in cAMP, and activation of MAP kinases (Howlett *et al*., 2004). To determine the signaling properties of the truncated hCB_1 receptors, basal and agonist-stimulated ERK activation was measured using in-cell western analysis in HEK 293A cells expressing each of the receptor. HEK 293A cells were transiently transfected with equimolar amounts of plasmids encoding the hCB_1-GFP^2, hCB_{1a}-GFP^2 or hCB_{1b}-GFP^2 receptors. Twenty-four hours post transfection; cells were pretreated with either 100 ng/ml pertussis (PTx) or DMEM

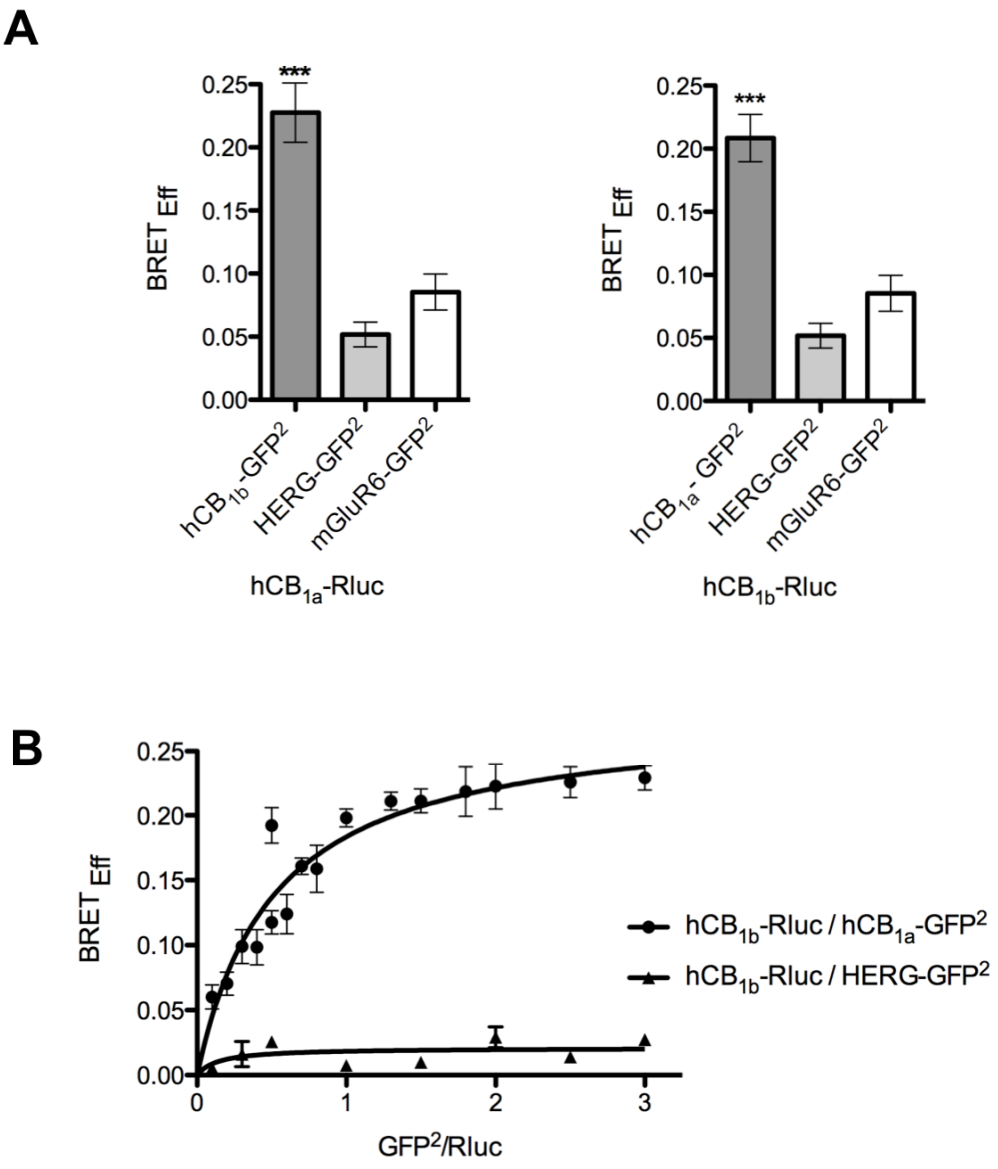

Figure 3.10: The hCB_1 receptor splice variants, hCB_{1a} and hCB_{1b}, can physically interact to form heterodimers in HEK 293A cells. **(A)** The co-expression of hCB_{1a}-Rluc/hCB_{1b}-GFP^2 or hCB_{1b}-Rluc/hCB_{1a}-GFP^2 yielded higher $BRET_{Eff}$ values, compared to when hCB_{1a}-Rluc or hCB_{1a}-Rluc was co-expressed with either HERG-GFP^2 or mGluR6-GFP^2 controls; ***$p<0.001$. **(B)** The BRET saturation curve obtained from cells transiently transfected with a constant amount of hCB_{1b}-Rluc and increasing amounts of hCB_{1a}- GFP^2 was significantly higher than the curve obtained from cells transfected with hCB_{1b}-Rluc/HERG-GFP^2. Data are presented as mean ± SEM of three independent experiments, n=6. Statistical significance was determined by using one-way ANOVA, followed by Tukey's post hoc test.

vehicle, then for 5 min with DMSO vehicle or 1 μM WIN 55212-2. pERK and total ERK were then measured. Cells expressing any of the receptor isoforms had measurable basal pERK that increased significantly upon stimulation with WIN 55212-2 ($P < 0.001$; Fig. 3.11A). There was a significant difference ($P > 0.05$) in pERK between cells expressing the hCB_1 receptor and either hCB_{1a} or hCB_{1b} splice variants. In all the three receptors the pERK responses to WIN 55212-2 were reduced by pre-treatment with PTx ($P < 0.001$). Furthermore, resulted WIN 55212-2 dose response curves (DRC) generated for each hCB_1variant resulting in E_{Max} values of 1.47 ± 0.03, 1.38 ± 0.024 and 1.30 ± 0.025 and pEC_{50} values of 7.33 ± 0.11, 7.05± 0.1 and 7.0 ± 0.12 for hCB_1-GFP^2, hCB_{1a}-GFP^2 or hCB_{1b}-GFP^2 receptors, respectively (Fig. 3.11B). Notably, the two hCB_1 splice variants showed a lower level of ERK efficacy and affinity, compared to the full-length receptor. These findings demonstrate that activation of the hCB_1 splice variants leads to an increase in pERK through a PTx-sensitive pathway, albeit with some differences to hCB_1.

To investigate further the pharmacology of the three hCB_1 receptors, cellular localization and cell surface expression were examined in HEK 293A cells. To follow the subcellular localization of the receptors in HEK 293A cells, confocal microscopy images were taken of cells transiently transfected with equimolar amounts of one of the following plasmids: hCB_1-GFP^2, hCB_{1a}-GFP^2 or hCB_{1b}-GFP^2. In contrast to the hCB_1 receptor, that where localized predominantly intracellular when expressed in HEK 293A cells, hCB_{1a} and hCB_{1b} receptors were observed at the plasma membrane (Fig. 3.12A). In order to quantify the cell surface expression of each receptor, on-cell western analysis was used. As shown in figure 3.12B, the truncated HA-hCB_{1a} and HA-hCB_{1b} receptors have significantly higher plasma membrane expression levels ($P < 0.001$ and $P < 0.05$)

Figure 3.11: Similarly to the hCB_1 receptor, hCB_{1a} and hCB_{1b} receptors signal through PTx sensitive pERK pathway in HEK 293A cells. (A) HEK 293A cells were transiently transfected with equimolar amounts of either hCB_1–GFP^2, hCB_{1a}–GFP^2 or hCB_{1b}–GFP^2 receptors, 24 hours later cells pre-treated for 24 h with either DMEM vehicle or 100 ng/ml PTx, then for 5 min with 0.05% DMSO vehicle or 1 **µ**M WIN. Data are presented as mean ± SEM of three independent experiments, n=6-10. *** $P < 0.001$ compared to unstimulated cells, ### $P < 0.001$ compared with appropriate PTx treatment, * $P < 0.05$ and ** $P < 0.01$ compared to stimulated cells transfected with the hCB_1 and treated with WIN. Statistical analysis was performed using a two-way ANOVA analyzing. **(B)** pERK dose-response curve from HEK 293A cells expressing either hCB_1–GFP^2, hCB_{1a}–GFP^2 or hCB_{1b}–GFP^2, n= 10-15.

A

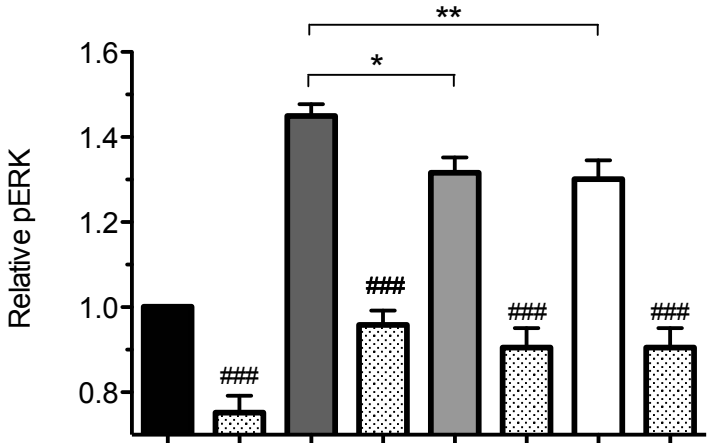

100 ng/ml PTx	-	+	-	+	-	+	-	+
Vehicle	+	+	-	-	-	-	-	-
1 µM WIN	-	-	+	+	+	+	+	+
hCB_1-GFP^2	+	+	+	+	-	-	-	-
hCB_{1a}-GFP^2	-	-	-	-	+	+	-	-
hCB_{1b}-GPF^2	-	-	-	-	-	-	+	+

B

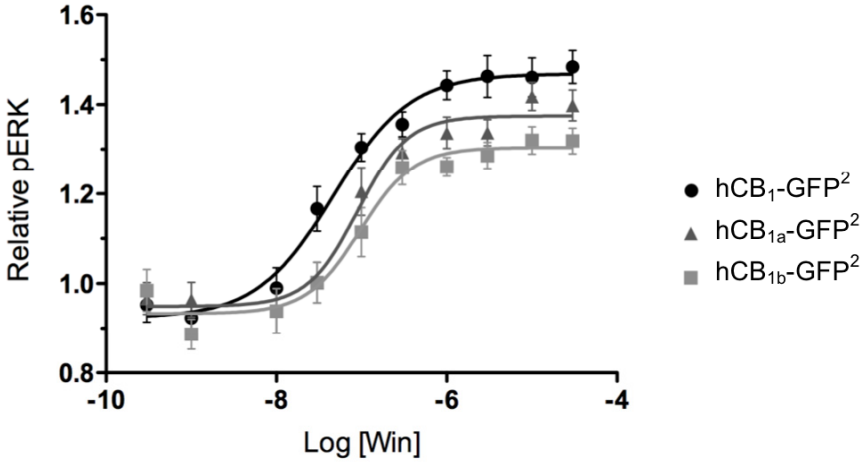

A

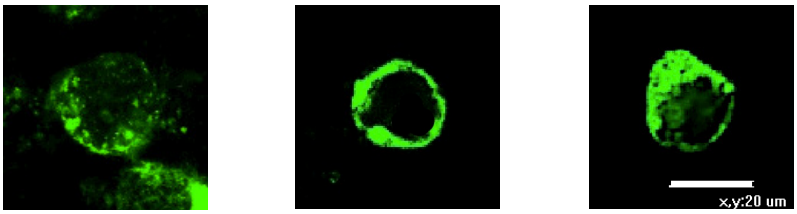

hCB_1-GFP^2 hCB_{1a}-GFP^2 hCB_{1b}-GFP^2

B

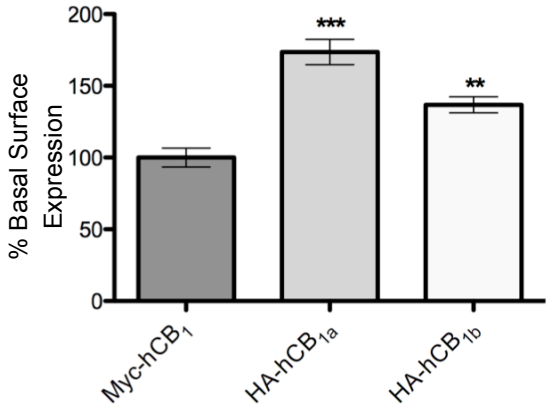

Figure 3.12: The hCB_{1a} and hCB_{1b} receptors have higher expression levels in HEK 293A cells. **(A)** Confocal images of HEK 293A cells transiently transfected with 100 ng of either hCB1-GFP^2, hCB_{1a}-GFP^2 or hCB_{1b}-GFP^2, scale bar is 20 µM. **(B)** On-cell western quantitative measure of hCB_1-GFP^2, hCB_{1a}-GFP^2 or hCB_{1b}-GFP^2 cell surface expression in transiently transfected HEK 293A cells. Data are presented as mean ± SEM of three independent experiments, n=6-12. *** $P < 0.001$; ** $P < 0.01$ compared to cells expressing Myc-hCB_1. Statistical analysis was performed using a one-way ANOVA, followed by Tukey's post hoc test.

respectively, compared to the full-length Myc-hCB_1 receptor. Thus, the truncated hCB_1 receptors have different patterns of cellular localization when expressed individually in HEK 293A cells.

3.5 Functional Interactions Between hCB_1 and its Splice Variants in HEK 293A Cells

Our previous data showed that the full-length hCB_1 receptor was able to dimerize with its splice variants in HEK 293A cells. Therefore, it was important to investigate the functional implications of hCB_1 heterodimerization. The influence of heterodimerization on receptor signaling was studied using the in-cell western technique to assess the level of ERK activation. HEK 293A cells were transfected with either 200 ng hCB_1-GFP^2 construct or 100 ng hCB_1-GFP^2 together with 100 ng hCB_{1a}-GFP^2, 100 ng of hCB_{1b}-GFP^2 or 100 ng HERG-GFP^2. Twenty-four hours later cells were treated with 1 μM WIN 55212-2 for 10 m. When HEK 293A cells expressed only the full-length hCB_1-GFP^2 receptor, an increase in pERK was observed following the treatment with WIN 55212-2 relative to vehicle treated cells (Fig. 3.13A). However, cells co-transfected with both the full-length hCB_1-GFP^2 receptor and one of the truncated receptor hCB_{1a}-GFP^2 or hCB_{1b}-GFP^2 resulted in a higher pERK ($P < 0.001$), compared when hCB_1-GFP^2 receptor was expressed alone or with HERG-GFP^2. The pERK dose response curve generated following WIN 55212-2 treatment in cells co-expressing hCB_1-GFP^2 alone yielded a pEC_{50} of 7.38 ± 0.1, an E_{Max} of 1.46 ± 0.021 and a Hill coefficient of 1.08 . The co-expression of hCB_1-GFP^2 together with one of the splice variants resulted in significantly different dose response curves ($P < 0.001$). Co-expressing hCB_1-GFP^2 and hCB_{1a}-GFP^2

Figure 3.13: Co-expression of hCB_1 with hCB_{1a} or hCB_{1b} receptors increases agonist-stimulated ERK response. (A) HEK 293 cells were transiently transfected with either 200 ng of hCB_1-GFP^2 alone, or 100 ng of hCB_1-GFP^2 with 100 ng of either hCB_{1a}-GFP^2, hCB_{1b}-GFP^2 or HERG-GFP^2, and treated with 0.05% DMSO vehicle or 1 μM WIN for 10 minutes before pERK was measured. *** $P < 0.001$ compared to cells expressing hCB_1 and treated with WIN; ### $P < 0.001$ compared to cells expressing hCB_1 and treated with vehicle. Data are presented as mean ± SEM of three independent experiments, n=10-12. Statistical analysis was performed using two-way ANOVA analyzing receptor expression and WIN stimulation. **(B)** pERK dose response curve from HEK 293A cells expressing hCB_1-GFP^2 or together with hCB_{1a}-GFP^2 or hCB_{1b}-GFP^2 and treated with WIN for 5 m. Data are presented as mean ± SEM of three independent experiments n=15-18.

A

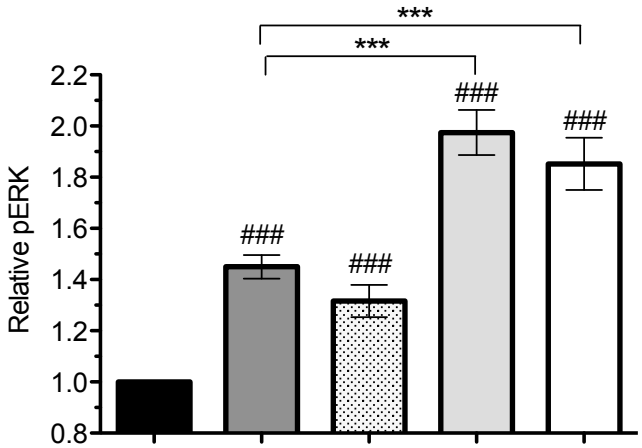

Vehicle	+	-	-	-	-
1 μM WIN	-	+	+	+	+
HERG-GFP^2	-	-	+	-	-
hCB$_1$-GFP^2	+	+	+	+	+
hCB$_{1a}$-GPF^2	-	-	-	+	-
hCB$_{1b}$-GFP^2	-	-	-	-	+

B

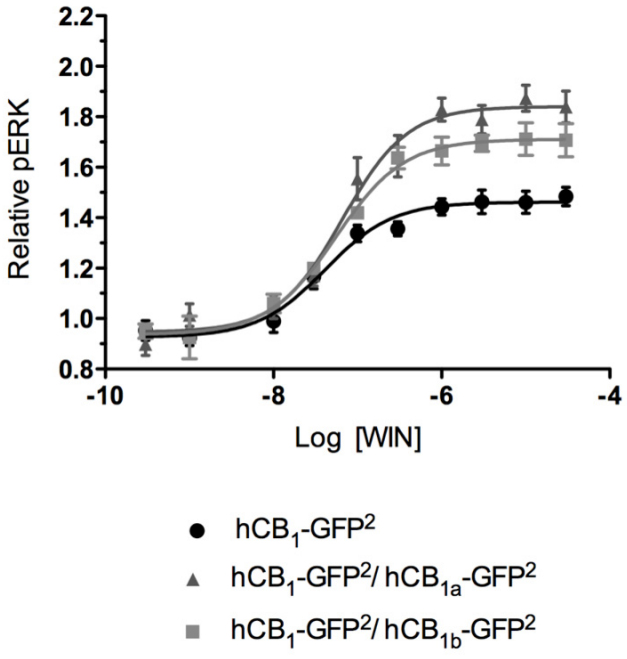

resulted in a pEC_{50} of 7.18 ±0.093, an E_{Max} of 1.84 ± 0.03 and a Hill coefficient of 1.12, while cells co-expressing hCB_1-GFP^2 and hCB_{1b}-GFP^2 yielded a pEC_{50} of 7.25 ± 0.092, an E_{Max} of 1.72 ± 0.029 and Hill coefficient of 1.072 (Fig. 3.13B) . The effect on signaling of the full-length hCB_1 receptor is dependent on the dose of the co-transfected truncated receptor, as the higher the ratio of the truncated receptor to the full-length receptor the higher the ERK activation (Fig. 3.14).

We hypothesized that the increase in ERK signaling could be due to the increase in hCB_1 cell-surface expression when co-expressing the hCB_{1a} or hCB_{1b}. Cell surface expression of the hCB_1.GFP^2 receptor alone, and in the presence of the truncated splice variant, HA-hCB_{1a} or HA-hCB_{1b}, was examined using confocal microscopy. When the full-length hCB_1-GFP^2 receptor was co-transfected with the truncated HA-hCB_{1a} or HA-hCB_{1b} receptor in HEK 293A cells, it was found that the localization of hCB_1-GFP^2 was increased at the cell surface membrane (Fig 3.15A). When the cells expressed only hCB_1-GFP^2, distribution of the receptor was consistent with a more internalized receptor (Fig. 3.15A). On-cell western analysis was also used to quantify the effect of co-expression of the truncated HA-hCB_{1a} and HA-hCB_{1b} receptors on the cell surface expression of Myc-hCB_1. The co-expression of Myc-hCB_1 with either of the splice variants resulted in a significant increase in Myc-hCB_1 cell surface expression ($P < 0.001$), while the co-expression of HERG-GFP^2 did not change Myc-CB_1 surface expression (Fig. 3.15B). Our data indicated that the co-expression of hCB_1 splice variants increased hCB_1 cell surface expression.

Next, we examined co-internalization of the Myc-hCB_1 following treatment with WIN 55212-2. Treatment of HEK 293A cells expressing Myc-hCB_1 with 10 μM CB_1

agonist WIN 55212-2 for 30 min resulted in reduction in Myc-hCB_1 cell surface expression ($P < 0.001$). However, when cells were co-transfected with both Myc-hCB_1 and HA-hCB_{1a} or HA-$hCB_{1b,}$ and treated with WIN, co-internalization of both receptors was observed (Fig. 3.16A). On-cell western analysis was also used to measure Myc-hCB_1 internalization (Fig. 3.16B). Cells expressing the Myc-hCB_1 receptors alone showed a significant reduction in cell-surface expression of the hCB_1 receptor after WIN 55212-2 treatment ($P < 0.001$) in relation to untreated cells. However, cells co-transfected with both the Myc-hCB_1 receptor and one of the splice variants and treated with WIN 55212-2 showed less internalization ($P < 0.01$), compared with WIN-treated cells expressing the hCB_1 receptor alone. Co-expression of Myc-hCB_1 and HERG-GFP[2] did not alter the trafficking of the hCB_1 receptor.

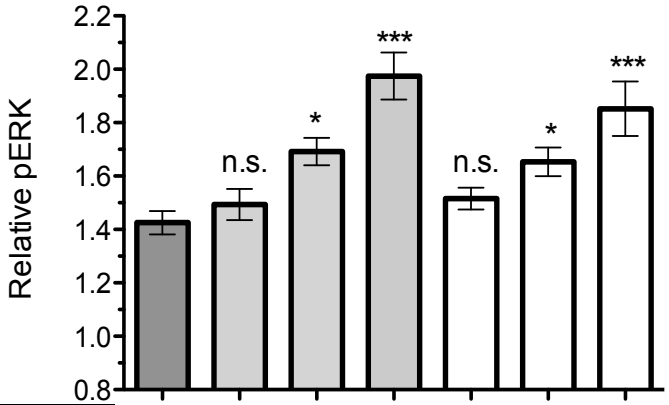

ng plasmid							
hCB_1-GFP^2	200	100	100	100	100	100	100
hCB_{1a}-GFP^2	-	50	75	100	-	-	-
hCB_{1b}-GPF^2	-	-	-	-	50	75	100
pcDNA 3.1	-	50	25	-	50	25	-

Figure 3.14: Co-expression of hCB_1 with hCB_{1a} or hCB_{1b} receptors increases agonist-stimulated ERK response. HEK cells were transfected with varying dose of hCB_1-GFP^2 and its splice variants and treated with 1 μM WIN 55212-2. *** $P < 0.001$; * $P < 0.05$; n.s. $P > 0.05$ compared to cells expressing 200 ng hCB_1. Data are presented as mean ± SEM of three independent experiments, n=10-12. Statistical analysis was performed using two-way ANOVA analyzing receptor expression and WIN 55212-2 stimulation.

Figure 3.15: Co-expression of hCB_{1a} or hCB_{1b} facilitates cell surface expression of hCB_1. (A) Confocal images of HEK 293A cells transiently transfected with hCB_1-GFP^2 and HA-hCB_{1a} or HA-hCB_{1b}. Left images show GFP^2 fluorescence, middle images are anti-HA immunofluorescence utilizing a Cy^3 conjugated antibody, and the right images are the merged images. Scale bar is 20 μm. **(B)** Quantitative measure of Myc-hCB_1 cell surface expression in HEK 293A cells transiently transfected with 100 ng Myc-hCB_1, or co-transfected with 100 ng of HA-hCB_{1a}, HA-hCB_{1b} or HERG-GFP^2. Data are presented as mean ± SEM of three independent experiments, n=6-10. ** $P < 0.01$ compared to cells expressing 100 ng Myc-hCB_1. Statistical analysis was performed using a one-way ANOVA, followed by Tukey's post hoc test.

A

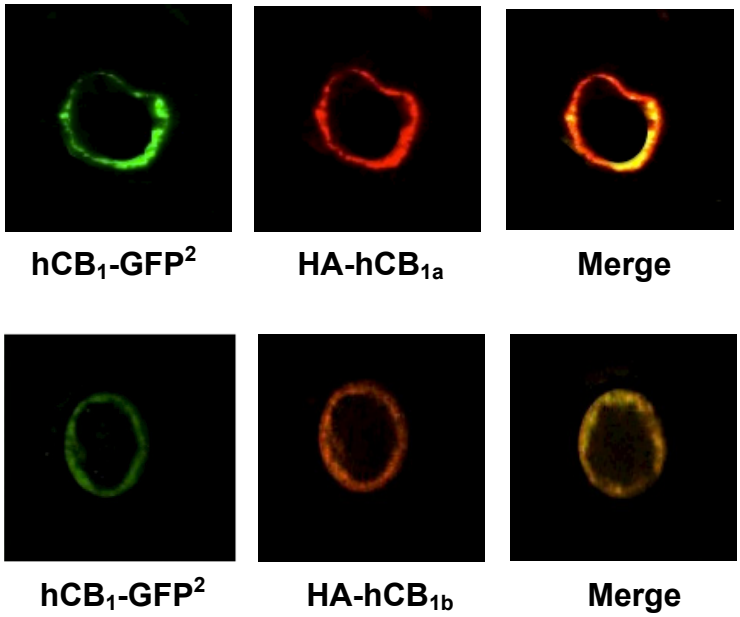

B

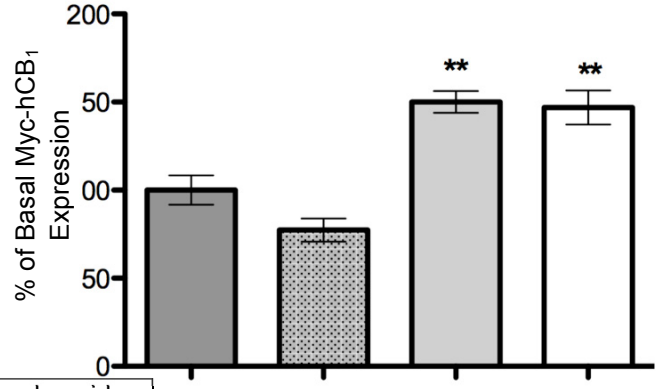

ng plasmids				
Myc-hCB$_1$	100	100	100	100
HA-hCB$_{1a}$	-	-	100	-
HA-hCB$_{1b}$	-	-	-	100
HERG-GFP^2	-	100	-	-
pcDNA 3.1	100	-	-	-

Figure 3.16. The hCB_1 receptor is co-internalized with its splice variant following WIN 55212-2 treatment. (A) Confocal images of HEK 293A cells transiently transfected with with hCB_1-GFP^2 and HA-hCB_{1a} or HA-hCB_{1b} and treated with 10 μM WIN 55212-2. Left images show GFP^2 fluorescence, middle images are anti-HA immunofluorescence utilizing a Cy^3 conjugated antibody, and the right images are the merged images. Scale bar = 20 μm. **(B)** Quantitative measure of Myc-hCB_1 cell surface expression in HEK 293A cells transiently transfected with 100 ng Myc-hCB_1, or co-transfected with 100 ng of HA-hCB_{1a}, HA-hCB_{1b} or HERG-GFP^2 and treated with 10 μM WIN 55212-2. Data are presented as mean ± SEM of three independent experiments, n=10-12. *** $P < 0.001$ compared to cells treated with vehicle; # $P < 0.05$ compared to cells expressing Myc-hCB_1 and treated with WIN 55212-2. Statistical analysis was performed using a two-way ANOVA, followed by Tukey's post hoc test.

A

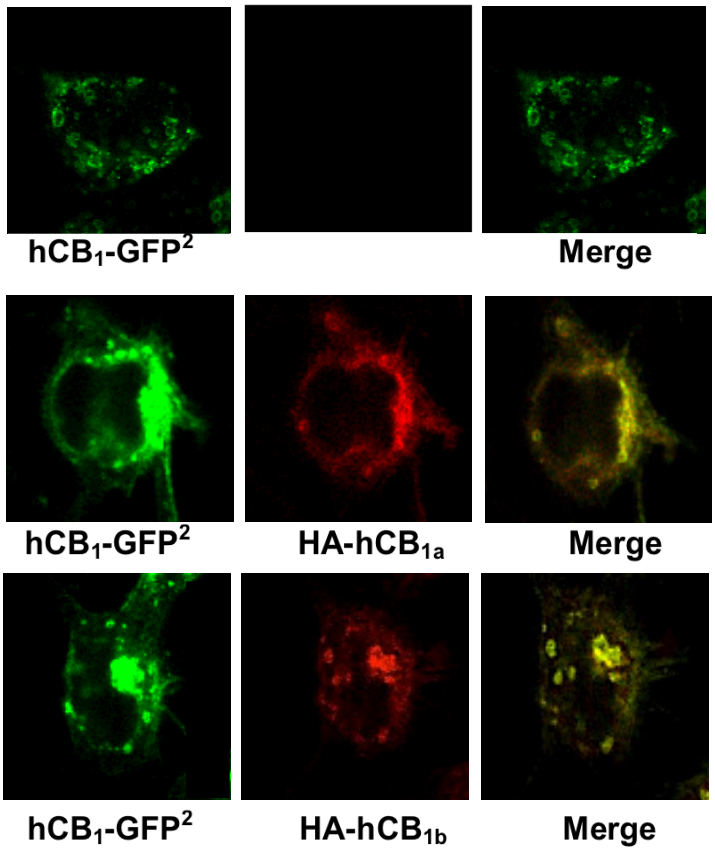

B

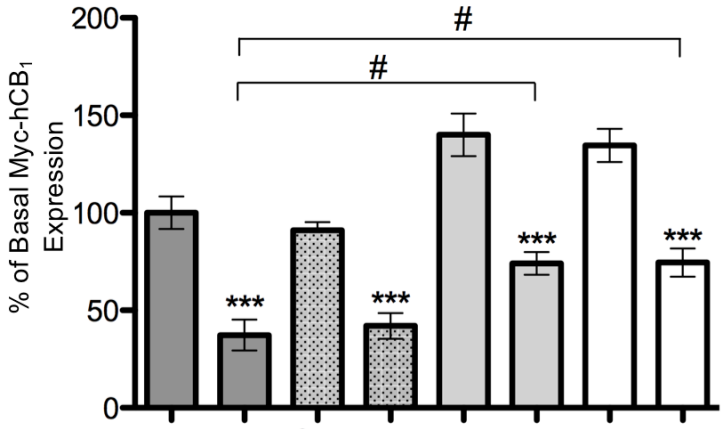

Vehicle	+	-	+	-	+	-	+	-
10 μM WIN	-	+	-	+	-	+	-	+
Myc-hCB$_1$	+	+	+	+	+	+	+	+
HA-hCB$_{1a}$	-	-	-	-	+	+	-	-
HA-hCB$_{1b}$	-	-	-	-	-	-	+	+
HERG-GFP^2	-	-	+	+	-	-	-	-

Chapter 4: Discussion

Dimerization between full-length GPCRs and their splice variants, under normal physiological conditions, has been reported to play an important role in regulating the functions of their full-length receptors (Bai, 2004). The recent discovery that the hCB_1 receptor is subjected to alternative splicing within the coding region, to form hCB_{1a} and hCB_{1b} transcripts, raises many questions regarding their distribution, functional differences and their biological roles (Shire *et al,* 1995; Ryberg *et al.,* 2005; Xiao, 2008). The present study aimed to determine the relative abundance and distribution of mRNAs encoding the three coding region CB_1 variants in human and monkey (*Macaca fascicularis*) brains, and to examine whether the hCB_{1a} and hCB_{1b} are expressed as proteins in the monkey brain. The overlapping patterns of distribution of the mRNAs of the three coding region variants raises the possibility that physical interaction through dimerization may occur and influence the function of hCB_1 receptor complexes. Finally we examined whether the hCB_1 variants can physically interact when co-expressed in a heterologous expression system, and looked to determine if co-expression of variants affects trafficking and signaling of hCB_1.

4.1 The hCB_{1a} and hCB_{1b} mRNAs were Distributed Throughout the Brain

In the present study, the CNS distribution of the hCB_1 variants was determined in a tissue derived from the brain of a 71 year-old human donor and a 4-year old monkey brain (equivalent to 12 human years). RT-PCR was conducted using a primer set common to the three-hCB_1 variants and all the three variant transcripts were detected in

all the regions examined in human and monkey brains. Although quantification was not possible, it appeared that each variant was amplified at the minimum number of cycles needed to observe any product, suggesting that template concentration was similar in each sample. Our findings agree with previously published data that reported that hCB_{1a} and hCB_{1b} mRNAs are expressed in adult human total brain tissue (Shire *et al,* 1995; Ryberg *et al.,* 2005; Xiao *et al*., 2008). However, the relative expression levels of the three variants in our results are not similar to previously published data. In earlier studies, hCB_1 mRNA was found to be the most abundant transcripts, while hCB_{1a} and hCB_{1b} mRNAs were found to be the minor transcript, as they represent fewer than 5% of the total hCB_1 transcripts (Shire *et al,* 1995; Ryberg *et al.,* 2005; Xiao *et al*., 2008). These discrepancies in the expression levels of the three hCB_1 variants could be due to a number of factors. RNAs used in the current study were obtained from a 71 year-old female donor and age might alter variant levels, however the age of the donors were not stated in previously studies. Age-related differences in levels of CB_1 mRNA and its protein have been reported in the human brain. It was found that CB_1 mRNA is expressed as early as 9 weeks gestation prenatal ages, and CB_1 mRNA level rises after birth to reach a plateau at one year of age. CB_1 mRNA level increases further during adolescence to reach a steady state level, thereafter decreasing throughout adulthood (Wang *et al*., 2003; Zurolo *et al*., 2010; Pinto *et al*., 2010). Another factor affecting the difference in the expression levels of the three CB_1 variant mRNAs observed in our study could be the different PCR conditions and primers used. In summary, our findings demonstrated that the three CB_1 variants are co-expressed together throughout human and monkey brains.

Whether CB_{1a} and CB_{1b} transcripts are translated into proteins *in vivo* has not yet been examined. Therefore, we performed western blots using the same monkey (*Macaca fascicularis*) brain tissues used for the RT-PCR reaction and an antibody directed against the C-terminal region of the receptor. Three bands were detected at the expected molecular weights for CB_1, CB_{1a} and CB_{1b} in all the tested brain regions. The CB_1 receptor appears to be the most abundant, while the two splice variants appear to be less abundant. To further confirm our result, western blot analysis was also conducted using an antibody raised against the first 14 amino acids of the N-terminal tail of the hCB_1 receptor (Chemicon), a region that is unique to hCB_1 and hCB_{1b} receptor, but is not found in hCB_{1a}. Two bands were detected at the expected molecular weight for both hCB_1 and hCB_{1b} (data not shown). An isoform specific antibody would be of great value to confirm our findings, since the two bands that were detected at the expected molecular weights for CB_{1a} and CB_{1b} could be degraded or incomplete CB_1 fragments.

GPCR splice variants can have different localization. For example, the dopamine receptor D_{2S} and D_{2L} receptors variants are differentially localized in CNS neurons, where the short isoform is localized pre-synaptically, while the long isoform is localized post-synaptically (Khan *et al*., 1998). It is well documented that the hCB_1 receptor is localized pre-synaptically in the CNS (Howlett *et al.*, 2004). Whether the two splice variants are localized pre- or post-synaptically has not been examined yet. For this reason, it is very important to determine the specific cellular localization of the two splice variants at both the mRNA and protein levels. To achieve these goals, we conducted single labeling *in situ* hybridization using sections of the monkey frontal cortex and CB_1 and CB_{1b} isoform-specific probe. The hybridization signal indicated no difference

between the expression levels and localizations of the two CB_1 variants. These findings might suggest that CB_1 and CB_{1b} transcripts have similar expression and cellular localization, or it might indicate that the isoform-specific probes for each variant are not specific (Data not shown). Using double labeled *in situ* hybridization would allow for colocalization of two different mRNAs simultaneously on the same brain section.

The full-length CB_1 receptor gene is highly conserved across species. Despite the high degree of primary sequence conservation, the CB_1 coding region splice variants have only been reported in human, non-human primates brain and rat astrocyte culture (Shire *et al.,* 1995; Ryberg *et al*., 2005; Eggan *et al*., 2007). This finding has been challenged by later studies that reported that neither of the splice variants was detected in the rat brain (Fig. 4-1; Xiao *et al*., 2008; Ryberg *et al*., 2005). Several attempts have been made in the current study to amplify CB_{1a} and CB_{1b} using cDNAs from mouse and rat brain using species-specific primers. However, we were unable to detect CB_{1a} and CB_{1b} in mouse or rat brains, despite repeated experiments with different primer sets and PCR conditions (data not shown). The consensus splicing sequence for the 5′ splice site (donor) is (NN/gt), while for the 3' splice site (acceptor) is (ag/NN). Both sites are highly conserved at splicing junctions in eukaryotes (Burset *et al*., 2000). The human and the monkey CB_1 sequences contain all consensus-splicing sites required to generate CB_{1a} and CB_{1b} transcripts (gt-ag). Splicing is, therefore, possible at both sites to generate CB_{1a} and CB_{1b}. In contrast, the rat and mouse CB_1 sequences lack the consensus 5' splice site sequence required to generate CB_{1a} and CB_{1b}. Instead, the rat and mouse sequences contain a non-consensus splicing site (/ct) at the 5' splicing site of CB_{1b} and (/ga) at the 5' splicing site for CB_{1a}. The rat and mouse sequences contain the consensus 3' splice sites for both

1 2

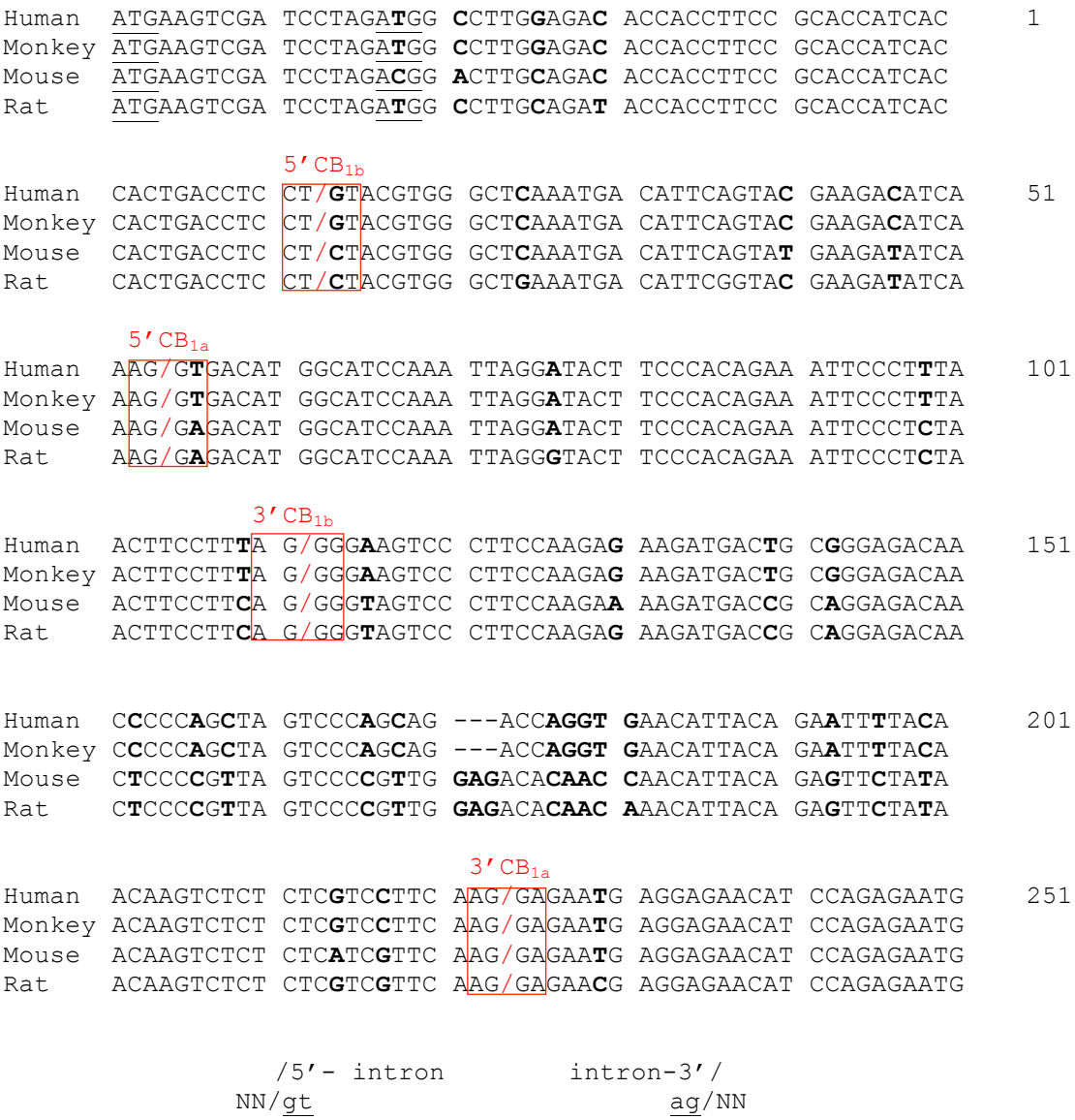

Figure 4.1: Genomic DNA sequences of human, monkey, mouse and rat CB_1 and the splicing sites for CB_{1a} and CB_{1b}. The initiation codon for CB_1 and CB_{1b} is ATG 1, while for CB_{1a} is ATG 2, both are underlined. Nucleotide differences among species are indicated in bold. Splicing sites for CB_{1a} and CB_{1b} are indicated by red boxes. Dashes represent gaps. (Figure was modified from Xiao *et al*., 2008; NCBI).

splice variants. In addition, the mouse CB_1 sequence lacks the initiation codon (ATG) for hCB_{1a}, indicating that translation of CB_{1a} in mouse is unlikely. Given the lack of consensus sequences splicing is less likely to occur to generate CB_{1a} and CB_{1b} in rodents than in human and monkey. Enrichment culture of a single astrocyte cell type may have allowed for detection of CB_{1a} splice variant by Shire and his colleague (1995). In conclusion, CB_{1a} and CB_{1b} receptors may be restricted to human and non-human primates.

4.2 hCB_1 Receptor Splice Variants can form Homo and Heterodimers

The dimerization of GPCRs represents an important phenomenon that modulates receptor function (Terrillon and Bouvier, 2004). Using $BRET^2$ and co-immunoprecipitation assays, previous studies have demonstrated that hCB_1 receptor was capable of forming dimeric or multimeric complexes when expressed alone in heterologous expression cell systems (Wager-Miller *et al.*, 2002; Hudson *et al*., 2010). In the current study, protein–protein interactions between and among hCB_1 and its splice variants were examined. We showed, using $BRET^2$, that hCB_{1a} and hCB_{1b} receptors, like hCB_1, could form homodimers when expressed alone in HEK 293A cells. Similar to hCB_1, the two variants exhibit specific and saturable homodimerization as determined by BRET saturation curves. Earlier studies have proposed that $BRET_{50}$ values reflect the affinity of donor and acceptor molecules for each other (Guan *et al*., 2009). By comparing the BRET saturation curves obtained for hCB_1, hCB_{1a} and hCB_{1b} homodimers, similar $BRET_{50}$ values were obtained, suggesting that the three hCB_1

variants have relatively similar affinity to form homodimers when expressed in HEK 293A cells (Mercier *et al.*, 2002). $BRET_{Max}$, however, reflects the relative orientations, distances, and expression levels of both donor and acceptor molecules (Guan *et al.*, 2009). The hCB_{1a} and hCB_{1b} homodimer saturation curve had significantly greater $BRET_{Max}$ values compared to the hCB_1-homodimer saturation curve. This indicates either that a larger proportion of hCB_{1a} and hCB_{1b} receptors can engage in dimerization than hCB_1 receptor or that the relative position of Rluc and GFP^2 within the hCB_{1a} and hCB_{1b} receptors are more permissive to energy transfer (Mercier *et al.*, 2002). Our results (using confocal images and on-cell western) showed that the two splice variants have higher cell-surface expression levels when heterologously expressed in HEK 293A cells, which might be the reason for the greater $BRET_{Max}$ observed.

Using a similar experimental approach, heterodimerization among hCB_1 and its splice variants was also demonstrated. These interactions were observed at low levels of expression, and were saturable as determined by BRET saturation curves. In addition, the interactions were competitively blocked by a receptor construct that was not tagged for BRET, suggesting that the interaction detected by BRET was specific. This was confirmed by co-expressing HERG, a non-competitive receptor, which is known not to interact with hCB_1 (Hudson *et al.*, 2010). Comparison of BRET saturation curves generated for the homodimers (hCB_1, hCB_{1a} and hCB_{1b}) and heterodimers (hCB_1-Rluc/hCB_{1a}-GFP^2, hCB_1-Rluc/hCB_{1b}-GFP^2 and hCB_{1a}-Rluc/hCB_{1b}-GFP^2), revealed that $BRET_{50}$ values for homodimers were lower than that for heterodimers. This finding might suggest that each hCB_1 variant has a higher affinity to form homodimers over heterodimers when the two receptors are heterologously expressed in HEK 293A cells.

When considering the maximal BRET values obtained for hCB_1-Rluc/hCB_{1a}-GFP^2, hCB_1-Rluc/hCB_{1b}-GFP^2 and hCB_{1a}-Rluc/hCB_{1b}-GFP^2 heterodimers, $BRET_{Max}$ values were found to be lower when compared to homodimers. The BRET saturation curve obtained from cells expressing the two splice variants hCB_{1a}-Rluc/hCB_{1b}-GFP^2 resulted in $BRET_{50}$ of 0.27 ± 0.014. This could indicate that dimerization between the two splice variants might occur with higher affinity compared to dimerization of each variant with hCB_1. However, it is hard to draw final conclusions regarding the affinity of each receptor to form homo- or heterodimers based on $BRET_{50}$ values obtained from BRET saturation curves, as interpretation of the $BRET_{50}$ values may be confounded by higher order GPCR oligomerization occurring in addition to dimerization (Guan *et al.*, 2009).

Given the affinity of hCB_1 and its splice variants to form homo- and heterodimers, $BRET_{Max}$ and $BRET_{50}$ values reflect a mixed population of dimeric forms when two different receptors are co-expressed. For example, if cells co-expressing hCB_1-Rluc and hCB_{1a}-GFP^2 fusion proteins, and we assumed that 100% of the expressed receptors will form dimers at equimolar concentrations of the two receptors (GFP^2/Rluc = 1), we would predict that 50% of the hCB_1-Rluc/hCB_{1a}-GFP^2 receptors would form heterodimers to produce BRET signals. The other 50% of the receptors would form homodimers (25% will form hCB_1 Rluc and 25% hCB_{1a}-GFP^2; Fig.4-2; Mercier *et al.*, 2002). The distribution will be influenced by *in vivo* affinity, intracellular distribution and it is possible that monomer, tetramer or higher-order oligomer scenarios may still occur.

Our data demonstrated that cannabinoid ligands are not required for the initiation of dimerization, since $BRET_{Eff}$ was detected for all receptor pairs (hCB_1, hCB_{1a}, hCB_{1b},

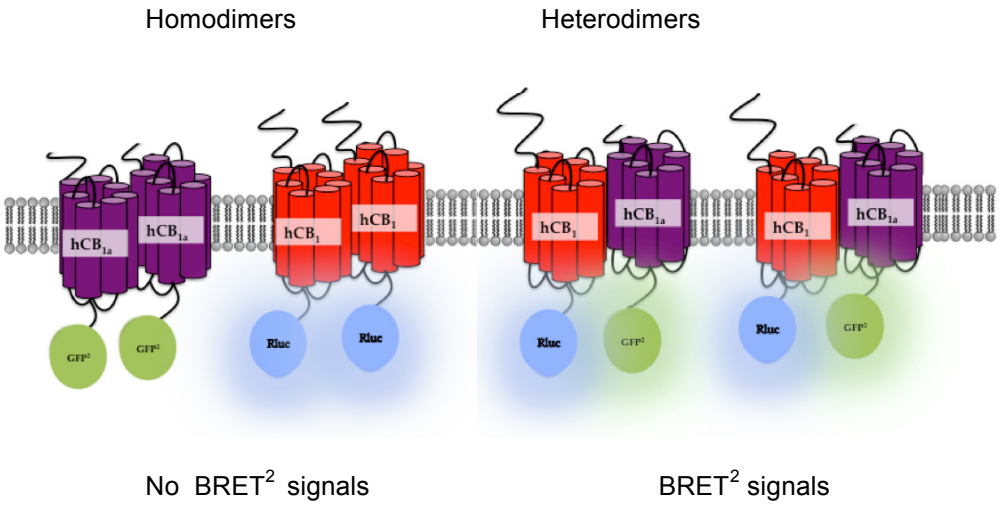

Figure 4.2: Schematic representation of the estimated percentage of hCB_1-Rluc and hCB_{1a}-GFP^2 dimers in living cells. At equimolar concentrations of the two receptors only 50% of the receptor will form heterodimers, resulting in a BRET signal, while the other 50% of receptor will form homodimers.

hCB_1/hCB_{1a}, hCB_1/hCB_{1b}, and hCB_{1a}/hCB_{1b}) in the absence of cannabinoids ligands. Treatment of cells with either the hCB_1 agonist WIN 55212-2, inverse agonist AM251 or neutral antagonist O-2050 did not alter $BRET_{Eff}$ values. This finding is in agreement with previous studies that reported that dimerization is a constitutive process that is not modulated by ligand binding, as binding of the ligand would only alter the conformation of the heterodimer in such a way that does not affect the $BRET_{Eff}$ (Terrillon and Bouvier, 2004; Guan *et al*., 2009).

The observed dimerization between and among hCB_1 and its N-terminal truncated variants also offers some insight into the main domains involved in dimerization. In general, the rhodopsin family of GPCRs is thought to dimerize by interaction of transmembrane domains (Milligan, 2004). However, some studies looking at the rhodopsin family of GPCRs reported that the N-terminal tail might be important for dimerization. For example, truncation of 53 amino acid at the N-terminal tail of the β_2-AR resulted in a receptor that is unable to dimerize with the bradykinin receptor (AbdAlla, *et a*l., 1999; Bai, 2004). Focusing on the hCB_1 receptor, the main domain involved in dimerization is not well known. However, a previous study has shown that the C-terminus of the hCB_1 receptor is not involved in the dimerization (Hudson *et al.,* 2010). Our results from the N-terminal truncated hCB_1 variants revealed that truncation of the N-terminal tail did not affect the ability of the receptor to dimerize. Consequently, we proposed that the N-terminal tail of the hCB_1 is not an obligate domain involved in hCB_1 dimerization, but might affect affinity. To precisely define the amino acid residues required for dimerization, additional experiment of site-directed mutagenesis of the receptor would be necessary.

4.3 Pharmacological Differences of hCB_1 Splice Variants Homo and Heterodimers

The signaling differences among hCB_1 and it splice variants remain controversial. Previous work has shown that the three hCB_1 receptor isoforms act through a $G_{i/o}$ protein to inhibit adenylyl cyclase and stimulate MAP kinase (Rinaldi-Carmona *et al*., 1996). In the present study, we assessed the difference in pERK signaling among hCB_1 receptor variants using the cannabinoid receptor agonist WIN 55212-2. In our results, significant differences among hCB_1 variants were found in their ability to stimulate ERK upon WIN 55212-2 treatment. The two variants showed lower efficiency (E_{max}) and affinity (pEC_{50}) values compared to hCB_1 receptors. Earlier studies have found that WIN 55212-2 exhibits a lower affinity to the truncated-receptor hCB_{1a} compared to the full-length receptor hCB_1 (Ryberg *et al*., 2005; Rinaldi-Carmona *et al*., 1996). The hydrophobic nature of cannabinoid ligands suggests that their ligand-binding site is localized within the transmembrane bundle of the receptor (McAllister *et al*., 2003). The N-terminal tail of the hCB_1 receptor is not directly involved in the formation of the ligand-binding pocket. The mechanism by which the N-terminal tail of the hCB_1 receptor is involved in ligand binding is still obscure. However, it has been suggested that the N-terminal tail could have some influence on the architecture of the ligand binding sites and truncation of the N-tail can reduce the affinity of ligand to the receptor. The reduced affinity may be the cause of the reduced efficiency observed with hCB_{1a} and hCB_{1b} receptors.

The role of the N-terminal tail in regulating GPCR trafficking is not well understood (Dong *et al*., 2007). There is some evidence that suggests that the N-terminal tail of the hCB_1 receptor might function in receptor trafficking from the endoplasmic reticulum to

the plasma membrane (Andersson *et al*., 2003). In the current study, we examined the differences in trafficking and subcellular localization patterns among hCB_1 and its variants when expressed in HEK 293A cells. The three variants were tagged at the C-terminus with GFP[2] and were transiently transfected into HEK 293A cells. By using confocal microscopy, we showed that the two splice variants, hCB_{1a} and hCB_{1b}, were mainly localized at the plasma membrane while the hCB_1 receptor was predominately accumulated intracellularly, which is consistent with previous studies (Bohn, 2007; Hudson *et al*., 2010). On-cell western analyses were also used to quantitatively measure total and cell-surface expression of each receptor variant. hCB_1 was tagged with a Myc tag antibody at the N-terminus, while hCB_{1a} and hCB_{1b} receptors were tagged with an HA tag. Similar to our confocal results, the hCB_{1a} and hCB_{1b} were expressed at higher levels and mainly localized at the cell membrane when transiently transfected into HEK 293A cells. The full-length hCB_1 receptor was mainly localized intracellularly. In order to eliminate the possibility that the differences in the measured expression levels are due to the use of different antibodies, similar experiments were conducted using untagged hCB_1 and hCB_{1b} receptors and an antibody directed against the first 14 amino acids of the N-terminal tail. Consistent results were found regarding their expression levels and cellular localization (data not shown). The findings in our study are supported by a study carried out by Andersson *et al*. (2003), who demonstrated that shortening the N-terminus of the CB_1 receptor greatly increases receptor stability, and results in increased targeting to the cell surface. In this study, the authors proposed that the large N- terminus of the hCB_1 receptor acts to inhibit efficient translocation of the receptor across the endoplasmic reticulum, leading to high levels of misfolded receptor that are subsequently degraded

(Andersson *et al*, 2003). In contrast, increasing the length of the N-terminal tail of the CB_1 receptor by adding a GFP tag was found to inhibit efficient receptor translocation across the endoplasmic reticulum (McDonald *et al.,* 2007). Taken together, these studies strongly support our findings that the N-terminal truncated hCB_1 variants have higher cell surface expression, than the full-length hCB_1.

Similar to other GPCRs, the hCB_1 receptor has been reported to associate with a variety of accessory proteins, which may direct both trafficking and cellular localization. These include G-protein receptor-associated sorting protein 1 (GASP1) and cannabinoid receptor-interacting protein 1a and 1b ($CRIP_{1a}$ and $CRIP_{1b}$; Smith *et al*., 2010). All these proteins bind at the C-terminal tail of the hCB_1 receptor and modulate cellular trafficking and signal transduction (Howlett *et al*., 2010; Smith *et al*., 2010). Alternatively spliced GPCR isoforms can differ in their ability to interact with accessory protein (Markovic & Challiss, 2009). It is still unclear, whether the increase cell surface expression observed with the two hCB_1 variants is caused solely by the truncated N-terminal tail, or by another accessory protein that interact with it.

Having revealed a physical interaction among hCB_1 and its variants, it was next important to demonstrate if this interaction had functional consequences for the full-length hCB_1. GPCR heterodimerization may influence the signaling pathways activated by the receptors present in the complex (Milligan, 2004; Terrillon and Bouvier, 2004). In HEK 293A cells transiently transfected with hCB_1-GFP^2 and either hCB_{1a}-GFP^2 or hCB_{1b}-GFP^2 and treated with the cannabinoid agonist WIN 55212-2, there was an increase in pERK, indicating that hCB_1-GFP^2 heterodimers couple to both $G_{i/o}$ pathway in these cells. Interestingly, co-expression of hCB_1 with its splice variant resulted in an

increase in both the E_{max} and Hill coefficient of the WIN-stimulated pERK dose-response of these cells, but not the pEC_{50}. This apparent increase in E_{max} could be explained either by an increase in the hCB_1 heterodimer complex coupling to $G_{i/o}$, or by an increase in cell-surface expression of the hCB_1 receptor. To examine these hypotheses, the trafficking of the Myc-hCB_1 was examined when expressed alone or with HA-hCB_{1a} or HA-hCB_{1b}. When hCB_1 receptor was expressed in HEK 293A cells, expression was observed in a punctate pattern. This is due to the high constitutive activity of the receptor resulted in a constitutive internalization of the receptor (Bohn, 2007), unlike the hCB_{1a} and hCB_1, which are mainly localized at the cell membrane. Similarly, dimerization of the hCB_1 receptor with the β_2-AR has been reported to enhance cell surface expression of the hCB_1 in HEK 293H cells (Hudson *et al*., 2010). Several examples of truncated GPCR variants have been reported to dimerize with their full-length receptors. Co-expression of these truncated receptors with their full-length receptors has been shown to decrease the membrane expression of their full-length receptors by dimerization (Bai, 2004). For example, a truncated splice variant of GnRH gonadotropin-releasing hormone, with altered trafficking was able to misroute the full-length receptor and reduce its membrane expression (Grosse *et al*., 1997; McElvaine and Mayo, 2006). However, this scenario does not seem the case for the hCB_1 receptor, since co-expression of the hCB_1 with its splice variants enhanced cell-surface expression of hCB_1 receptor in HEK 293A cells.

4.4 Future Directions

Our findings raised several interesting and important questions for further investigation. First, does the expression of the hCB_1 variants at both the transcript and

protein levels differ during development? and if so does that alter the function of the cannabinoid system during development?. To address this, a more detailed knowledge of the age-related brain distribution of the hCB_{1a} and hCB_{1b} transcripts and proteins is required and would increase our understanding of the physiological roles of these receptors. However, these studies face challenges due to the difficulty in obtaining postmortem human brain tissue of different ages suitable for anatomical investigation. For such studies, an isoform specific antibody would be useful and would complement our western blot analysis. Second, do the relative expression levels of hCB_1 and its variants alter during diseases? For example, the expression levels of the hCB_1 variant transcripts have been reported to change in non-Hodgkin lymphoma. Overexpression of the hCB_1 transcript was observed in lymph nodes of patients with non-Hodgkin's lymphoma compared to lymph nodes of normal individuals. However, low levels of the hCB_{1a} splice variant were detected in 44% of the tested patients, while hCB_{1b} expression was not detected (Gustafsson *et al.,* 2008). This study clearly demonstrated that during the progression of non-Hodgkin's lymphoma, not only is the full-length receptor level altered, but also that of the two truncated variants. It is well documented that normal GPCR expression levels are required for their appropriate physical interactions and functions; however, alterations in the expression level of one or all subunits in the heteromeric protein complexes would be expected to have profound effects on function, leading to abnormal signaling, and disease progression (Dalrymple *et al.,* 2008). Further studies focusing on analysis of the relationship between the expression levels of all hCB_1 and splice variant transcripts and protein levels are required in order to establish the role of these variants in human diseases. Third, do the three hCB_1 variants physically interact

in vivo and do they have higher affinities to form homo- or heterodimers? To answer this, an isoform specific antibody would be of great value to confirm that physical interaction can occur *in vivo* by using co-immunoprecipitation approach.

4.5 Conclusion

In summary, the present work showed overlapping distribution of the hCB_1 variant transcripts in different regions of the human brain. Similarly, hCB_1 protein variants were distributed throughout the monkey brain. We identified a novel mechanism of the hCB_1 receptor splice variants function, in which the truncated receptors can form a physical complex with the full-length hCB_1 receptor and increase cell surface expression of hCB_1, thereby enhancing the signaling activity of the full-length hCB_1 receptor through ERK in HEK 293A cells. Having demonstrated that the hCB_1 can dimerize with its variants, I suggest that future work should take this finding in to consideration when studying the pharmacology of the endocannabinoid system, or designing ligands that target the endocannabinoids system for the treatment of various diseases.

References

AbdAlla, S., Zaki, E., Lother, H. and Quitterer, U. (1999) Involvement of the amino terminus of the B (2) receptor in agonist- induced receptor dimerization. *J Biol Chem*, **274**, 26079-26084.

Abood, M.E., & Martin, B.R. (1992) Neurobiology of marijuana abuse. *Trends Pharmacol. Sci,* **13**, 201-6.

Andersson, H., D'antona, A.M., Kendall, D.A., Von Heijne, G. & Chen, N.C. (2003) Membrane assembly of the cannabinoid receptor 1: impact of a long N-terminal tail. *Mol Pharmacol*, **64**, 570-577.

Apaja, P.M., Tuusa, J.T., Pietila, E.M., Rajaniemi, H.J. & Petaja-Repo,U.E. (2006) Luteinizing hormone receptor ectodomain splice variant misroutes the full-length receptor into a subcompartment of the endoplasmic reticulum. *Molecular Biology of the Cell*, 17, 2243–2255.

Bai, M. (2003) Dimerization of G-protein-coupled receptors: roles in signal transduction. *Cellular Signaling,* **16**, 175–186.

Benkirane, M., Jin, D.Y., Chun, R.F., Koup, R.A. & Jeang, K.T. (1997) Mechanism of transdominant inhibition of CCR5-mediated HIV-1 infection by CCR5**Δ**32. *J. Biol. Chem*, **272**, 30603**–**30606.

Bohn, L.M. (2007) Constitutive trafficking more than just running in circles? *Mol. Pharmacol.***71**, 957-.-8.

Bosier, B., Muccioli, G.G., Hermans, E. & Lambert, D.M. (2010) Functionally selective cannabinoid receptor signalling: Therapeutic implications and opportunities. *Biochemical Pharmacology*, **80**, 1–12.

Bovolin, P., S. Bovetti, S., Fasolo, A., Katarova, Z., Szabo, G., Shipley, M.T., Margolis, F.L. & Puche A.C. (2009) Developmental regulation of metabotropic glutamate receptor 1 splice variants in olfactory bulb mitral cells. *J Neurosci Res*, **87**, 369–379

Burset, M., Seledkov, I.A. & Solovyev, V.V. (2000) Analysis of canonical and non-canonical splice sites in mammalian genomes. *Nucleic Acids Res*, **28**, 4364-4375.

Carriba, P., Ortiz, O., Patkar, K., Justinova, Z., Stroik, J., Themann, A., Muller, C., Woods, A.S., Hope, B.T., Ciruela, F., Casado, V., Canela, E.I., Lluis, C., Goldberg, S.R., Moratalla, R. & Franco, R., Ferre, S. (2007) Striatal adenosine A (2A) and cannabinoid CB_1 receptors form functional heteromeric complexes that mediate the motor effects of cannabinoids. *Neuropsychopharmacology*, **32**,49-59.

Claeysen, S., Sebben, J., Becamel, C., Bockaert, J. & Dumuis. (1999) A. Novel brain-specific 5-HT4 receptor splice variants show marked constitutive activity: Role of the C-terminal intracellular domain. *Mol. Pharmacol,* **55**, 910-920.

Conn, P.J. & Pin J. (1997) Pharmacology and functions of metabotropic glutamate receptors. *Annu. Rev. Pharmacol. Toxicol*, **37**, 205–37.

Dalrymple, M.B., Pfleger, K.D.G. & Eidne, K.A. (2008) G protein-coupled receptor dimers: Functional consequences, disease states and drug targets. *Pharmacology & Therapeutics*, **118**, 359–371.

Demuth, D.G. & Molleman, A. (2006) Cannabinoid signaling. *Life Sci,* **78**, 549-63.

Denovan-Wright, E.M., Gilby, K.L., Howlett, S.E. & Robertson, H.A. Isolation of total cellular RNA from brain tissue. http://fds.oup.com/www.oup.co.uk/pdf/pas/5-7-2.pdf (23 August. 2001)

Devane, W.A., Hanus, L., Breuer, A., Pertwee, R.G., Stevenson, L.A., Griffin, G., Gibson, D., Mandelbaum, A., Etinger, A. & Mechoulam, R. (1992) Isolation and structure of a brain constituent that binds to the cannabinoid receptor. *Science,* **258**,1946-9.

Dong, C., Filipeanu, C.M., Duvernay, M.T. & Wu, G. (2007) Regulation of G protein-coupled receptor export trafficking. *Biochim Biophys Acta*, **1768**, 853–870.

Dupré, D.J., Robitaille, M., Ethier, N., Villeneuve, L.R., Mamarbachi, A.M. & Hebert, T.E. (2006) Seven transmembrane receptor core signaling complexes are assembled prior to plasma membrane trafficking. *J. Biol. Chem,* **281**, 34561-73.

Duvernay, M.T., Filipeanu, C.M., Wu, G. (2005) The regulatory mechanisms of export trafficking of G protein-coupled receptors.*Cellular Signalling* , **17**, 1457-1465.

Eggan, S.M. & Lewis, D.A. (2007) Immunocytochemical distribution of the cannabinoid CB1 receptor in the primate neocortex: a regional and laminar analysis. *Cereb Cortex*, **17**,175-191.

Ellis, J., Pediani, J.D., Canals, M., Milasta, S. & Milligan, G. (2006). Orexin-1 receptor cannabinoid CB_1 receptor heterodimerization results in both ligand-dependent and independent coordinated alterations of receptor localization and function. *J. Biol. Chem,* **281**, 38812-24.

Galvez, T., Duthey, B., Kniazeff, J., Blahos, J., Rovelli, G., Bettler,B., Pr**é**zeau, L. & Pin, J.P. (2001) Allosteric interactions between GB1 and GB2 subunits are required for optimal GABAB receptor function. *EMBO J.*, **20,** 2152-2159.

George, S.R., O'Dowd, B.F. & Lee S.P. (2002) G-protein-coupled receptor oligomerization and its potential for drug discovery. *Nat. Rev. Drug Discov*, **1**, 808-820.

Glass, M. & Felder, C.C. (1997) Concurrent stimulation of cannabinoid CB_1 and dopamine D2 receptors augments cAMP accumulation in striatal neurons: Evidence for a Gs linkage to the CB_1 receptor. *J. Neurosci,* **17**, 5327-33.

Grosse, R., Schoneberg, T., Schultz, G. & Gudermann, T. (1997) Inhibition of gonadotropin-releasing hormone receptor signaling by expression of a splice variant of the human receptor. *Mol. Endocrinol*, **11**, 1305**–**1318.

Guan, R., Feng, X., Wu, X., Zhang, M., Zhang, X., Hebert, T.E. & Segaloff, D.L. (2009) Bioluminescence resonance energy transfer studies reveal constitutive dimerization of the human lutropin receptor and a Lack of correlation between receptor activation and the propensity for dimerization. *The Journal of Biological Chemistry,* **284**, 7483–7494.

Gurevich, V.V & Gurevich, E.V. (2008) GPCR monomers and oligomers: it takes all kinds.*Trends Neurosci*, **31**, 74-81.

Gustafsson, K., Wang, X., Severa, D., Eriksson, M., Kimby, E., Merup, M., Christensson, B., Jenny Flygare & Sander, B. (2008) Expression of cannabinoid receptors type 1 and type 2 in non-Hodgkin lymphoma: growth inhibition by receptor activation. *Int. J. Cancer*, **123**, 1025–1033.

Hague, C., Chen, Z., Pupo, A.S., Schulte, N.A, Toews, M.L. & Minneman, K.P. (2004) The N terminus of the human alpha1D-adrenergic receptor prevents cell surface expression. *J Pharmacol Exp Ther,* **309**, 388-397.

Hosking, R.D. & Zajicek, J.P. (2008) Therapeutic potential of cannabis in pain medicine. *BJA*, 10159-68.

Howlett, A.C., Breivogel, C.S., Childers, S.R., Deadwyler, S.A., Hampson, R.E. & Porrino, L.J. (2004) Cannabinoid physiology and pharmacology: 30 years of progress. *Neuropharmacology,* **47,** 345–358.

Howlett, A.C., Blume, L.C. & Dalton, G.D. (2010) CB_1 cannabinoid receptors and their associated proteins. *Curr Med Chem*, **17**, 1382-1393.

Hu, C.D., Chinenov, Y. & Kerppola, T.K. (2002) Visualization of interactions among bZIP and rel family proteins in living cells using bimolecular fluorescence complementation. *Mol. Cell,* **9**, 789-98.

Hudson, B.D., Hébert, T.E. & Kelly, M. E. (2010) Physical and functional interaction between CB_1 cannabinoid receptors and β_2-adrenoceptors. *British Journal of Pharmacology*, **160**, 627–642.

Hughes, T.A. 2006) Regulation of gene expression by alternative untranslated regions. *Trends Genet*, **22**,119-22.

Karpa, K.D., Lin, R., Kabbani, N. & Levenson, R. (2000) The Dopamine D3 Receptor interacts with itself and the truncated D3 splice variant D3nf: D3-D3nf interaction causes mislocalization of D3 receptors. *Mol Pharmacol,* **58**, 677-683.

Kearn, C.S., Blake-Palmer, K., Daniel, E. Mackie, K. & Glass, M. (2005) Concurrent Stimulation of cannabinoid CB1 and dopamine D2 receptors enhances heterodimer formation: a mechanism for receptor cross-talk?. *Mol Pharmacol*, **67**,1697–1704.

Khan, Z.U, Mrzljak, L., Gutierrez, A.T., De La Calle, A. & Goldman-Rakic, P.S. (1998) Prominence of the dopamine D2 short isoform in dopaminergic pathways. *PNAS*, **95**, 7731-7736

Kilpatrick, G.J., Dautzenberg, F.M., Martin, G.R. & Eglen, R.M. (1999) 7TM receptors: the splicing on the cake. *Trends Pharmacol Sci*, **20**, 294-301.

McElvaine, A.T. & Mayo K.E. (2006) A dominant-negative human growth hormone-releasing hormone (GHRH) receptor splice variant inhibits GHRH binding. *Endocrinology*, **147**, 1884–1894.

Mackie, K. (2005) Cannabinoid receptor homo- and heterodimerization. *Life Sci,* **77**, 1667-1673.

Mackie, K. (2005) Distribution of cannabinoid receptors in the central and peripheral Nervous System. *HEP*, **168**, 299–325.

McDonald, N.A., Henstridge, C.M., Connolly, C.N. & Irving, A.J. (2007) Generation and functional characterization of fluorescent, N-terminally tagged CB_1 receptor chimeras for live-cell imaging. *Mol. Cell. Neurosci*, **35**, 237–248.

Markovic, D. & Challiss, R.A. (2009) Alternative splicing of G protein-coupled receptors: physiology and pathophysiology. *Cell. Mol. Life Sci,* **66**, 3337–3352.

Markovic, D. & Grammatopoulos, D.K. (2009) Focus on the splicing of secretin GPCRs transmembrane-domain 7. *Trends Biochem Sci*, **34**, 443-52.

Marcellino, D., Carriba, P., Filip, M., Borgkvist, A., Frankowska, M., Bellido, I., Tanganelli, S., Muller, C.E., Fisone, G., Lluis, C., Agnati, L.F., Franco, R. & Fuxe, K. (2008) Antagonistic cannabinoid CB_1/dopamine D_2 receptor interactions in striatal CB_1/D_2 heteromers. A combined neurochemical and behavioral analysis. *Neuropharmacology.* **54**, 815-23.

Matsuda, L.A., Lolait, S.J.,Brownstein, M.J., Young, A.C. & Bonner, T.I. (1990) Structure of a cannabinoid receptor and functional expression of the cloned cDNA. *Nature,* **346**, 561-4.

Maudsley, S., Bronwen, M. & Luttrell, L., M. (2005) The origins of diversity and specificity in G protein-coupled receptor signaling. *JPET*, **314**, 485-494.

McAllister, C.D., Rizvi,G., Anavi-Goffer, S., Hurst, D.P., Barnett-Norris,J.,Lynch, D.L., Reggio, P.H. & Mary E. Abood, M.E.(2003) An aromatic microdomain at the cannabinoid CB_1 Receptor constitutes anagonist/inverse agonist binding region. *J. Med. Chem*, ***46***, 5139-5152.

McElvaine, A.T. & Mayo, K.E. (2005) A dominant-negative human growth hormone-releasing hormone (GHRH) receptor splice variant inhibits GHRH binding. *Endocrinology*, **147**, 1884–1894.

Mechoulam, R., & Gaoni, Y. (1967). The absolute configuration of Δ-1 tetrahydrocannabinol, the major active constituent of hashish. *Tetrahedron Lett*, **12**,1109-11.

Mechoulam, R. (1970). Marihuana chemistry. *Science*, **168**, 1159-66.

Mechoulam, R., Ben-Shabat, S., Hanus, L., Ligumsky, M., Kaminski, N.E., Schatz, A.R.,Gopher, A., Almog, S., Martin, B.R. & Compton, D.R. (1995). Identification of an endogenous 2-monoglyceride, present in canine gut, that binds to cannabinoid receptors. *Biochem. Pharmacol*, **50**, 83-90.

Mercier, J.F., Salahpour, A., Angers, S., Breit, A. & Bouvier, M. (2002) Quantitative assessment of β_1- and β_2-adrenergic receptor homo- and heterodimerization by bioluminescence resonance energy transfer. *The Journal of Biological Chemistry*, **277**, 44925-44931.

Minneman, K.P. (2001) Splice variants of G protein-coupled receptors. *Mol Interv*, **1**, 108-16.

Milligan, G. (2004) G protein-coupled receptor dimerization: function and ligand pharmacology. *Mol Pharmacol,* **66**, 1–7.

Millar, R.P. & Newton, C.L. (2010) The year in G protein-coupled receptor research. *Mol Endocrinol*, **24**, 261–274.

Miller, J. (2004) Tracking G protein-coupled receptor trafficking using Odyssey Imaging. http://www.licor.com/bio/PDF/Miller_GPCR.pdf (25 Jul. 2006).

Miller, L.K. & Devi, L.A. (2011) The highs and lows of cannabinoid receptor expression in disease: mechanisms and their therapeutic implications. *Pharmacol Rev,* **63**, 461–470.

Miyake, A. (1995) A truncated isoform of human CCK-B/gastrin receptor generated by alternative usage of a novel exon. *Biochem Biophys Res Commun*, **208**, 230-7.

Munro, S., Thomas, K.L. & Abu-Shaar, M. (1993) Molecular characterization of a peripheral receptor for cannabinoids. *Nature*, **365**, 61-5.

Nakamura, K., Yamashita, S., Omori, Y. & Minegishi, T. (2004) A Splice variant of the human luteinizing hormone (LH) receptor modulates the expression of wild-type human LH receptor. *Molecular Endocrinology*, **18**, 1461–1470.

Pinto, J.G., Hornby, K.R., Jones, D.G. & Murphy K.M. (2010) Developmental changes in GABAergic mechanisms in human visual cortex across the lifespan. *Front Cell Neurosci*, **10**: 4-16.

Pfleger, K.D. & Eidne, K.A. (2005) Monitoring the formation of dynamic G-protein-coupled receptor-protein complexes in living cells. *Biochem. J,* **385**, 625-37.

Prinster, S.C., Hague, C. & Hall, R.A. (2005) Heterodimerization of G protein-coupled receptors: specificity and functional significance. *Pharmacol Rev,* **57,** 289-298.

Przybyla, J.A., & Watts, V.J. (2010). Ligand-induced regulation and localization of cannabinoid CB_1 and dopamine D2L receptor heterodimers. *J. Pharmacol. Exp. Ther.* **332**, 710-9.

Rinaldi-Carmona, M., Calandra, B., Shire, D., Bouaboula, M., Oustric, D., Barth, F., Casellas, P., Ferrara, P. & Le Fur, G. (1996) Characterization of two cloned human CB1 cannabinoid receptor isoforms. *J Pharmacol Exp Ther*, **278**, 871-8.

Richtand, N.M. (2006) Behavioral Sensitization, Alternative Splicing, and D3 Dopamine Receptor-Mediated Inhibitory Function. *Neuropsychopharmacology*, **31**, 2368–2375.

Rios, C.D., Jordan, B.A., Gomes, I. & Devi, L. A. (2001). G-protein-coupled receptor dimerization: Modulation of receptor function. *Pharmacol. Ther,* **92**, 71-87.

Rios, C.D., Gomes, I. & Devi, L.A. (2006). μ opioid and CB_1 cannabinoid receptor interactions: Reciprocal inhibition of receptor signaling and neuritogenesis. *Br. J. Pharmacol,* **148**, 387-95.

Rozenfeld, R., Gupta, A., Gagnidze, K., Lim, M.P., Gomes, I., Lee-Ramos, D., Nieto, N. & Devi L.A. (2011) AT_1R–CB_1R heteromerization reveals a new mechanism for the pathogenic properties of angiotensin II. *The EMBO Journal*, **30**, 2350–2363.

Ryberg, E., Vu, H.K., Larsson, N., Groblewski, T., Hjorth, S., Elebring, T., Sjögren, S. & Greasley, P.J. (2005) Identification and characterization of a novel splice variant of the human CB1 receptor. *FEBS Letters*. **579**, 259–264.

Sarzania, R., Bordicchiaa, M., Marcuccia, P., Bedettaa, S., Santinia, S., Giovagnolia, A., Scappinia, L., Minardib, D., Muzzonigrob, G., Dessì-Fulgheria, P. & Rappellia, A. (2009) Altered pattern of cannabinoid type 1 receptor expression in adipose tissue of dysmetabolic and overweight patients. *Metabolism Clinical and Experimental*. **58**, 361–367.

Shioda, T., Nakayama, E.E., Tanaka, Y., Xin, X., Liu, H., Kawana-Tachikawa, A., Kato, A., Sakai, Y., Nagai, Y. & Iwamoto, A. (2001) Naturally occurring deletional mutation in the C-terminal cytoplasmic tail of CCR5 affects surface trafficking of CCR5. *J Virol*, **75**, 3462–3468.

Shire, D., Carillon, C., Kaghad, M., Calandra, B., Rinaldi-Carmona, M., Le Fur, G., Caput, D. & Ferrara, P. (1995) An amino-terminal variant of the central cannabinoid receptor resulting from alternative splicing. *J Biol Chem*, **270**, 3726-3731.

Smith, T.H., Sim-Selley, L.J. & Selley, D.E. (2010) Cannabinoid CB1 receptor-interacting proteins: novel targets for central nervous system drug discovery?. *Br J Pharmacol*, **160**, 454-466.

Szidonya, L., Cserzo, M., and Hunyady, L. (2008) Dimerization and oligomerization of G-protein-coupled receptors: debated structures with established and emerging functions. *Journal of Endocrinology*. 1**96**, 435–453.

Terrillon, S. & Bouvier, M. (2004) Roles of G-protein-coupled receptor dimerization. From ontogeny to signalling regulation. *EMBO reports,* **5**, 3 –34.

Tress, M.L., Martelli, P.L., Frankish, A., Reeves, G.A, Wesselink, J.J., Yeats, C., Olason, P.I., Albrecht, M., Hegyi, H., Giorgetti, A., Raimondo, D., Lagarde, J., Laskowski, R.A., López, G., Sadowski, M.I., Watson, J. D., Fariselli, P., Rossi, I., Nagy, A., Kai, W., Storling, Z., Orsini, M., Assenov, Y., Blankenburg, H., Huthmacher, C., Ramírez, F., Schlicker, A., Denoeud, F., Jones, P., Kerrien, S., Orchard, S., Antonarakis, S. E., Reymond, A., Birney, E., Brunak, S., Casadio, R., Guigo, R., Harrow, J., Hermjakob, H., Jones, D.T., Lengauer, T., Orengo, C. A., Patthy, L., Thornton, J.M., Tramontano, A., Valencia A. (2007) The implications of alternative splicing in the ENCODE protein complement. *PNAS,* **104**, 5495-500.

Vilardaga, J.P., Bünemann, M., Feinstein T.N., Lambert N., Nikolaev, V.O., Engelhardt,S., Lohse, M.J. & Hoffmann, C. (2009) GPCR and G protein: drug efficacy and activation in live cells. *Molecular Endocrinology,* **23**,590-599.

Wager-Miller, J., Ruth Westenbroek, R., Mackie, K. (2002) Dimerization of G protein-coupled receptors: CB1 cannabinoid receptors as an example. *Chemistry and Physics of Lipids*, 121, 83- 89.

Wang, X., Dow-Edwards, D., Keller, E. & Hurd, Y.L. (2003) Preferential limbic expression of the cannabinoid receptor mRNA in the human fetal brain. Neuroscience, **118**, 681-94.

Wilkie, T.M. (2001) Treasures throughout the life-cycle of G-protein-coupled receptors. *Trends Pharmacol.Sci,* **22**, 396-397.

Wilson, R.I. & Nicoll, R.A. (2001) Endogenous cannabinoids mediate retrograde signaling at hippocampal synapses. *Nature*, **410**, 588-92.

Xiao, J.C., Jewell, J.P., Lin, L.S., Hagmann, W.K., Fong, T.M. & Shen, C. (2008) Similar in vitro pharmacology of human cannabinoid CB1 receptor variants expressed in CHO cells. *Brain Res*, **1238**, 36-43.

Xu, J., Xu, M., Yasmin L. Hurd, Y. L., Pasternak, G.W. Pan, Y. (2009) Isolation and characterization of new exon 11-associated N-terminal splice variants of the human mu opioid receptor gene. *J Neurochem*, **108**,962-972.

Zhang, P.W., Ishiguro, H., Ohtsuki, T., Hess, J., Carillo, F., Walther , D., Onaivi, E.S., Arinami, T. & Uhl, G.R. (2004) Human cannabinoid receptor 1: 50 exons, candidate regulatory regions, polymorphisms, haplotypes and association with polysubstance abuse. *Molecular Psychiatry*, **9**, 916–931.

Zhu, X. & Wess, J. (1998) Truncated V2 vasopressin receptors as negative regulators of wild-type V2 receptor function. *Biochemistry,* **37**, 15773–15784.

Zurolo, E., Iyer, A.M., Spliet, W.G.M, Van Rijen, P.C., Troost, D., Gorter, J.A. & Aronica. E. (2010) CB_1 and CB_2 cannabinoid receptor expression during development and in epileptogenic developmental pathologies. *Neuroscience*, **170**, 28-41.

Distribution, Dimerization and Function of Human Cannabinoid Receptor Type 1 Coding Region Splice Variants

by

Amina Mustafa Bagher

Submitted in partial fulfilment of the requirements
for the degree of Master of Science

at

Dalhousie University
Halifax, Nova Scotia
July 2012

DALHOUSIE UNIVERSITY
DEPARTMENT OF PHARMACOLOGY

The undersigned hereby certify that they have read and recommend to the Faculty of Graduate Studies for acceptance a thesis entitled "Distribution, Dimerization and Function of Human Cannabinoid Receptor Type 1 Coding Region Splice Variants" by Amina Mustafa Bagher in partial fulfilment of the requirements for the degree of Master of Science.

Dated: 19-July-2012

Co-Supervisors: _____

_____

Readers: _____

_____

Departmental Representative: _____

DALHOUSIE UNIVERSITY

DATE: 19-July-2012

AUTHOR: Amina Mustafa Bagher

TITLE: Distribution, Dimerization and Function of Human Cannabinoid Receptor Type 1 Coding Region Splice Variants.

DEPARTMENT OR SCHOOL: Department of Pharmacology.

DEGREE: M.Sc. CONVOCATION: October YEAR: 2012

_____

Signature of Author

Table of Contents

List of Tables

List of Figures

Abstract

The pharmacological functions of the type 1 human cannabinoid receptor (hCB_1) are thought to be modulated through the isoform encoded by the fourth exon of the *CNR1* gene. Two other mRNA variants of the coding region of this receptor have been described, hCB_{1a} and hCB_{1b}. The contribution of these variants to endocannabinoid physiology and pharmacology remains unclear. In the present study, the three hCB_1 coding region variants mRNAs were detected in all human brain regions examined. Western blot analysis of homogenates from different regions of the monkey brain demonstrated that proteins with the expected molecular weights of CB_1, CB_{1a} and CB_{1b} receptors are present throughout the brain. In HEK cells, each of the receptor variants could form homodimers and variants formed heterodimers. Heterodimerization affected both the trafficking of hCB_1 receptor complexes and signalling in response to cannabinoid agonists.

List of Abbreviations and Symbols Used

2-AG	2-arachidonyl glycerol
A	adenosine
AEA	N-arachidonoylethanolamine, or anandamide
AM251	(N-(piperidin-1-yl)-5-(4-iodophenyl)-1-(2,4-dichlorophenyl)-4-methyl-1H- pyrazole-3-carboxamide)
ANOVA	analyses of variance
ATG	translation initiation codon
β_2AR	β_2 adrenergic receptor
BiFC	bimolecular fluorescence complementation
bp	base pair
BRET	bioluminescence resonance energy transfer
BSA	bovine serum albumin
cAMP	cyclic adenosine monophosphate
CCK	cholecystokinin
CCKR5	cholecystokinin receptor 5
CHO	Chinese hamster ovary cells
CNS	central nervous system
Co-IP	co-immunoprecipitation
$CRIP_{1a}$	cannabinoid receptor-interacting protein 1a
$CRIP_{1b}$	cannabinoid receptor-interacting protein 1b
D_{2S}	dopamine receptor 2 short isoform
D_{2L}	dopamine receptor 2 long isoform
D_3	dopamine receptor 3
DGL	diacylglycerol lipase
DTT	dithiothreitol
DMEM	Dulbecco's modified eagle's medium
DMSO	dimethyl sulfoxide
dNTP	deoxyribonucleotide

DNA	deoxyribonucleic acid
DRC	dose-response curve
ECS	endocannabinoid system
EDTA	ethylenediaminetetraacetic acid
ER	endoplasmic reticulum
ERK	extracellular-signal regulated kinase
G	guanine
FBS	fetal bovine serum
GABA	γ-aminobutyric acid
GFP^2	green fluorescent protein2
GDP	guanosine diphosphate
GPCR	G-protein coupled receptor
G protein	guanine nucleotide binding protein
GRK	g protein kinase
GTP	guanosine triphosphate
FITC	fluorescein isothiocyanate
FRET	fluorescence resonance energy transfer
H_2O	water
hMOR	human mu opioid receptor
HEPES	(4-(2-hydroxyethyl)-1-piperazineethanesulfonic acid)
HERG	human *ether--a--go--go* related gene
HEK	human embryonic kidney
HIV	human immunodeficiency virus
h	hours
IgG	immunoglobulin G
kDa	kilodaltons
m	minute
MAP kinase	mitogen activated protein kinase
mGluR6	metabotropic glutamate receptor 6
mGluR1	metabotropic glutamate receptor 1
mRNA	messenger RNA

NAT	N-acyltransferase
NCBI	National center for biotechnology information
O-2050	((6aR,10aR)-3-(1-Methanesulfonylamino-4-hexyn-6-yl)-6a,7,10,10a-tetrahydro-6,6,9-trimethyl-6H-dibenzo[b,d]pyran)
ORF	open reading frame
PBS	phosphate-buffered saline
PBST	phosphate-buffered saline with 0.1%tween-20
PCR	polymerase chain reaction
PFA	paraformaldehyde
PKA	protein kinase A
PTx	pertussis toxin
qPCR	quantitative polymerase chain reaction
RGS	regulator of G protein signaling proteins
Rluc	*Renilla* luciferase
RNA	ribonucleic acid
RT-PCR	reverse transcription polymerase chain reaction
s	seconds
SDS-PAGE	sodium dodecyl sulfate polyacrylamide gel electrophoresis
THC	Δ9-tetrahydrocannabinol
T	thymidine
TM	transmembrane
UTR	untranslated regions
VGCC	voltage gated calcium channel
WIN 55,212-2	WIN (R)-(+)-WIN55,212-2 mesylate (WIN) ((R)-(+)-[2,3-Dihydro-5-methyl-3-(4-morpholinylmethyl)pyrrolo[1,2,3-de]-1,4-benzoxazin-6 yl]-1-naphthalenylmethanone mesylate

Acknowledgements

In the name of ALLAH (GOD), the most merciful, the most compassionate

"The more you thank Me, the more I give you." Quran, 14:7

"Say: My Lord increase me in knowledge." Quran, 20:114

First of all, I would like to thank my supervisor Dr. Melanie Kelly for giving me this great opportunity to be a grad student at Dalhousie University and for her guidance. I also would like to thank my co-supervisor Dr. Eileen Denovan-Wright for her outstanding supervision, support and patience, without her guidance, I would not have been able to finish this thesis. I would like to thank my parents Norma and Mustafa for their support and encouragement who without them I would not be here. Thanks to my siblings Sarah, Kassem and Mariam for their support through the years. Thanks to my husband Abdullah and my big boy Louie for their love and patience. Thanks to our lovely lab technician Kay Murphy for all her technical help, and thanks to all the current and the past members of the Denovan-Wright lab, Robert Laprairie, Gregory Hosier, Mathew Hogel, Sophie Rowlands and Sarah Hutchings for their continuous help and sharing a good time. Finally I need to thank all the faculty and staff of the Department of Pharmacology for their help and support, in particular the members of my thesis advisory committee and examining committee, Dr. Christopher Sinal, Dr. Elizabeth Cowley and Dr. Denis Dupré.

Chapter 1: Introduction

G protein-coupled receptors (GPCRs) are the largest family of transmembrane receptors. GPCRs can physically interact with each other to form homo- and heterodimers. These interactions have profound impact on receptor trafficking, ligand binding and G protein coupling (Milligan, 2004). GPCR transcripts can undergo alternative splicing within their coding regions to generate receptor variants that may differ in their pharmacological, signaling and regulatory properties (Kilpatrick *et al*., 1999). The human cannabinoid receptor 1 (hCB_1), a GPCR that is highly expressed in the central nervous system, plays an important role in regulating neurotransmitter release (Howlett *et al*., 2004). Two mRNA variants of the hCB_1 coding region have been identified: hCB_{1a} and hCB_{1b} (Shire *et al*., 1995; Ryberg *et al*., 2005). The main aim of my thesis was to examine the distribution of CB_1 variant transcripts in human and monkey brain, to examine if hCB_{1a} and hCB_{1b} protein are expressed in the monkey brain, and to study physical interactions between hCB_1 receptor variants.

1.1 G Protein-Coupled Receptors

G protein-coupled receptors (GPCRs) are integral membrane proteins involved in signal transduction (Millar and Newton, 2010). GPCRs share a common architecture, which consists of an extracellular amino (N)-terminus, seven transmembrane spanning segments (TM) and an intracellular carboxyl (C)-terminus. They are activated by a diverse range of ligands including: light, odorants, hormones, neurotransmitters, chemokines, amino acids and Ca^{+2} ions. GPCRs can be broadly subdivided into five families according to their protein sequence and receptor function, including the

rhodopsin family, the secretin family, the glutamate family, the adhesion family, and the frizzled/taste2 family (Gurevich, 2008; Millar & Newton, 2010).

Signal transduction at GPCRs begins with an agonist binding to the receptor, which in turn switches the receptor from an inactive state to an active state conformation (Fig. 1.1). The activated receptor catalyzes the exchange of GDP for GTP on the α-subunit of heterotrimeric G proteins (Gαβγ), which in turn engages conformational and/or dissociational events between the Gα and dimeric Gβγ subunits. Both the GTP-bound Gα subunit and the Gβγ dimer can then initiate or suppress the activity of effector enzymes (*e.g*. adenylyl cyclases, phosphodiesterases, phospholipases), and ion channels (*e.g*. G protein-activated inwardly rectifying K+ channels) that modulate diverse signaling pathways (Vilardaga *et al*., 2009). Signaling ceases when GTP is hydrolyzed to GDP by intrinsic GTPase activity of the Gα subunit. The primary pathway leading to desensitization of a GPCR is initiated by phosphorylation of the intracellular C-terminus of the receptor by G-protein receptor kinase (GRK). Following phosphorylation, an arrestin scaffolding protein facilitates the internalization of the receptor, where it may either be degraded or recycled back to the cell surface (Millar & Newton, 2010; Duvernay *et al*., 2005).

In recent years, it has become clear that GPCR signaling is more complex and diverse than has been previously known. This complexity in signaling arises from numerous factors, among which are the ability of GPCRs to form both homo- and heterodimers, which modulates nearly every aspect of receptor pharmacology and function; the ability of receptors to adopt multiple "active" states with different effector coupling profiles; and the ability of non-G protein effectors to mediate some aspects of

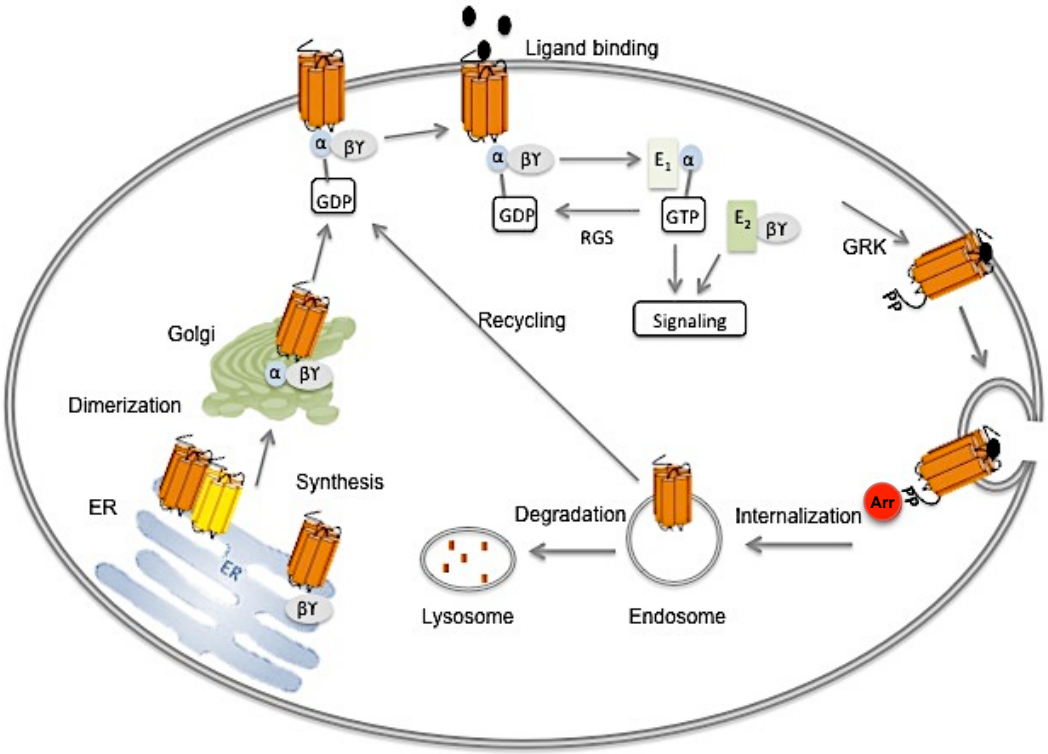

Figure 1.1: The life-cycle of a GPCR. GPCRs are synthesized and folded in the endoplasmic reticulum. Following this, the receptor is transported via secretory vesicle to the Golgi apparatus and eventually to the plasma membrane. Signal transduction at GPCRs begins with the agonist binding to the receptor, which catalyzes the exchange of GDP for GTP on the α-subunit of heterotrimeric G proteins (Gαβγ). This allows the activated G protein to act on downstream effectors and produce a biological response through their own effector 1 (E_1) and effector 2 (E_2). Signaling is then turned off by the hydrolysis of GTP back to GDP by the regulator of G protein signaling (RGS) proteins. The receptor will be internalized by phosphorylation of the intracellular region of the receptor by G protein kinase (GRK) and the recruitment of arrestin protein (Arr). The internalized receptor will either be degraded by the lysosome, or recycled back to the cell surface. GPCR dimerization persists throughout the cycle (Figure was modified from Wilkie *et al.,* 2001).

GPCR signaling (Maudsley *et al*., 2005). In addition, the discovery that GPCRs can undergo alternative splicing to generate multiple isoforms with distinct biochemical properties further increases the complexity of GPCR (Kilpatrick *et al*., 1999).

1.2 Alternative Splicing of GPCRs

Alternative splicing is a mechanism that increases the diversity of proteins that are encoded by the genome. Alternative splicing is the process by which introns are removed from precursor-mRNA (pre-mRNA) and exons are reconnected in multiple ways, resulting in alternative and sometimes multiple mature mRNA variants. The resulting different mRNA may be translated into different protein isoforms. Thus, a single gene may code for multiple proteins. In humans, over 90% of genes undergo alternative splicing giving rise to the exceptional complexity of human proteins (Kilpatrick *et al*., 1999; Markovic and Challiss, 2009). To date, alternative splicing has been reported for more than 50 GPCRs and some GPCRs have multiple variants (Markovic and Grammatopoulos, 2009). Alternative splicing of GPCRs can result from exon skipping, alternative exon insertion, and intron retention and consequently several receptor isoforms may be encoded by the same gene (Kilpatrick *et al*., 1999; Minneman, 2001). Many members of the rhodopsin family are expressed as multiple isoforms and all members of the secretin and glutamate families identified to date undergo extensive alternative splicing (Markovic and Challiss, 2009). Interestingly, alterative splicing of GPCRs is not limited to the open reading frame (ORF), but it can also occur in the 5'-untranslated region (5'-UTR) of the pre-mRNAs. The retention of alternate 5'-UTR may play an important role in controlling the translational efficiency, message stability and

subcellular localization of mRNAs (Hughes, 2006). GPCR splice variants have been identified by reverse transcriptase- polymerase chain reaction (RT-PCR) and by *in situ* hybridization. Whether alternatively spliced coding regions GPCRs are translated and expressed *in vivo* as receptors, or they undergo degradation, has not been determined for all alternatively spliced GPCRs mRNAs (Minneman, 2001).

1.2.1 Influence of Alternative Splicing on GPCRs Structure and Function

GPCR open reading frame splice variants can differ in the amino acid sequence of their C-terminal tails, N-terminal tails or transmembrane regions (Kilpatrick *et al*., 1999). There is a growing body of evidence showing that alternatively spliced GPCR isoforms might exhibit altered pharmacological properties, ranging from changes in ligand binding, signaling, G-protein coupling, constitutive activity and distribution (Minneman, 2001).

Knowing the sites of variation in GPCR structures that arise through splicing may give an insight regarding their pharmacological differences (Minneman, 2001). For example, the N-termini of GPCRs are usually involved in ligand recognition and binding. It has been reported that some N-terminal GPCR splice variants display altered ligand-binding properties. Cholecystokinin ΔCCK-B, an isoform of the CCK-B receptor, has lower affinity for CCK and gastrin compared to the full-length isoform (Miyake *et al*., 1995). In contrast, human μ opioid receptor (hMOR-1i), a splice variant for hMOR-1, having an additional 93 amino acids at the N-terminus, shows no significant difference in binding affinity compared to the hMOR-1 (Xu *et al*., 2009). Alternative splicing at the C-

terminal and the transmembrane domains of GPCRs has effects on the signaling pathways used by the receptors. For instance, the $mGluR_{1a}$ receptor, a C-terminal splice variant of the metabotropic glutamine receptor ($mGluR_1$), stimulates adenylate cyclase, as well as the production of inositol phosphate, unlike the other C-terminal splice variants that don't activate inositol phosphate (Coon and Pin, 1997). In addition to ligand binding and signaling, alternative GPCR splicing at the C-terminus has also been reported to alter the constitutive activity of the receptor. For example, $5\text{-}HT_{4a}$, a splice variant of the $5\text{-}HT_4$ receptor, has a much higher constitutive activity compared to the full-length receptor (Claeysan *et al*., 1999). However, constitutive activity is difficult to quantify, and is generally inferred from differences in second messenger levels caused by changes in receptor density following heterologous overexpression (Minneman, 2001). Lastly, GPCR splice variants might also exhibit different distribution patterns. A well-known example is the D_2 dopamine receptor, which exists in two isoforms including the short isoform (D_{2S}) and long isoform (D_{2L}). D_{2S} and D_{2L} receptors are formed by alternate splicing of the third intracellular loop. D_2 variants are differentially localized in central nervous system (CNS) neurons; the short isoform is localized pre-synaptically, especially in the hypothalamus and mesencephalon regions known to synthesize and release dopamine, while the long isoform is localized post-synaptically in the striatum and nucleus accumbens regions that receive dopaminergic output (Khan *et al*., 1998).

1.3 GPCRs Dimerization and its Functional Consequences

For many years, GPCRs were thought to exist and function as monomers. However, recent evidence has shown that many GPCRs can physically interact to form functional

homodimers, and can physically interact with other member of GPCRs to form heterodimers (Milligan, 2004; Prinster *et al*., 2005). Dimerization of GPCRs has been reported to have profound effects on receptor biosynthesis, trafficking, ligand binding and signal transduction (Rios *et al*., 2001; Terrillon and Bouvier, 2004).

Dimerization occurs early during the biosynthesis of the receptor in the endoplasmic reticulum (ER), and appears to persist through all phases of receptor trafficking to the cell membrane (Dupré *et al.*, 2006). Several studies have demonstrated that GPCR heterodimerization can affect receptor synthesis and trafficking to the plasma membrane. A good example is the gamma-aminobutyric acid B receptor ($GABA_B$), which exists as a heterodimer composed of $GABA_{B1}$ and $GABA_{B2}$. When each receptor is expressed alone, $GABA_{B1}$ is retained in the ER, whereas $GABA_{B2}$ reaches the cell surface as a nonfunctional receptor. Co-expression of $GABA_{B1}$ and $GABA_{B2}$ results in efficient surface expression of the receptor and the agonist affinity of these heterodimeric receptors were similar to the native $GABA_B$ receptor (Galvez *et al*., 2001). This observation confirms that dimerization of GPCRs is required for the appropriate maturation and trafficking of these receptors from the ER to the cell membrane (Milligan, 2004). Another aspect of GPCR function that is affected by dimerization is the ligand pharmacology of the interacting receptors. It has been reported that GPCR heterodimerization leads to both positive and negative ligand binding cooperativity between the receptors (Terrillon and Bouvier, 2004). An interesting consequence of dimerization with respect to ligand pharmacology is the concept that heterodimer-selective ligands could be created, which may be useful in reducing the side-effect of drug, as they act only on cells expressing the heterodimer (Milligan *et al*., 2004; Terrillon

and Bouvier, 2004). Another aspect of GPCR function that is altered by dimerization is signal transduction. Many studies have shown that the G-protein coupling preference for receptors may be altered by heterodimerization, while others have simply suggested that heterodimerization may either potentiate or inhibit receptor signaling through specific pathways (Bai, 2003; Milligan *et al*., 2004; Terrillon and Bouvier, 2004). A final aspect of GPCR function that is affected by dimerization is desensitization and internalization of the GPCRs following agonist activation. In a heterodimer, it has been found that activation of one receptor will lead to a cross-internalization and a cross-desensitization of the second receptor. These findings are supported by the observation that dimers appear to internalize as intact entities, instead of disassociating prior to internalization (Terrillon and Bouvier, 2004).

1.4 Physiological and Pathophysiological Roles of GPCR Splice Variants

There is a growing body of evidence that suggests that GPCR splice variants play important roles under normal as well as diseased conditions (Markovic and Grammatopoulos, 2009). Changes in expression of the full-length and spliced mRNAs during development have been reported for some GPCRs. A good example is the mGlu1b receptor variant. The $mGluR_{1b}$ mRNA was found to be the predominant isoform in embryonic mouse olfactory mitral cells, compared to postnatal day 7 when this variant is a minor component and the $mGluR_{1a}$ receptor predominates. This finding suggests a physiological function for $mGluR_{1b}$ in mitral embryonic cell maturation (Bovolin *et al.*, 2009). Moreover, it has been reported that some GPCRs are capable of physically

interacting with their splice variants to form heterodimers. Such interaction was found to affect every aspect of the full-length receptor function. Many members of the rhodopsin family GPCRs have been reported to dimerize with their splice variants, including GnRH gonadotropin-releasing hormone (Grosse *et al*., 1997; McElvaine and Mayo, 2005), vasopressin V2R (Zhu and Wess, 1998), D3 dopamine (Karpa *et al.*, 2000), and CCR5 chemokine receptors (Benkirane *et al.*, 1997; Shioda *et al*., 2001) and hLHR human luteinizing hormone (Nakamura *et al*., 2004; Apaja *et al.*, 2006). In all cases, it was found that the co-expression of the full-length receptor and its splice variants in a heterologous expression system resulted in a reduction in the cell surface expression of the full-length receptor. Studies suggest that this reduction in cell-surface expression is due to the retention of the wild-type receptor in the ER (Bai, 2003).

Dimerization of GPCRs with their splice variants has been linked to the pathophysiology of some diseases. For example, increase in the expression level of the truncated dopamine D_{3nf} mRNA was observed in the cortex of postmortem tissue from schizophrenia patients. D_{3nf} expression inhibits dopamine binding to full-length D_3 receptor, and also redirects full-length D_3 receptor localization away from the plasma membrane, and instead into an intracellular compartment. Alternation in the expression level of the truncated D_3 receptor was hypothesized to contribute to the abnormal dopamine activity observed in schizophrenia (Richtand, 2006; Karpa *et al*, 2000). Another example is the CCR5 receptor. It has been shown that a truncated variant of the human CCR5 receptor can reduce cell surface expression of the full-length CCR5 receptor, which inhibits CCR5 receptor-mediated human immunodeficiency virus (HIV) infection in individuals who are heterozygous for the mutant GPCR by forming

heterodimers with the wild-type receptor and thereby preventing its transport and delaying the development of HIV syndromes by 2-4 years (Benkirane *et al.*, 1997; George *et al*., 2002). Clearly, dimerization of GPCRs with their variants has profound influences on the full-length receptor functions.

1.5 The Cannabinoid System: the Cannabinoid Receptor 1 (CB_1)

The plant *Cannabis sativa* has been used for centuries for medical, religious, and recreational purposes due to its antiemetic, sedative, anti-inflammatory and psychotropic effects (Mechoulam & Gaoni, 1967). These effects have been attributed to the effect of delta-9-tetrahydrocannabinol (Δ9-THC), one of the active constituent of the plant, on two GPCRs: the cannabinoid receptor 1 (CB_1), predominantly found in the CNS and other peripheral tissues, and the cannabinoid receptor 2 (CB_2), mainly associated with immune cells (Mechoulam, 1970; Matsuda *et al*., 1990; Munro *et al.*, 1993). The CB_1 receptor regulates a variety of central and peripheral physiological functions, including neuronal development, neuromodulatory processes, energy metabolism as well as cardiovascular, respiratory and reproductive functions. The CB_2 receptor plays a role in modulating the immune system (Howlett *et al*., 2004; Bosier *et al.,* 2010).

The cannabinoid receptors, their endogenous ligands (endocannabinoids) and enzymes for their synthesis and degradation are referred to as the endocannabinoid system (ECS). The ECS activity is regulated by the enzymes responsible for the synthesis and the degradation of the endocannabinoids. Endocannabinoids are lipid neurotransmitters derived from arachidonic acid. The primary endocannabinoids are arachidonylethanolamide (anandamide or AEA), 2-arachidonoylglycerol (2-AG),

virodhamine and noladin ether (Devane *et al*., 1992; Mechoulam *et al*., 1995). These endocannabinoids are synthesized on demand at the site of action in response to specific signals, such as increases in intracellular calcium or activation of phospholipase Cβ by $G_{q/11}$ metabotropic receptors. Degradation of the endocannabinoids occurs locally by fatty-acid amide hydrolase (FAAH) and monoacylglycerol lipase (MGL; Howlett *et al*., 2004; Bosier *et al.,* 2010).

In the CNS, the CB_1 receptor is located presynaptically where it plays a modulatory role in the regulation of neurotransmitters release including: noradrenaline, acetylcholine, dopamine, GABA, glutamine, serotonin and glycine (Fig. 1.2; Abood & Martin, 1992; Wilson & Nicoll, 2001; Howlett *et al*., 2004). The CB_1 receptor preferentially couples to $G\alpha_i$, and CB_1 activation is associated with inhibition of adenylyl cyclase, decreases in the concentrations of cAMP, and activation of mitogen activated protein kinases (MAP kinase). In addition, CB_1 receptors are associated with inhibition of voltage-gated Ca^{2+} channels and activation of inward rectifying K^+ channels. In some cells CB_1 has been shown to signal through both $G\alpha_s$ and $G\alpha_{q/11}$ pathways to increase cAMP, and intracellular Ca^{2+}, respectively (Demuth and Molleman, 2006; Bosier *et al.,* 2010).

Cannabinoid agonists are divided into four structurally distinct groups. The first group contains the 'classical cannabinoids' derived from the plant *C. sativa* such as Δ9-THC and related synthetic derivatives such as, HU-210. The second group contains the non-classical cannabinoids, which are synthetic derivatives of the classical cannabinoids that lack the dihydropyran ring, for example, CP 55,940. The third group contains aminoalkylindoles, such as WIN 55212-2 and its related compounds. The fourth group

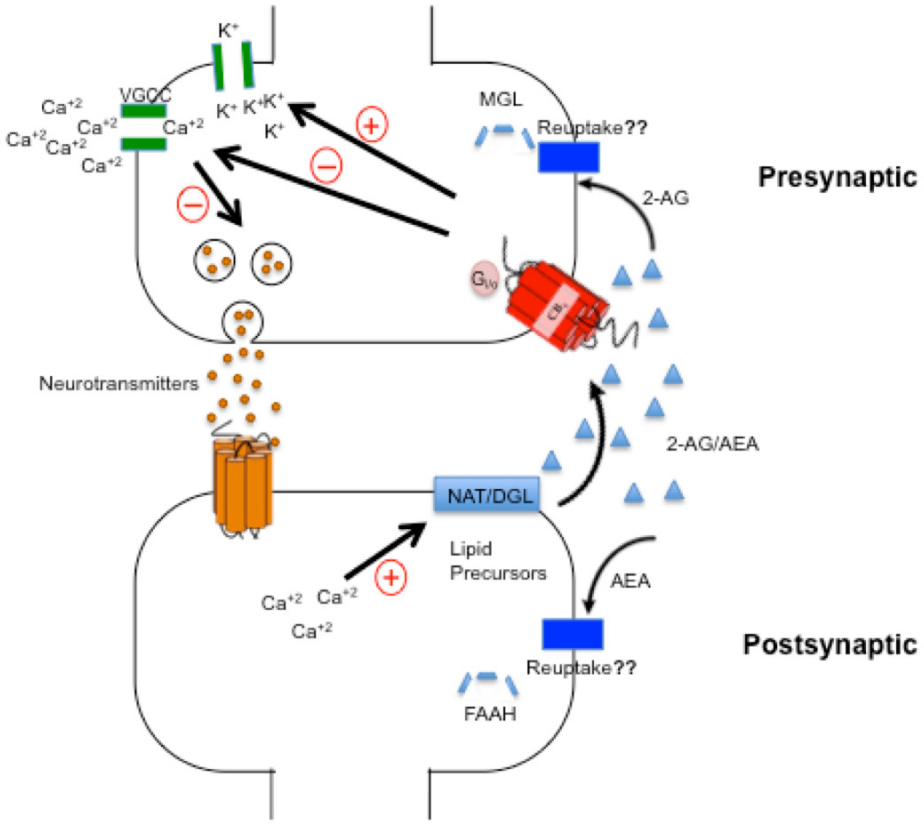

Figure 1.2: Diagram of CB_1 retrograde inhibition of neurotransmitter release. The increase in intracellular calcium levels in the postsynaptic terminal activates N-acyltransferase (NAT) or diacylglycerol lipase (DGL), which synthesize anadamide (AEA) or 2-arachidonyl glycerol (2-AG), respectively, from cellular phospholipids. AEA and 2-AG then travel back to the presynaptic terminal to activate CB_1 receptors (retrograde signaling). Activation of CB_1 receptors inhibit voltage gated calcium channel (VGCC), in addition to other presynaptic changes, which lowers the probability of Ca^{+2} dependent neurotransmitter release. Then, AEA is taken back up by the postsynaptic terminal, possibly by a plasma membrane protein transporter and/or by passive diffusion, and its signaling function terminated by conversion to arachidonic acid by fatty acid amide hydrolase (FAAH), while the 2-AG is taken up by the presynaptic terminal and is degraded by monoacylglycerol lipase (MGL; Figure was modified from Hosking, R.D. & Zajicek, J.P., 2008).

contains the endocannabinoids, which are eicosanoid compounds rather than cannabinoid compounds and includes the endocannabinoids AEA and 2-AG (Bosier *et al.,* 2010).

1.5.1 Human CB_1 Gene Structure and Splicing Pattern

The human CB_1 gene (*CNR1*) is located on chromosome 6 locus q14-q15. The *CNR1* gene was originally described as consisting of four exons and three introns. Exon 4 contains the entire protein coding regions of hCB_1, while the three non-coding exons, named exon 1, 2, and 3 are located 5' to the protein-coding region and are separated by three introns (introns 1, 2, and 3; Zhang *et al*., 2004). Alternative splicing of the 5'-UTR of the hCB_1 gene results in the formation of six hCB_1 transcripts with variable 5' UTR, termed variants 1, 2, 3, 4, 5 and 6 (Fig. 1.3). Each of these variants has a unique 5'- UTR, transcription initiation site and distribution pattern in the human brain and peripheral tissues. Alternations in the relative abundance of these variants have been reported in the visceral adipose tissue of obese patients (Sarzania *et al*., 2009). The translation of the hCB_1 receptor starts at the first ATG located at the 5' end of unspliced exon 4 and produces a polypeptide chain of 472 amino acids. This chain forms an exceptionally long extracellular N-terminal tail of 116 amino acids connected to seven transmembrane domains and ended by an intracellular carboxyl terminus (The National Center for Biotechnology Information, NCBI; Zhang *et al*., 2004). Alternative splicing of hCB_1 within the coding region has been totally ignored, as the fourth exon of the *CNR1* gene, that encodes the whole coding region of hCB_1 receptor was thought to be intronless,

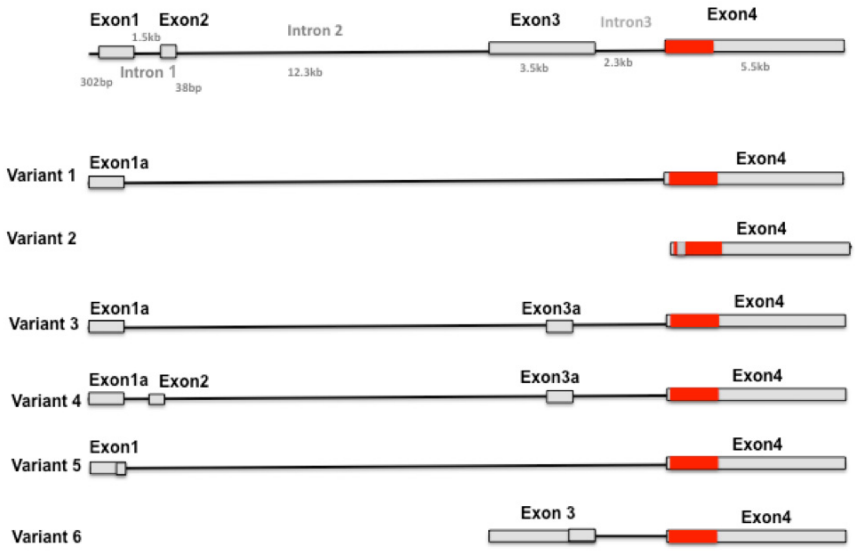

Figure 1.3: Schematic diagram of the human *CNR1* gene and mRNA variants. Six splice variants of the 5'UTR of hCB_1 gene have been identified. Exons are indicated by boxes, while introns are indicated by interconnecting lines. The coding region is indicated in red, while the non-coding region is indicated in grey (Figure was modified from Zhang *et al*., 2004).

which led to the belief that hCB_1 mRNA is not subjected to alternative splicing. As a result, all the pharmacological functions of the hCB_1 were thought to be modulated through the isoform encoded by the fourth exon of the *CNR1* gene. However, this view has now changed with the identification of the first hCB_1 receptor mRNA coding region splice variant, hCB_{1a} (411 amino acids; Shire *et al.*, 1995). Subsequently, the second hCB_1 splice variant mRNA, hCB_{1b} (439 amino acids) has been identified (Ryberg *et al*, 2005). Splicing within the coding region of transcript variant 2 results in the formation of hCB_{1a} and hCB_{1b} transcripts. The hCB_{1a} transcript lacks an internal segment of 167 base pairs within the sequence encoding the N-terminal tail of the receptor. Translation of the hCB_{1a} receptor starts at the second ATG located at the 5' end of exon 4 (Fig.1.4). The resulting receptor is shorter than hCB_1 by 61 amino acids at its N-terminus. In addition, the first 28 amino acids of the N-terminus are totally different to hCB_1, while the remaining 27 amino acids are similar to the hCB_1 receptor (Fig. 1.5 &1.6). hCB_{1a} also lacks two out of three glycosylation sites and resulted in a more hydrophobic receptor. hCB_{1b} transcript is missing an internal segment of 99 base pairs resulting in a protein lacking 33 amino acids at the N-terminus tail. However, unlike hCB_{1a}, translation of hCB_{1b} starts at the first ATG located in exon 4 as hCB_1 (Fig. 1.4, 1.5. & 1.6; Shire *et al*., 1995; Ryberg *et al*., 2005; Zhang *et al*., 2004). It has not been demonstrated yet if the hCB_{1a} and hCB_{1b} mRNAs are translated and expressed as functional receptors *in vivo*. Transcripts formed through alternative splicing within the coding region of the gene are of particular interest, as they have the potential to alter the biological function of the expressed protein (Tress *et al*., 2007).

Figure 1.4: Aligned sequences of the 5' end of hCB_1, hCB_{1b} and hCB_{1a} cDNA. hCB_1 translation start at the first ATG from mRNA that is unspliced in the coding region. hCB_{1b} translation starts at the same ATG from mRNA that is spliced at the 5' end of the coding region. Specifically, hCB_{1b} results from a 99-nucleotide excision between donor (5'hCB_{1b}) and acceptor (3' hCB_{1b}). hCB_{1a} results from a 167-nucleotide excision between donor (5'hCB_{1a}) and acceptor (3' hCB_{1a}),while translation starts at the second ATG. TM1 codes for the first transmembrane region. Splicing sites are indicated in red boxes. Dashes represent gaps. (Figure was modified from Shire *et al*., 1995; Xiao *et al*., 2008; NCBI).

```
hCB1    MKSILDGLAD TTFRTITTDL LYVGSNDIQY EDIKGDMASK LGYFPQKFPL          1
hCB1b   MKSILDGLAD TTFRTITTDL L--------- ---------- ----------
hCB1a         MALQ IPPSAPSPLT SCTWAQMTFS TKTSK----- ----------

                                       *      *
hCB1    TSFRGSPFQE KMTAGDNPQL VPADQVNITE FYNKSLSSFK ENEENIQCGE         51
hCB1b   ----GSPFQE KMTAGDNPQL VPADQVNITE FYNKSLSSFK ENEENIQCGE
hCB1a   ---------- ---------- ---------- ---------- ENEENIQCGE

                    *
hCB1    NFMDIECFMV LNPSQQLAIA VLSLTLGTFT VLENLLVLCV ILHSRSLRCR        101
hCB1b   NFMDIECFMV LNPSQQLAIA VLSLTLGTFT VLENLLVLCV ILHSRSLRCR
hCB1a   NFMDIECFMV LNPSQQLAIA VLSLTLGTFT VLENLLVLCV ILHSRSLRCR

hCB1    PSYHFIGSLA VADLLGSVIF VYSFIDFHVF HRKDSRNVFL FKLGGVTASF        151
hCB1b   PSYHFIGSLA VADLLGSVIF VYSFIDFHVF HRKDSRNVFL FKLGGVTASF
hCB1a   PSYHFIGSLA VADLLGSVIF VYSFIDFHVF HRKDSRNVFL FKLGGVTASF

hCB1    TASVGSLFLT AIDRYISIHR PLAYKRIVTR PKAVVAFCLM WTIAIVIAVL        201
hCB1b   TASVGSLFLT AIDRYISIHR PLAYKRIVTR PKAVVAFCLM WTIAIVIAVL
hCB1a   TASVGSLFLT AIDRYISIHR PLAYKRIVTR PKAVVAFCLM WTIAIVIAVL

hCB1    PLLGWNCEKL QSVCSDIFPH IDETYLMFWI GVTSVLLLFI VYAYMYILWK        251
hCB1b   PLLGWNCEKL QSVCSDIFPH IDETYLMFWI GVTSVLLLFI VYAYMYILWK
hCB1a   PLLGWNCEKL QSVCSDIFPH IDETYLMFWI GVTSVLLLFI VYAYMYILWK

hCB1-   AHSHAVRMIQ RGTQKSIIIH TSEDGKVQVT RPDQARMDIR LAKTLVLILV        301
hCB1b   AHSHAVRMIQ RGTQKSIIIH TSEDGKVQVT RPDQARMDIR LAKTLVLILV
hCB1a   AHSHAVRMIQ RGTQKSIIIH TSEDGKVQVT RPDQARMDIR LAKTLVLILV

hCB1    VLIICWGPLL AIMVYDVFGK MNKLIKTVFA FCSMLCLLNS TVNPIIYALR        351
hCB1b   VLIICWGPLL AIMVYDVFGK MNKLIKTVFA FCSMLCLLNS TVNPIIYALR
hCB1a   VLIICWGPLL AIMVYDVFGK MNKLIKTVFA FCSMLCLLNS TVNPIIYALR

hCB1    SKDLRHAFRS MFPSCEGTAQ PLDNSMGDSD CLHKHANNAA SVHRAAESCI        401
hCB1b   SKDLRHAFRS MFPSCEGTAQ PLDNSMGDSD CLHKHANNAA SVHRAAESCI
hCB1a   SKDLRHAFRS MFPSCEGTAQ PLDNSMGDSD CLHKHANNAA SVHRAAESCI

hCB1    KSTVKIAKVT MSVSTDTSAE AL                                      451
hCB1b   KSTVKIAKVT MSVSTDTSAE AL
hCB1a   KSTVKIAKVT MSVSTDTSAE AL
```

Figure 1.5: Amino acid sequence alignment of hCB_1, hCB_{1b} and hCB_{1a}. The N-terminus of the hCB_1 receptor consists of 116 amino acids, indicated in bold. The hCB_{1b} receptor lacks an internal segment of 33 amino acids within the sequence encoding the amino-terminal tail of the receptor, resulting in a receptor with 84-amino acid N-terminal tail. The hCB_{1a} receptor uses a different initiation coding leading to a frameshift from the reading frame of hCB_1; in addition it misses an internal segment of 56 amino acids. This results in a receptor with only 55 amino acids N-terminal tail that differs from hCB_1 in the first 28 amino acids (highlighted in grey). However, after the splice junction, the reading frame of hCB_1 is restored, and the remaining 27 amino acids of the NH_2 terminal of hCB_{1a} are identical to hCB_1. Glycosylation sites are indicated in red *. Dashes represent gaps

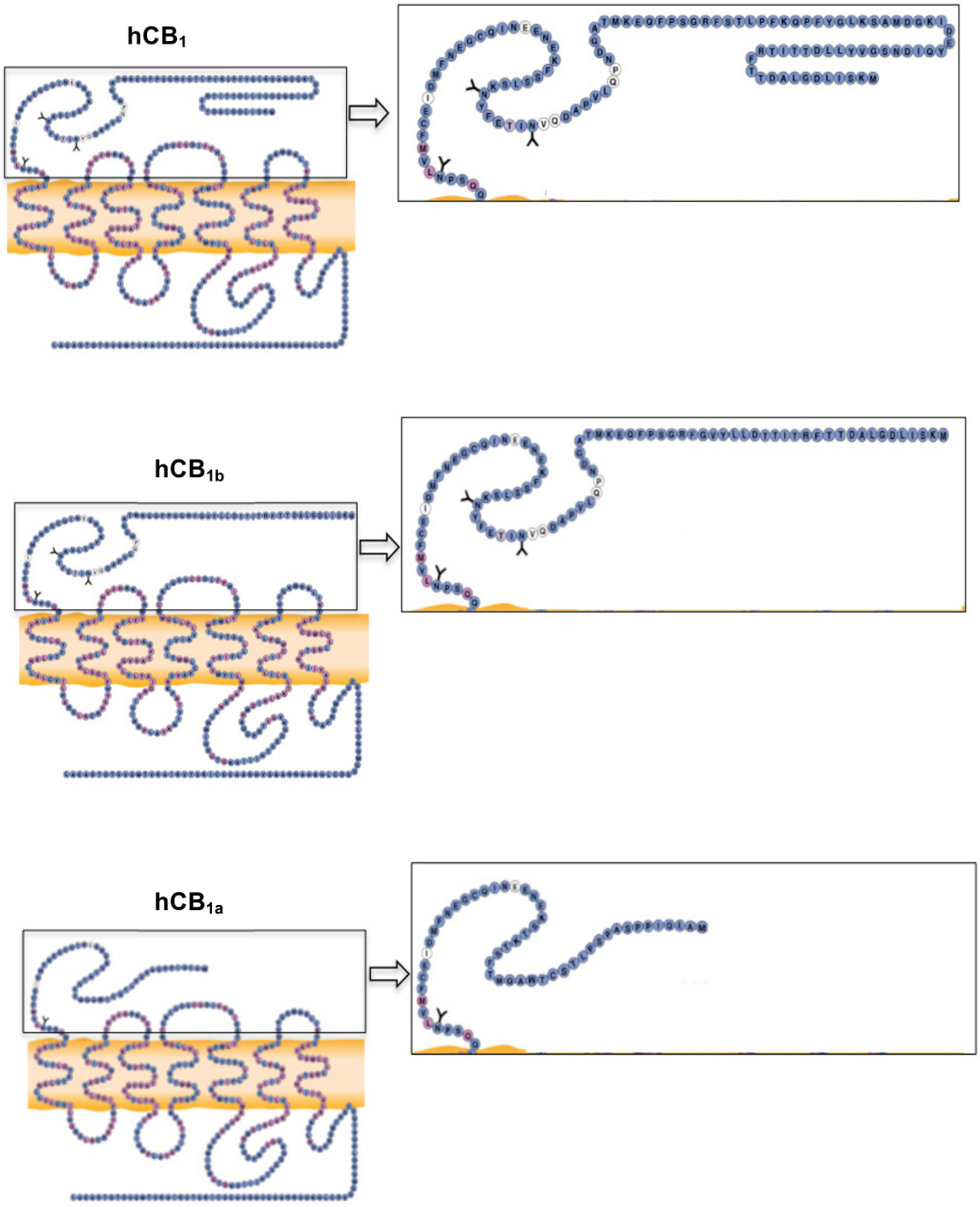

Figure 1.6: Schematic illustration of the amino acid sequences of hCB_1, hCB_{1b} and hCB_{1a} (Modified with permission of Cayman chemical company).

1.5.2 Distribution of hCB_1, hCB_{1a} and hCB_{1b} Receptors

The distribution of hCB_1 receptors has been extensively mapped by quantitative autoradiography, *in situ* hybridization and immunocytochemistry. High levels of the hCB_1 are expressed in neocortical association areas such as the prefrontal cortex and the cingulate cortex, which are known to mediate executive functions. Other brain regions involved in cognitive functioning, such as the hippocampus, basal ganglia, and cerebellum, also express high levels of the hCB_1. hCB_1 transcript is expressed in many regions of the human brain as early as the prenatal age (Wang *et al.,* 2003). The hCB_1 mRNA expression levels change during development. In the visual cortex of infants (<1 year) and pre-teens (5–11 years), the hCB_1 mRNA levels are about 40% higher compared to young children (1–2 years), adults (21–55 years), and the elderly (>55 years) (Pinto *et al*., 2010). In addition to the CNS, hCB_1 is expressed in several peripheral organs including the eye, gut, uterus, testis, vascular endothelium, spleen, and tonsils (Howlett *et al.,* 2004; Mackie, 2005).

The mRNAs of the hCB_{1a} and hCB_{1b} are expressed in the human brain and some peripheral tissues. Alteration in the distribution profiles of these transcripts has been reported during development and disease states (Shire *et al.,* 1995; Ryberg *et al.,* 2005; Xiao *et al*., 2008; Gustafsson *et al*., 2008). In the human brain, the hCB_1 and hCB_{1a} transcripts have been detected, using RT-PCR, in human adult total brain, brain stem, cortex, cerebellum, inferior hemisphere and temporal lobe (Shire *et al.,* 1995). Unlike hCB_1, hCB_{1a} mRNA was not detected in all the tested human infant brain regions including the brain stem and temporal lobe. The expression of the hCB_{1b} transcript has only been investigated in human fetal and adult total brain. It has not yet been determined if there is an overlap in the distribution patterns of the mRNAs of the three hCB_1 protein

variants in different regions of human adult brain. In the periphery, the transcripts of three hCB_1 coding region variants were detected in many peripheral tissues (adipose, testis, lung, kidney, jejunum, uterus, muscle, duodenum, and colon; Ryberg *et al.,* 2005). hCB_{1a} and hCB_{1b} transcripts were reported to be the minor transcripts compared to the hCB_1 transcript, as they represent fewer than 5% of the total hCB_1 transcripts depending on the examined tissues (Shire *et al,* 1995; Ryberg *et al.,* 2005; Xiao, 2008).

1.5.3 Functional Differences Between of hCB_1 and its Splice Variants

The existence of three isoforms of the human cannabinoid receptor 1 (hCB_1, hCB_{1a} and hCB_{1b}) has raised questions concerning their functional variations. A limited number of studies have attempted to address the functional differences between the hCB_1 receptor and its splice variants, as well as their physiological significance of these variants on the endocannabinoid system. One of the initial reports that characterized the hCB_{1a} splice variant, found that the binding of THC, CP55940 and WIN 5521-2 was slightly higher for hCB_1 than hCB_{1a} receptor, when either isoform was stably expressed in Chinese hamster ovary (CHO) cells. However, the endocannabinoid anandamide showed a similar affinity for both isoforms. Activation of hCB_{1a} by the cannabinoid agonists is able to inhibit cAMP and increase MAP kinase phosphorylation in a slightly lower extent compared to the full-length hCB_1 receptor (Rinaldi-Carmona *et al*., 1996). These results are consistent with the findings of Xiao *et al*. (2008). In this study, no significant difference in ligand binding and cAMP levels was observed among hCB_1, hCB_{1a} and hCB_{1b} receptors, in CHO cells, in responses to either endogenous cannabinoids (anandamide, 2-AG,

virodhamine and noladin ether) or synthetic cannabinoid ligands (CP55940 and AM251). In contrast, a study carried out by Ryberg *et al.*, (2005), reported that expression of hCB_{1a} and hCB_{1b} variants in human embryonic kidney (HEK) 293 cells displayed significantly less affinity and efficacy when treated with the endogenous cannabinoid ligands (anandamide, virodhamine and noladin ether) compared to hCB_1 receptor. In this study, 2-AG was found to act as an inverse agonist on both hCB_{1a} and hCB_{1b} receptors, while it acted as a full agonist on the hCB_1 receptors. The three receptors showed similar binding affinity and efficacy to synthetic ligands (Δ9-THC, CP55940, WIN 5521-2, HU210 and SR141716; Ryberg *et al*., 2005). A more recent study published in 2011 by Straiker *et al*., reported that hCB_1 variants signal more robustly compared to the hCB_1 in cultured hippocampal neurons. Given differences in general studies, the signaling properties for the hCB_1 variants are still poorly understood and further investigation is required.

1.5.4 Dimerization of the Cannabinoid Receptor 1 (CB_1)

Similar to other member of the Rhodopsin family of GPCR, the hCB_1 receptor forms both homodimers (Wager-Miller *et al*., 2002) and heterodimers with other GPCRs such as the D_2 dopamine receptor (Glass and Felder, 1997; Kearn *et al*., 2005), μ-, κ- and δ-opioid receptors (Rios *et al.,* 2006), orexin-1 (Ellis *et al*., 2006), A_{2a} adrenergic receptor (Carriba *et al.,* 2007) β_2-adrenergic receptor (β_2-AR; Hudson *et al*., 2010) and angiotensin II receptor (Rozenfeld *et al.,* 2011). These interactions have a profound functional implications on the function and pharmacology of the CB_1 receptor, including receptor trafficking, G protein coupling and signaling.

Homodimerization of the CB_1 receptor has been demonstrated by the observation of

a high molecular weight band on SDS-PAGE using an antibody directed against the C-terminal tail of CB_1 receptor; the high molecular weight bands have been anticipated as a dimer of higher molecular (Wager-Miller *et al.*, 2002). Homodimerization of the CB_1 receptor was further confirmed using the bioluminescence resonance energy transfer (BRET; Hudson *et al*., 2010). There is substantial evidence, using a variety of techniques, demonstrating that CB_1 can form dimers and higher order oligomers with a number of members the rhodopsin family of GPCRs. The first receptor demonstrated to form a heterodimer with CB_1 was the D_2 dopamine receptor. The functional interaction between the two receptors was first observed by Glass and Felder in 1997. They demonstrated that the co-activation of D_2 and CB_1, in both transfected cell lines and cultured striatal neurons, caused an increase in cAMP production, however stimulation of only one of the receptor results in an inhibition of cAMP. This response was found to be the result of stabilizing the CB_1 active state with increased coupling to G_s instead of G_i when the two receptors were co-activated (Kearn *et al.*, 2005). Physical interaction between the CB_1 and the D_2 receptors was confirmed using co-immunoprecipitation (Co-IP), fluorescence resonance energy transfer (FRET) and bimolecular fluorescence complementation (BiFC; Marcellino *et al.*, 2008, Przybyla and Watts, 2010). The CB_1 receptor has also been reported to form heterodimers with the μ, κ and δ opioid receptors using the BRET and FRET. The functional result of the CB_1/μ opioid receptor interaction is that signaling from both receptors is attenuated in the heterodimer, only when agonists for both receptors are present (Rios *et al.*, 2006). Using the fluorescence resonance energy transfer (FRET) technique, Ellis *et al.* (2006), reported that the CB_1 receptor dimerize with the orexin-1 receptor. In this study, it was shown that co-expression of the CB_1 and orexin-1

receptors altered the distribution of orexin-1 to a more intracellular distribution, similar to that of CB_1. Inverse agonists for either receptor were then able to return both receptors to the cell surface (Ellis *et al.*, 2006). In addition to D_2, opioid and orexin-1 receptors, the CB_1 receptor has also been reported to heterodimerize with the A_{2A} adenosine receptor. This was demonstrated both by Co-IP from rat striatal membranes, and by BRET in HEK 293 cells (Carriba *et al.*, 2007). Such an interaction was found to influence CB_1 signaling, such that CB_1 receptor did not signal through $G\alpha_i$ in HEK 293 cells co-expressing A_{2A} (Carriba *et al.*, 2007). Recently, Hudson *et al.*, (2010) was able to demonstrate functional and physical interactions between the hCB_1 receptor and the β_2-adrenergic receptor (β_2-AR) in both HEK 293 cells and primary human ocular cells using BRET. In HEK 293H cells, co-expression of β_2-AR increased cell surface expression of hCB_1 receptors and altered the signaling properties of CB_1 receptors, resulting in increased $G\alpha_i$ -dependent ERK phosphorylation, but decreased non-$G\alpha_i$-mediated CREB phosphorylation. Lastly, the CB_1 receptor has been reported to form heterodimers with the angiotensin II receptor (AT1R) using Co-IP, BRET and heteromer-selective antibodies (Rozenfeld *et al.,* 2011). Such an interaction was found to potentiate AT1R signaling and resulted in coupling of AT1R to multiple G proteins. In the same study, the physiological relevance of this interaction was examined in hepatic stellate cells from ethanol-administered rats in which CB_1 receptor is down regulated. They found a significant upregulation of AT1–CB_1 heteromers and enhancement of angiotensin II-mediated signaling, as compared with cells from control animals (Rozenfeld *et al.,* 2011).

1.6 Research Objectives

Similar to other members of the family of type A GPCRs, the hCB1 receptor is able to physically interact and form heterodimers with other type A GPCRs. Homo- and heterodimerization between and among hCB_1 variants has not been examined. The overlapping patterns of distribution of the mRNAs of the three coding region variants in addition to alterations in the relative abundance of the mRNAs of the three variants raises the possibility that dimerization may occur and influence the function of hCB_1 receptor complexes. Therefore, the present study aimed to address these issues with four primary research objectives:

1- Determine the relative distribution of the human cannabinoid hCB_1 receptor and its splice variant mRNAs in selected regions of the human brain.

2-Determine if the CB_1 variant proteins are expressed in the monkey (*Macaca fascicularis*) brain.

3- Determine the functional differences among the human cannabinoid hCB_1 receptor and its variants.

4- Determine if physical interactions occur between and among human cannabinoid hCB_1 receptor and its variants when expressed in heterologous expression systems and examine the functional consequences of these interactions.

Chapter 2: Methods

2.1 Isolation of Total RNA from *Macaca Fascicularis*, Mouse and Rat Brains

All animal work was done in accordance with the Canadian Council on Animal Care guidelines and is approved by the University Committee on Laboratory Animals at Dalhousie University. The *Macaca fascicularis* brain tissue was a kind gift from Dr. Jim C. Gourdon, McGill University, Montreal. The brain tissue was obtained from animals that were part of a research study of McGill University. All animal care, use and handling were approved by the McGill Animal Care Committee. The use of the post-mortem tissue was approved by Dalhousie University Committee on Laboratory Animals. The *Macaca fascicularis* brain was stored and handled following the standard operating procedure (McGill University) for hazardous material. The brain was shipped on dry ice and it was stored at -80ºC until use. Human brain RNA from different brain regions (total brain, frontal cortex, parietal cortex, caudate/putamen and cerebellum) from a 71-year-old female donor was obtained from Agilent Technologies (Cedar Creek, TX).

Total brain RNA from different brain regions (total brain, frontal cortex, parietal cortex, striatum, cerebellum, hippocampus, substantia nigra and brain stem) was isolated from mouse, rat and *Macaca fascicularis* brains. The isolated RNA was used in RT-PCR analysis to determine whether the CB_1 splice variant transcripts were expressed. RNA was isolated following the protocol described previously (Denovan-Wright *et al*., 2001). Briefly, the brain tissue was added to a tube containing 1 ml of TRIzol® reagent (Invitrogen Canada Inc., Burlington, ON, CA) per 50 mg of brain tissue. The tissue was homogenized using a Dounce homogenizer before 0.2 ml of chloroform was added.

Then, the homogenate was mixed vigorously for 15 s, incubated for 3 m on ice and centrifuged at 12,000 x *g* for 15 m at 4°C. The aqueous phase was removed to a new microcentrifuge tube and 0.5 ml of isopropanol was added. The solution was mixed well and placed on ice for 15 m before being centrifuged at 12,000 x *g* for 15 m at 4°C. The supernatant was then removed and the RNA pellet was washed twice using 1.0 ml of 75% ethanol, vortexed and centrifuged at 7,500 x *g* for 3 m at 4°C. The RNA pellet was allowed to air dry for approximately 10 m before being suspended in ddH_2O. The purity and concentration of the collected RNA were determined by measuring the A260/280 ratio of the samples. RNA samples were stored at -70°C.

2.2 Reverse Transcription Polymerase Chain Reaction (RT-PCR)

RT-PCR analysis was conducted to determine the relative abundance of the CB_1 variants and CNS distribution in human, monkey and rodents brains. Using human RNA, first strand cDNA was generated using 2 µg RNA from each brain region using reverse transcriptase SuperScript® II (GibcoBRL, ON, CA) following the protocol supplied by the manufacturer in a 20 µl reaction volume. The forward Human-CB_1-F and the reverse Human-CB_1-R primers (Table 2.1) common to the three-hCB_1 mRNAs were used to amplify cDNA (Fig. 2.1). PCR reactions contained 5 µl of 1/100 dilution of RT reaction, 2 µl 10X *Pfu* buffer with $MgSO_4$ (final concentration of 2 mM), 2 mM each deoxyribonucleoside triphosphate and 1 unit of *Pfu* DNA polymerase (Fermentas, ON, CA). These reactions were subjected to an initial denaturation step at 95°C for 3 m, and then 30 cycles of amplification at 95°C for 30 s, primer annealing at 54°C for 30 s and

A

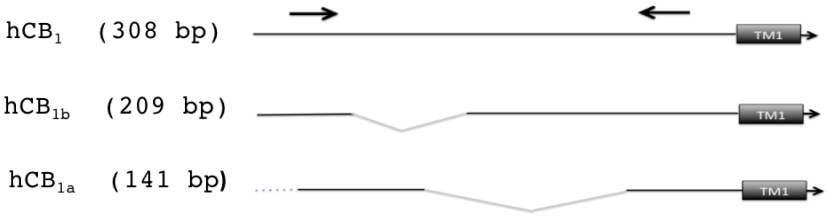

B

```
                                    Human-CB1-F
hCB1    ATGAAGTCGA TCCTAGATGG CCTTGCAGAT ACCACCTTCC GCACCATCAC       1
hCB1b   ATGAAGTCGA TCCTAGATGG CCTTGCAGAT ACCACCTTCC GCACCATCAC
hCB1a   ---------- ------ATGG CCTTGCAGAT ACCACCTTCC GCACCATCAC

hCB1    CACTGACCTC CTGTACGTGG GCTCAAATGA CATTCAGTAC GAAGACATCA      51
hCB1b   CACTGACCTC CT-------- ---------- ---------- ----------
hCB1a   CACTGACCTC CTGTACGTGG GCTCAAATGA CATTCAGTAC GAAGACATCA

hCB1    AAGGTGACAT GGCATCCAAA TTAGGGTACT TCCCACAGAA ATTCCCTTTA     101
hCB1b   ---------- ---------- ---------- ---------- ----------
hCB1a   AAG------- ---------- ---------- ---------- ----------

hCB1    ACTTCCTTTA GGGGAAGTCC CTTCCAAGAG AAGATGACTG CGGGAGACAA     151
hCB1b   ---------- -GGGAAGTCC CTTCCAAGAG AAGATGACTG CGGGAGACAA
hCB1a   ---------- ---------- ---------- ---------- ----------

hCB1    CCCCCAGCTA GTCCCAGCAG ACCAGGTGAA CATTACAGAA TTTTACAACA     201
hCB1b   CCCCCAGCTA GTCCCAGCAG ACCAGGTGAA CATTACAGAA TTTTACAACA
hCB1a   ---------- ---------- ---------- ---------- ----------

hCB1    AGTCTCTCTC GTCCTTCAAG GAGAATGAGG AGAACATCCA GAGAATGAGG     251
hCB1b   AGTCTCTCTC GTCCTTCAAG GAGAATGAGG AGAACATCCA GAGAATGAGG
hCB1a   ---------- ---------- GAGAATGAGG AGAACATCCA GAGAATGAGG

                   Human-CB1-R
hCB1    AGAACATCCA GTGTGGGGAG AACTTCATGG ACATAGAGTG TTTCATGGTC     301
hCB1b   AGAACATCCA GTGTGGGGAG AACTTCATGG ACATAGAGTG TTTCATGGTC
hCB1a   AGAACATCCA GTGTGGGGAG AACTTCATGG ACATAGAGTG TTTCATGGTC

hCB1    CTGAACCCCA GCCAGCAGCT GGCCATTGCA GTCCTGTCCC TCACGCTGGG     351
hCB1b   CTGAACCCCA GCCAGCAGCT GGCCATTGCA GTCCTGTCCC TCACGCTGGG
hCB1a   CTGAACCCCA GCCAGCAGCT GGCCATTGCA GTCCTGTCCC TCACGCTGGG
                                  TM1
```

Figure 2.1: **Detecting the human CB_1 receptor variants in the human brain using RT-PCR (A)** A schematic diagram of primers used for RT-PCR (indicated by arrows) and the expected length of the PCR products corresponding to hCB_1 (308 bp), hCB_{1b} (209 bp) and hCB_{1a} (141 bp). **(B)** Aligned sequences of the 5' end of hCB_1, hCB_{1b} and hCB_{1a} cDNA. The forward Human-CB_1-F and the reverse Human-CB_1-R primers used to detect hCB_1, hCB_{1a} and hCB_{1b} are underlined. TM1 codes for the first transmembrane region. Dashes represent gaps (Figure was modified from Ryberg *et al.,* 2005

Table 2.1: Primer sequences used in RT-PCR and cloning. Restriction sites are shown in bold.

Primer Name	Orientation	Primer sequence (5' to 3')	References
Human-CB_1-F	Sense	ATGGCCTTGCAGATACCACC	
Human-CB_1-R	Anti-sense	AGTTCTCCCCACACTGGATG	Ryberg *et al*., 2005
Mouse-CB_1-F	Sense	ACGGACTTGGAGACACCACC	
Rat-CB_1-F	Sense	ATGGCCTTGCAGACACCACC	
hCB_{1a}-87-F	Sense	CGAC**GAATTC**ATGGCCTTGCAGATACCACC	
hCB_{1a}-87-R	Anti-sense	PCTTTGATGTCTTCGTACTGAATGTCATTT GAGCC	
hCB_{1a}-1146-F	Sense	PGAGAATGAGGAGAACATCCAGTGTGGGGA GAAC	
hCB_{1a}-1146-R	Anti-sense	TGACAT**GGATCC**CACAGAGCCTCGGCAGAC	Hudson *et al*., 2010
hCB_{1b}-63-F	Sense	CGAC**GAATTC**ATGAAGTCGATCCTAGATGG CC	
hCB_{1b}-63-R	Anti-sense	PCAGGAGGTCAGTGGTGATGGTG	
hCB_{1b}-1254-F	Sense	PGGGAAGTCCCTTCCAAGAGAAG	
hCB_{1b}-1254-R	Anti-sense	TGACAT**GGATCC**CACAGAGCCTCGGCAGAC	Hudson *et al.*, 2010
Myc-hCB_1-F	Sense	CGAC**GAATTC**GCGCCATGGAACAAAAACTT ATTTCTGAAGAAGATCTGAAGTCGATCCTA GATGGCC	
Myc-hCB_1-R	Anti-sense	TGACAT**AAGCTT**ACAGAGCCTCGGCAGACG TGCTG	
HA-hCB_{1a}-F	Sense	CGAC**GAATTC**GCGCCATGTACCCATACGAT GTTCCAGATTACGCTGCCTTGCAGATACCA CCTTCC	
HA-hCB_{1b}-F	Sense	CGAC**GAATTC**GCGCCATGTACCCATACGAT GTTCCAGATTACGCTAAGTCGATCCTAGAT GGCC	

extension at 72°C for 40 s with a final extension at 72°C for 10 m. Products were fractionated on a 2% agarose gel containing 0.5 μg/ml ethidium bromide and visualized with a UV transilluminator and Kodak EDAS 290 docking station. Similar RT-PCR conditions were used to examine the expression and relative abundance of the CB_1 variants and CNS distribution in the *Macaca fascicularis* brain. The RT-PCR analysis was also used to examine whether the two splice variants, CB_{1a} and $CB_{1b,}$ are expressed in the rodent brains. The RT-PCR was conducted using the same conditions described to amplify human CB_1 variants with the exception that the forward primer used was Mouse-CB_1-F or Rat-CB_1-F for mouse and rat samples, respectively (Table 2-1). The reverse primer was Human-CB_1-R primer.

2.3 *Macaca Fascicularis* Tissue Preparation

In order to extract total protein from the brain, the protocol previously described by Miller *et al.,* (2002) was followed. In brief, frozen brain tissue was allowed to thaw slightly on dry ice and sterile razor blades were used to dissect tissues from the brain regions. The tissue pieces were immediately homogenized in 10:1 volume:weight of 4ºC homogenization buffer (25 mM HEPES pH 7.4, 1 mM EDTA, 6 mM $MgCl_2$, 1mM DTT, 1 tablet Complete mini protease inhibitor/10 ml buffer; Roche Canada, Mississauga, ON). Samples were centrifuged at 700 x *g* at 4ºC. Supernatants were collected and the pellets were re-extracted in homogenization buffer. The pellets were then discarded and supernatants were centrifuged at 14,000 x *g* for 30 m at 4ºC. The protein pellets were resuspended in homogenization buffer, quantified using Bio-Rad reagent (Bio-Rad Laboratories, Mississauga, ON), and adjusted to a final concentration of 5 mg/ml in

homogenization buffer. Samples were divided into aliquots and were stored at -80ºC

2.4 Western Blot Analysis

Macaca fascicularis total protein samples (20 µg) were mixed with double the volume Laemmli sample buffer containing 10% ß-mercaptoethanol. The proteins were separated on a 4–20% tris-glycine gel (Bio-Rad) at 90 volts for 20 m, followed by 120 volts for 180 m. The fractionated proteins were transferred to 0.2 mm nitrocellulose at 100 volts for 120 m (Bio-Rad). Membranes were allowed to air-dry overnight before being blocked with 100% Odyssey blocking buffer (Li-Cor Biotechonology, Lincoln, NE) for 3 h at room temperature with shaking. The primary antibody, rabbit anti-CB_1 C-terminus antibody (Caymen Chemical, Ann Arbor, MI) was diluted 1:10000 in the diluted Odyssey blocking buffer (1:10 Odyssey blocking buffer in 1X PBS with 0.1% Tween-20; PBST). Blots were incubated overnight at 4ºC in antibody. Following overnight incubation blots were then washed three times with PBST for 5 m each, and then incubated for 1 h with anti-rabbit IR800CW secondary antibody (Rockland Immunochemical, Gilbertsville, PA) diluted 1:1000. The blots were washed three times with PBST, once with 1X PBS and ddH_2O. The membrane was scanned using an Odyssey infrared imaging system (Li-Cor Biotechnologis) with intensity settings of 5 for 800 nm channel and a focus offset of 0 mm.

2.5 Generating hCB_{1a} and hCB_{1b} Receptors

The hCB_1 receptor splice variants in the coding region, hCB_{1a} and hCB_{1b}, were genetically engineered using a full-length human CB_1 receptor cDNA clone as a template

(kind gift from Tom Bonner, NIH, Bethesda, MD). To generate hCB_{1a} (Fig. 2.2, 2.3), the 5'-end of the coding region of the hCB_{1a} receptor (87 nucleotides) was amplified from hCB_1 by PCR utilizing a high fidelity *Pfu* DNA polymerase (Fermentas) with the forward primer hCB_{1a}-87-F possessing an *EcoR1* restriction site and the reverse primer hCB_{1a}-87-R that was manufactured with a 5'phosphate. The 3'-end of the hCB_{1a} receptor-coding region (1146 bp) was amplified using hCB_{1a}-1146-F and hCB_{1a}-1146-R containing a *BamH1* site. The PCR products were then fractionated on a 2% gel containing ethidium bromide and the bands were extracted using GenElute™ Gel Extraction Kit (Sigma, ON). To generate the complete coding sequence of hCB_{1a} receptor, the two PCR products 87 bp and 1146 bp were blunt-end ligated overnight using T4 DNA ligase. The ligation mixture contained 100 ng of each PCR product, 1 µl ligase 10X buffer and 1 unit T4 DNA ligase in 10 µl reaction (Promega Fisher Scientific Ltd., Ottawa, CA). The ligation products (1233 bp) were amplified using *Taq* polymerase to make the products combatable for TA cloning (Fermentas), forward primer hCB_{1a}-87-F and the reverse primer hCB_{1a}-1148-R were used. The PCR products (1233 bp) were cloned into pGEM®-T vector (Promega), and transformed using One Shot® TOP10 Chemically Competent *E. coli* (Invitrogen). Transformed cells were plated on LB/carbenicillin plates with 30 µl of 20 µg/ml X-gal for a blue/white screen. White colonies were cultured in 2 ml LB broth with 50 µg/ml of carbenicillin. Plasmids were extracted using a GenElute™ Plasma Miniprep Kit (Sigma), and clones containing appropriate inserts were identified by restriction digestion of each individual DNA sample with *EcoR1* and *BamH1* followed by gel electrophoresis. A clone containing appropriate sized insert was subjected to

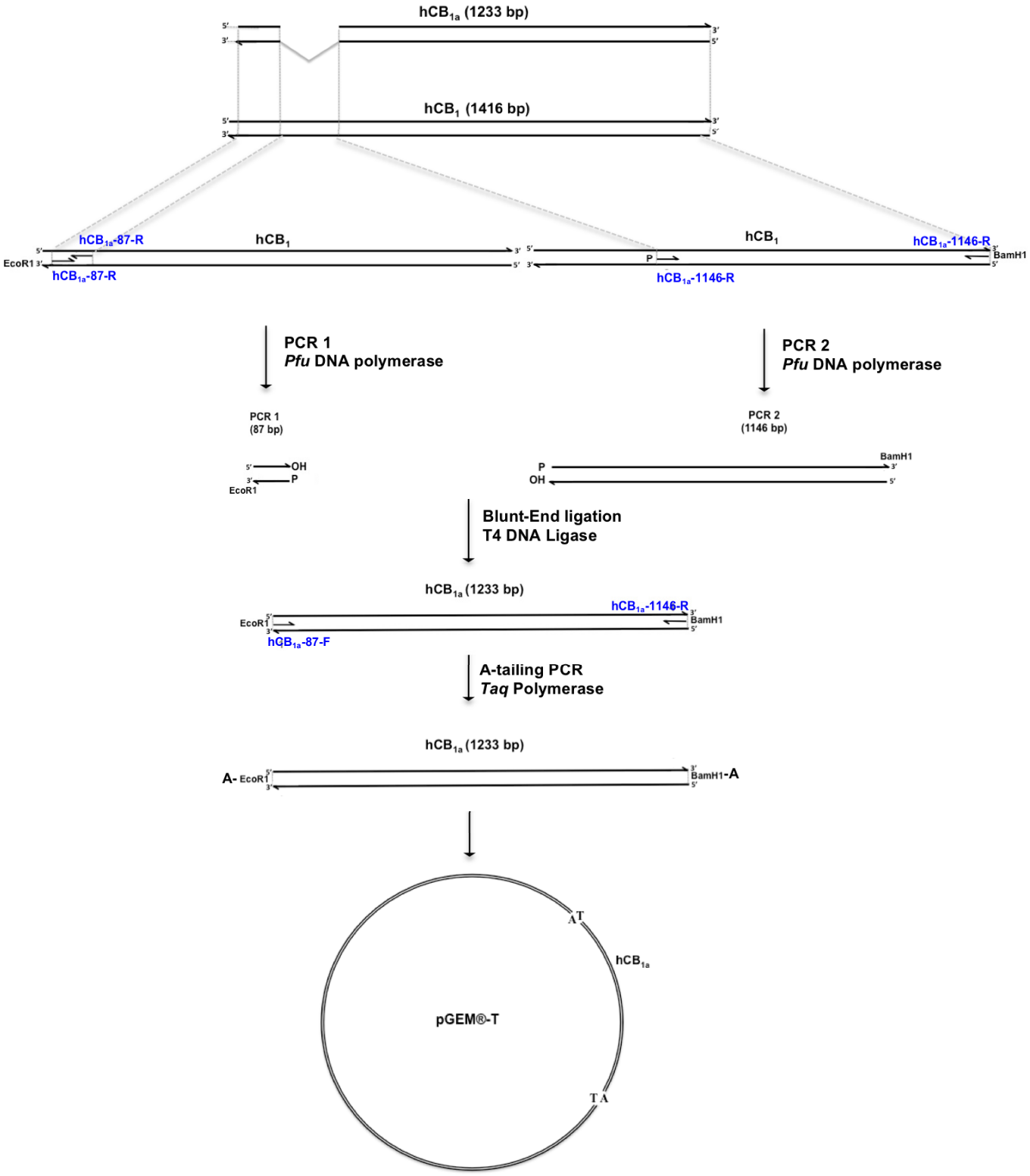

Figure 2.2: A schematic diagram of the cloning strategy of the hCB_{1a} receptor using the hCB_1 as a template. All PCR products have 5' and 3' hydroxyl groups.

hCB$_{1a}$-87-F

```
ATGAAGTCGA TCCTAGATGG CCTTGCAGAT ACCACCTTCC GCACCATCAC       1
```

hCB$_{1a}$-87-R

```
CACTGACCTC CTGTACGTGG GCTCAAATGA CATTCAGTAC GAAGACATCA      51

AAGGTGACAT GGCATCCAAA TTAGGGTACT TCCCACAGAA ATTCCCTTTA     101

ACTTCCTTTA GGGGAAGTCC CTTCCAAGAG AAGATGACTG CGGGAGACAA     151

CCCCCAGCTA GTCCCAGCAG ACCAGGTGAA CATTACAGAA TTTTACAACA     201
```

hCB$_{1a}$-1146-F

```
AGTCTCTCTC GTCCTTCAAG GAGAATGAGG AGAACATCCA GTGTGGGGAG     251

AACTTCATGG ACATAGAGTG TTTCATGGTC CTGAACCCCA GCCAGCAGCT     301

GGCCATTGCA GTCCTGTCCC TCACGCTGGG ACCTTCACGG TCCTGGAGAA     351
CCTCCTGGTG CTGTGCGTCA TCCTCCACTC CCGCAGCCTC CGCTGCAGGC     401
CTTCCTACCA CTTCATCGGC AGCCTGGCGG TGGCAGACCT CCTGGGGAGT     451
GTCATTTTTG TCTACAGCTT CATTGACTTC CACGTGTTCC ACCGCAAAGA     501
TAGCCGCAAC GTGTTTCTGT TCAAACTGGG TGGGGTCACG GCCTCCTTCA     551
CTGCCTCCGT GGGCAGCCTG TTCCTCACAG CCATCGACAG GTACATATCC     601
ATTCACAGGC CCCTGGCCTA TAAGAGGATT GTCACCAGGC CCAAGGCCGT     651
GGTGGCGTTT TGCCTGATGT GGACCATAGC CATTGTGATC GCCGTGCTGC     701
CTCTCCTGGG CTGGAACTGC GAGAAACTGC AATCTGTTTG CTCAGACATT     751
TTCCCACACA TTGATGAAAC CTACCTGATG TTCTGGATCG GGGTCACCAG     801
CGTACTGCTT CTGTTCATCG TGTATGCGTA CATGTATATT CTCTGGAAGG     851
CTCACAGCCA CGCCGTCCGC ATGATTCAGC GTGGCACCCA GAAGAGCATC     901
ATCATCCACA CGTCTGAGGA TGGGAAGGTA CAGGTGACCC GGCCAGACCA     951
AGCCCGCATG GACATTAGGT TAGCCAAGAC CCTGGTCCTG ATCCTGGTGG    1001
TGTTGATCAT CTGCTGGGGC CCTCTGCTTG CAATCATGGT GTATGATGTC    1051
TTTGGGAAGA TGAACAAGCT CATTAAGACG GTGTTTGCAT TCTGCAGTAT    1101
GCTCTGCCTG CTGAACTCCA CCGTGAACCC CATCATCTAT GCTCTGAGGA    1151
GTAAGGACCT GCGACACGCT TTCCGGAGCA TGTTTCCCTC TTGTGAAGGC    1201
ACTGCGCAGC CTCTGGATAA CAGCATGGGG GACTCGGACT GCCTGCACAA    1251
ACACGCAAAC AATGCAGCCA GTGTTCACAG GGCCGCAGAA AGCTGCATCA    1301

AGAGCACGGT CAAGATTGCC AAGGTAACCA TGTCTGTGTC CACAGACACG    1351
```

hCB$_{1a}$-1146-R

```
TCTGCCGAGG CTCTGT                                        1401
```

Figure 2.3: The sequence of hCB$_1$ cDNA and primers sequences used to generate hCB$_{1a}$. Primers are indicated in (Table 2.1).

bidirectional sequencing using M13 forward and reverse universal primers (Genewiz, NJ).

The coding sequence of the hCB_{1b} receptor was generated using a similar cloning strategy and initial template as was described for hCB_{1a} (Fig. 2.4, 2.5). The 5'-end of the coding region of the hCB_{1b} receptor (63 bp) was amplified from the hCB_1 using *Pfu* polymerase and hCB_{1b}-63-F containing an *EcoR1* restriction site, and hCB_{1b}-63-R that was manufactured with a 5'phosphate. The 3'-end of the coding region of the hCB_{1b} (1254 bp) was amplified using the forward primer hCB_{1b}-1254-F and the reverse primer hCB_{1b}-1256-R possessing a *BamH1* site. The two PCR products (63 bp and 1254 bp) were blunt-end ligated, amplified using *Taq* polymerase and cloned into a pGEM®-T vector. The hCB_{1b}-pGEM-T was subjected to bidirectional sequencing using M13 forward and reverse primers (GeneWiz).

2.6 hCB_1, hCB_{1a} and hCB_{1b} Constructs

Both hCB_{1a} and hCB_{1b} receptors were cloned such that either Green Fluorescent protein^2 (GFP^2) or *Renilla* luciferase (Rluc) was expressed as fusion protein at the intracellular carboxy terminus of each receptor. To generate hCB_{1a}-GFP^2 and hCB_{1a}-Rluc, the hCB_{1a} was digested from hCB_{1a}-pGEM-T using *EcoR1* and *BamH1* restriction enzymes. The same restriction enzyme digestions were performed on the pGFP^2-N3 and pRluc-N1 plasmids (PerkinElmer, Waltham, MA). The digested hCB_{1a} and plasmids were run on 1% agarose gel and the bands were extracted using GenElute™ Gel Extraction Kit (Sigma). The hCB_{1a} was inserted into both plasmids using a T4 DNA ligase and the ligated plasmids were then transformed using One Shot® TOP10

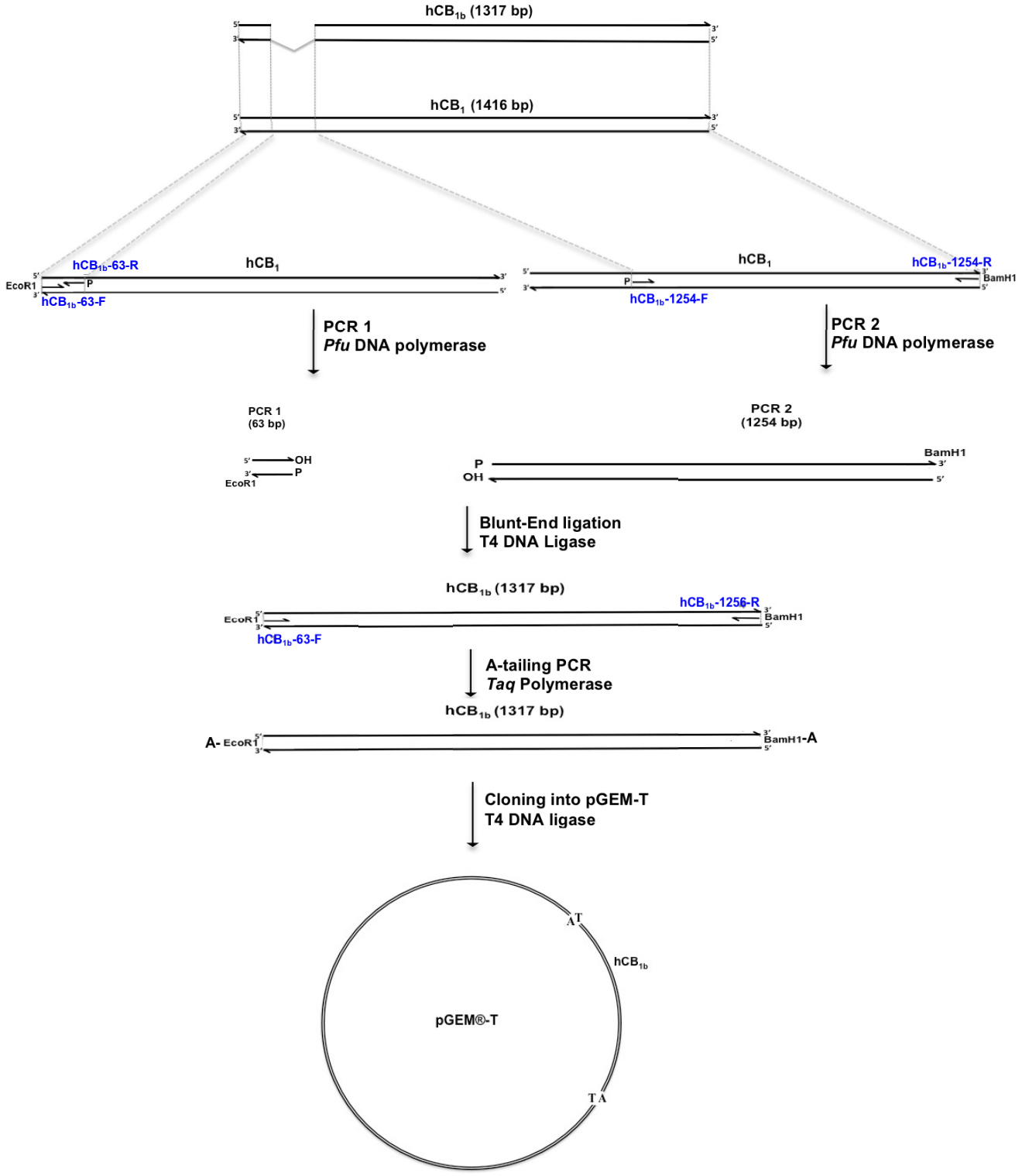

Figure 2.4: A schematic diagram of the cloning strategy of the hCB_{1b} receptor using the hCB_1 as a template. All PCR products have 5' and 3' hydroxyl groups.

hCB$_{1b}$-63-F

```
ATGAAGTCGA TCCTAGATGG CCTTGCAGAT ACCACCTTCC GCACCATCAC       1
```

hCB$_{1b}$-63-R

```
CACTGACCTC CTGTACGTGG GCTCAAATGA CATTCAGTAC GAAGACATCA      51

AAGGTGACAT GGCATCCAAA TTAGGGTACT TCCCACAGAA ATTCCCTTTA     101
```

hCB$_{1b}$-1254-R

```
ACTTCCTTTA GGGGAAGTCC CTTCCAAGAG AAGATGACTG CGGGAGACAA     151

CCCCCAGCTA GTCCCAGCAG ACCAGGTGAA CATTACAGAA TTTTACAACA     201
AGTCTCTCTC GTCCTTCAAG GAGAATGAGG AGAACATCCA GTGTGGGGAG     251
AACTTCATGG ACATAGAGTG TTTCATGGTC CTGAACCCCA GCCAGCAGCT     301
GGCCATTGCA GTCCTGTCCC TCACGCTGGG ACCTTCACGG TCCTGGAGAA     351
CCTCCTGGTG CTGTGCGTCA TCCTCCACTC CCGCAGCCTC CGCTGCAGGC     401
CTTCCTACCA CTTCATCGGC AGCCTGGCGG TGGCAGACCT CCTGGGGAGT     451
GTCATTTTTG TCTACAGCTT CATTGACTTC CACGTGTTCC ACCGCAAAGA     501
TAGCCGCAAC GTGTTTCTGT TCAAACTGGG TGGGGTCACG GCCTCCTTCA     551
CTGCCTCCGT GGGCAGCCTG TTCCTCACAG CCATCGACAG GTACATATCC     601
ATTCACAGGC CCCTGGCCTA TAAGAGGATT GTCACCAGGC CCAAGGCCGT     651
GGTGGCGTTT TGCCTGATGT GGACCATAGC CATTGTGATC GCCGTGCTGC     701
CTCTCCTGGG CTGGAACTGC GAGAAACTGC AATCTGTTTG CTCAGACATT     751
TTCCCACACA TTGATGAAAC CTACCTGATG TTCTGGATCG GGGTCACCAG     801
CGTACTGCTT CTGTTCATCG TGTATGCGTA CATGTATATT CTCTGGAAGG     851
CTCACAGCCA CGCCGTCCGC ATGATTCAGC GTGGCACCCA GAAGAGCATC     901
ATCATCCACA CGTCTGAGGA TGGGAAGGTA CAGGTGACCC GGCCAGACCA     951
AGCCCGCATG GACATTAGGT TAGCCAAGAC CCTGGTCCTG ATCCTGGTGG    1001
TGTTGATCAT CTGCTGGGGC CCTCTGCTTG CAATCATGGT GTATGATGTC    1051
TTTGGGAAGA TGAACAAGCT CATTAAGACG GTGTTTGCAT TCTGCAGTAT    1101
GCTCTGCCTG CTGAACTCCA CCGTGAACCC CATCATCTAT GCTCTGAGGA    1151
GTAAGGACCT GCGACACGCT TTCCGGAGCA TGTTTCCCTC TTGTGAAGGC    1201
ACTGCGCAGC CTCTGGATAA CAGCATGGGG GACTCGGACT GCCTGCACAA    1251
ACACGCAAAC AATGCAGCCA GTGTTCACAG GGCCGCAGAA AGCTGCATCA    1301

AGAGCACGGT CAAGATTGCC AAGGTAACCA TGTCTGTGTC CACAGACACG    1351
```

hCB$_{1b}$-1254-R

```
TCTGCCGAGG CTCTGTGA                                      1401
```

Figure 2.5: The sequence of hCB$_1$ cDNA and primers sequences used to generate hCB$_{1b}$. Primers are indicated in (Table 2.1).

chemically Competent *E. coli* (Invitrogen). Positive colonies were selected on an agar plate containing either Zeocin (25 μg/ml) or kanamycin (25 μg/ml) for GFP^2 –N3 and Rluc-N1 constructs, respectively. Similarly, hCB_{1b} receptor was cloned into $pGFP^2$-N3 and pRluc-N1 plasmids, using *EcoR1* and *BamH1* sites, to generate hCB_{1b}-GFP^2 and hCB_{1b}-Rluc constructs. The hCB_1 receptor had been previously cloned with GFP^2 and Rluc tags in the laboratory by Brian Hudson (Hudson *et al*., 2010). The carboxy-terminus fusion GFP^2 of the human ether-a-go-go-related gene construct (HERG-GFP^2) was provided by Dr. Terry Herbert and was previously described (Dupré *et al*., 2007). The carboxy-terminus construct of the human metabotropic glutamate receptor type 6 (mGluR6-GFP^2) was provided by Dr.Robert Duvoisin of the Oregan Health and Science University, Portland, OR.

The hCB_1 receptor was tagged with the Myc-tag at the N-terminus of the receptor (Myc-hCB_1) using PCR. Myc-hCB_1-F and Myc-hCB_1-R were used in PCR reaction containing hCB_1 cDNA as a template. The PCR products were digested with *EcoR1* and *HindIII* before being ligated into pcDNA3.1/Zeo(-) (Invitrogen). Following transformation, positive colonies were selected on agar plates containing 50 μg/ml carbenicillin. The hCB_1 splice variants, hCB_{1a} and hCB_{1b}, were tagged with the influenza hemagglutinin tag (HA tag) at their N-terminal extremities. HA-hCB_{1a} and HA-hCB_{1b} constructs were generated in the same manner as the Myc-hCB_1 construct, with the exception of using the forward primer HA-hCB_{1a}-F or HA-hCB_{1b}-F for HA-hCB_{1a} and HA-hCB_{1b}, respectively. All of the generated constructs were sequenced to confirm the correct reading frame and insert sequence (Genewize, NJ).

2.7 Cell Culture

All the experiments were performed using human embryonic kidney HEK 293A cells (HEK 293A) a kind gift from Dr. Denis J. Dupré, Dalhousie University, Canada. Cells were maintained in high glucose Dulbecco's Modified Eagle Medium (DMEM; Invitrogen) supplied with 10% Fetal Bovine Serum (FBS), 100 U/ml penicillin and 100 µg/ml streptomycin. Cells were cultured in cell culture treated flasks (BD) at 37ºC and 5% CO_2. At confluency, cells were subcultured at a 1:10 ratio. All experiments were carried out using cells between passages 3-15.

2.8 Transfection

HEK 293A cells were transfected using Lipofectamine 2000 reagent (Invitrogen) following the manufacturer's protocol. For BRET experiments, HEK 293A cells were plated on a 6-well plate (10 cm^2/ml) with DMEM and 10% FBS for 24-48 h, until cells reached 90% confluence. Each well of the 6-well plate received 4 µg of the required plasmids diluted in 250 µl Opti-MEM® Reduced-Serum Medium (Invitrogen; the total amount of DNA/well was kept constant by using pcDNA3.1+ empty vector as required), and mixed with 250 ul Opti-MEM® Reduced-Serum Medium containing 10 µl of Lipofectamine® 2000 reagent. The solution was then incubated at room temperature for 20 m before being added to one well of the 6-well plate containing fresh DMEM media without serum. Cells were cultured at 37°C and 5% CO_2 for 48 h. The same method was used to transfect HEK 293A cells used for confocal microscopy using 24 well plates, and for In- and On-cell western® analysis using poly-D-lysine-coated 96 well plates (Nunc, Rochester, NY).

2.9 Bioluminescence Resonance Energy Transfer 2 ($BRET^2$)

$BRET^2$ was used to study the physical interaction between the hCB_1 receptor and hCB_{1a} and hCB_{1b} splice variants. In $BRET^2$, Renilla luciferase (Rluc) is used as the donor protein, while green-fluorescent protein 2 (GFP^2) is used as the acceptor protein (Fig. 2.6). $BRET^2$ utilizes a unique Rluc substrate, coelenterazine 400 a, that emits light between 290-400 nm. If the Rluc molecule is in sufficiently close proximity (approximately 50-100 Å) to the GFP^2 molecule, then there will be a non-radiative resonance energy transfer to the GFP^2, which in turn will lead to its subsequent fluorescent emission at 505-508 nm. The efficiency of this energy transfer is dependent upon a number of factors including the relative distance between the donor and acceptor molecules, estimated to be less than 100 Å, and their relative orientation (Pfleger and Eidne, 2005).

To carry out $BRET^2$ experiments, HEK 293A cells were plated in a 6-well plate and transfected with the required constructs. Forty-eight h post-transfection, the $BRET^2$ experiment was conducted. Cells were washed twice with cold 1X PBS before being suspended in 90 µl of PBS supplemented with glucose (1 mg/ml), benzamidine (10 mg/ml), leupeptin (5 mg/ml) and a trypsin inhibitor (5 mg/ml). Cells were dispensed into a white 96 well plate (PerkinElmer). Following the addition of 10 µl of 50 µM coelenterazine 400a substrate (Biotium, Hayward, CA, USA) emissions of Rluc and GFP^2 were measured at 405 nm and 510 nm using Luminoskan Ascent plate reader (Thermo Scientific, Waltham, MA), with the integration time set to 10 s and the photomultiplier tube voltage set to 1200 volts. The ratio of 510/405 nm was converted to

A

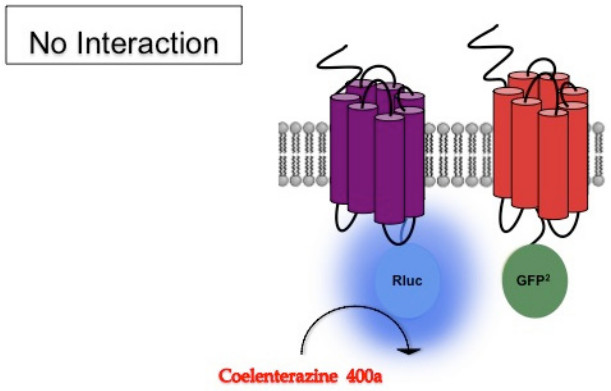

B

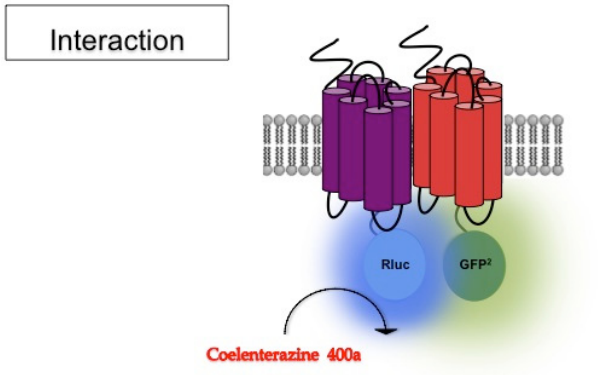

Figure 2.6: Bioluminescence Resonance Energy Transfer 2 (BRET^2). GPCRs are tagged at their carboxy-termini with either Rluc or GFP2. **(A)** GPCRs are not interacting. Thus, on the addition of the Rluc substrate, coelenterazine 400a, blue light is emitted by Rluc, but no energy is transferred to GFP^2, and therefore no green light is emitted. **(B)** GPCRs are interacting. As a result of this, on the addition of coelenterazine 400a blue light is still emitted by Rluc, but since GFP^2 is now in close enough proximity to Rluc, resonance energy transfer to GFP^2 occurs, resulting in the emission of green light (Figure was modified from Pfleger and Eidne, 2005).

BRET efficiency ($BRET_{Eff}$) by first determining the 510/405 ratio of each sample, subtracting the minimum 510/405 nm emission obtained from cells expressing only a Rluc-N1 construct, then divided by the maximum measurable 510/405 nm ratio obtained from cells expressing a GFP^2-Rluc fusion construct (PerkinElmer).

The most common problem with using BRET experiments is that because the receptor constructs are heterologously expressed, there is the possibility that an observed BRET signal may be the result of random collisions of the over-expressed receptors within the cell membrane (Pfleger and Eidne, 2005). This problem has been resolved by several modifications to the BRET assay, specifically the use of BRET saturation and competition assays, both of them help demonstrate the specificity of the interaction being measured by BRET (Pfleger and Eidne, 2005).

In BRET saturation experiments cells were transfected with fixed amounts of the BRET donor (Rluc-tagged receptor), together with increasing amounts of BRET acceptor (GFP^2- tagged receptor). $BRET_{Eff}$ values were then plotted against the ratio of GFP^2 to Rluc concentration. The resulting data was then fit to a rectangular hyperbola curve. If the interaction is specific this should result in a hyperbolic increase in BRET signal to a maximum value, or $BRET_{Max}$, while non-specific interactions will only result in a gradual linear increase. An added benefit to the BRET saturation approach is that by comparing the amount of receptor required to achieve 50% of the maximum BRET signal, the $BRET_{50}$, a rough estimate for the affinity of the interaction can be inferred. B_{Max} and K_d determinations were taken as the $BRET_{Max}$ and $BRET_{50}$, respectively (Pfleger and Eidne, 2005).

BRET competition experiments have also been used to demonstrate the specificity of an interaction between the donor and the acceptor. In these experiments, cells were transfected with constant amount of both donor (Rluc-tagged receptor), and BRET acceptor (GFP^2- tagged receptor) and increasing amounts of one of the interacting receptors untagged with either donor or acceptor is expressed. The untagged receptor should compete with the acceptor-tagged construct for the available donor-tagged constructs, thus reducing the BRET signal.

In BRET experiments examining the effect of CB_1 ligands on $BRET_{Eff}$ signal, HEK 293A cells were plated in 6 well-plate 24 h before being transfected with the required constructs. Forty-eight h later, the cells were collected from each well, washed and resuspended in 300 µl BRET buffer. The 300 µl of the resuspended cells were dispensed into four wells of a 96 well plate. Cells were treated with 10 µl of either vehicle, WIN 55,212-2 (agonist), AM-251 (inverse agonist) or O-2050 (neutral antagonist) to reach final concentrations of 10 µM for 30 m (Tocris Bioscience, Ellisville, MO). BRET signals were measured at 510 and 405 nm immediately after the addition of 10 µl of a 50 µM Coelenterazine 400a substrate.

2.10 Confocal Microscopy and Immunofluorescence

HEK 293A cells were plated onto glass cover slips in a 24-well plate. At 50% confluence, cells were transfected with HA and/or GFP^2 tagged receptors using Lipofectamine 2000 reagent. Forty-eight h post-transfection, culture media was removed and cells were fixed with ice-cold 100% ethanol for 5 m. After washing the cells three times with 1X PBS, cells were blocked with 1% bovine serum albumin (BSA) for 60 m at

room temperature. Cells expressing HA-tagged receptors were incubated with 1:1000 primary monoclonal mouse anti-HA antibody overnight at 4°C (Covance, Emeryville, CA). The next day, the cells were washed three times with 1X PBS and incubated with a Cy^3-conjugated anti-mouse immunoglobulin G (IgG) secondary antibody, 1:500 (Jackson Immuno Research Laboratories Inc., West Grove, PA) for 1 h at room temperature, then washed 3 times with 1X PBS and once with ddH_2O. Finally, cover slips were mounted on microscopic slides (Fisher Scientific) using Fluorsave reagent® (Calbiochem, San Diego, CA). Images of cells were acquired with a Nikon Eclipse E800 microscope attached to the D-Eclapse C1 confocal system (Nikon Canada Inc., Mississauga, ON). Cy^3 was imaged by a 543 nm Helium-Neon laser (JDS Uniphase, Milpitas, CA), while GFP^2 was imaged using a 488 nm air-cooled argon laser (Spectra-Physics Lasers Inc., Mountain View, CA). Images were taken using a 100X oil immersion objective.

2.11 In-Cell Western™ Analysis

In-cell western analysis was used to measure phosphorylation of the extracellular kinase 1 and 2 (ERK). HEK 293A cells were plated in poly-D-lysine coated 96 well plates and cultured for 24-48 h or until confluency. Culture media was then removed and replaced with serum free DMEM and transfected with 200 ng of the required constructs. Twenty-four h later, cells were treated with vehicle (0.05% DMSO) or 1 μM WIN 55,212-2 in 0.05% DMSO for 5 m. HEK 293A cells were fixed for 20 m at room temperature with 4% paraformaldehyde (PFA) in 0.1 M $NaPO_4$ buffer pH 7.4. Cells were washed three times with PBS, permeabilized with 0.1% Triton X-100 in PBS for 1 h at room temperature and then washed again three times with PBS. Cells were blocked using

1% BSA in PBST for 90 m at room temperature. Cells were then incubated overnight at 4°C with rabbit anti phospho-ERK antibody (Tyr 204; Santa Cruz Biotechnology Inc., Santa Cruz, CA), diluted 1:200 in the blocking buffer. After washing the cells three times with PBST, the cells were incubated for 1 h with the IR800CW conjugated anti-rabbit IgG secondary antibody, diluted 1:500 in the blocking buffer (Rockland Immunochemical). Plates were washed three times with PBST, and incubated with goat anti-total ERK2 primary antibody (c-14,; Santa Cruz Biotechnology) for 1 h, diluted 1:200 in PBST containing 1% BSA. After washing three times with PBST, cells were incubated for 1 h with Alexa Fluor 680 anti-goat secondary antibody diluted 1:800 (Invitrogen), washed three times with PBST, three times with PBS and once with ddH_2O before being allowed to air-dry. Plates were scanned using the Odyssey infrared imaging system (Li-Cor Biotechnology), with intensity settings of 5 for both 700 nm and 800 nm channel and a focus offset of 5 mm.

To obtain relative pERK, the background fluorescence was determined from wells receiving only the secondary antibodies and the background was then subtracted from the pERK and total ERK2 signals. The ratio of the background-subtracted pERK/total ERK2 signals was then determined for each well and normalized to the ratios obtained from the wells treated with vehicle (0.05% DMSO).

2.12 On- Cell Western™ Analysis

To measure cell surface expression of Myc-hCB_1, HA-hCB_{1a} and HA-$hCB_{1b,}$ on-cell western analysis was used. The protocol described previously by Miller *et al*. (2004) was followed. HEK 293A cells were plated on poly-D-lysine-coated 96 well plates and

cultured for 24 h to confluence. Twenty-four h post-transfection, the cells were fixed with 4% paraformaldehyde for 1 h at room temperature and washed three times with PBS. Cells were blocked using 1% BSA in PBS for 90 m at room temperature. Wells expressing HA-tagged receptors were incubated with 1:1000 primary monoclonal mouse anti-HA antibody (Covance), while wells expressing Myc-tagged receptors received 1:1000 primary rabbit anti-Myc antibody (Abcam, Cambridge, MA) overnight at 4°C. The following day, cells were washed three times with PBS, before being incubated with an anti-rabbit IR800CW conjugated secondary antibody (Rockland Immunochemicals) diluted 1:800 in 1% BSA in PBS. Cells were washed three times with PBS, then incubated with an Alexa Flour 680 conjugated anti-mouse IgG secondary antibody (Invitrogen) diluted 1:500 with 1% BSA in PBS. Finally, cells were washed 5 times in PBS and once with ddH_2O. The plates were allowed to air-dry and scanned using an Odyssey infrared imaging system (Li-Cor Biotechnology) with intensity settings of 5 for both the 700 and 800 nm channels and a focus offset of 3 mm.

After imaging the cell surface expression of the receptors using the Odyssey, the same wells were used to determine the total receptor expression. The cells were permeabilized using 0.1% Triton X-100 in PBS for 1 h at room temperature and washed three times with PBS. Cells were then exposed to primary anti-HA and/or anti-Myc antibodies, secondary antibodies and scanned following the same protocol described for on cell-western. To obtain the percent of basal surface expression, the background fluorescence was determined from wells receiving only the secondary antibodies and the background was then subtracted from the surface and total receptor expression signals.

The ratio of the background-subtracted surface/total signals was then determined for each well.

2.13 Statistics

Statistical analysis was performed using Graphpad Prism v.4 (GraphPad Software Inc. San Diego, CA). All data are reported as mean ± standard error of the mean (SEM). One-way and two-way ANOVA with the statistical significance set at $P < 0.05$ were performed. Tukey's post-hoc test was applied.

Chapter 3: Results

3.1 CB_1, CB_{1a} and CB_{1b} mRNAs were Distributed Throughout Human and Monkey Brains

The first aim of this study was to determine the relative abundance and CNS distribution of the hCB_1 variants in the human brain. RT-PCR was carried out using a primer set capable of amplifying the three hCB_1 variants with products of 308, 141 and 209 bp corresponding to hCB_1, hCB_{1a} and hCB_{1b}, respectively. Five regions of the human brain were examined, including total brain, frontal cortex, parietal cortex, cerebellum and caudate/putamen. After 30 cycles, PCR products were subjected to electrophoresis on a 2% agarose gel (Fig. 3.1). Three amplicons were detected of the expected sizes for hCB_1, hCB_{1a} and hCB_{1b} in each cDNA sample derived from different regions of the human brain. All of the PCR products were extracted from the agarose gel and sequenced to confirm their identities (GeneWiz).

Several hCB_1 variant-specific primer pairs were designed and tested by PCR reaction using plasmid DNA templates containing the full sequence of each variant. None of the tested primer sets specifically amplified the individual variants despite several attempts to optimize annealing temperature, buffer conditions and cycling parameters. For this reason we were unable to perform quantitative PCR (qPCR) analysis. We did attempt to examine the relative abundance of variants after different numbers of PCR amplification cycles. However, the relative abundance of the three receptors did not differ irrespective of different numbers of PCR amplification (results not shown). Our results showed that hCB_1, hCB_{1a} and hCB_{1b} mRNAs are distributed throughout the regions of the human

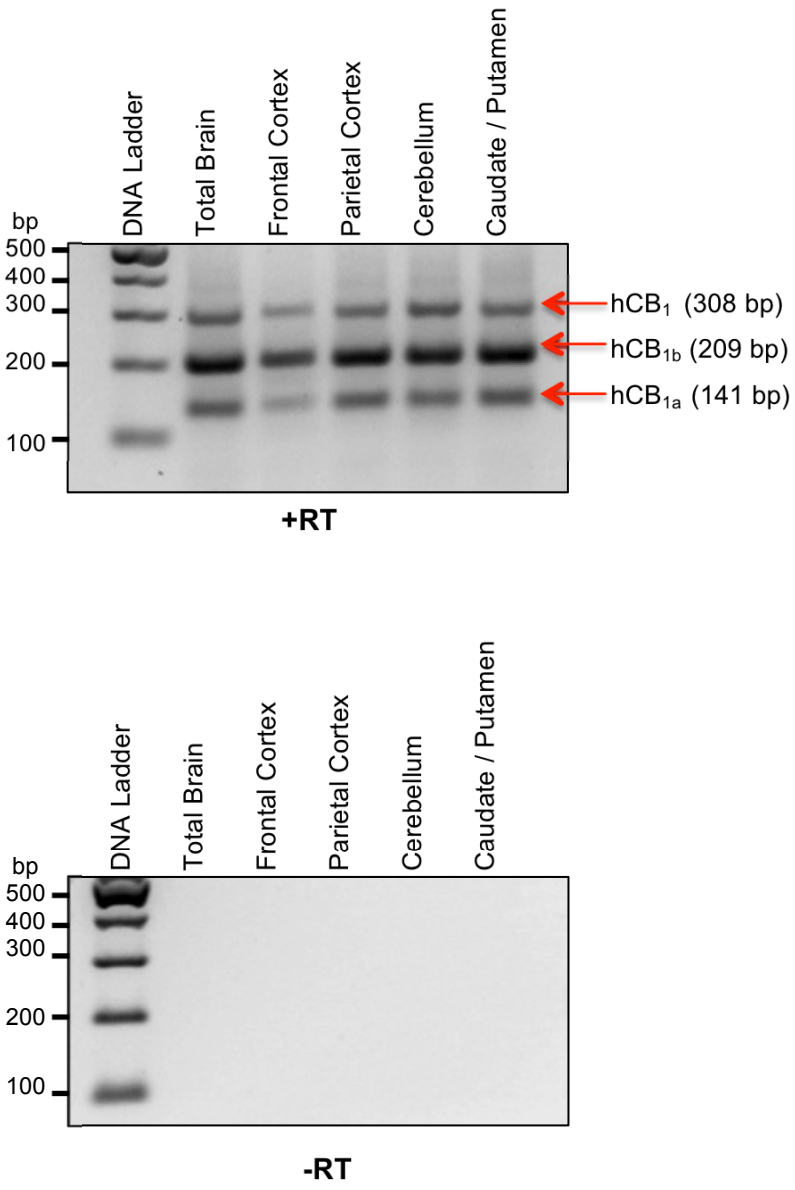

Figure 3.1: The hCB_1, hCB_{1a} and hCB_{1b} mRNAs are distributed throughout the human brain. PCR products obtained using a primer set that amplifies the three-hCB_1 variants. PCR products were fractionated on 2% agarose gel containing ethidium bromide and visualized under UV light.

brain tested and can easily be detected via RT-PCR.

Next, we wanted to determine if CB_{1a} and CB_{1b} mRNAs are expressed in the brain of different species. To examine whether the CB_1 splice variants are expressed in rodent brains, RT-PCR was performed on RNA extracted from various tissues of adult mouse and rat brains using species-specific primers. We employed multiple primer sets, PCR conditions and buffer compositions to attempt to amplify the CB_1 splice variants in the rat and mouse brains. Other than CB_1, we could not detect the variants CB_{1a} and CB_{1b} in rodent cDNA (data not shown).

We tested if the two splice variants, CB_{1a} and $CB_{1b,}$ were expressed in the brain of a non-human primate (*Macaca fascicularis)*. First, RT-PCR was conducted on RNA extracted from different brain regions of the *Macaca fascicularis* using similar primers and reaction conditions to those used to amplify human CB_1 variants using human brain RNA. Three bands were detected at the expected sizes for CB_1, CB_{1a} and CB_{1b} (Fig. 3.2). PCR products were extracted from the agarose gel and sequenced to confirm their identities (GeneWiz). Our results showed that the monkey brain expresses CB_1, CB_{1a} and CB_{1b}.

3.2 CB_1, CB_{1a} and CB_{1b} Proteins were Expressed in the Monkey Brain

It still remains unclear whether the hCB_1 splice variants mRNAs are translated into proteins *in vivo*. In addition, GPCR mRNA and protein levels do not necessarily correlate (Markovic and Challiss, 2009). Therefore, it was important not only to demonstrate the presence of the transcript of each isoform, but also to determine the relative protein level

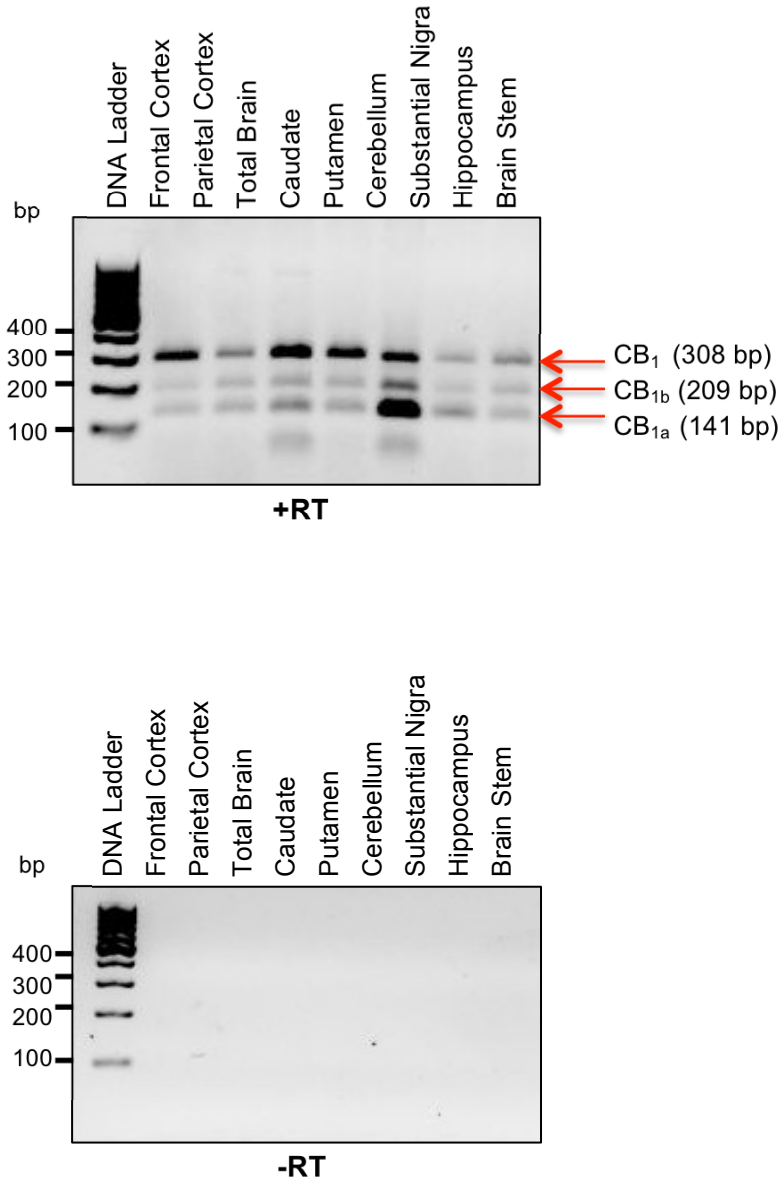

Figure 3.2: The CB_1, CB_{1a} and CB_{1b} mRNAs are distributed throughout the *Macaca Fascicularis* brain. PCR products using a primer set that amplify the three-hCB_1 variants. PCR products were fractionated on 2% agarose gel containing ethidium bromide and visualized under UV light. Upper panel represents positive reverse transcriptase (+RT) reaction, while lower panel represent negative reverse transcriptase (-RT) reaction.

in different brain regions. Since we showed that rodents don't express the CB_1 variants, and we were unable to obtain fresh or frozen human brain tissue for appropriate analysis, we chose to determine the expression levels of CB_1 variants in different brain regions of the monkey (*Macaca fascicularis)* brain. Human and monkey CB_1 receptors exhibit 100% sequence identity at the amino acid level over the complete protein (NCBI). A variety of cortical and subcortical structures from the monkey (*Macaca fascicularis*) brain were dissected and analyzed for CB_1 by western blotting. The antibody used was raised against the C-terminal (amino acids 461-472) intracellular sequences common to all three hCB_1 receptor variants (Cayman Chemical, Ann Arbor, MI). Western blot analysis of homogenates from different regions of the monkey brain revealed a prominent immunoreactive band with a molecular mass of ≈53 kDa, which is consistent with the predicted band size for human CB_1. In addition, two less abundant bands at approximately ≈49 kDa and ≈46 kDa were detected, which is the predicted size for CB_{1b} and CB_{1a}, respectively (Fig. 3.3A). The antibody detected the three different molecular weight bands in all tested brain regions. There were only slight differences in the band intensity across different brain regions. These bands were not detected when the C-terminal antibody was pre-incubated with the blocking peptide (Fig. 3.3C), or when the secondary antibody was applied alone without the primary antibody (Fig. 3.3D). We did not have enough numbers of animals to quantify the relative amounts of each variant in different brain regions. However, we can conclude that the monkey brain expressed proteins with the expected molecular weights of CB_1, CB_{1a} and CB_{1b} receptors. Although, CB_1 receptor appeared to be most abundant; the other variants were present in approachable quantities.

Figure 3.3: The CB_1, CB_{1a} and CB_{1b} proteins are distributed throughout the *Macaca fascicularis* brain. Western blot of proteins extracted from different regions of monkey brain using CB_1 antibody directed against the C-terminal tail (A) and housekeeping gene β-III tubulin **(B)**. Bands were detected at the expected molecular weight for CB_1 (53kDa) CB_{1a} (46 kDa), CB_{1b} (49 kDa) and β-III tubulin (55 kDa). No bands were detected when the antibody was pre-incubated with a blocking peptide (1:10 dilution) **(C)** or when the membrane was incubated with the secondary antibody alone **(D)**.

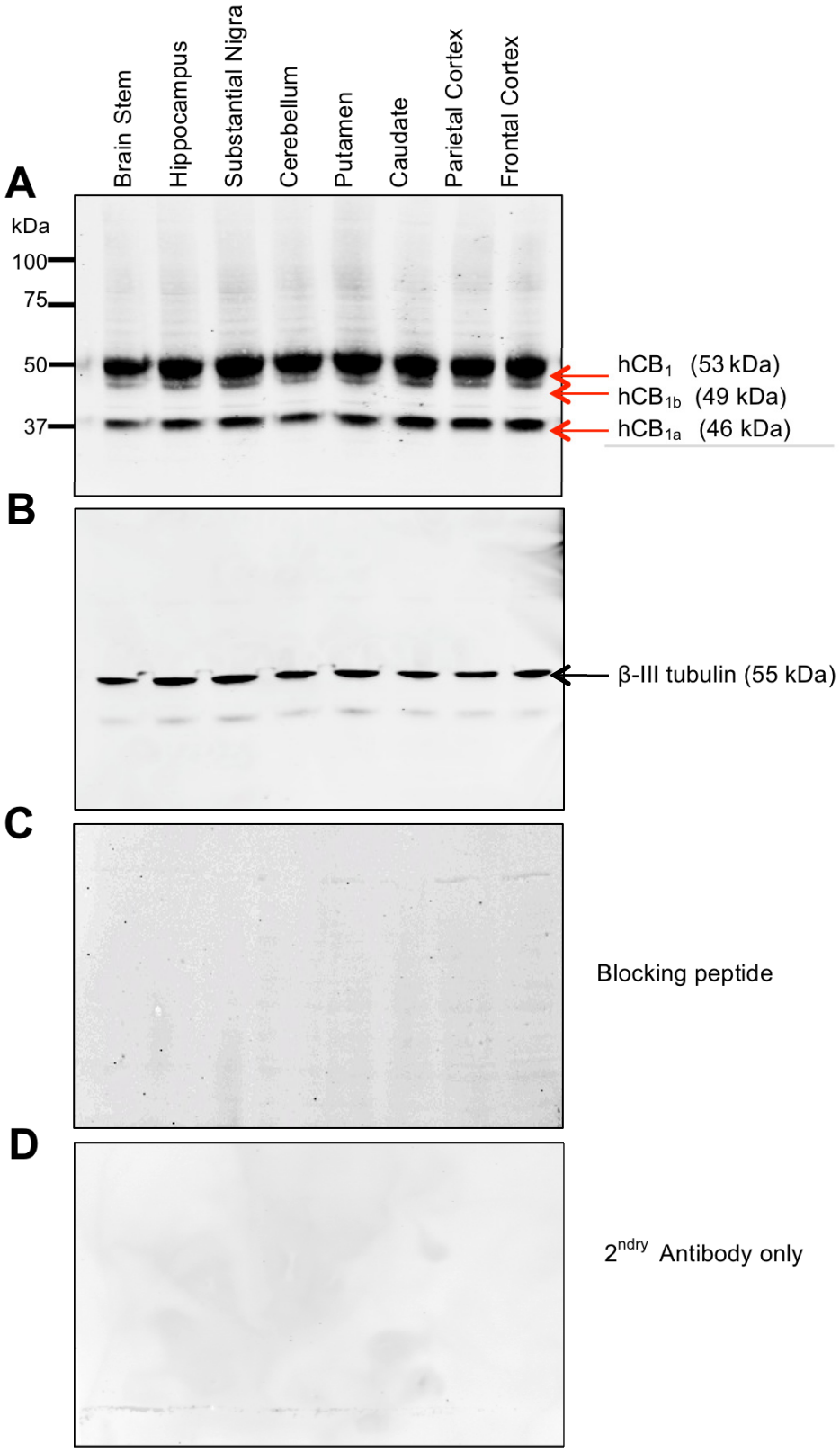
A
Brain Stem
Hippocampus
Substantial Nigra
Cerebellum
Putamen
Caudate
Parietal Cortex
Frontal Cortex
kDa
100
75
50
37
hCB1 (53 kDa)
hCB1b (49 kDa)
hCB1a (46 kDa)
B
β-III tubulin (55 kDa)
C
Blocking peptide
D
2ndry Antibody only

3.3 Dimerization of hCB_1 Receptor and its Splice Variants

3.3.1 Homodimerization of hCB_1 Receptor Splice Variants

$BRET^2$ was used to determine whether hCB_1 splice variants could form homodimers in HEK 293A cells. Cells were co-transfected with hCB_{1a}-Rluc and hCB_{1a}-GFP^2, or with two two-membrane proteins that do not interact with hCB_1, HERG-GFP^2, a membrane localized K^+ channel, or mGluR6-GFP^2 (Hudson *et al*., 2010). Forty-eight hours later, BRET efficiency ($BRET_{Eff}$) was measured. The combination of hCB_{1a}-Rluc and hCB_{1a}-GFP^2 resulted in an increased $BRET_{Eff}$ compared with the $BRET_{Eff}$ observed when hCB_{1a}-Rluc was co-transfected with mGluR6-GFP^2 or HERG-GFP^2 ($P < 0.001$; Fig. 3.4A). A BRET saturation curve was generated to demonstrate the ability of hCB_{1a} to form homodimers at constant donor expression levels and increasing acceptor expression levels. For the BRET saturation curve, cells were co-transfected with a constant amount of hCB_1-Rluc with increasing amounts of hCB_{1a}-GFP^2 or HERG-GFP^2. The combination of hCB_{1a}-Rluc with hCB_{1a}-GFP^2 resulted in a significantly different saturation curve ($P < 0.001$) than the control curve, which was generated with a combination of hCB_{1a}-Rluc with HERG-GFP^2 (Fig. 3.4B). The hCB_{1a} homodimer saturation curve resulted in a $BRET_{Max}$ of 0.32 ± 0.02 and a $BRET_{50}$ of 0.39 ± 0.043.

Similar experiments were also carried out to demonstrate the ability of hCB_{1b} to form homodimers in HEK 293A cells. A significantly higher $BRET_{Eff}$ resulted ($P < 0.001$) when hCB_{1b}-Rluc and hCB_{1b}-GFP^2 constructs were co-expressed, compared to the two controls (Fig. 3.5A). The hCB_{1b} homodimer saturation curve resulted in a $BRET_{Max}$ of 0.31 ± 0.016 ($P < 0.001$), and $BRET_{50}$ of 0.40 ± 0.048 ($P < 0.001$) (Fig. 3.5B).

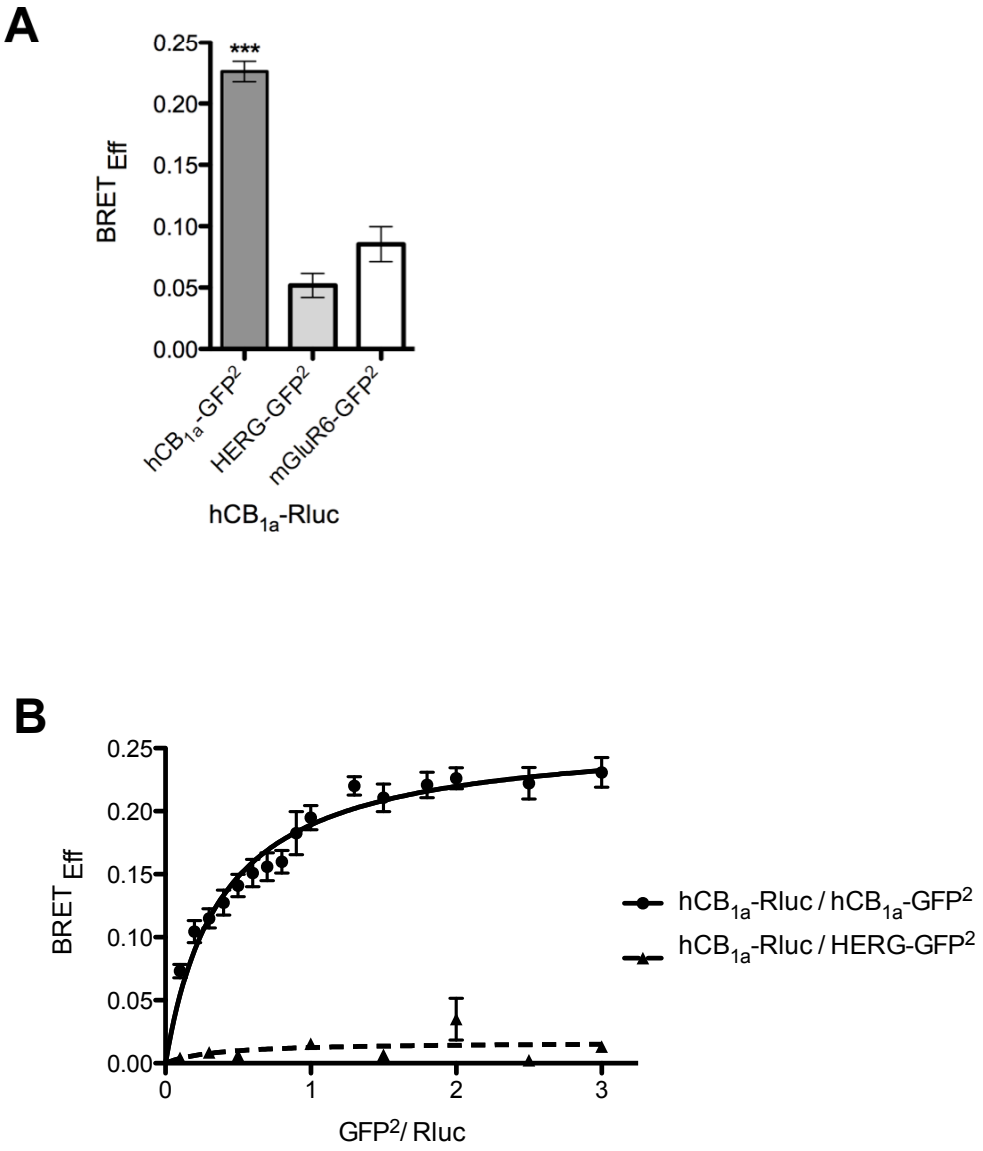

Fig. 3.4: The hCB_{1a} receptor forms homodimers in HEK 293A cells. **(A)** The co-expression of hCB_{1a}-Rluc and hCB_{1a}-GFP^2 in HEK 293A cells resulted in a higher $BRET_{Eff}$ value, compared to when hCB_{1a}-Rluc was co-expressed with either HERG-GFP^2 or mGluR6-GFP^2 controls. **(B)** BRET saturation curve obtained from cells transiently transfected with hCB_{1a}-Rluc/hCB_{1a}-GFP^2 was higher than the curve of hCB_{1a}-Rluc/HERG-GFP^2. Data are presented as mean ± SEM of three independent experiments, n=6-8. Statistical significance was determined by using one-way ANOVA, followed by Tukey's post hoc test. *** $P < 0.001$ compared to controls.

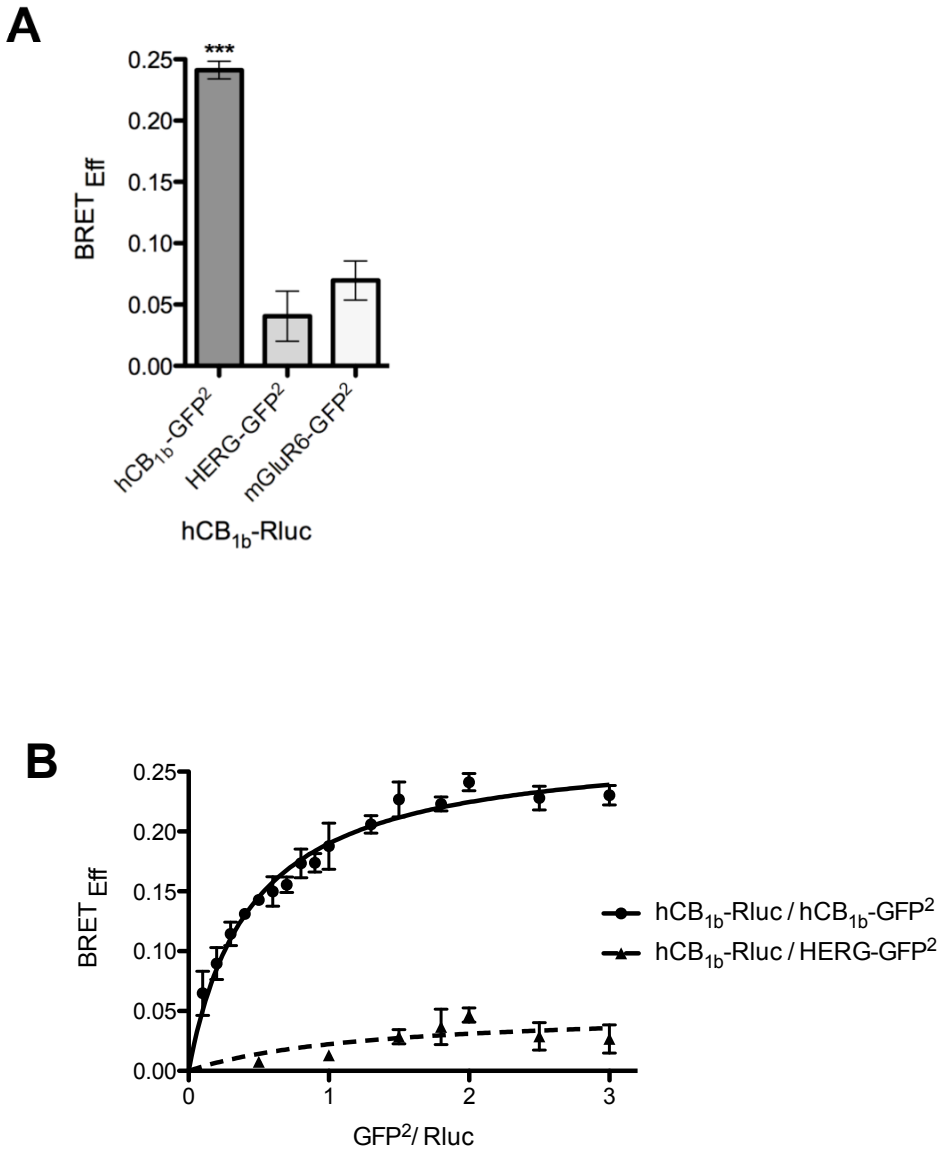

Figure 3.5: The hCB_{1b} receptor forms homodimers in HEK 293A cells. (A) The co-expression of hCB_{1b}-Rluc and hCB_{1b}-GFP^2 in HEK cells resulted in a higher $BRET_{Eff}$ value, compared when hCB_{1b} was co-expressed with either HERG-GFP^2 or mGluR6-GFP^2 controls. **(B)** The BRET saturation curve obtained from cells transiently transfected with hCB_{1b}-Rluc/hCB_{1b}-GFP^2 increases exponentially and had $BRET^{Eff}$ higher than the hCB_{1b}-Rluc/HERG-GFP^2, which showed a linear change curve over full range. Data are presented as mean ± SEM of three independent experiments, n=6-8. Statistical significance was determined by using one-way ANOVA, followed by Tukey's post hoc test. *** $P < 0.001$ compared to controls.

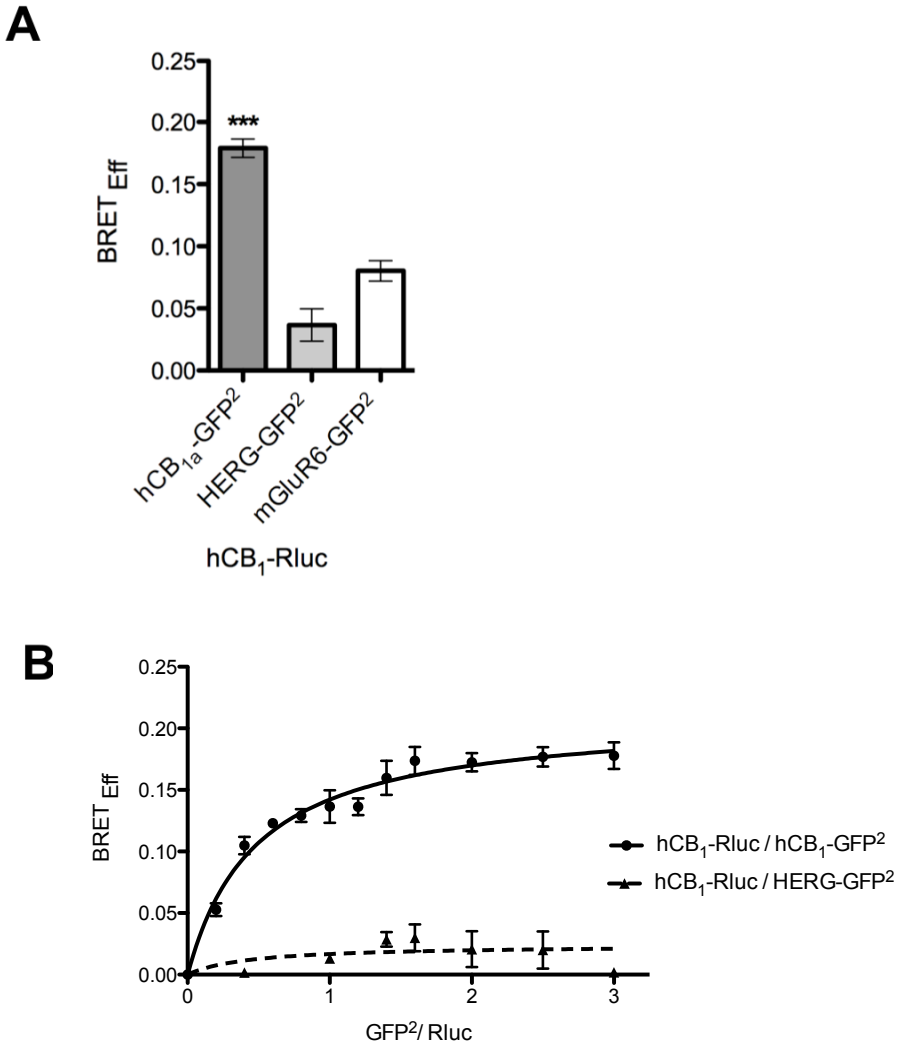

Figure. 3.6: The hCB_1 receptor forms homodimers in HEK 293A cells. **(A)** The co-expression of hCB_1-Rluc and hCB_1-GFP^2 in HEK 293A cells resulted in a higher $BRET_{Eff}$ value, compared when hCB_{1a}-Rluc was co-expressed with either HERG-GFP^2 or mGluR6-GFP^2 controls; ***p<0.001, n=6-8 of three independent experiments. **(B)** BRET saturation curve obtained from cells transiently transfected with hCB_1-Rluc/hCB_1-GFP^2 was higher than the curve of hCB_{1a}-Rluc/HERG-GFP^2. Data are presented as mean ± SEM of three independent experiments, n=6-8. Statistical significance was determined by using one-way ANOVA, followed by Tukey's post hoc test. *** $P < 0.001$ compared to controls.

Homodimerization of hCB_1 receptor was also carried out. A significantly higher $BRET_{Eff}$ resulted ($P < 0.001$) when hCB_1-Rluc and hCB_1-GFP^2 constructs were co-expressed, compared to the two controls (Fig. 3.6A). BRET saturation curve for the hCB_1 receptor resulted in a $BRET_{Max}$ of 0.23 ± 0.02 ($P < 0.001$), and $BRET_{50}$ of 0.48 ± 0.05 ($P < 0.001$; Fig. 3.6B), which further confirm previously published data of hCB_1 homodimerization (Wager-Miller *et al*., 2002; Hudson *et al*., 2010). Taken together, the $BRET^2$ data suggest that hCB_1, hCB_{1a} and hCB_{1b} are capable of forming homodimers, when expressed in HEK 293A cells.

3.3.2 Heterodimerization Between hCB_1 Receptor and its Splice Variants

GPCRs have been reported to physically interact with their splice variants under normal physiological conditions to form heterodimers (Rios *et al*., 2001; Milligan, 2004; Pfleger and Edine, 2005). These interactions were found to have substantial effects on the trafficking and signaling of the full-length receptors (Milligan, 2004). RT-PCR and western blot assays indicated that there was an overlapping pattern of distribution of the mRNAs and proteins of the three CB_1 coding region variants in different regions of the human and monkey brain, raising the possibility that heterodimerization may occur and influence the function of CB_1 receptor complexes in these tissues. For this reason, the next aim of this study was to determine whether dimerization would occur between the hCB_1 receptor and hCB_{1a} and hCB_{1b} splice variants. For these experiments, $BRET^2$ was also used to demonstrate dimerization between hCB_1 and hCB_{1a} and hCB_{1b} splice variants in HEK 293A cells. $BRET_{Eff}$ was measured from cells co-transfected with either hCB_1-

Rluc or hCB_{1a}-Rluc, and one of the following: hCB_1-GFP^2, hCB_{1a}-GFP^2, HERG-GFP^2 or mGluR6-GFP^2 (Fig. 3.7A). The co-expression of hCB_{1a}-Rluc and hCB_1-GFP^2 produced an increased $BRET_{Eff}$ ($P < 0.01$) compared to the two controls. Similarly, when hCB_1-Rluc was co-expressed with hCB_{1a}-GFP^2 it produced an increased $BRET_{Eff}$ ($P < 0.001$) compared with either HERG-GFP^2 or mGluR6-GFP^2. A BRET saturation curve was also generated (Fig. 3.7B). The hCB_1-Rluc/hCB_{1a}-GFP^2 saturation curve was higher than the curve for the hCB_{1a}-Rluc/ HERG-GFP^2 ($p<0.001$). The saturation curve yielded a $BRET_{Max}$ of 0.28 ± 0.018 and $BRET_{50}$ of 0.7 ± 0.064. To confirm the specificity of the interaction between hCB_1 and hCB_{1a}, a BRET competition assay was carried out. In a BRET competition assay, cells were transfected with constant amounts of hCB1-Rluc/hCB_{1a}-GFP^2 and an increasing amount of non-fluorescent HA-hCB_{1a} as competitor (Fig. 3.7C). The $BRET_{Eff}$ of hCB_1-Rluc/hCB_{1a}-GFP^2 was decreased by the co-expression of 1 μg of HA-hCB_{1a} ($P < 0.05$). Increasing the HA-hCB_{1a} concentration to 2 and 3 μg resulted in a further reduction in $BRET_{Eff}$ values ($P < 0.001$) and ($P < 0.01$), respectively. The physical interaction between hCB_1 and hCB_{1b} was also studied using $BRET^2$ experiments (Fig. 3.8). The BRET saturation curve of hCB_1-Rluc/hCB_{1b}-GFP^2 resulted in a $BRET_{Max}$ of 0.27 ± 0.017 and $BRET_{50}$ of 0.71 ± 0.05 (Fig.3.8B). Our results demonstrate that there is a specific interaction between hCB_1 and its splice variants, when hCB_1 is co-expressed with hCB_{1a} or hCB_{1b}.

The effect of several CB_1 ligands on the dimerization of hCB_1 with its splice variants was studied (Fig. 3.9). Treating cells expressing hCB_1-Rluc/hCB_{1a}-GFP^2 or hCB_1-Rluc/hCB_{1b}-GFP^2 for 30 m with either an inverse agonist AM-251, full agonist WIN 55212-2, or neutral antagonist, O-2050, did not significantly alter the observed $BRET_{Eff}$

Figure 3.7: The hCB_1 receptor can forms heterodimers with its splice variant hCB_{1a} in HEK 293A cells. **(A)** The co-expression of hCB_{1a}-Rluc and hCB_1-GFP^2 in HEK cells resulted in a higher $BRET_{Eff}$ value, compared when hCB_{1a}-Rluc was co-expressed with either HERG-GFP^2 or mGluR6-GFP^2 controls; ** $P < 0.01$. Similarly, the co-expression of hCB_1-Rluc and hCB_{1a}-GFP^2 in HEK cells resulted in a higher $BRET_{Eff}$ value, compared to the controls; *** $P < 0.001$. **(B)** BRET saturation curve obtained from cells transiently transfected with hCB_1-Rluc/hCB_{1a}-GFP^2 was higher than the curve of hCB_{1b}-Rluc/HERG-GFP^2. **(C)** BRET competition experiment was performed with HEK cells transfected with a constant amount of hCB_1-Rluc and hCB_{1a}-GFP^2 and increasing amounts of HA-hCB_{1a} or HERG-GFP^2. * $P < 0.05$, ** $P < 0.01$ and *** $P < 0.001$ compared to cells expressing only hCB_1-Rluc/hCB_{1a}-GFP^2. Data are presented as mean ± SEM of three independent experiments, n=6. Statistical significance was confirmed by using one-way ANOVA, followed by Tukey's post hoc test.

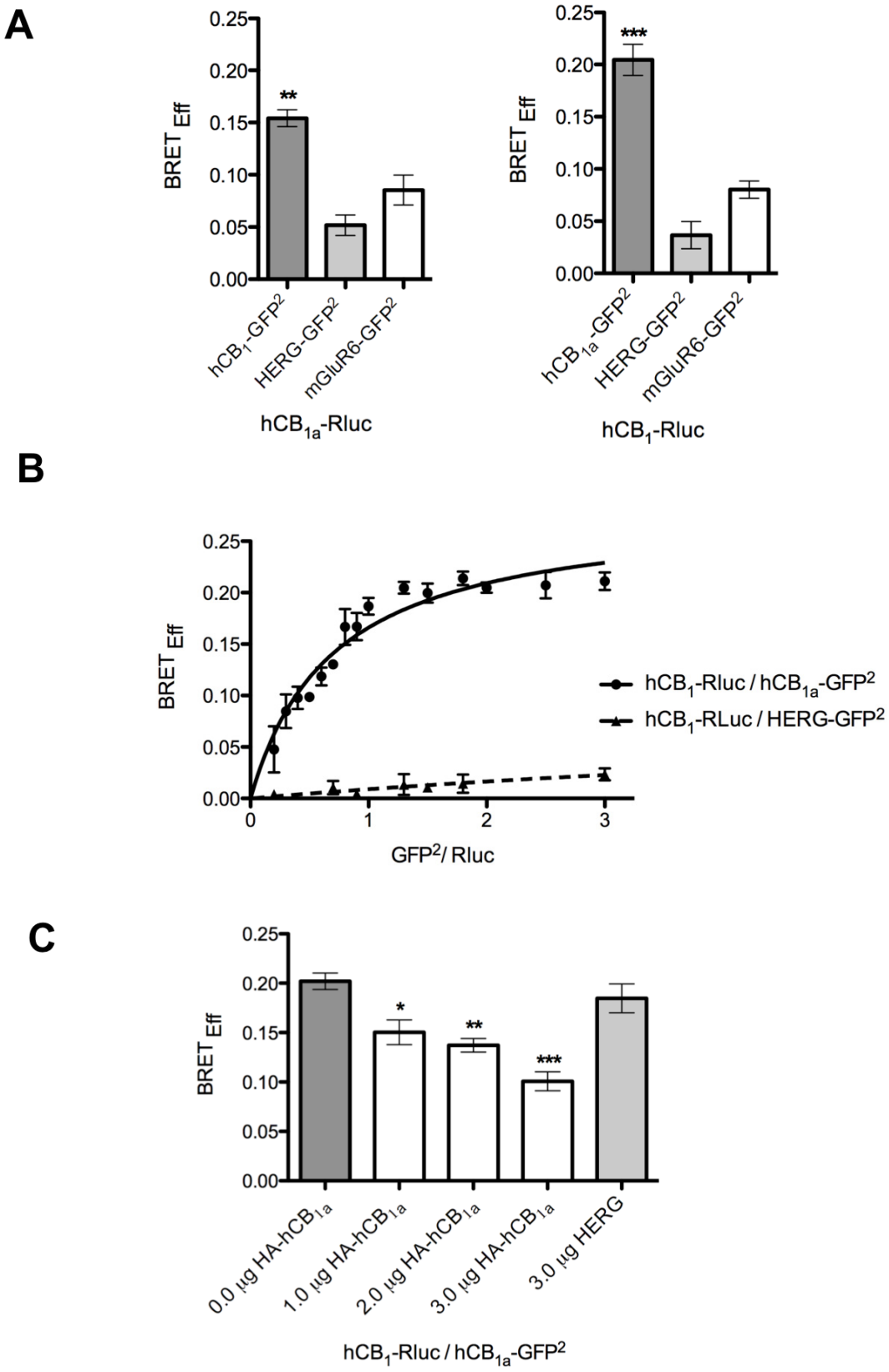
A
BRET Eff
0.25
0.20
0.15
0.10
0.05
0.00
**
hCB1-GFP2
HERG-GFP2
mGluR6-GFP2
hCB1a-Rluc
***
hCB1a-GFP2
hCB1-Rluc
B
GFP2/ Rluc
hCB1-Rluc / hCB1a-GFP2
hCB1-RLuc / HERG-GFP2
C
*
**
***
0.0 µg HA-hCB1a
1.0 µg HA-hCB1a
2.0 µg HA-hCB1a
3.0 µg HA-hCB1a
3.0 µg HERG
hCB1-Rluc / hCB1a-GFP2

Figure 3.8: The hCB_1 receptor can form heterodimers with its splice variant hCB_{1b} in HEK 293A cells. (A) The co-expression of hCB_{1b}-Rluc and hCB_1-GFP^2 in HEK cells resulted in a higher $BRET_{Eff}$ value, compared when hCB_{1a}-Rluc was co-expressed with either HERG-GFP^2 or mGluR6-GFP^2 controls; ** $P < 0.01$. Similarly, the co-expression of hCB_1-Rluc and hCB_{1a}-GFP^2 in HEK cells resulted in a higher $BRET_{Eff}$ value, compared to the controls; *** $P < 0.001$. **(B)** BRET saturation curve obtained from HEK cells transiently transfected with a constant amount of hCB_{1b}-Rluc and increasing amount of hCB_{1b}-GFP^2 was higher than the curve of hCB_{1b}-Rluc/HERG-GFP^2. **(C)** BRET competition experiment was performed with HEK 293A cells transfected with a constant amount of hCB_1-Rluc and hCB_{1b}-GFP^2 and increasing amounts of HA-hCB_{1b} or HERG-GFP^2 . * $P < 0.05$, ** $P < 0.01$ and *** $P < 0.001$ compared to the cells expressing only hCB_1-Rluc/hCB_{1b}-GFP^2. Data are presented as mean ± SEM of three independent experiments, n=6. Statistical significance was determined by using one-way ANOVA, followed by Turkey's post hoc test.

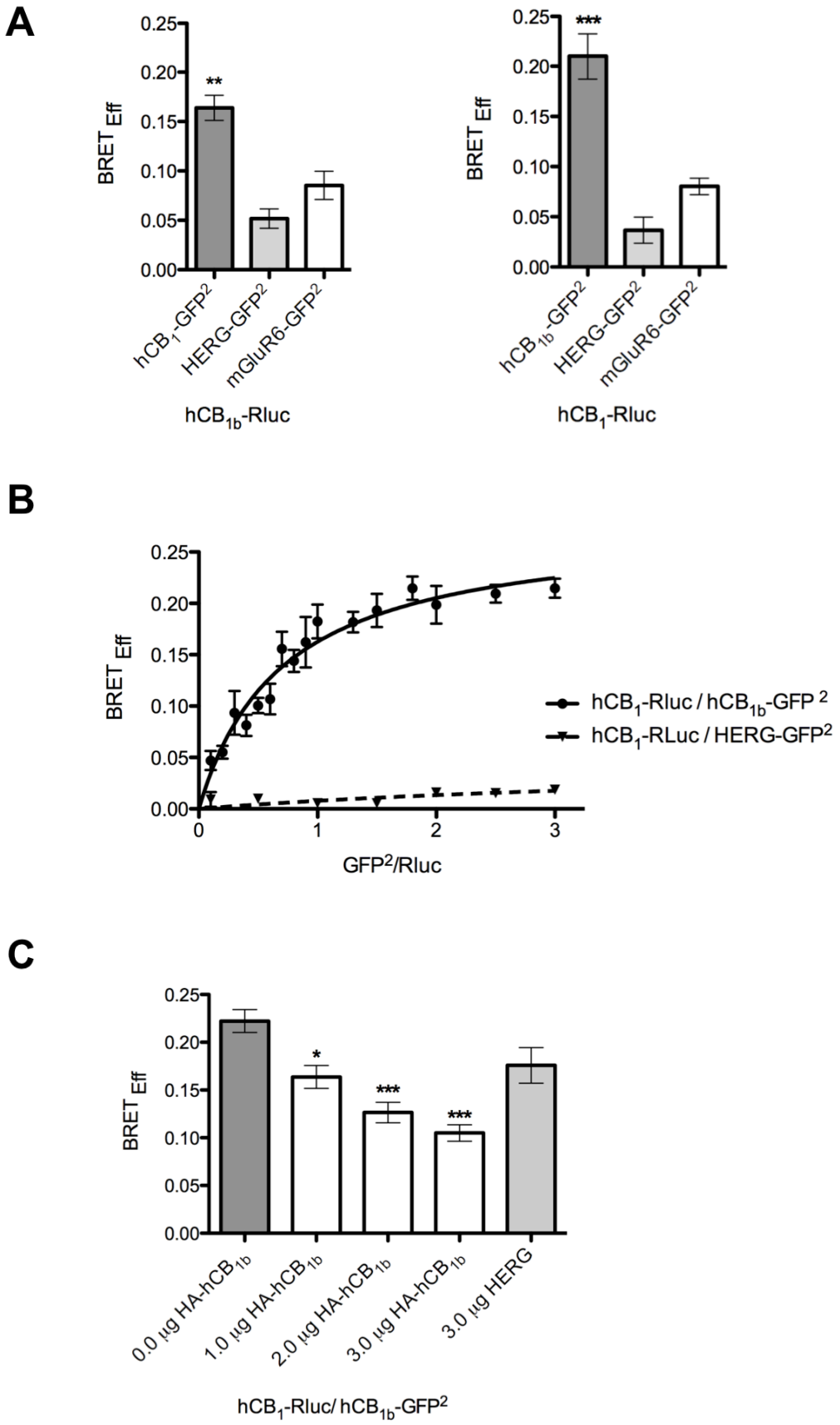
A
BRET Eff
0.25
0.20
0.15
0.10
0.05
0.00
**
***
hCB1-GFP2
HERG-GFP2
mGluR6-GFP2
hCB1b-Rluc
hCB1-Rluc
B
BRET Eff
GFP2/Rluc
hCB1-Rluc / hCB1b-GFP 2
hCB1-RLuc / HERG-GFP2
C
BRET Eff
*
***
0.0 µg HA-hCB1b
1.0 µg HA-hCB1b
2.0 µg HA-hCB1b
3.0 µg HA-hCB1b
3.0 µg HERG
hCB1-Rluc/ hCB1b-GFP2

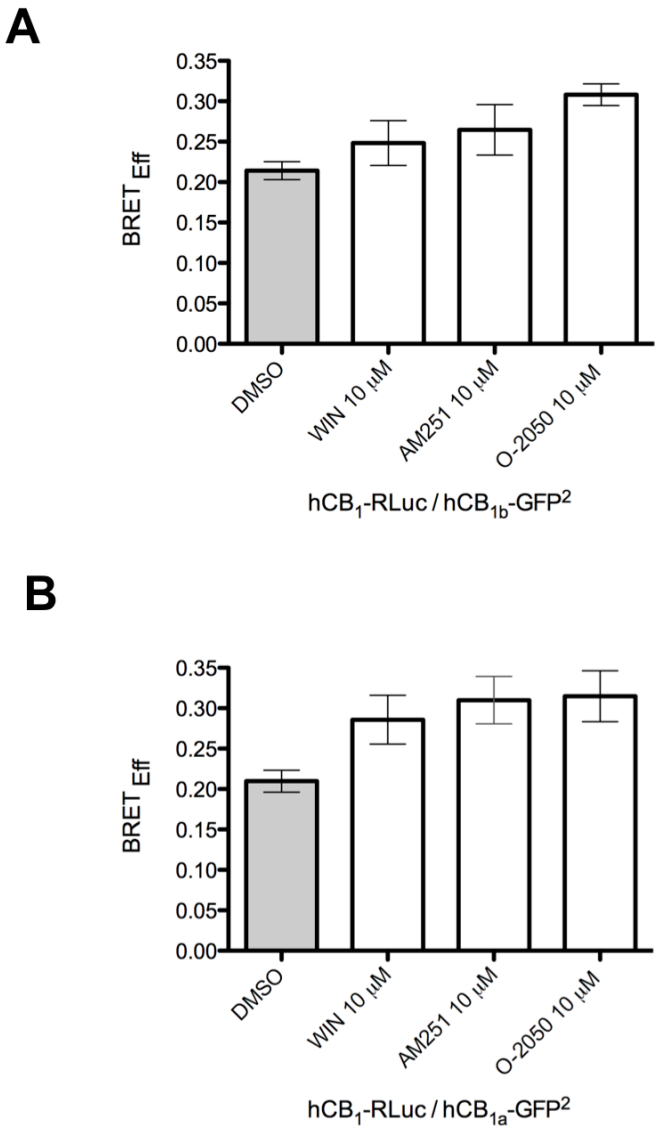

Figure 3.9: Dimerization of the hCB_1 receptor with its splice variants is not affected by CB_1 ligand treatment. $BRET_{Eff}$ obtained from cells transfected with hCB_1-Rluc/hCB1a-GFP^2 **(A)**, and hCB_1 –Rluc/hCB_{1b}-GFP^2 **(B)**, forty-eight hours later cells were treated with either DMSO (0.05%), WIN (10 µM), AM251 (10 µM) or O-2050 (10 µM) for 30 min before $BRET_{Eff}$ was measured. Data are presented as mean ± SEM of three independent experiments; n=4-6. n.s., $P > 0.05$ compared to cells treated with DMSO. Statistical significance was determined by using one-way ANOVA, followed by Tukey's post hoc test.

signals. This finding suggested that heterodimerization of hCB_1 with its splice variants is independent of ligand binding.

3.3.3 Heterodimerization Between hCB_{1a} and hCB_{1b} Receptors

We examined whether dimerization could occur between the splice variants hCB_{1a} and hCB_{1b}. HEK 293A cells were transfected with hCB_{1a}-Rluc or hCB_{1b}-Rluc, in addition to one of the following constructs: hCB_{1b}-GFP^2, hCB_{1a}-GFP^2, HERG-GFP^2 or mGluR6-GFP^2. Cells co-expressing either hCB_{1a}-Rluc/hCB_{1b}-GFP2 or hCB_{1b}-Rluc/hCB_{1a}-GFP^2 revealed a higher $BRET_{Eff}$ values compared to the controls ($P < 0.001$; Fig. 3.10A). The BRET saturation curve was also used to confirm the specificity of the interaction between the two hCB_1 splice variants and resulted in a $BRET_{Max}$ of 0.29 ± 0.015 and $BRET_{50}$ of 0.27 ± 0.014 (Fig. 3.10B). These results revealed that hCB_{1a} and hCB_{1b} were able to form heterodimers when expressed together in HEK 293A cells.

3.4 Pharmacological Characterizations of hCB_1 Splice Variants

The hCB_1 receptor preferentially couples to $G_{i/o}$, and its activation is typically associated with inhibition of adenylyl cyclase, a decrease in cAMP, and activation of MAP kinases (Howlett *et al*., 2004). To determine the signaling properties of the truncated hCB_1 receptors, basal and agonist-stimulated ERK activation was measured using in-cell western analysis in HEK 293A cells expressing each of the receptor. HEK 293A cells were transiently transfected with equimolar amounts of plasmids encoding the hCB_1-GFP^2, hCB_{1a}-GFP^2 or hCB_{1b}-GFP^2 receptors. Twenty-four hours post transfection; cells were pretreated with either 100 ng/ml pertussis (PTx) or DMEM

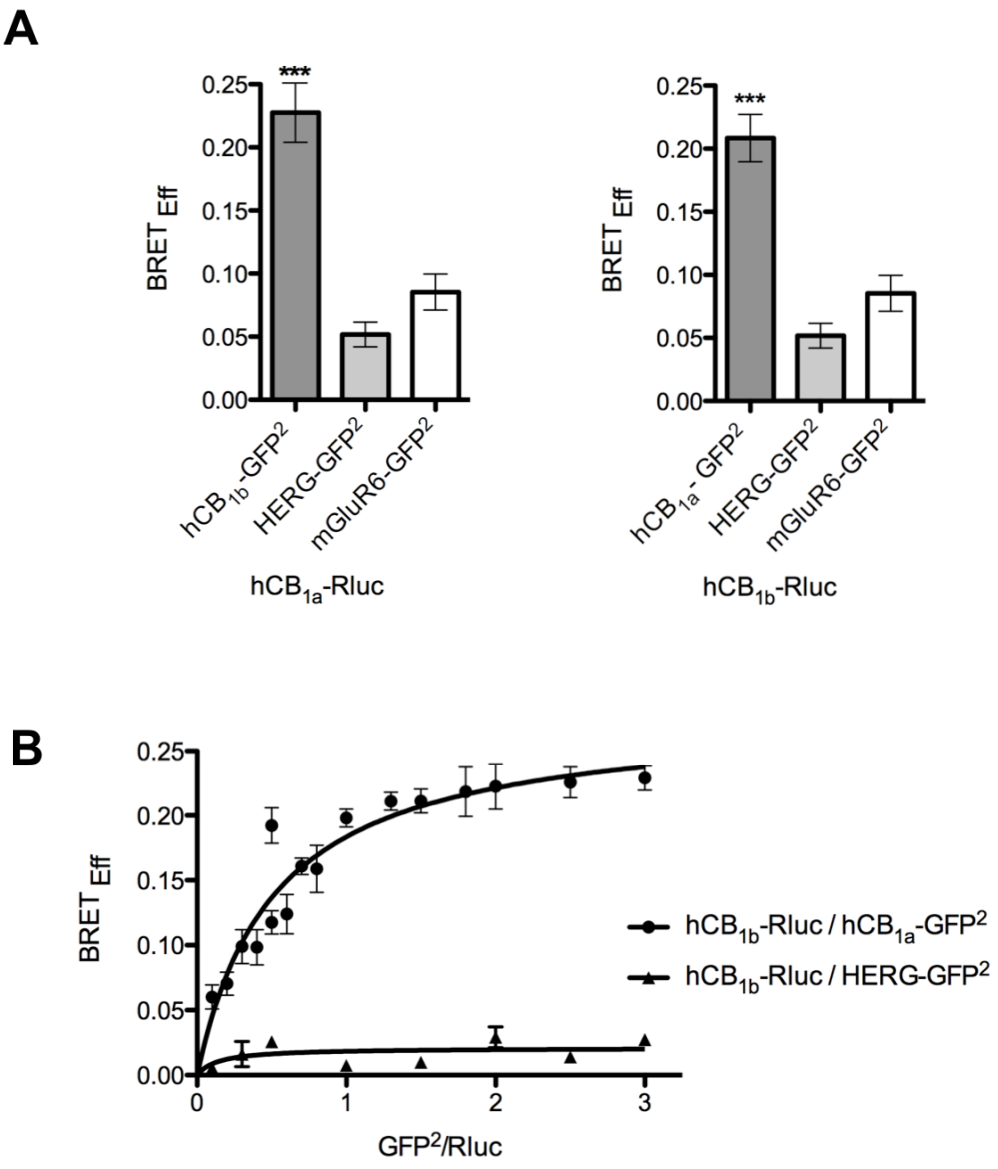

Figure 3.10: The hCB_1 receptor splice variants, hCB_{1a} and hCB_{1b}, can physically interact to form heterodimers in HEK 293A cells. **(A)** The co-expression of hCB_{1a}-Rluc/hCB_{1b}-GFP^2 or hCB_{1b}-Rluc/hCB_{1a}-GFP^2 yielded higher $BRET_{Eff}$ values, compared to when hCB_{1a}-Rluc or hCB_{1a}-Rluc was co-expressed with either HERG-GFP^2 or mGluR6-GFP^2 controls; ***$p<0.001$. **(B)** The BRET saturation curve obtained from cells transiently transfected with a constant amount of hCB_{1b}-Rluc and increasing amounts of hCB_{1a}- GFP^2 was significantly higher than the curve obtained from cells transfected with hCB_{1b}-Rluc/HERG-GFP^2. Data are presented as mean ± SEM of three independent experiments, n=6. Statistical significance was determined by using one-way ANOVA, followed by Tukey's post hoc test.

vehicle, then for 5 min with DMSO vehicle or 1 μM WIN 55212-2. pERK and total ERK were then measured. Cells expressing any of the receptor isoforms had measurable basal pERK that increased significantly upon stimulation with WIN 55212-2 ($P < 0.001$; Fig. 3.11A). There was a significant difference ($P > 0.05$) in pERK between cells expressing the hCB_1 receptor and either hCB_{1a} or hCB_{1b} splice variants. In all the three receptors the pERK responses to WIN 55212-2 were reduced by pre-treatment with PTx ($P < 0.001$). Furthermore, resulted WIN 55212-2 dose response curves (DRC) generated for each hCB_1variant resulting in E_{Max} values of 1.47 ± 0.03, 1.38 ± 0.024 and 1.30 ± 0.025 and pEC_{50} values of 7.33 ± 0.11, 7.05± 0.1 and 7.0 ± 0.12 for hCB_1-GFP^2, hCB_{1a}-GFP^2 or hCB_{1b}-GFP^2 receptors, respectively (Fig. 3.11B). Notably, the two hCB_1 splice variants showed a lower level of ERK efficacy and affinity, compared to the full-length receptor. These findings demonstrate that activation of the hCB_1 splice variants leads to an increase in pERK through a PTx-sensitive pathway, albeit with some differences to hCB_1.

To investigate further the pharmacology of the three hCB_1 receptors, cellular localization and cell surface expression were examined in HEK 293A cells. To follow the subcellular localization of the receptors in HEK 293A cells, confocal microscopy images were taken of cells transiently transfected with equimolar amounts of one of the following plasmids: hCB_1-GFP^2, hCB_{1a}-GFP^2 or hCB_{1b}-GFP^2. In contrast to the hCB_1 receptor, that where localized predominantly intracellular when expressed in HEK 293A cells, hCB_{1a} and hCB_{1b} receptors were observed at the plasma membrane (Fig. 3.12A). In order to quantify the cell surface expression of each receptor, on-cell western analysis was used. As shown in figure 3.12B, the truncated HA-hCB_{1a} and HA-hCB_{1b} receptors have significantly higher plasma membrane expression levels ($P < 0.001$ and $P < 0.05$)

Figure 3.11: Similarly to the hCB_1 receptor, hCB_{1a} and hCB_{1b} receptors signal through PTx sensitive pERK pathway in HEK 293A cells. (A) HEK 293A cells were transiently transfected with equimolar amounts of either hCB_1–GFP^2, hCB_{1a}–GFP^2 or hCB_{1b}–GFP^2 receptors, 24 hours later cells pre-treated for 24 h with either DMEM vehicle or 100 ng/ml PTx, then for 5 min with 0.05% DMSO vehicle or 1 **µ**M WIN. Data are presented as mean ± SEM of three independent experiments, n=6-10. *** $P < 0.001$ compared to unstimulated cells, ### $P < 0.001$ compared with appropriate PTx treatment, * $P < 0.05$ and ** $P < 0.01$ compared to stimulated cells transfected with the hCB_1 and treated with WIN. Statistical analysis was performed using a two-way ANOVA analyzing. **(B)** pERK dose-response curve from HEK 293A cells expressing either hCB_1–GFP^2, hCB_{1a}–GFP^2 or hCB_{1b}–GFP^2, n= 10-15.

A

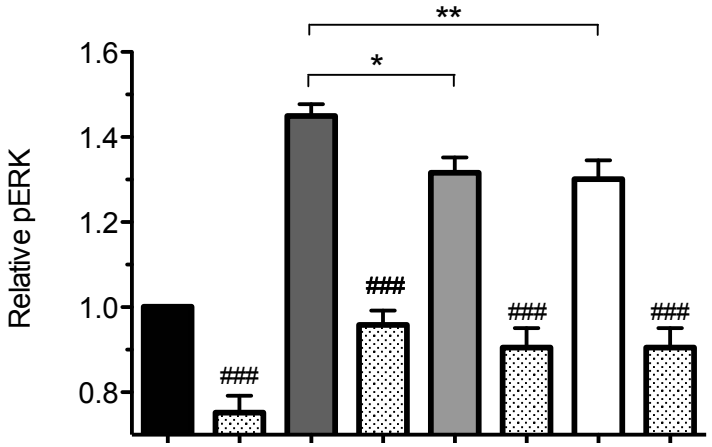

100 ng/ml PTx	-	+	-	+	-	+	-	+
Vehicle	+	+	-	-	-	-	-	-
1 µM WIN	-	-	+	+	+	+	+	+
hCB_1-GFP^2	+	+	+	+	-	-	-	-
hCB_{1a}-GFP^2	-	-	-	-	+	+	-	-
hCB_{1b}-GPF^2	-	-	-	-	-	-	+	+

B

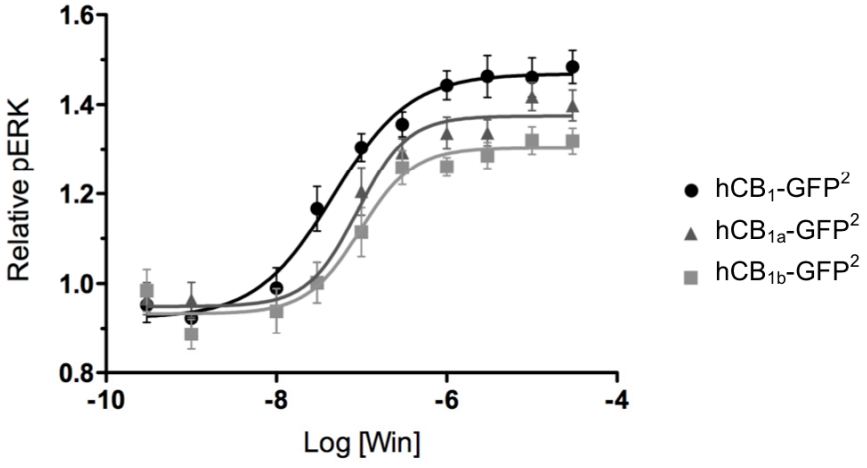

A

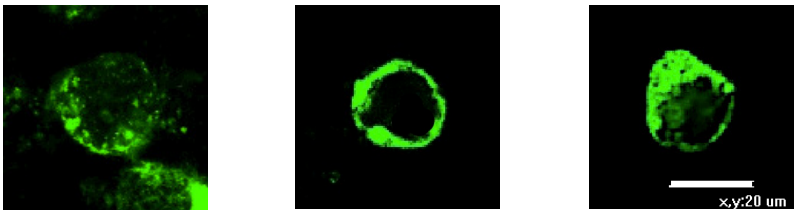

hCB_1-GFP^2 hCB_{1a}-GFP^2 hCB_{1b}-GFP^2

B

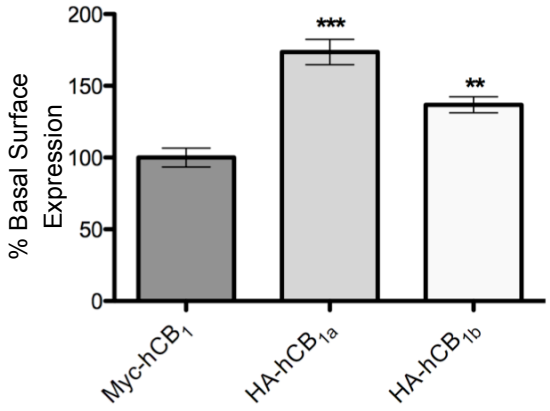

Figure 3.12: The hCB_{1a} and hCB_{1b} receptors have higher expression levels in HEK 293A cells. **(A)** Confocal images of HEK 293A cells transiently transfected with 100 ng of either hCB1-GFP^2, hCB_{1a}-GFP^2 or hCB_{1b}-GFP^2, scale bar is 20 µM. **(B)** On-cell western quantitative measure of hCB_1-GFP^2, hCB_{1a}-GFP^2 or hCB_{1b}-GFP^2 cell surface expression in transiently transfected HEK 293A cells. Data are presented as mean ± SEM of three independent experiments, n=6-12. *** $P < 0.001$; ** $P < 0.01$ compared to cells expressing Myc-hCB_1. Statistical analysis was performed using a one-way ANOVA, followed by Tukey's post hoc test.

respectively, compared to the full-length Myc-hCB_1 receptor. Thus, the truncated hCB_1 receptors have different patterns of cellular localization when expressed individually in HEK 293A cells.

3.5 Functional Interactions Between hCB_1 and its Splice Variants in HEK 293A Cells

Our previous data showed that the full-length hCB_1 receptor was able to dimerize with its splice variants in HEK 293A cells. Therefore, it was important to investigate the functional implications of hCB_1 heterodimerization. The influence of heterodimerization on receptor signaling was studied using the in-cell western technique to assess the level of ERK activation. HEK 293A cells were transfected with either 200 ng hCB_1-GFP^2 construct or 100 ng hCB_1-GFP^2 together with 100 ng hCB_{1a}-GFP^2, 100 ng of hCB_{1b}-GFP^2 or 100 ng HERG-GFP^2. Twenty-four hours later cells were treated with 1 μM WIN 55212-2 for 10 m. When HEK 293A cells expressed only the full-length hCB_1-GFP^2 receptor, an increase in pERK was observed following the treatment with WIN 55212-2 relative to vehicle treated cells (Fig. 3.13A). However, cells co-transfected with both the full-length hCB_1-GFP^2 receptor and one of the truncated receptor hCB_{1a}-GFP^2 or hCB_{1b}-GFP^2 resulted in a higher pERK ($P < 0.001$), compared when hCB_1-GFP^2 receptor was expressed alone or with HERG-GFP^2. The pERK dose response curve generated following WIN 55212-2 treatment in cells co-expressing hCB_1-GFP^2 alone yielded a pEC_{50} of 7.38 ± 0.1, an E_{Max} of 1.46 ± 0.021 and a Hill coefficient of 1.08 . The co-expression of hCB_1-GFP^2 together with one of the splice variants resulted in significantly different dose response curves ($P < 0.001$). Co-expressing hCB_1-GFP^2 and hCB_{1a}-GFP^2

Figure 3.13: Co-expression of hCB_1 with hCB_{1a} or hCB_{1b} receptors increases agonist-stimulated ERK response. (A) HEK 293 cells were transiently transfected with either 200 ng of hCB_1-GFP^2 alone, or 100 ng of hCB_1-GFP^2 with 100 ng of either hCB_{1a}-GFP^2, hCB_{1b}-GFP^2 or HERG-GFP^2, and treated with 0.05% DMSO vehicle or 1 μM WIN for 10 minutes before pERK was measured. *** $P < 0.001$ compared to cells expressing hCB_1 and treated with WIN; ### $P < 0.001$ compared to cells expressing hCB_1 and treated with vehicle. Data are presented as mean ± SEM of three independent experiments, n=10-12. Statistical analysis was performed using two-way ANOVA analyzing receptor expression and WIN stimulation. **(B)** pERK dose response curve from HEK 293A cells expressing hCB_1-GFP^2 or together with hCB_{1a}-GFP^2 or hCB_{1b}-GFP^2 and treated with WIN for 5 m. Data are presented as mean ± SEM of three independent experiments n=15-18.

A

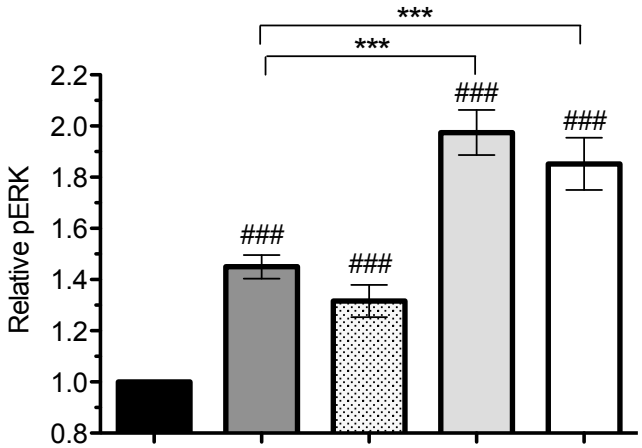

Vehicle	+	-	-	-	-
1 μM WIN	-	+	+	+	+
HERG-GFP^2	-	-	+	-	-
hCB$_1$-GFP^2	+	+	+	+	+
hCB$_{1a}$-GPF^2	-	-	-	+	-
hCB$_{1b}$-GFP^2	-	-	-	-	+

B

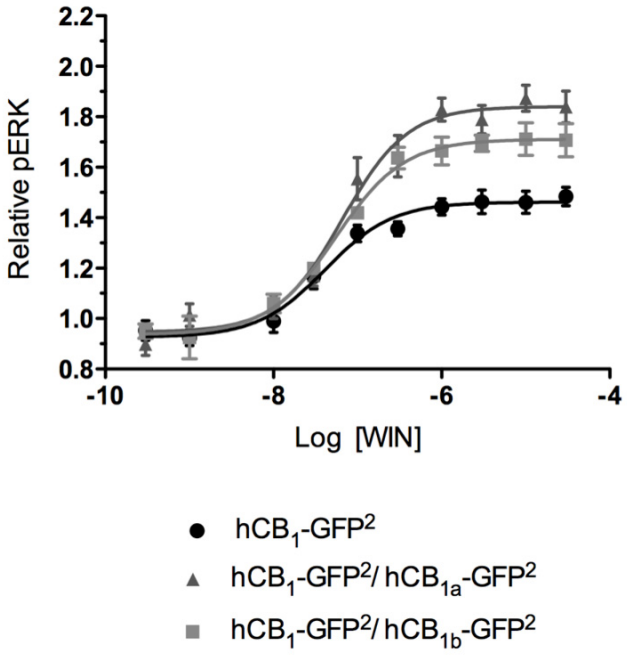

resulted in a pEC_{50} of 7.18 ±0.093, an E_{Max} of 1.84 ± 0.03 and a Hill coefficient of 1.12, while cells co-expressing hCB_1-GFP^2 and hCB_{1b}-GFP^2 yielded a pEC_{50} of 7.25 ± 0.092, an E_{Max} of 1.72 ± 0.029 and Hill coefficient of 1.072 (Fig. 3.13B) . The effect on signaling of the full-length hCB_1 receptor is dependent on the dose of the co-transfected truncated receptor, as the higher the ratio of the truncated receptor to the full-length receptor the higher the ERK activation (Fig. 3.14).

We hypothesized that the increase in ERK signaling could be due to the increase in hCB_1 cell-surface expression when co-expressing the hCB_{1a} or hCB_{1b}. Cell surface expression of the hCB_1.GFP^2 receptor alone, and in the presence of the truncated splice variant, HA-hCB_{1a} or HA-hCB_{1b}, was examined using confocal microscopy. When the full-length hCB_1-GFP^2 receptor was co-transfected with the truncated HA-hCB_{1a} or HA-hCB_{1b} receptor in HEK 293A cells, it was found that the localization of hCB_1-GFP^2 was increased at the cell surface membrane (Fig 3.15A). When the cells expressed only hCB_1-GFP^2, distribution of the receptor was consistent with a more internalized receptor (Fig. 3.15A). On-cell western analysis was also used to quantify the effect of co-expression of the truncated HA-hCB_{1a} and HA-hCB_{1b} receptors on the cell surface expression of Myc-hCB_1. The co-expression of Myc-hCB_1 with either of the splice variants resulted in a significant increase in Myc-hCB_1 cell surface expression ($P < 0.001$), while the co-expression of HERG-GFP^2 did not change Myc-CB_1 surface expression (Fig. 3.15B). Our data indicated that the co-expression of hCB_1 splice variants increased hCB_1 cell surface expression.

Next, we examined co-internalization of the Myc-hCB_1 following treatment with WIN 55212-2. Treatment of HEK 293A cells expressing Myc-hCB_1 with 10 μM CB_1

agonist WIN 55212-2 for 30 min resulted in reduction in Myc-hCB_1 cell surface expression ($P < 0.001$). However, when cells were co-transfected with both Myc-hCB_1 and HA-hCB_{1a} or HA-$hCB_{1b,}$ and treated with WIN, co-internalization of both receptors was observed (Fig. 3.16A). On-cell western analysis was also used to measure Myc-hCB_1 internalization (Fig. 3.16B). Cells expressing the Myc-hCB_1 receptors alone showed a significant reduction in cell-surface expression of the hCB_1 receptor after WIN 55212-2 treatment ($P < 0.001$) in relation to untreated cells. However, cells co-transfected with both the Myc-hCB_1 receptor and one of the splice variants and treated with WIN 55212-2 showed less internalization ($P < 0.01$), compared with WIN-treated cells expressing the hCB_1 receptor alone. Co-expression of Myc-hCB_1 and HERG-GFP[2] did not alter the trafficking of the hCB_1 receptor.

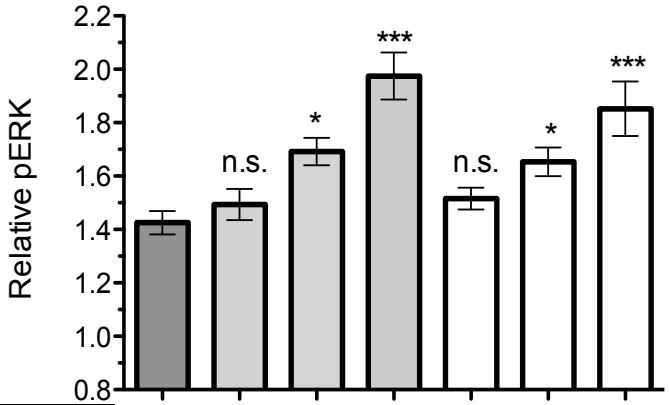

ng plasmid							
hCB_1-GFP^2	200	100	100	100	100	100	100
hCB_{1a}-GFP^2	-	50	75	100	-	-	-
hCB_{1b}-GPF^2	-	-	-	-	50	75	100
pcDNA 3.1	-	50	25	-	50	25	-

Figure 3.14: Co-expression of hCB_1 with hCB_{1a} or hCB_{1b} receptors increases agonist-stimulated ERK response. HEK cells were transfected with varying dose of hCB_1-GFP^2 and its splice variants and treated with 1 μM WIN 55212-2. *** $P < 0.001$; * $P < 0.05$; n.s. $P > 0.05$ compared to cells expressing 200 ng hCB_1. Data are presented as mean ± SEM of three independent experiments, n=10-12. Statistical analysis was performed using two-way ANOVA analyzing receptor expression and WIN 55212-2 stimulation.

Figure 3.15: Co-expression of hCB_{1a} or hCB_{1b} facilitates cell surface expression of hCB_1. (A) Confocal images of HEK 293A cells transiently transfected with hCB_1-GFP^2 and HA-hCB_{1a} or HA-hCB_{1b}. Left images show GFP^2 fluorescence, middle images are anti-HA immunofluorescence utilizing a Cy^3 conjugated antibody, and the right images are the merged images. Scale bar is 20 μm. **(B)** Quantitative measure of Myc-hCB_1 cell surface expression in HEK 293A cells transiently transfected with 100 ng Myc-hCB_1, or co-transfected with 100 ng of HA-hCB_{1a}, HA-hCB_{1b} or HERG-GFP^2. Data are presented as mean ± SEM of three independent experiments, n=6-10. ** $P < 0.01$ compared to cells expressing 100 ng Myc-hCB_1. Statistical analysis was performed using a one-way ANOVA, followed by Tukey's post hoc test.

A

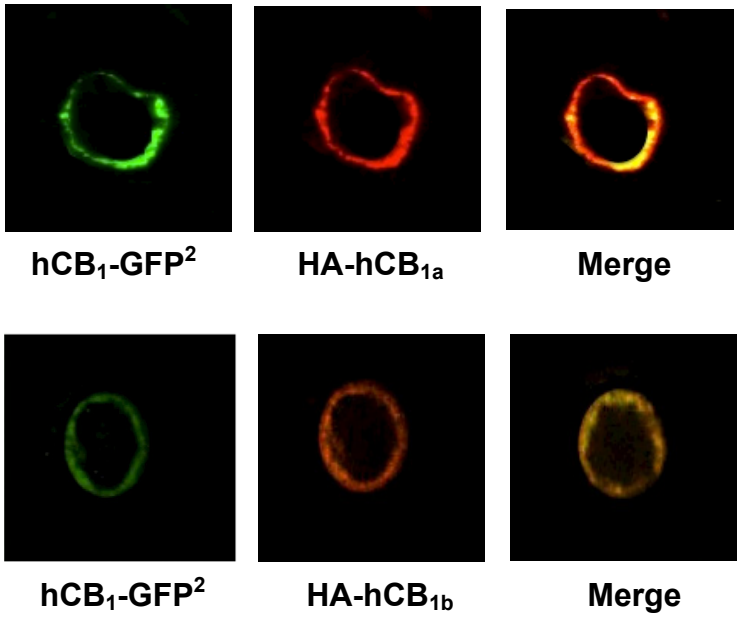

B

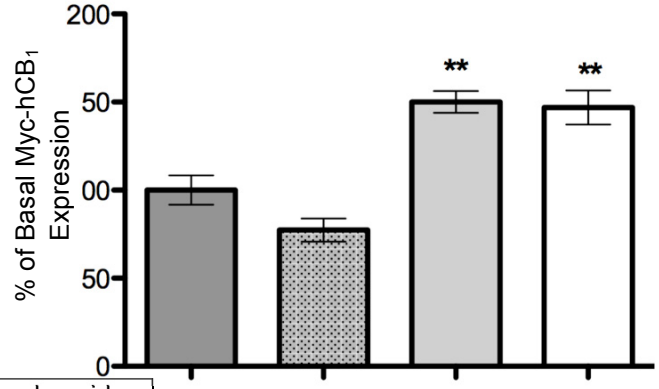

ng plasmids				
Myc-hCB$_1$	100	100	100	100
HA-hCB$_{1a}$	-	-	100	-
HA-hCB$_{1b}$	-	-	-	100
HERG-GFP^2	-	100	-	-
pcDNA 3.1	100	-	-	-

Figure 3.16. The hCB_1 receptor is co-internalized with its splice variant following WIN 55212-2 treatment. (A) Confocal images of HEK 293A cells transiently transfected with with hCB_1-GFP^2 and HA-hCB_{1a} or HA-hCB_{1b} and treated with 10 μM WIN 55212-2. Left images show GFP^2 fluorescence, middle images are anti-HA immunofluorescence utilizing a Cy^3 conjugated antibody, and the right images are the merged images. Scale bar = 20 μm. **(B)** Quantitative measure of Myc-hCB_1 cell surface expression in HEK 293A cells transiently transfected with 100 ng Myc-hCB_1, or co-transfected with 100 ng of HA-hCB_{1a}, HA-hCB_{1b} or HERG-GFP^2 and treated with 10 μM WIN 55212-2. Data are presented as mean ± SEM of three independent experiments, n=10-12. *** $P < 0.001$ compared to cells treated with vehicle; # $P < 0.05$ compared to cells expressing Myc-hCB_1 and treated with WIN 55212-2. Statistical analysis was performed using a two-way ANOVA, followed by Tukey's post hoc test.

A

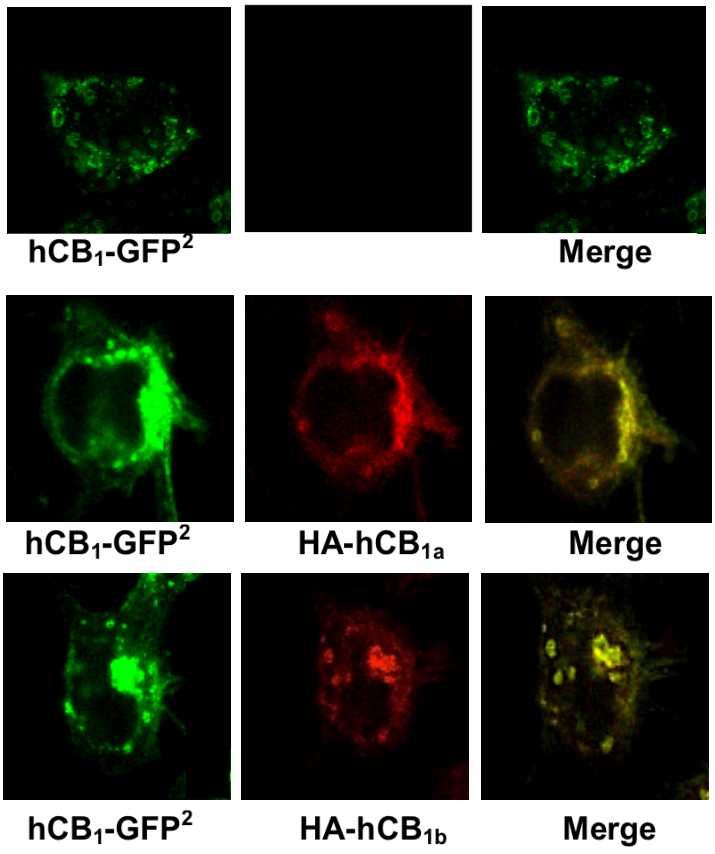

B

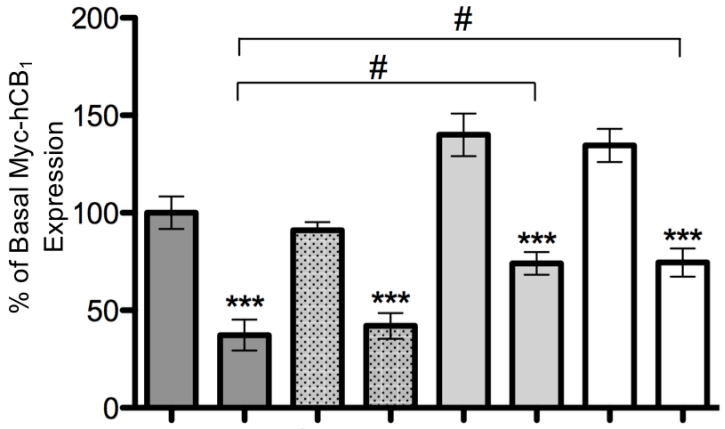

Vehicle	+	-	+	-	+	-	+	-
10 μM WIN	-	+	-	+	-	+	-	+
Myc-hCB$_1$	+	+	+	+	+	+	+	+
HA-hCB$_{1a}$	-	-	-	-	+	+	-	-
HA-hCB$_{1b}$	-	-	-	-	-	-	+	+
HERG-GFP^2	-	-	+	+	-	-	-	-

Chapter 4: Discussion

Dimerization between full-length GPCRs and their splice variants, under normal physiological conditions, has been reported to play an important role in regulating the functions of their full-length receptors (Bai, 2004). The recent discovery that the hCB_1 receptor is subjected to alternative splicing within the coding region, to form hCB_{1a} and hCB_{1b} transcripts, raises many questions regarding their distribution, functional differences and their biological roles (Shire *et al,* 1995; Ryberg *et al.,* 2005; Xiao, 2008). The present study aimed to determine the relative abundance and distribution of mRNAs encoding the three coding region CB_1 variants in human and monkey (*Macaca fascicularis*) brains, and to examine whether the hCB_{1a} and hCB_{1b} are expressed as proteins in the monkey brain. The overlapping patterns of distribution of the mRNAs of the three coding region variants raises the possibility that physical interaction through dimerization may occur and influence the function of hCB_1 receptor complexes. Finally we examined whether the hCB_1 variants can physically interact when co-expressed in a heterologous expression system, and looked to determine if co-expression of variants affects trafficking and signaling of hCB_1.

4.1 The hCB_{1a} and hCB_{1b} mRNAs were Distributed Throughout the Brain

In the present study, the CNS distribution of the hCB_1 variants was determined in a tissue derived from the brain of a 71 year-old human donor and a 4-year old monkey brain (equivalent to 12 human years). RT-PCR was conducted using a primer set common to the three-hCB_1 variants and all the three variant transcripts were detected in

all the regions examined in human and monkey brains. Although quantification was not possible, it appeared that each variant was amplified at the minimum number of cycles needed to observe any product, suggesting that template concentration was similar in each sample. Our findings agree with previously published data that reported that hCB_{1a} and hCB_{1b} mRNAs are expressed in adult human total brain tissue (Shire *et al,* 1995; Ryberg *et al.,* 2005; Xiao *et al*., 2008). However, the relative expression levels of the three variants in our results are not similar to previously published data. In earlier studies, hCB_1 mRNA was found to be the most abundant transcripts, while hCB_{1a} and hCB_{1b} mRNAs were found to be the minor transcript, as they represent fewer than 5% of the total hCB_1 transcripts (Shire *et al,* 1995; Ryberg *et al.,* 2005; Xiao *et al*., 2008). These discrepancies in the expression levels of the three hCB_1 variants could be due to a number of factors. RNAs used in the current study were obtained from a 71 year-old female donor and age might alter variant levels, however the age of the donors were not stated in previously studies. Age-related differences in levels of CB_1 mRNA and its protein have been reported in the human brain. It was found that CB_1 mRNA is expressed as early as 9 weeks gestation prenatal ages, and CB_1 mRNA level rises after birth to reach a plateau at one year of age. CB_1 mRNA level increases further during adolescence to reach a steady state level, thereafter decreasing throughout adulthood (Wang *et al*., 2003; Zurolo *et al*., 2010; Pinto *et al*., 2010). Another factor affecting the difference in the expression levels of the three CB_1 variant mRNAs observed in our study could be the different PCR conditions and primers used. In summary, our findings demonstrated that the three CB_1 variants are co-expressed together throughout human and monkey brains.

Whether CB_{1a} and CB_{1b} transcripts are translated into proteins *in vivo* has not yet been examined. Therefore, we performed western blots using the same monkey (*Macaca fascicularis*) brain tissues used for the RT-PCR reaction and an antibody directed against the C-terminal region of the receptor. Three bands were detected at the expected molecular weights for CB_1, CB_{1a} and CB_{1b} in all the tested brain regions. The CB_1 receptor appears to be the most abundant, while the two splice variants appear to be less abundant. To further confirm our result, western blot analysis was also conducted using an antibody raised against the first 14 amino acids of the N-terminal tail of the hCB_1 receptor (Chemicon), a region that is unique to hCB_1 and hCB_{1b} receptor, but is not found in hCB_{1a}. Two bands were detected at the expected molecular weight for both hCB_1 and hCB_{1b} (data not shown). An isoform specific antibody would be of great value to confirm our findings, since the two bands that were detected at the expected molecular weights for CB_{1a} and CB_{1b} could be degraded or incomplete CB_1 fragments.

GPCR splice variants can have different localization. For example, the dopamine receptor D_{2S} and D_{2L} receptors variants are differentially localized in CNS neurons, where the short isoform is localized pre-synaptically, while the long isoform is localized post-synaptically (Khan *et al*., 1998). It is well documented that the hCB_1 receptor is localized pre-synaptically in the CNS (Howlett *et al.*, 2004). Whether the two splice variants are localized pre- or post-synaptically has not been examined yet. For this reason, it is very important to determine the specific cellular localization of the two splice variants at both the mRNA and protein levels. To achieve these goals, we conducted single labeling *in situ* hybridization using sections of the monkey frontal cortex and CB_1 and CB_{1b} isoform-specific probe. The hybridization signal indicated no difference

between the expression levels and localizations of the two CB_1 variants. These findings might suggest that CB_1 and CB_{1b} transcripts have similar expression and cellular localization, or it might indicate that the isoform-specific probes for each variant are not specific (Data not shown). Using double labeled *in situ* hybridization would allow for colocalization of two different mRNAs simultaneously on the same brain section.

The full-length CB_1 receptor gene is highly conserved across species. Despite the high degree of primary sequence conservation, the CB_1 coding region splice variants have only been reported in human, non-human primates brain and rat astrocyte culture (Shire *et al.,* 1995; Ryberg *et al*., 2005; Eggan *et al*., 2007). This finding has been challenged by later studies that reported that neither of the splice variants was detected in the rat brain (Fig. 4-1; Xiao *et al*., 2008; Ryberg *et al*., 2005). Several attempts have been made in the current study to amplify CB_{1a} and CB_{1b} using cDNAs from mouse and rat brain using species-specific primers. However, we were unable to detect CB_{1a} and CB_{1b} in mouse or rat brains, despite repeated experiments with different primer sets and PCR conditions (data not shown). The consensus splicing sequence for the 5′ splice site (donor) is (NN/gt), while for the 3' splice site (acceptor) is (ag/NN). Both sites are highly conserved at splicing junctions in eukaryotes (Burset *et al*., 2000). The human and the monkey CB_1 sequences contain all consensus-splicing sites required to generate CB_{1a} and CB_{1b} transcripts (gt-ag). Splicing is, therefore, possible at both sites to generate CB_{1a} and CB_{1b}. In contrast, the rat and mouse CB_1 sequences lack the consensus 5' splice site sequence required to generate CB_{1a} and CB_{1b}. Instead, the rat and mouse sequences contain a non-consensus splicing site (/ct) at the 5' splicing site of CB_{1b} and (/ga) at the 5' splicing site for CB_{1a}. The rat and mouse sequences contain the consensus 3' splice sites for both

1 2

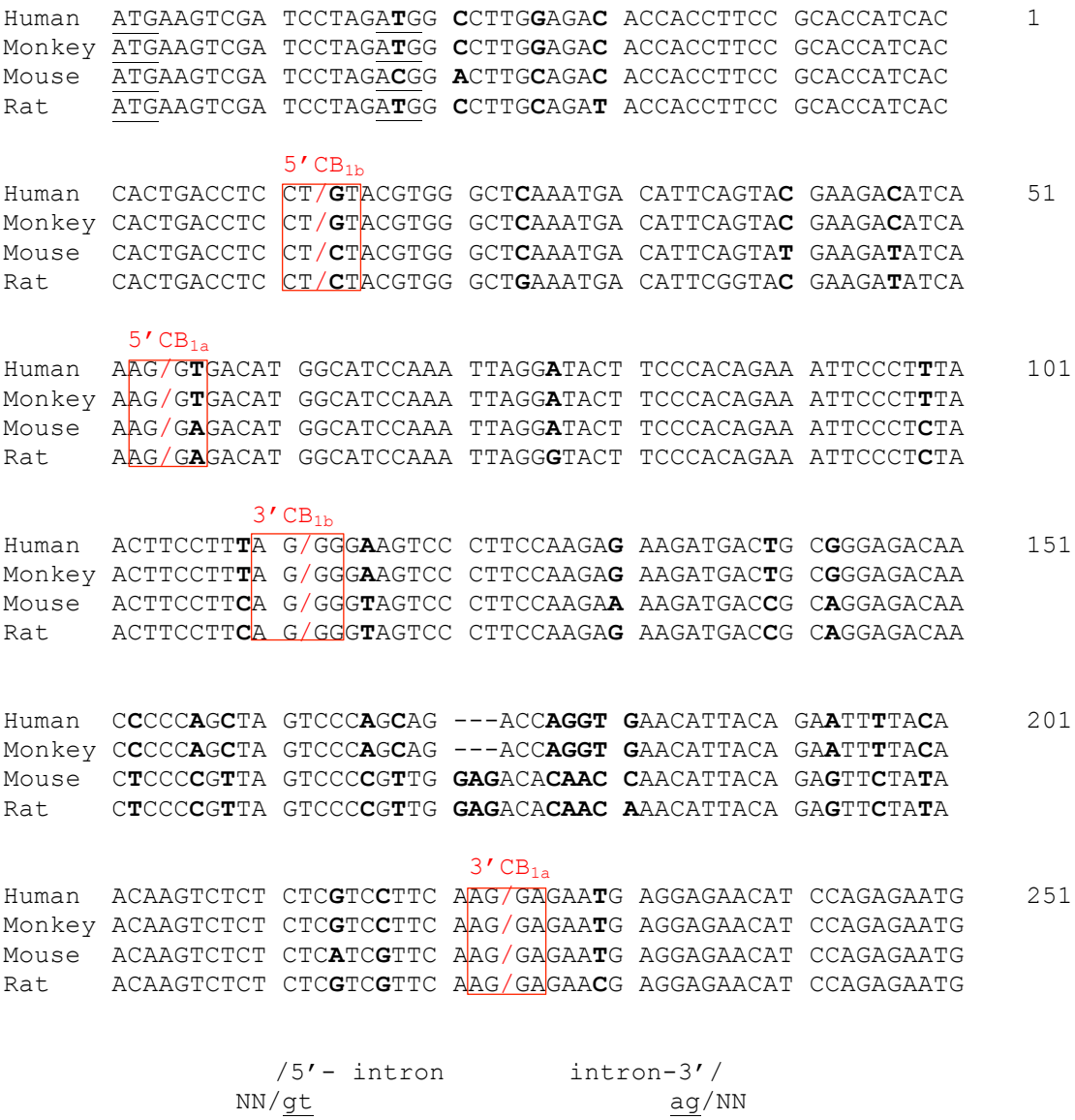

Figure 4.1: Genomic DNA sequences of human, monkey, mouse and rat CB_1 and the splicing sites for CB_{1a} and CB_{1b}. The initiation codon for CB_1 and CB_{1b} is ATG 1, while for CB_{1a} is ATG 2, both are underlined. Nucleotide differences among species are indicated in bold. Splicing sites for CB_{1a} and CB_{1b} are indicated by red boxes. Dashes represent gaps. (Figure was modified from Xiao *et al*., 2008; NCBI).

splice variants. In addition, the mouse CB_1 sequence lacks the initiation codon (ATG) for hCB_{1a}, indicating that translation of CB_{1a} in mouse is unlikely. Given the lack of consensus sequences splicing is less likely to occur to generate CB_{1a} and CB_{1b} in rodents than in human and monkey. Enrichment culture of a single astrocyte cell type may have allowed for detection of CB_{1a} splice variant by Shire and his colleague (1995). In conclusion, CB_{1a} and CB_{1b} receptors may be restricted to human and non-human primates.

4.2 hCB_1 Receptor Splice Variants can form Homo and Heterodimers

The dimerization of GPCRs represents an important phenomenon that modulates receptor function (Terrillon and Bouvier, 2004). Using $BRET^2$ and co-immunoprecipitation assays, previous studies have demonstrated that hCB_1 receptor was capable of forming dimeric or multimeric complexes when expressed alone in heterologous expression cell systems (Wager-Miller *et al.*, 2002; Hudson *et al*., 2010). In the current study, protein–protein interactions between and among hCB_1 and its splice variants were examined. We showed, using $BRET^2$, that hCB_{1a} and hCB_{1b} receptors, like hCB_1, could form homodimers when expressed alone in HEK 293A cells. Similar to hCB_1, the two variants exhibit specific and saturable homodimerization as determined by BRET saturation curves. Earlier studies have proposed that $BRET_{50}$ values reflect the affinity of donor and acceptor molecules for each other (Guan *et al*., 2009). By comparing the BRET saturation curves obtained for hCB_1, hCB_{1a} and hCB_{1b} homodimers, similar $BRET_{50}$ values were obtained, suggesting that the three hCB_1

variants have relatively similar affinity to form homodimers when expressed in HEK 293A cells (Mercier *et al.*, 2002). $BRET_{Max}$, however, reflects the relative orientations, distances, and expression levels of both donor and acceptor molecules (Guan *et al.*, 2009). The hCB_{1a} and hCB_{1b} homodimer saturation curve had significantly greater $BRET_{Max}$ values compared to the hCB_1-homodimer saturation curve. This indicates either that a larger proportion of hCB_{1a} and hCB_{1b} receptors can engage in dimerization than hCB_1 receptor or that the relative position of Rluc and GFP^2 within the hCB_{1a} and hCB_{1b} receptors are more permissive to energy transfer (Mercier *et al.*, 2002). Our results (using confocal images and on-cell western) showed that the two splice variants have higher cell-surface expression levels when heterologously expressed in HEK 293A cells, which might be the reason for the greater $BRET_{Max}$ observed.

Using a similar experimental approach, heterodimerization among hCB_1 and its splice variants was also demonstrated. These interactions were observed at low levels of expression, and were saturable as determined by BRET saturation curves. In addition, the interactions were competitively blocked by a receptor construct that was not tagged for BRET, suggesting that the interaction detected by BRET was specific. This was confirmed by co-expressing HERG, a non-competitive receptor, which is known not to interact with hCB_1 (Hudson *et al.*, 2010). Comparison of BRET saturation curves generated for the homodimers (hCB_1, hCB_{1a} and hCB_{1b}) and heterodimers (hCB_1-Rluc/hCB_{1a}-GFP^2, hCB_1-Rluc/hCB_{1b}-GFP^2 and hCB_{1a}-Rluc/hCB_{1b}-GFP^2), revealed that $BRET_{50}$ values for homodimers were lower than that for heterodimers. This finding might suggest that each hCB_1 variant has a higher affinity to form homodimers over heterodimers when the two receptors are heterologously expressed in HEK 293A cells.

When considering the maximal BRET values obtained for hCB_1-Rluc/hCB_{1a}-GFP^2, hCB_1-Rluc/hCB_{1b}-GFP^2 and hCB_{1a}-Rluc/hCB_{1b}-GFP^2 heterodimers, $BRET_{Max}$ values were found to be lower when compared to homodimers. The BRET saturation curve obtained from cells expressing the two splice variants hCB_{1a}-Rluc/hCB_{1b}-GFP^2 resulted in $BRET_{50}$ of 0.27 ± 0.014. This could indicate that dimerization between the two splice variants might occur with higher affinity compared to dimerization of each variant with hCB_1. However, it is hard to draw final conclusions regarding the affinity of each receptor to form homo- or heterodimers based on $BRET_{50}$ values obtained from BRET saturation curves, as interpretation of the $BRET_{50}$ values may be confounded by higher order GPCR oligomerization occurring in addition to dimerization (Guan *et al.*, 2009).

Given the affinity of hCB_1 and its splice variants to form homo- and heterodimers, $BRET_{Max}$ and $BRET_{50}$ values reflect a mixed population of dimeric forms when two different receptors are co-expressed. For example, if cells co-expressing hCB_1-Rluc and hCB_{1a}-GFP^2 fusion proteins, and we assumed that 100% of the expressed receptors will form dimers at equimolar concentrations of the two receptors (GFP^2/Rluc = 1), we would predict that 50% of the hCB_1-Rluc/hCB_{1a}-GFP^2 receptors would form heterodimers to produce BRET signals. The other 50% of the receptors would form homodimers (25% will form hCB_1 Rluc and 25% hCB_{1a}-GFP^2; Fig.4-2; Mercier *et al.*, 2002). The distribution will be influenced by *in vivo* affinity, intracellular distribution and it is possible that monomer, tetramer or higher-order oligomer scenarios may still occur.

Our data demonstrated that cannabinoid ligands are not required for the initiation of dimerization, since $BRET_{Eff}$ was detected for all receptor pairs (hCB_1, hCB_{1a}, hCB_{1b},

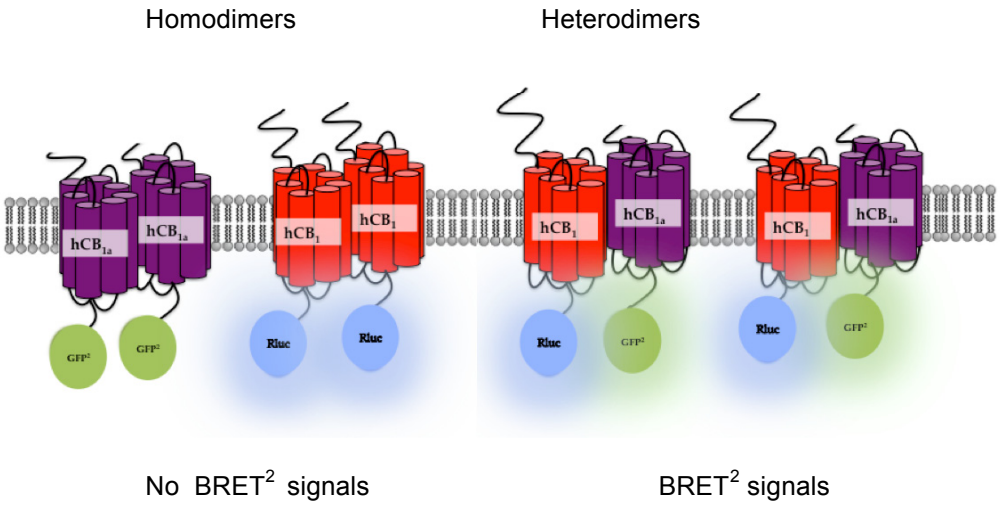

Figure 4.2: Schematic representation of the estimated percentage of hCB_1-Rluc and hCB_{1a}-GFP^2 dimers in living cells. At equimolar concentrations of the two receptors only 50% of the receptor will form heterodimers, resulting in a BRET signal, while the other 50% of receptor will form homodimers.

hCB_1/hCB_{1a}, hCB_1/hCB_{1b}, and hCB_{1a}/hCB_{1b}) in the absence of cannabinoids ligands. Treatment of cells with either the hCB_1 agonist WIN 55212-2, inverse agonist AM251 or neutral antagonist O-2050 did not alter $BRET_{Eff}$ values. This finding is in agreement with previous studies that reported that dimerization is a constitutive process that is not modulated by ligand binding, as binding of the ligand would only alter the conformation of the heterodimer in such a way that does not affect the $BRET_{Eff}$ (Terrillon and Bouvier, 2004; Guan *et al*., 2009).

The observed dimerization between and among hCB_1 and its N-terminal truncated variants also offers some insight into the main domains involved in dimerization. In general, the rhodopsin family of GPCRs is thought to dimerize by interaction of transmembrane domains (Milligan, 2004). However, some studies looking at the rhodopsin family of GPCRs reported that the N-terminal tail might be important for dimerization. For example, truncation of 53 amino acid at the N-terminal tail of the β_2-AR resulted in a receptor that is unable to dimerize with the bradykinin receptor (AbdAlla, *et a*l., 1999; Bai, 2004). Focusing on the hCB_1 receptor, the main domain involved in dimerization is not well known. However, a previous study has shown that the C-terminus of the hCB_1 receptor is not involved in the dimerization (Hudson *et al.,* 2010). Our results from the N-terminal truncated hCB_1 variants revealed that truncation of the N-terminal tail did not affect the ability of the receptor to dimerize. Consequently, we proposed that the N-terminal tail of the hCB_1 is not an obligate domain involved in hCB_1 dimerization, but might affect affinity. To precisely define the amino acid residues required for dimerization, additional experiment of site-directed mutagenesis of the receptor would be necessary.

4.3 Pharmacological Differences of hCB_1 Splice Variants Homo and Heterodimers

The signaling differences among hCB_1 and it splice variants remain controversial. Previous work has shown that the three hCB_1 receptor isoforms act through a $G_{i/o}$ protein to inhibit adenylyl cyclase and stimulate MAP kinase (Rinaldi-Carmona *et al*., 1996). In the present study, we assessed the difference in pERK signaling among hCB_1 receptor variants using the cannabinoid receptor agonist WIN 55212-2. In our results, significant differences among hCB_1 variants were found in their ability to stimulate ERK upon WIN 55212-2 treatment. The two variants showed lower efficiency (E_{max}) and affinity (pEC_{50}) values compared to hCB_1 receptors. Earlier studies have found that WIN 55212-2 exhibits a lower affinity to the truncated-receptor hCB_{1a} compared to the full-length receptor hCB_1 (Ryberg *et al*., 2005; Rinaldi-Carmona *et al*., 1996). The hydrophobic nature of cannabinoid ligands suggests that their ligand-binding site is localized within the transmembrane bundle of the receptor (McAllister *et al*., 2003). The N-terminal tail of the hCB_1 receptor is not directly involved in the formation of the ligand-binding pocket. The mechanism by which the N-terminal tail of the hCB_1 receptor is involved in ligand binding is still obscure. However, it has been suggested that the N-terminal tail could have some influence on the architecture of the ligand binding sites and truncation of the N-tail can reduce the affinity of ligand to the receptor. The reduced affinity may be the cause of the reduced efficiency observed with hCB_{1a} and hCB_{1b} receptors.

The role of the N-terminal tail in regulating GPCR trafficking is not well understood (Dong *et al*., 2007). There is some evidence that suggests that the N-terminal tail of the hCB_1 receptor might function in receptor trafficking from the endoplasmic reticulum to

the plasma membrane (Andersson *et al*., 2003). In the current study, we examined the differences in trafficking and subcellular localization patterns among hCB_1 and its variants when expressed in HEK 293A cells. The three variants were tagged at the C-terminus with GFP[2] and were transiently transfected into HEK 293A cells. By using confocal microscopy, we showed that the two splice variants, hCB_{1a} and hCB_{1b}, were mainly localized at the plasma membrane while the hCB_1 receptor was predominately accumulated intracellularly, which is consistent with previous studies (Bohn, 2007; Hudson *et al*., 2010). On-cell western analyses were also used to quantitatively measure total and cell-surface expression of each receptor variant. hCB_1 was tagged with a Myc tag antibody at the N-terminus, while hCB_{1a} and hCB_{1b} receptors were tagged with an HA tag. Similar to our confocal results, the hCB_{1a} and hCB_{1b} were expressed at higher levels and mainly localized at the cell membrane when transiently transfected into HEK 293A cells. The full-length hCB_1 receptor was mainly localized intracellularly. In order to eliminate the possibility that the differences in the measured expression levels are due to the use of different antibodies, similar experiments were conducted using untagged hCB_1 and hCB_{1b} receptors and an antibody directed against the first 14 amino acids of the N-terminal tail. Consistent results were found regarding their expression levels and cellular localization (data not shown). The findings in our study are supported by a study carried out by Andersson *et al*. (2003), who demonstrated that shortening the N-terminus of the CB_1 receptor greatly increases receptor stability, and results in increased targeting to the cell surface. In this study, the authors proposed that the large N- terminus of the hCB_1 receptor acts to inhibit efficient translocation of the receptor across the endoplasmic reticulum, leading to high levels of misfolded receptor that are subsequently degraded

(Andersson *et al*, 2003). In contrast, increasing the length of the N-terminal tail of the CB_1 receptor by adding a GFP tag was found to inhibit efficient receptor translocation across the endoplasmic reticulum (McDonald *et al.,* 2007). Taken together, these studies strongly support our findings that the N-terminal truncated hCB_1 variants have higher cell surface expression, than the full-length hCB_1.

Similar to other GPCRs, the hCB_1 receptor has been reported to associate with a variety of accessory proteins, which may direct both trafficking and cellular localization. These include G-protein receptor-associated sorting protein 1 (GASP1) and cannabinoid receptor-interacting protein 1a and 1b ($CRIP_{1a}$ and $CRIP_{1b}$; Smith *et al*., 2010). All these proteins bind at the C-terminal tail of the hCB_1 receptor and modulate cellular trafficking and signal transduction (Howlett *et al*., 2010; Smith *et al*., 2010). Alternatively spliced GPCR isoforms can differ in their ability to interact with accessory protein (Markovic & Challiss, 2009). It is still unclear, whether the increase cell surface expression observed with the two hCB_1 variants is caused solely by the truncated N-terminal tail, or by another accessory protein that interact with it.

Having revealed a physical interaction among hCB_1 and its variants, it was next important to demonstrate if this interaction had functional consequences for the full-length hCB_1. GPCR heterodimerization may influence the signaling pathways activated by the receptors present in the complex (Milligan, 2004; Terrillon and Bouvier, 2004). In HEK 293A cells transiently transfected with hCB_1-GFP^2 and either hCB_{1a}-GFP^2 or hCB_{1b}-GFP^2 and treated with the cannabinoid agonist WIN 55212-2, there was an increase in pERK, indicating that hCB_1-GFP^2 heterodimers couple to both $G_{i/o}$ pathway in these cells. Interestingly, co-expression of hCB_1 with its splice variant resulted in an

increase in both the E_{max} and Hill coefficient of the WIN-stimulated pERK dose-response of these cells, but not the pEC_{50}. This apparent increase in E_{max} could be explained either by an increase in the hCB_1 heterodimer complex coupling to $G_{i/o}$, or by an increase in cell-surface expression of the hCB_1 receptor. To examine these hypotheses, the trafficking of the Myc-hCB_1 was examined when expressed alone or with HA-hCB_{1a} or HA-hCB_{1b}. When hCB_1 receptor was expressed in HEK 293A cells, expression was observed in a punctate pattern. This is due to the high constitutive activity of the receptor resulted in a constitutive internalization of the receptor (Bohn, 2007), unlike the hCB_{1a} and hCB_1, which are mainly localized at the cell membrane. Similarly, dimerization of the hCB_1 receptor with the β_2-AR has been reported to enhance cell surface expression of the hCB_1 in HEK 293H cells (Hudson *et al*., 2010). Several examples of truncated GPCR variants have been reported to dimerize with their full-length receptors. Co-expression of these truncated receptors with their full-length receptors has been shown to decrease the membrane expression of their full-length receptors by dimerization (Bai, 2004). For example, a truncated splice variant of GnRH gonadotropin-releasing hormone, with altered trafficking was able to misroute the full-length receptor and reduce its membrane expression (Grosse *et al*., 1997; McElvaine and Mayo, 2006). However, this scenario does not seem the case for the hCB_1 receptor, since co-expression of the hCB_1 with its splice variants enhanced cell-surface expression of hCB_1 receptor in HEK 293A cells.

4.4 Future Directions

Our findings raised several interesting and important questions for further investigation. First, does the expression of the hCB_1 variants at both the transcript and

protein levels differ during development? and if so does that alter the function of the cannabinoid system during development?. To address this, a more detailed knowledge of the age-related brain distribution of the hCB_{1a} and hCB_{1b} transcripts and proteins is required and would increase our understanding of the physiological roles of these receptors. However, these studies face challenges due to the difficulty in obtaining postmortem human brain tissue of different ages suitable for anatomical investigation. For such studies, an isoform specific antibody would be useful and would complement our western blot analysis. Second, do the relative expression levels of hCB_1 and its variants alter during diseases? For example, the expression levels of the hCB_1 variant transcripts have been reported to change in non-Hodgkin lymphoma. Overexpression of the hCB_1 transcript was observed in lymph nodes of patients with non-Hodgkin's lymphoma compared to lymph nodes of normal individuals. However, low levels of the hCB_{1a} splice variant were detected in 44% of the tested patients, while hCB_{1b} expression was not detected (Gustafsson *et al.,* 2008). This study clearly demonstrated that during the progression of non-Hodgkin's lymphoma, not only is the full-length receptor level altered, but also that of the two truncated variants. It is well documented that normal GPCR expression levels are required for their appropriate physical interactions and functions; however, alterations in the expression level of one or all subunits in the heteromeric protein complexes would be expected to have profound effects on function, leading to abnormal signaling, and disease progression (Dalrymple *et al.,* 2008). Further studies focusing on analysis of the relationship between the expression levels of all hCB_1 and splice variant transcripts and protein levels are required in order to establish the role of these variants in human diseases. Third, do the three hCB_1 variants physically interact

in vivo and do they have higher affinities to form homo- or heterodimers? To answer this, an isoform specific antibody would be of great value to confirm that physical interaction can occur *in vivo* by using co-immunoprecipitation approach.

4.5 Conclusion

In summary, the present work showed overlapping distribution of the hCB_1 variant transcripts in different regions of the human brain. Similarly, hCB_1 protein variants were distributed throughout the monkey brain. We identified a novel mechanism of the hCB_1 receptor splice variants function, in which the truncated receptors can form a physical complex with the full-length hCB_1 receptor and increase cell surface expression of hCB_1, thereby enhancing the signaling activity of the full-length hCB_1 receptor through ERK in HEK 293A cells. Having demonstrated that the hCB_1 can dimerize with its variants, I suggest that future work should take this finding in to consideration when studying the pharmacology of the endocannabinoid system, or designing ligands that target the endocannabinoids system for the treatment of various diseases.

References

AbdAlla, S., Zaki, E., Lother, H. and Quitterer, U. (1999) Involvement of the amino terminus of the B (2) receptor in agonist- induced receptor dimerization. *J Biol Chem*, **274**, 26079-26084.

Abood, M.E., & Martin, B.R. (1992) Neurobiology of marijuana abuse. *Trends Pharmacol. Sci,* **13**, 201-6.

Andersson, H., D'antona, A.M., Kendall, D.A., Von Heijne, G. & Chen, N.C. (2003) Membrane assembly of the cannabinoid receptor 1: impact of a long N-terminal tail. *Mol Pharmacol*, **64**, 570-577.

Apaja, P.M., Tuusa, J.T., Pietila, E.M., Rajaniemi, H.J. & Petaja-Repo,U.E. (2006) Luteinizing hormone receptor ectodomain splice variant misroutes the full-length receptor into a subcompartment of the endoplasmic reticulum. *Molecular Biology of the Cell*, 17, 2243–2255.

Bai, M. (2003) Dimerization of G-protein-coupled receptors: roles in signal transduction. *Cellular Signaling,* **16**, 175–186.

Benkirane, M., Jin, D.Y., Chun, R.F., Koup, R.A. & Jeang, K.T. (1997) Mechanism of transdominant inhibition of CCR5-mediated HIV-1 infection by CCR5**Δ**32. *J. Biol. Chem*, **272**, 30603**–**30606.

Bohn, L.M. (2007) Constitutive trafficking more than just running in circles? *Mol. Pharmacol.***71**, 957-.-8.

Bosier, B., Muccioli, G.G., Hermans, E. & Lambert, D.M. (2010) Functionally selective cannabinoid receptor signalling: Therapeutic implications and opportunities. *Biochemical Pharmacology*, **80**, 1–12.

Bovolin, P., S. Bovetti, S., Fasolo, A., Katarova, Z., Szabo, G., Shipley, M.T., Margolis, F.L. & Puche A.C. (2009) Developmental regulation of metabotropic glutamate receptor 1 splice variants in olfactory bulb mitral cells. *J Neurosci Res*, **87**, 369–379

Burset, M., Seledkov, I.A. & Solovyev, V.V. (2000) Analysis of canonical and non-canonical splice sites in mammalian genomes. *Nucleic Acids Res*, **28**, 4364-4375.

Carriba, P., Ortiz, O., Patkar, K., Justinova, Z., Stroik, J., Themann, A., Muller, C., Woods, A.S., Hope, B.T., Ciruela, F., Casado, V., Canela, E.I., Lluis, C., Goldberg, S.R., Moratalla, R. & Franco, R., Ferre, S. (2007) Striatal adenosine A (2A) and cannabinoid CB_1 receptors form functional heteromeric complexes that mediate the motor effects of cannabinoids. *Neuropsychopharmacology*, **32**,49-59.

Claeysen, S., Sebben, J., Becamel, C., Bockaert, J. & Dumuis. (1999) A. Novel brain-specific 5-HT4 receptor splice variants show marked constitutive activity: Role of the C-terminal intracellular domain. *Mol. Pharmacol,* **55**, 910-920.

Conn, P.J. & Pin J. (1997) Pharmacology and functions of metabotropic glutamate receptors. *Annu. Rev. Pharmacol. Toxicol*, **37**, 205–37.

Dalrymple, M.B., Pfleger, K.D.G. & Eidne, K.A. (2008) G protein-coupled receptor dimers: Functional consequences, disease states and drug targets. *Pharmacology & Therapeutics*, **118**, 359–371.

Demuth, D.G. & Molleman, A. (2006) Cannabinoid signaling. *Life Sci,* **78**, 549-63.

Denovan-Wright, E.M., Gilby, K.L., Howlett, S.E. & Robertson, H.A. Isolation of total cellular RNA from brain tissue. http://fds.oup.com/www.oup.co.uk/pdf/pas/5-7-2.pdf (23 August. 2001)

Devane, W.A., Hanus, L., Breuer, A., Pertwee, R.G., Stevenson, L.A., Griffin, G., Gibson, D., Mandelbaum, A., Etinger, A. & Mechoulam, R. (1992) Isolation and structure of a brain constituent that binds to the cannabinoid receptor. *Science,* **258**,1946-9.

Dong, C., Filipeanu, C.M., Duvernay, M.T. & Wu, G. (2007) Regulation of G protein-coupled receptor export trafficking. *Biochim Biophys Acta*, **1768**, 853–870.

Dupré, D.J., Robitaille, M., Ethier, N., Villeneuve, L.R., Mamarbachi, A.M. & Hebert, T.E. (2006) Seven transmembrane receptor core signaling complexes are assembled prior to plasma membrane trafficking. *J. Biol. Chem,* **281**, 34561-73.

Duvernay, M.T., Filipeanu, C.M., Wu, G. (2005) The regulatory mechanisms of export trafficking of G protein-coupled receptors.*Cellular Signalling* , **17**, 1457-1465.

Eggan, S.M. & Lewis, D.A. (2007) Immunocytochemical distribution of the cannabinoid CB1 receptor in the primate neocortex: a regional and laminar analysis. *Cereb Cortex*, **17**,175-191.

Ellis, J., Pediani, J.D., Canals, M., Milasta, S. & Milligan, G. (2006). Orexin-1 receptor cannabinoid CB_1 receptor heterodimerization results in both ligand-dependent and independent coordinated alterations of receptor localization and function. *J. Biol. Chem,* **281**, 38812-24.

Galvez, T., Duthey, B., Kniazeff, J., Blahos, J., Rovelli, G., Bettler,B., Pr**é**zeau, L. & Pin, J.P. (2001) Allosteric interactions between GB1 and GB2 subunits are required for optimal GABAB receptor function. *EMBO J.*, **20,** 2152-2159.

George, S.R., O'Dowd, B.F. & Lee S.P. (2002) G-protein-coupled receptor oligomerization and its potential for drug discovery. *Nat. Rev. Drug Discov*, **1**, 808-820.

Glass, M. & Felder, C.C. (1997) Concurrent stimulation of cannabinoid CB_1 and dopamine D2 receptors augments cAMP accumulation in striatal neurons: Evidence for a Gs linkage to the CB_1 receptor. *J. Neurosci,* **17**, 5327-33.

Grosse, R., Schoneberg, T., Schultz, G. & Gudermann, T. (1997) Inhibition of gonadotropin-releasing hormone receptor signaling by expression of a splice variant of the human receptor. *Mol. Endocrinol*, **11**, 1305**–**1318.

Guan, R., Feng, X., Wu, X., Zhang, M., Zhang, X., Hebert, T.E. & Segaloff, D.L. (2009) Bioluminescence resonance energy transfer studies reveal constitutive dimerization of the human lutropin receptor and a Lack of correlation between receptor activation and the propensity for dimerization. *The Journal of Biological Chemistry,* **284**, 7483–7494.

Gurevich, V.V & Gurevich, E.V. (2008) GPCR monomers and oligomers: it takes all kinds.*Trends Neurosci*, **31**, 74-81.

Gustafsson, K., Wang, X., Severa, D., Eriksson, M., Kimby, E., Merup, M., Christensson, B., Jenny Flygare & Sander, B. (2008) Expression of cannabinoid receptors type 1 and type 2 in non-Hodgkin lymphoma: growth inhibition by receptor activation. *Int. J. Cancer*, **123**, 1025–1033.

Hague, C., Chen, Z., Pupo, A.S., Schulte, N.A, Toews, M.L. & Minneman, K.P. (2004) The N terminus of the human alpha1D-adrenergic receptor prevents cell surface expression. *J Pharmacol Exp Ther,* **309**, 388-397.

Hosking, R.D. & Zajicek, J.P. (2008) Therapeutic potential of cannabis in pain medicine. *BJA*, 10159-68.

Howlett, A.C., Breivogel, C.S., Childers, S.R., Deadwyler, S.A., Hampson, R.E. & Porrino, L.J. (2004) Cannabinoid physiology and pharmacology: 30 years of progress. *Neuropharmacology,* **47,** 345–358.

Howlett, A.C., Blume, L.C. & Dalton, G.D. (2010) CB_1 cannabinoid receptors and their associated proteins. *Curr Med Chem*, **17**, 1382-1393.

Hu, C.D., Chinenov, Y. & Kerppola, T.K. (2002) Visualization of interactions among bZIP and rel family proteins in living cells using bimolecular fluorescence complementation. *Mol. Cell,* **9**, 789-98.

Hudson, B.D., Hébert, T.E. & Kelly, M. E. (2010) Physical and functional interaction between CB_1 cannabinoid receptors and β_2-adrenoceptors. *British Journal of Pharmacology*, **160**, 627–642.

Hughes, T.A. 2006) Regulation of gene expression by alternative untranslated regions. *Trends Genet*, **22**,119-22.

Karpa, K.D., Lin, R., Kabbani, N. & Levenson, R. (2000) The Dopamine D3 Receptor interacts with itself and the truncated D3 splice variant D3nf: D3-D3nf interaction causes mislocalization of D3 receptors. *Mol Pharmacol,* **58**, 677-683.

Kearn, C.S., Blake-Palmer, K., Daniel, E. Mackie, K. & Glass, M. (2005) Concurrent Stimulation of cannabinoid CB1 and dopamine D2 receptors enhances heterodimer formation: a mechanism for receptor cross-talk?. *Mol Pharmacol*, **67**,1697–1704.

Khan, Z.U, Mrzljak, L., Gutierrez, A.T., De La Calle, A. & Goldman-Rakic, P.S. (1998) Prominence of the dopamine D2 short isoform in dopaminergic pathways. *PNAS*, **95**, 7731-7736

Kilpatrick, G.J., Dautzenberg, F.M., Martin, G.R. & Eglen, R.M. (1999) 7TM receptors: the splicing on the cake. *Trends Pharmacol Sci*, **20**, 294-301.

McElvaine, A.T. & Mayo K.E. (2006) A dominant-negative human growth hormone-releasing hormone (GHRH) receptor splice variant inhibits GHRH binding. *Endocrinology*, **147**, 1884–1894.

Mackie, K. (2005) Cannabinoid receptor homo- and heterodimerization. *Life Sci,* **77**, 1667-1673.

Mackie, K. (2005) Distribution of cannabinoid receptors in the central and peripheral Nervous System. *HEP*, **168**, 299–325.

McDonald, N.A., Henstridge, C.M., Connolly, C.N. & Irving, A.J. (2007) Generation and functional characterization of fluorescent, N-terminally tagged CB_1 receptor chimeras for live-cell imaging. *Mol. Cell. Neurosci*, **35**, 237–248.

Markovic, D. & Challiss, R.A. (2009) Alternative splicing of G protein-coupled receptors: physiology and pathophysiology. *Cell. Mol. Life Sci,* **66**, 3337–3352.

Markovic, D. & Grammatopoulos, D.K. (2009) Focus on the splicing of secretin GPCRs transmembrane-domain 7. *Trends Biochem Sci*, **34**, 443-52.

Marcellino, D., Carriba, P., Filip, M., Borgkvist, A., Frankowska, M., Bellido, I., Tanganelli, S., Muller, C.E., Fisone, G., Lluis, C., Agnati, L.F., Franco, R. & Fuxe, K. (2008) Antagonistic cannabinoid CB_1/dopamine D_2 receptor interactions in striatal CB_1/D_2 heteromers. A combined neurochemical and behavioral analysis. *Neuropharmacology.* **54**, 815-23.

Matsuda, L.A., Lolait, S.J.,Brownstein, M.J., Young, A.C. & Bonner, T.I. (1990) Structure of a cannabinoid receptor and functional expression of the cloned cDNA. *Nature,* **346**, 561-4.

Maudsley, S., Bronwen, M. & Luttrell, L., M. (2005) The origins of diversity and specificity in G protein-coupled receptor signaling. *JPET*, **314**, 485-494.

McAllister, C.D., Rizvi,G., Anavi-Goffer, S., Hurst, D.P., Barnett-Norris,J.,Lynch, D.L., Reggio, P.H. & Mary E. Abood, M.E.(2003) An aromatic microdomain at the cannabinoid CB_1 Receptor constitutes anagonist/inverse agonist binding region. *J. Med. Chem*, ***46***, 5139-5152.

McElvaine, A.T. & Mayo, K.E. (2005) A dominant-negative human growth hormone-releasing hormone (GHRH) receptor splice variant inhibits GHRH binding. *Endocrinology*, **147**, 1884–1894.

Mechoulam, R., & Gaoni, Y. (1967). The absolute configuration of Δ-1 tetrahydrocannabinol, the major active constituent of hashish. *Tetrahedron Lett*, **12**,1109-11.

Mechoulam, R. (1970). Marihuana chemistry. *Science*, **168**, 1159-66.

Mechoulam, R., Ben-Shabat, S., Hanus, L., Ligumsky, M., Kaminski, N.E., Schatz, A.R.,Gopher, A., Almog, S., Martin, B.R. & Compton, D.R. (1995). Identification of an endogenous 2-monoglyceride, present in canine gut, that binds to cannabinoid receptors. *Biochem. Pharmacol*, **50**, 83-90.

Mercier, J.F., Salahpour, A., Angers, S., Breit, A. & Bouvier, M. (2002) Quantitative assessment of β_1- and β_2-adrenergic receptor homo- and heterodimerization by bioluminescence resonance energy transfer. *The Journal of Biological Chemistry*, **277**, 44925-44931.

Minneman, K.P. (2001) Splice variants of G protein-coupled receptors. *Mol Interv*, **1**, 108-16.

Milligan, G. (2004) G protein-coupled receptor dimerization: function and ligand pharmacology. *Mol Pharmacol,* **66**, 1–7.

Millar, R.P. & Newton, C.L. (2010) The year in G protein-coupled receptor research. *Mol Endocrinol*, **24**, 261–274.

Miller, J. (2004) Tracking G protein-coupled receptor trafficking using Odyssey Imaging. http://www.licor.com/bio/PDF/Miller_GPCR.pdf (25 Jul. 2006).

Miller, L.K. & Devi, L.A. (2011) The highs and lows of cannabinoid receptor expression in disease: mechanisms and their therapeutic implications. *Pharmacol Rev,* **63**, 461–470.

Miyake, A. (1995) A truncated isoform of human CCK-B/gastrin receptor generated by alternative usage of a novel exon. *Biochem Biophys Res Commun*, **208**, 230-7.

Munro, S., Thomas, K.L. & Abu-Shaar, M. (1993) Molecular characterization of a peripheral receptor for cannabinoids. *Nature*, **365**, 61-5.

Nakamura, K., Yamashita, S., Omori, Y. & Minegishi, T. (2004) A Splice variant of the human luteinizing hormone (LH) receptor modulates the expression of wild-type human LH receptor. *Molecular Endocrinology*, **18**, 1461–1470.

Pinto, J.G., Hornby, K.R., Jones, D.G. & Murphy K.M. (2010) Developmental changes in GABAergic mechanisms in human visual cortex across the lifespan. *Front Cell Neurosci*, **10**: 4-16.

Pfleger, K.D. & Eidne, K.A. (2005) Monitoring the formation of dynamic G-protein-coupled receptor-protein complexes in living cells. *Biochem. J,* **385**, 625-37.

Prinster, S.C., Hague, C. & Hall, R.A. (2005) Heterodimerization of G protein-coupled receptors: specificity and functional significance. *Pharmacol Rev,* **57,** 289-298.

Przybyla, J.A., & Watts, V.J. (2010). Ligand-induced regulation and localization of cannabinoid CB_1 and dopamine D2L receptor heterodimers. *J. Pharmacol. Exp. Ther.* **332**, 710-9.

Rinaldi-Carmona, M., Calandra, B., Shire, D., Bouaboula, M., Oustric, D., Barth, F., Casellas, P., Ferrara, P. & Le Fur, G. (1996) Characterization of two cloned human CB1 cannabinoid receptor isoforms. *J Pharmacol Exp Ther*, **278**, 871-8.

Richtand, N.M. (2006) Behavioral Sensitization, Alternative Splicing, and D3 Dopamine Receptor-Mediated Inhibitory Function. *Neuropsychopharmacology*, **31**, 2368–2375.

Rios, C.D., Jordan, B.A., Gomes, I. & Devi, L. A. (2001). G-protein-coupled receptor dimerization: Modulation of receptor function. *Pharmacol. Ther,* **92**, 71-87.

Rios, C.D., Gomes, I. & Devi, L.A. (2006). μ opioid and CB_1 cannabinoid receptor interactions: Reciprocal inhibition of receptor signaling and neuritogenesis. *Br. J. Pharmacol,* **148**, 387-95.

Rozenfeld, R., Gupta, A., Gagnidze, K., Lim, M.P., Gomes, I., Lee-Ramos, D., Nieto, N. & Devi L.A. (2011) AT_1R–CB_1R heteromerization reveals a new mechanism for the pathogenic properties of angiotensin II. *The EMBO Journal*, **30**, 2350–2363.

Ryberg, E., Vu, H.K., Larsson, N., Groblewski, T., Hjorth, S., Elebring, T., Sjögren, S. & Greasley, P.J. (2005) Identification and characterization of a novel splice variant of the human CB1 receptor. *FEBS Letters*. **579**, 259–264.

Sarzania, R., Bordicchiaa, M., Marcuccia, P., Bedettaa, S., Santinia, S., Giovagnolia, A., Scappinia, L., Minardib, D., Muzzonigrob, G., Dessì-Fulgheria, P. & Rappellia, A. (2009) Altered pattern of cannabinoid type 1 receptor expression in adipose tissue of dysmetabolic and overweight patients. *Metabolism Clinical and Experimental*. **58**, 361–367.

Shioda, T., Nakayama, E.E., Tanaka, Y., Xin, X., Liu, H., Kawana-Tachikawa, A., Kato, A., Sakai, Y., Nagai, Y. & Iwamoto, A. (2001) Naturally occurring deletional mutation in the C-terminal cytoplasmic tail of CCR5 affects surface trafficking of CCR5. *J Virol*, **75**, 3462–3468.

Shire, D., Carillon, C., Kaghad, M., Calandra, B., Rinaldi-Carmona, M., Le Fur, G., Caput, D. & Ferrara, P. (1995) An amino-terminal variant of the central cannabinoid receptor resulting from alternative splicing. *J Biol Chem*, **270**, 3726-3731.

Smith, T.H., Sim-Selley, L.J. & Selley, D.E. (2010) Cannabinoid CB1 receptor-interacting proteins: novel targets for central nervous system drug discovery?. *Br J Pharmacol*, **160**, 454-466.

Szidonya, L., Cserzo, M., and Hunyady, L. (2008) Dimerization and oligomerization of G-protein-coupled receptors: debated structures with established and emerging functions. *Journal of Endocrinology*. 1**96**, 435–453.

Terrillon, S. & Bouvier, M. (2004) Roles of G-protein-coupled receptor dimerization. From ontogeny to signalling regulation. *EMBO reports,* **5**, 3 –34.

Tress, M.L., Martelli, P.L., Frankish, A., Reeves, G.A, Wesselink, J.J., Yeats, C., Olason, P.I., Albrecht, M., Hegyi, H., Giorgetti, A., Raimondo, D., Lagarde, J., Laskowski, R.A., López, G., Sadowski, M.I., Watson, J. D., Fariselli, P., Rossi, I., Nagy, A., Kai, W., Storling, Z., Orsini, M., Assenov, Y., Blankenburg, H., Huthmacher, C., Ramírez, F., Schlicker, A., Denoeud, F., Jones, P., Kerrien, S., Orchard, S., Antonarakis, S. E., Reymond, A., Birney, E., Brunak, S., Casadio, R., Guigo, R., Harrow, J., Hermjakob, H., Jones, D.T., Lengauer, T., Orengo, C. A., Patthy, L., Thornton, J.M., Tramontano, A., Valencia A. (2007) The implications of alternative splicing in the ENCODE protein complement. *PNAS,* **104**, 5495-500.

Vilardaga, J.P., Bünemann, M., Feinstein T.N., Lambert N., Nikolaev, V.O., Engelhardt,S., Lohse, M.J. & Hoffmann, C. (2009) GPCR and G protein: drug efficacy and activation in live cells. *Molecular Endocrinology,* **23**,590-599.

Wager-Miller, J., Ruth Westenbroek, R., Mackie, K. (2002) Dimerization of G protein-coupled receptors: CB1 cannabinoid receptors as an example. *Chemistry and Physics of Lipids*, 121, 83- 89.

Wang, X., Dow-Edwards, D., Keller, E. & Hurd, Y.L. (2003) Preferential limbic expression of the cannabinoid receptor mRNA in the human fetal brain. Neuroscience, **118**, 681-94.

Wilkie, T.M. (2001) Treasures throughout the life-cycle of G-protein-coupled receptors. *Trends Pharmacol.Sci,* **22**, 396-397.

Wilson, R.I. & Nicoll, R.A. (2001) Endogenous cannabinoids mediate retrograde signaling at hippocampal synapses. *Nature*, **410**, 588-92.

Xiao, J.C., Jewell, J.P., Lin, L.S., Hagmann, W.K., Fong, T.M. & Shen, C. (2008) Similar in vitro pharmacology of human cannabinoid CB1 receptor variants expressed in CHO cells. *Brain Res*, **1238**, 36-43.

Xu, J., Xu, M., Yasmin L. Hurd, Y. L., Pasternak, G.W. Pan, Y. (2009) Isolation and characterization of new exon 11-associated N-terminal splice variants of the human mu opioid receptor gene. *J Neurochem*, **108**,962-972.

Zhang, P.W., Ishiguro, H., Ohtsuki, T., Hess, J., Carillo, F., Walther , D., Onaivi, E.S., Arinami, T. & Uhl, G.R. (2004) Human cannabinoid receptor 1: 50 exons, candidate regulatory regions, polymorphisms, haplotypes and association with polysubstance abuse. *Molecular Psychiatry*, **9**, 916–931.

Zhu, X. & Wess, J. (1998) Truncated V2 vasopressin receptors as negative regulators of wild-type V2 receptor function. *Biochemistry,* **37**, 15773–15784.

Zurolo, E., Iyer, A.M., Spliet, W.G.M, Van Rijen, P.C., Troost, D., Gorter, J.A. & Aronica. E. (2010) CB_1 and CB_2 cannabinoid receptor expression during development and in epileptogenic developmental pathologies. *Neuroscience*, **170**, 28-41.